Design of Bio-Inspired Materials and Total Synthesis of *Securinega* Alkaloids

Inauguraldissertation

zur

Erlangung der Würde eines Doktors der Philosophie

vorgelegt der

Philosophisch-Naturwissenschaftlichen Fakultät

der Universität Basel

von

Robin Wehlauch

aus Wolfen, Deutschland

Basel 2017

Genehmigt von der Philosophisch-Naturwissenschaftlichen Fakultät

auf Antrag von:

Prof. Dr. Karl Gademann

Prof. Dr. Konrad Tiefenbacher

Basel, den 13.12.2016

Prof. Dr. Jörg Schibler

Dekan

Für meine Familie

Table of Content

Abstract

This thesis is divided into four chapters presenting distinct research projects that address challenges in the fields of functional systems chemistry, chemical biology, and the total synthesis of natural products. Experimental details, analytical data and appendices are enclosed at the end of this work.

Chapter 1 introduces the concept of electron-poor catechols as surface binding agents and highlights some of the natural role models. The development of a synthetic surface modification platform for the controlled release of small molecules is described. Nitrocatechol-based anchoring units allowed for the immobilization of a molecular cargo on titanium dioxide surfaces and cleavage on demand by UV irradiation.

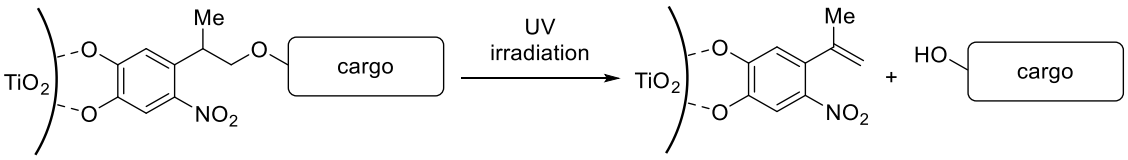

Chapter 2 expands the application of small catechol binders. The design and synthesis of new polar derivatives facilitated the use of boronate esters in dynamic functional systems and led to the discovery of the third orthogonal dynamic covalent bond.

Chapter 3 reports on the preparation of biochemical probes for the investigation of the cellular target of rapamycin. An efficient assembly of natural product hybrids from rapamycin was achieved without the need for protection of the macrolide. The antiproliferative activity of the parent compound was shown to be largely conserved in the novel substances.

Chapter 4 provides a detailed review of the literature on *Securinega* alkaloids. The first enantioselective total synthesis of secu'amamine E was accomplished in twelve linear synthetic steps and 8.5% overall yield. Three examples of an intriguing rearrangement process were studied allowing for the direct interconversion of natural products with implications for a new biogenetic hypothesis.

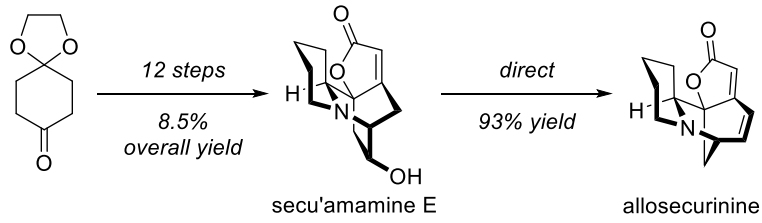

Abbreviations, Acronyms and Symbols

°C ..... degree centigrade

[α] ..... specific optical rotation

2,2-DMP 2,2-dimethoxypropane

Ac ..... acetyl

aq. ..... aqueous

AuNP ..... gold nanoparticle

Bn ..... benzyl

Boc ..... *tert*-butyloxycarbonyl

brsm ..... based on recovered starting material

Bu ..... butyl

Bz ..... benzoyl

c ..... concentration

calcd. ..... calculated

cat. ..... catalytic

CD ..... circular dichroism

cf. ..... confer

conc. ..... concentrated

δ ..... chemical shift

d ..... doublet

D ..... deuterium

d.r. ..... diastereomeric ratio

dec. ..... decomposed

DIAD ..... diisopropyl azodicarboxylate

DIPEA ..... *N*,*N*-diisopropylethylamine

DMAP 4-dimethylaminopyridine

DMF .....dimethylformamide

DMP ..... Dess-Martin periodinane

DMSO ..... dimethyl sulfoxide

DNA .....deoxyribonucleic acid

DOPA 3,4-dihydroxyphenylalanine

ee ..... enantiomeric excess

EDC .....1-ethyl-3-(3-dimethylaminopropyl)carbodiimide

EM .....electron microscopy

eq. .....equivalent

ESI .....electrospray ionization

Et ..... ethyl

FKBP12 ..... FK-506-binding protein 12

FTIR ..... Fourier transform infrared spectroscopy

g ..... gram

h .....hour

HBTU ..... *O*-(benzotriazol-1-yl)-*N*,*N*,*N*′,*N*′-tetramethyluronium hexafluorophosphate

hν .....photon energy according to Planck-Einstein relation

HMDS ..... hexamethyldisilazide

HOBt ..... *N*-hydroxybenzotriazole

HPLC..... high-performance liquid chromatography

HRMS.....high-resolution mass spectrometry

Hz ..... hertz

IBX .....2-iodoxybenzoic acid

IR .....infrared

J ..... coupling constant

L ..... liter

LDA ..... lithium diisopropylamide

M ..... molarity

m ..... multiplet

M.p. ..... melting point

*m*CPBA ..... *meta*-chloroperbenzoic acid

Me ..... methyl

Mfp ..... mussel foot protein

min ..... minute

MOM ..... methoxymethyl

MOPS ..... 3-(*N*-morpholino)propanesulfonic acid

MS ..... mass spectrometry

Ms ..... methanesulfonyl

μw ..... microwave heating

NBS ..... *N*-bromosuccinimide

NCS ..... *N*-chlorosuccinimide

NDI ..... naphthalenediimide

NIS ..... *N*-iodosuccinimide

NMP *N*-methyl-2-pyrrolidone

NMR ..... nuclear magnetic resonance

PEG ..... polyethylene glycol

Ph ..... phenyl

PPG ..... photoremovable protecting group

ppm ..... parts per million

Pr ..... propyl

*p*TsOH ..... *para*-toluenesulfonic acid

q ..... quartet

quant. ..... quantitative

Rapa ..... rapamycin(yl)

rac. ..... racemic

R_f ..... retention factor

rt ..... room temperature

s ..... singlet

SAM ..... self-assembled monolayer

SAR ..... structure-activity relationship

sat. ..... saturated

SOSIP ..... self-organizing surface-initiated polymerization

t ..... triplet

TBAF ..... tetrabutylammonium fluoride

TBS ..... *tert*-butyldimethylsilyl

TBDPS ..... *tert*-butyldiphenylsilyl

TES ..... triethylsilyl

Tf ..... trifluoromethanesulfonyl

TFA ..... trifluoroacetic acid

THF ..... tetrahydrofuran

TIPS ..... triisopropylsilyl

TLC ..... thin-layer chromatography

TMS ..... trimethylsilyl

TOR ..... target of rapamycin

TORC ..... target of rapamycin complex

TSE..... templated stack exchange

UPLC.....ultra-performance liquid chromatography

UV .....ultraviolet

$\tilde{\nu}$.....wavenumber

1 Nitrocatechols for Light-Induced Small Molecule Release

1.1 Introduction

1.1.1 Catechols in Nature

Catechols are *ortho*-dihydroxyaryl compounds serving a variety of different functions in nature. Already from the structure itself a chemist can augur the broad range of catechol chemistry. The two vicinal hydroxyl groups may serve as weak acid or be oxidized to a highly reactive *ortho*-quinone. They could engage in hydrogen bonding or act as bidentate ligand for coordination chemistry.

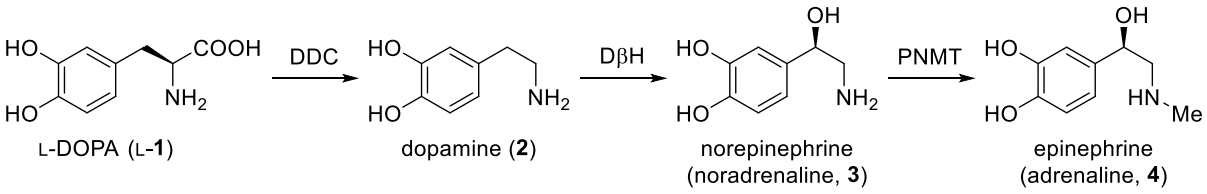

Scheme 1: Biogenesis of catecholamine neurotransmitters.

A prominent example from nature are the catecholamine neurotransmitters, tightly regulated signaling molecules within neural networks (Scheme 1). Dopamine (**2**) is enzymatically derived from L-3,4-dihydroxyphenylalanine (L-DOPA, L-**1**) by DOPA decarboxylase (DDC). Further transformation by dopamine β-hydroxylase (DβH) produces norepinephrine (**3**), which is methylated by phenolethanolamine-*N*-methyltransferase (PNMT) to epinephrine (**4**).[1] In the human brain dopamine (**2**) is closely linked to rewarding and alerting systems, and it serves several other roles in the peripheral nervous system.[2] Norepinephrine (**3**) and epinephrine (**4**) also act as hormones and are released under physical and psychological stress.[3] The catecholamines exhibit their high activities *via* two G protein-coupled receptors, the adrenergic and dopamine receptors.[4] Narcotic drugs like amphetamines also act partially *via* these receptors and their strong acute effects as well as the high addiction potential (methamphetamine) arise from their interference with catecholamine neurotransmitter metabolism in the brain.[5]

[1] G. Eisenhofer, I. J. Kopin, D. S. Goldstein, *Pharmacol. Rev.* **2004**, *56*, 331–349.
[2] E. S. Bromberg-Martin, M. Matsumoto, O. Hikosaka, *Neuron* **2010**, *68*, 815–834.
[3] D. L. Wong, *Cell. Mol. Neurobiol.* **2006**, *26*, 891–900.
[4] O.-E. Brodde, H. Bruck, K. Leineweber, *J. Pharmacol. Sci.* **2006**, *100*, 323–337.
[5] D. Sulzer, M. S. Sonders, N. W. Poulson, A. Galli, *Prog. Neurobiol.* **2005**, *75*, 406–433.

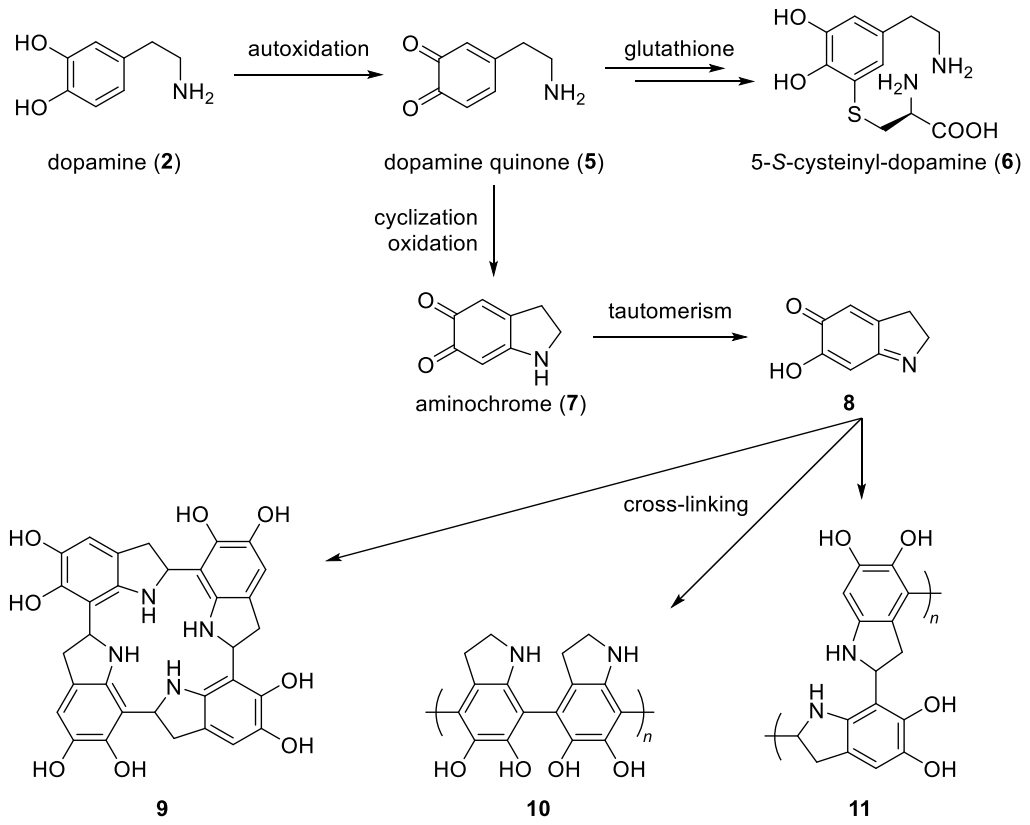

Scheme 2: Oxidative metabolism of dopamine in the human brain producing neurotoxic dopamine derivatives and melanin pigments.

But also, catecholamines themselves are attributed with neurotoxic effects and play a role in the development of neurodegenerative diseases, especially in the Parkinson's disease. While dopamine (**2**), norepinephrine (**3**) and epinephrine (**4**) are usually metabolized enzymatically by catechol-*O*-methyltransferase (COMT) and monoamine oxidase (MAO), autoxidation of dopamine (**2**) leads to reactive dopamine quinone (**5**, Scheme 2), which is transformed to neurotoxic compounds like 5-*S*-cysteinyl-dopamine (**6**) or aminochrome (**7**).[6] Spontaneous cyclization and oxidation of dopamine quinone (**5**) lead to aminochrome (**7**), which by tautomerization (**8**) and cross-linking of aryl moieties, produces melanin (poly-5,6-dihydroxyindole, **9**–**11**). Increased formation of neuromelanin pigments together with largely reduced amounts of dopamine (**2**) producing cells has been observed in patients suffering from Parkinson's disease.

[6] (a) J. Smythies, L. Galzigna, *Biochim. Biophys. Acta* **1998**, *1380*, 159–162; (b) C. Aureli, T. Cassano, A. Masci, A. Francioso, S. Martire, A. Cocciolo, S. Chichiarelli, A. Romano, S. Gaetani, P. Mancini, M. Fontana, M. d'Erme, L. Mosca, *J. Neurosci. Res.* **2014**, *92*, 347–358.

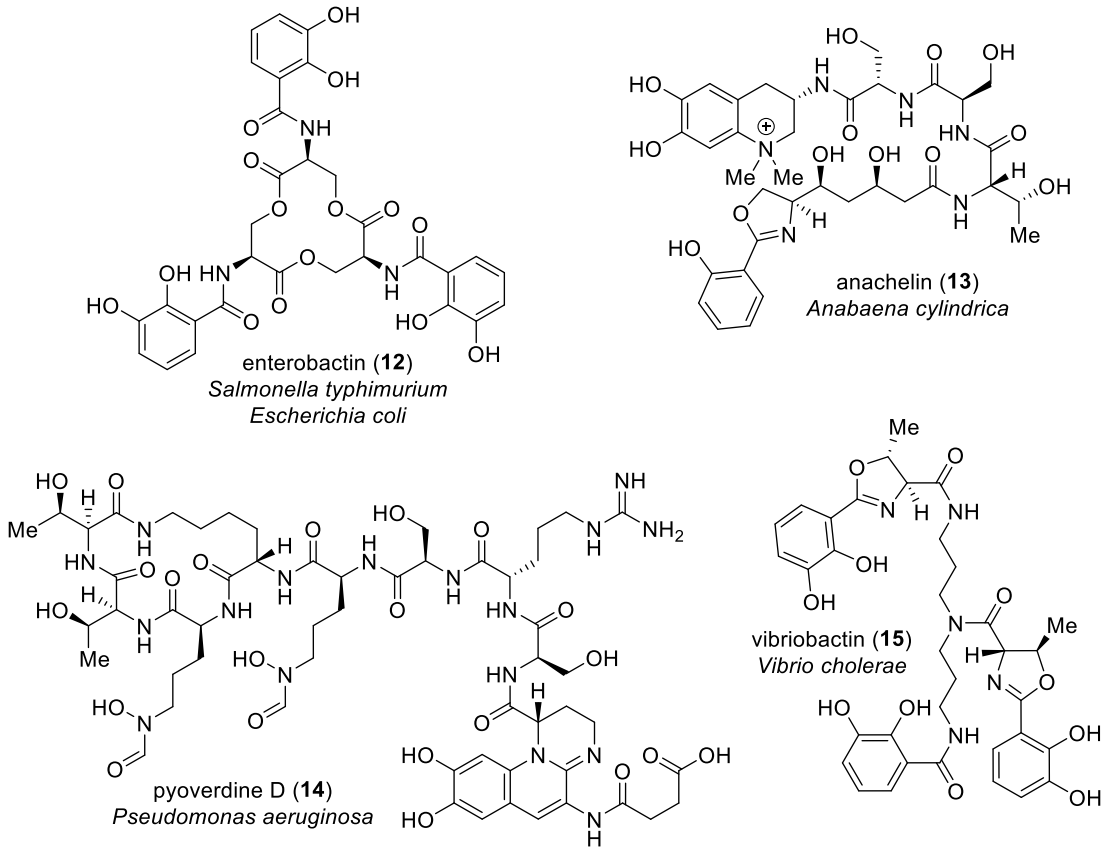

Figure 1: Examples of bacterial catechol-containing siderophores and their natural sources.

Another example of natural catechols are siderophores, iron chelators produced by bacteria, fungi and plants. In the extracellular environment, these compounds bind and transport inorganic Fe^{3+} making it bioavailable to the parent organism. Hundreds of siderophores have been described in the literature and can be classified by the functional groups complexing the ferric ions.[7] The siderophores produced by graminaceous plants (phytosiderophores) are usually carboxylate siderophores whereas fungi predominantly possess hydroxamate siderophores. The largest structural variety is found in bacteria, which, in addition to the afore mentioned, also synthesize catecholate siderophores (**12**–**15**, Figure 1). Siderophores are only produced and secreted under iron starvation conditions to supply the organism with iron from mineral sources. Ferric ions are complexed and transported to the membrane where specific receptors recognize these complexes and transport them into the cell. Transport of the ferric siderophore complexes has been studied to a great extend in Gram-negative bacteria where several homologous TonB-dependent transporters consisting of 22-stranded transmembrane β barrels have been characterized.[8] To release the ions, the siderophores are either degraded, or the ferric ions are

[7] For general reviews on siderophores, see: (a) H. Drechsel, G. Jung, *J. Peptide Sci.* **1998**, *4*, 147–181; (b) R. C. Hider, X. Kong, *Nat. Prod. Rep.* **2010**, *27*, 637–657.

[8] (a) K. P. Locher, B. Rees, R. Koebnik, A. Mitschler, L. Moulinier, J. P. Rosenbusch, D. Moras, *Cell* **1998**, *95*, 771–778; (b) A. D. Ferguson, E. Hofmann, J. W. Coulton, K. Diederichs, W. Welte, *Science*

reduced to ferrous ions with decreased affinity to the complexing ligand. Many siderophores contain peptide building blocks which are synthesized non-ribosomally and the biosyntheses of enterobactin (**12**),[9] pyoverdine D (**14**)[10] and others[11] have been reported. Their structures can be very diverse, containing alkaloid and polyketide fragments as exemplified by the structure of anachelin (**13**).[12]

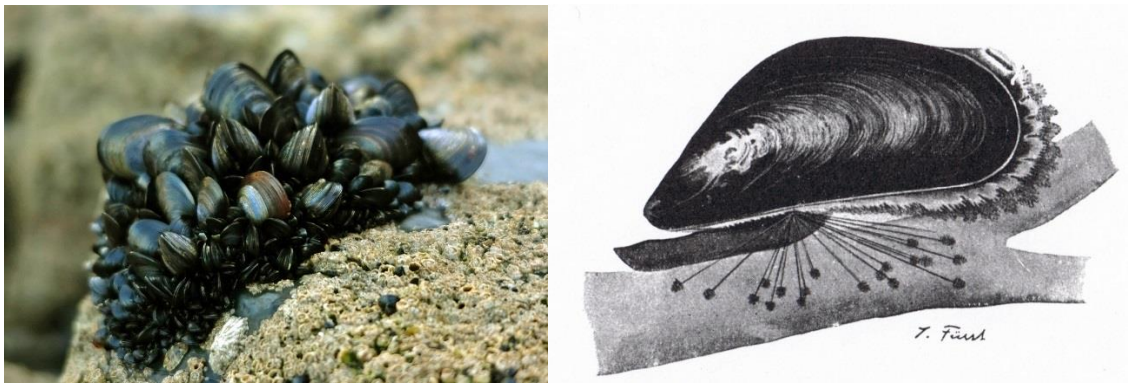

Figure 2: Blue mussels, *Mytilus edulis*, on a rock in Cornwall, UK (left)[13] and a drawing of *M. edulis* by Julius Fürst indicating the byssus' filaments and plaque tips (around 1895, right).[14]

The ability to efficiently complex ions and coordinate to solid surfaces is existential for the mussels of the genus *Mytilus*. These bivalve mollusks live stationary in the intertidal zones of ocean shores. To brave the constant waves in their habitat, mussels adhere permanently to virtually any surface found in the marine environment. Adhesion is accomplished under wet conditions by a bundle of filaments reaching out radially. The filaments carry adhesive plaques at the tips, which bind to the foreign surface. The plaques secrete a proteinaceous gel, which darkens, solidifies, and leads to the strong adhesion. Analyses showed that the secretion contains so called mussel foot proteins (Mfps) of which Mfp-3 and Mfp-5 contain up to

1998, *282*, 2215–2220; (c) S. K. Buchanan, B. S. Smith, L. Venkatramani, D. Xia, L. Esser, M. Palnitkar, R. Chakraborty, D. van der Helm, J. Deisenhofer, *Nat. Struct. Biol.* **1999**, *6*, 56–63; (d) D. Cobessi, H. Celia, F. Pattus, *J. Mol. Biol.* **2005**, *352*, 893–904.

[9] D. P. Frueh, H. Arthanari, A. Koglin, D. A. Vosburg, A. E. Bennett, C. T. Walsh, G. Wagner, *Nature* **2008**, *454*, 903–907.

[10] (a) P. Visca, F. Imperi, I. L. Lamont, *Trends Microbiol.* **2007**, *15*, 22–30; (b) I. J. Schalk, L. Guillon, *Environ. Microbiol.* **2013**, *15*, 1661–1673.

[11] (a) J. J. De Voss, K. Rutter, B. G. Schroeder, C. E. Barry III, *J. Bacteriol.* **1990**, *181*, 4443–4451; (b) L. E. N. Quadri, *Mol. Microbiol.* **2000**, *37*, 1–12.

[12] (a) Y. Itou, S. Okada, M. Murakami, *Tetrahedron* **2001**, *57*, 9093–9099; (b) Y. Ito, K. Ishida, S. Okada, M. Murakami, *Tetrahedron* **2004**, *60*, 9075–9080.

[13] https://commons.wikimedia.org/wiki/File:Blue_mussel_clump.jpg; public domain.

[14] https://commons.wikimedia.org/wiki/File:Miesmuschel_(Mytilus_edulis).jpg; Julius Fürst, public domain.

30 mol% of L-DOPA (L-**1**).[15] The complex interplay of the Mfps as well as the influence of surrounding factors have not yet been fully understood but many studies have been carried out to elucidate those details.[16] Attractive interactions between specific Mfps and mineral surfaces as well as protein-protein binding interactions have been reported.[17] Also, the implementation of metal ions (Ca^{2+}, Fe^{3+}) into the protein films can enable adhesion through ion bridging of proteins.[18] Covalent crosslinking between Mfps proceeds through oxidation of the L-DOPA (L-**1**) residues by seawater or redox exchange with Fe^{3+}.[19] The extent of crosslinking remains unclear and is thought to be closely regulated as oxidation to the quinone results in a much reduced binding affinity to mineral surfaces. These crosslinking events enable the protein film to also adhere to organic surfaces by the formation of covalent bonds to surface bound nucleophiles. Furthermore, the oxidation of catechol groups as well as the incorporation of metal ions at sites of film rupture and defect enable self-healing of the macromolecular network.

[15] (a) J. H. Waite, X. X. Qin, *Biochemistry* **2001**, *40*, 2887–2893; (b) H. Zhao, N. B. Robertson, S. A. Jewhurst, J. H. Waite, *J. Biol. Chem.* **2006**, *281*, 11090–11096.

[16] Review: B. P. Lee, P. B. Messersmith, J. N. Israelachvili, J. H. Waite, *Annu. Rev. Mater. Res.* **2011**, *41*, 99–132.

[17] Q. Lin, D. Gourdon, C. Sun, N. Holten-Andersen, T. H. Anderson, J. H. Waite, J. N. Israelachvili, *Proc. Natl. Acad. Sci. USA* **2007**, *104*, 3782–3786.

[18] (a) D. S. Hwang, H. Zeng, A. Masic, M. J. Harrington, J. N. Israelachvili, J. H. Waite, *J. Biol. Chem.* **2010**, *285*, 25850–25858; (b) H. Zeng, D. S. Hwang, J. N. Israelachvili, J. H. Waite, *Proc. Natl. Acad. Sci. USA* **2010**, *107*, 12850–12853.

[19] (a) L. M. McDowell, L. A. Burzio, J. H. Waite, J. Schaefer, *J. Biol. Chem.* **1999**, *274*, 20293–20295; (b) M. J. Sever, J. T. Weisser, J. Monahan, S. Srinivasan, J. J. Wilker, *Angew. Chem. Int. Ed.* **2004**, *43*, 448–450.

1.1.2 Catecholic Surface Coatings

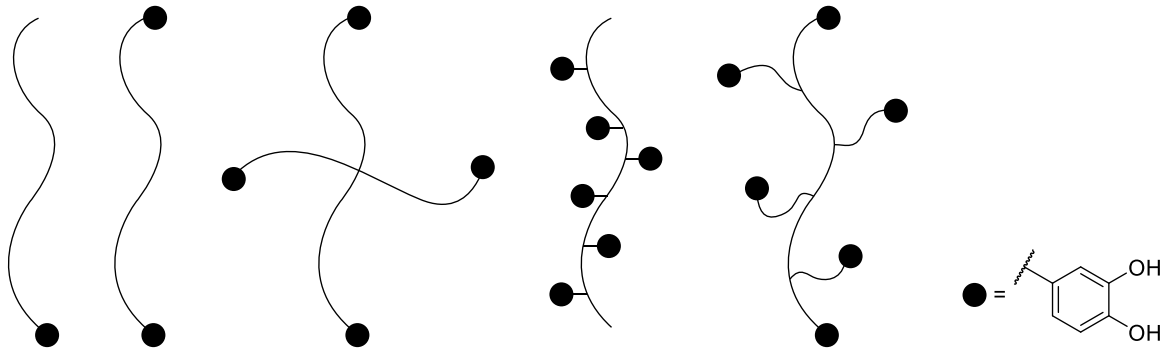

Figure 3: Schematic representation of designs of polymers with catechol residues.

Inspired by the outstanding adhesive capabilities of Mfps, scientists have developed a wide range of biomimetic molecular architectures primarily for medical and materials science applications. Several molecular setups have been designed consisting of a linear or branched polymer backbone carrying from a single catechol side-chain to up to ca. 30 mol% catechol groups (Figure 3).[20] While the first examples of such polymers were relatively simple DOPA polypeptides produced *via* common peptide synthesis,[21] the field expanded rapidly. Thus adhesive proteins have been produced applying DNA recombination for expression by a microbial host[22] or copolymerization of *N*-carboxyanhydride amino acid precursors to obtain DOPA/lysine co-polypeptides on gram-scale.[23] Also, synthetic polymers have been introduced as backbone and photocopolymerization of DOPA *N*-methacrylate and polyethylene glycol (PEG) diacrylate monomers produced adhesive hydrogels.[24] A very versatile approach for the generation of coatings is the deposition of a polydopamine film on a substrate surface in alkaline medium, followed by one of several techniques to further modify the layer including metallization, thiol self-assembly, and grafting of polymers onto the polydopamine film.[25] The

[20] Review: E. Faure, C. Falentin-Daudré, C. Jérôme, J. Lyskawa, D. Fournier, P. Woisel, C. Detrembleur, *Prog. Polym. Sci.* **2013**, *38*, 236–270.

[21] (a) H. Yamamoto, *J. Adhes. Sci. Tecnol.* **1987**, *1*, 177–183; (b) H. Yamamoto, S. Yamauchi, S. Ohara, *Biomimetics* **1992**, *1*, 219–238; (c) H. Yamamoto, K. Ohkawa, *Amino Acids* **1993**, *5*, 71–75.

[22] (a) R. L. Strausberg, D. M. Anderson, D. Filpula, M. Finkelman, R. Link, R. McCandliss, S. A. Orndorff, S. L. Strausberg, T. Wei, *ACS Symp. Ser.* **1989**, *385*, 453–464; (b) D. R. Filpula, S. M. Lee, R. P. Link, S. L. Strausberg, R. L. Strausberg, *Biotechnol. Prog.* **1990**, *6*, 171–177.

[23] (a) M. Yu, T. J. Deming, *Macromolecules* **1998**, *31*, 4739–4745; (b) M. Yu, J. Hwang, T. J. Deming, *J. Am. Chem. Soc.* **1999**, *121*, 5825–5826.

[24] B. P. Lee, K. Huang, F. N. Nunalee, K. R. Shull, P. B. Messersmith, *J. Biomater. Sci. Polym. Ed.* **2004**, *15*, 449–464.

[25] H. Lee, S. M. Dellatore, W. M. Miller, P. B. Messersmith, *Science* **2007**, *318*, 426–430.

formation and structure of the polydopamine film are still under investigation.[26] Mechanistically, the oxidation and cross-linking events are thought to parallel those in the formation of eumelanin (cf. **12**–**15**, Scheme 2). Analogous films can be generated using norepinephrine (**3**) as initial monomer and the resulting OH groups on the surface may be used for further functionalization by surface-initiated ring-opening polymerization.[27]

These catecholic polymers are desirable, especially for applications in the medical and clinical area. The ability to effectively bind to a large variety of surfaces under wet conditions makes these compounds prime candidates as wound sealants and medical adhesives. In solutions of branched and linear DOPA-capped PEG, hydrogel formation can be triggered by the addition of an oxidant (*e.g.* periodate, horseradish peroxidase) and, depending on the nature and concentration of the oxidant, can be achieved in only 30 seconds.[28] Strong tissue adhesion has been reported for different catecholic PEG-based polymers and fine tuning of the polymer structure allows for further adjustment of properties such as the hydrogel degradation rate.[29] Studies in mice focusing on the biocompatibility of such polymers showed that the applied non-degradable wound sealant was in place even one year after implantation with an intact tissue interface and healthy surrounding tissues.[30] A broad variety of further applications has been reported including the generation of antifouling, anticorrosion, and hydrophobic coatings or chemo- and biosensing applications.[16,31]

[26] (a) V. Ball, D. D. Frari, M. Michel, M. J. Buehler, V. Toniazzo, M. K. Singh, J. Gracio, D. Ruch, *Bionanoscience* **2012**, *2*, 16–34; (b) J. Yang, M. A. Cohen Stuart, M. Kamperman, *Chem. Soc. Rev.* **2014**, *43*, 8271–8298.

[27] S. M. Kang, J. Rho, I. S. Choi, P. B. Messersmith, H. Lee, *J. Am. Chem. Soc.* **2009**, *131*, 13224–13225.

[28] B. P. Lee, J. L. Dalsin, P. B. Messersmith, *Biomacromolecules* **2002**, *3*, 1038–1047.

[29] S. A. Burke, M. Ritter-Jones, B. P. Lee, P. B. Messersmith, *Biomed. Mater.* **2007**, *2*, 203–210.

[30] C. E. Brubaker, H. Kissler, L.-J. Wang, D. B. Kaufman, P. B. Messersmith, *Biomaterials* **2010**, *31*, 420–427.

[31] Reviews: (a) M. E. Lynge, R. van der Westen, A. Postma, B. Städler, *Nanoscale* **2011**, *3*, 4916–4928; (b) Q. Ye, F. Zhou, W. Liu, *Chem. Soc. Rev.* **2011**, *40*, 4244–4258; (c) S. Sedó, J. Saiz-Poseu, F. Busqué, D. Ruiz-Molina, *Adv. Mater.* **2013**, *25*, 653–701; (d) S. Moulay, *Polym. Rev.* **2014**, *54*, 436–513.

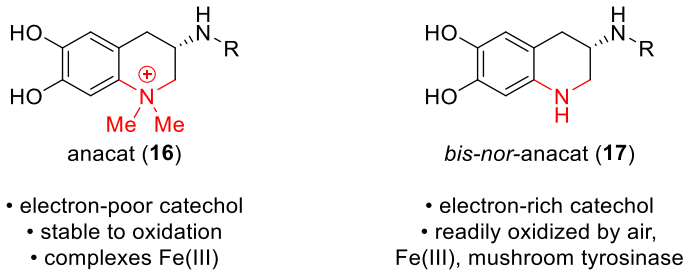

Figure 4: Studies on the anachelin chromophore **16** revealed the influence of an EWG attached to the catechol. R = L-Ser.

Based on the strong iron complexing capabilities of the cyanobacterial siderophore anachelin (**13**), its catecholic chromophore has been developed into a surface anchoring unit (anacat, **16**) for bare metal oxide substrates (Figure 4).[32] Studies on the *bis-nor* derivative **17** lacking the two *N*-methyl groups revealed that the positively charged ammonium group reduces liability towards oxidation of the catechol significantly,[33] rendering the anchor **16** suitable for the generation of self-assembled monolayers (SAMs). This approach avoids the formation of a thick and structurally undefined polymer layer.

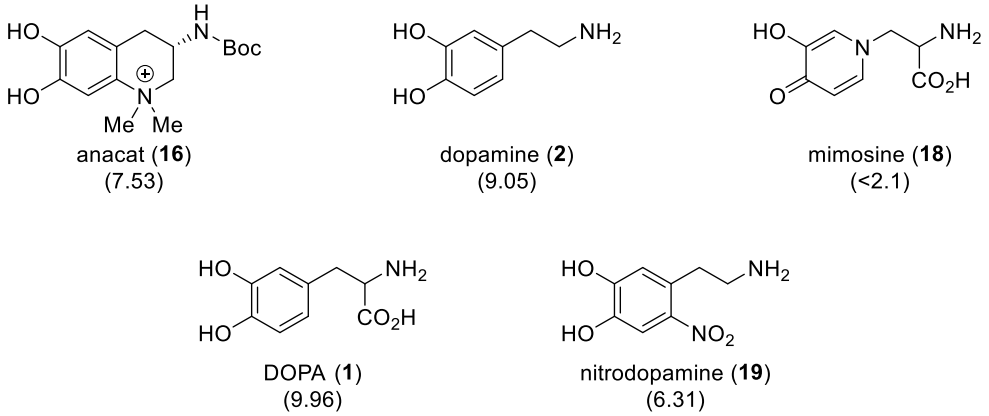

Figure 5: A series of catechols tested for their anchoring ability on metal oxide surfaces. Numbers in brackets represent the first dissociation constant of the catechol hydroxyl groups, pK_{a1}(OH).

[32] (a) S. Zürcher, D. Wäckerlin, Y. Bethuel, B. Malisova, M. Textor, S. Tosatti, K. Gademann, *J. Am. Chem. Soc.* **2006**, *128*, 1064–1065; (b) K. Gademann, J. Kobylinska, J.-Y. Wach, T. M. Woods, *BioMetals* **2009**, *22*, 595–604.

[33] Y. Bethuel, K. Gademann, *J. Org. Chem.* **2005**, *70*, 6258–6264.

A series of derived biomimetic anchoring units with varying electron density of their catechol moieties has been investigated (Figure 5).[34] Besides the protection towards oxidation, the electron-withdrawing groups (EWGs) also lead to acidification of the catechol OH groups and adlayer thickness and stability were found to increase with decreasing pK_a. In particular, nitrodopamine (**19**) proved to be a valuable surface anchor as it can be obtained from commercial dopamine (**2**) by nitration in one synthetic step while possessing excellent surface binding properties. The SAMs can be generated by operationally simple dip-and-rinse procedures using dilute aqueous solutions of catechol in high-salt buffer. Temperature as well as pH can be adjusted to the substrate to achieve optimal surface coverage.[34]

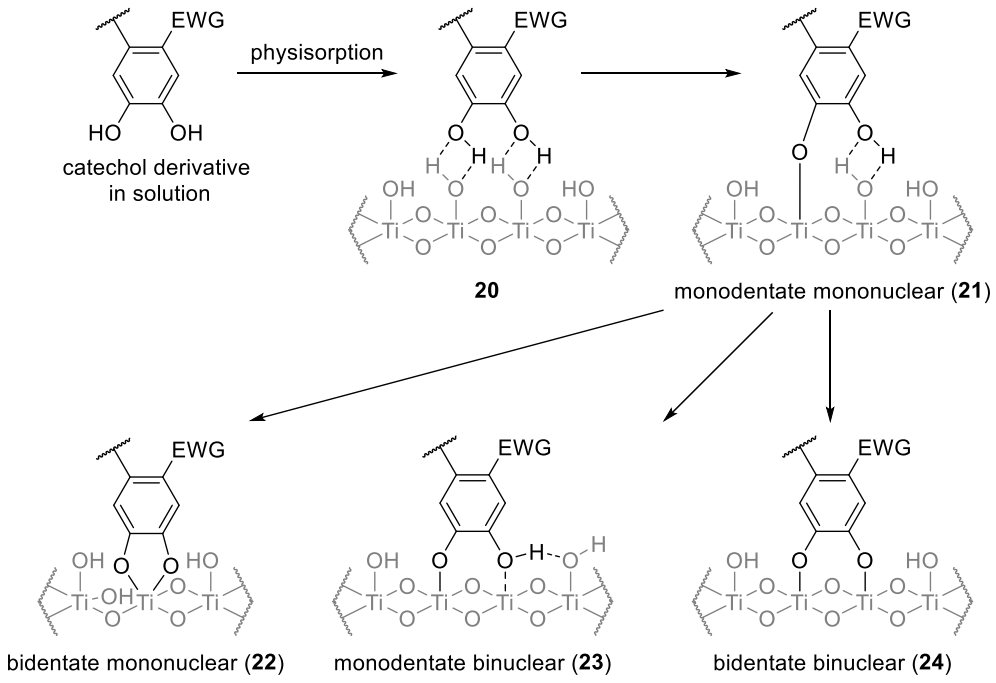

Scheme 3: Different binding modes of catechol derivatives on a titania surface.

Investigations concerning the structure of catecholic SAMs on metal oxides, especially TiO_2, have revealed a number of possible binding modes (Scheme 3).[31b,35] After physisorption, the catechol is bound only by hydrogen bonds (**20**). A hydroxyl group from the metal oxide is then replaced by the catechol forming a monodentate mononuclear complex **21**. This intermediate then forms one of three possible complexes: a bidentate mononuclear chelate complex **22**, a monodentate binuclear complex **23** with an adjacent second surface hydroxyl group displaced by the catechol and bridging hydrogen bonds, or a bidentate binuclear complex **24**.

[34] B. Malisova, S. Tosatti, M. Textor, K. Gademann, S. Zürcher, *Langmuir* **2010**, *26*, 4018–4026.

[35] S. P. Pujari, L. Scheres, A. T. M. Marcelis, H. Zuilhof, *Angew. Chem. Int. Ed.* **2014**, *53*, 6322–6356.

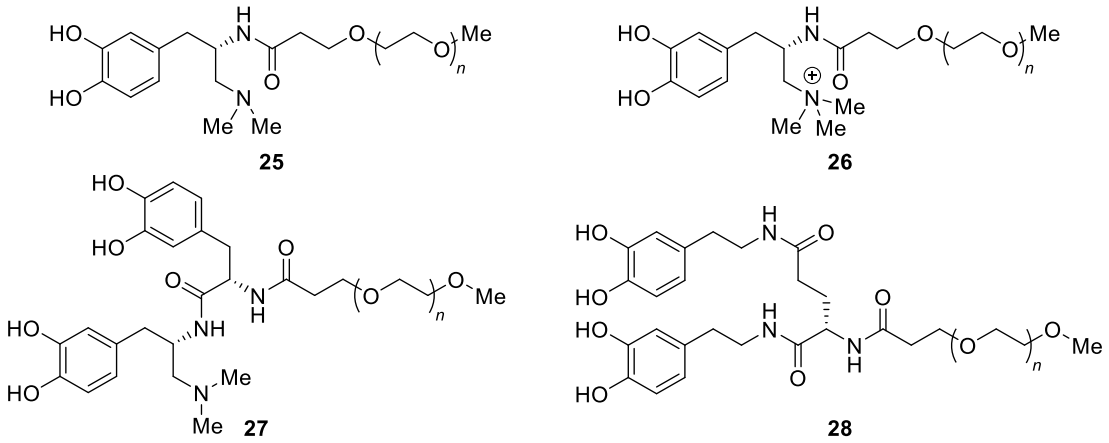

Figure 6: Biomimetic catechol anchoring units attached to mPEG for the generation of protein-resistant surfaces.

Catecholic SAMs have been used for the generation of protein-resistant surfaces using different anchoring units (such as the series shown in Figure 5) attached to the end of methoxy polyethylene glycol (mPEG).[32a,34] A similar study focused on the identification of structurally analogous anchors, which are easier to produce then the anacat (**16**) reference compound (Figure 6).[36] The resulting coatings **25**–**28** significantly reduced protein adsorption compared to bare TiO_2 when exposed to human serum. Furthermore, it was shown that a positively charged ammonium substituent facilitates PEG adlayer formation, but also easily accessible bis-dopamine anchoring units are efficient.

Building on these results, the passively acting antifouling coatings were interfaced with antimicrobial agents to generate active functional surfaces. The clinically used glycopeptide antibiotic vancomycin was merged with an anacat-capped PEG unit to generate the natural product hybrid **29** (Figure 7).[37] In addition to strong metal oxide surface anchoring and prevention of the nonspecific adsorption of proteins and cells, hybrid **29** acts as an active antimicrobial surface coating agent. Due to the high local concentration of the vancomycin unit in proximity to the surface, bacterial growth of *Bacillus subtilis* was inhibited efficiently and the attachment of dead cells to the surface was inhibited by the PEG chains. Activity of the coating was retained even after five cycles of incubation with bacteria followed by washing. Another class of antimicrobial coating agents was designed to interfere with quorum sensing (QS),[38] bacterial communication pathways based on small chemical signaling agents (autoinducers) dependent on the cell density of a population. QS enables a bacterial population

[36] J.-Y. Wach, B. Malisova, S. Bonazzi, S. Tosatti, M. Textor, S. Zürcher, K. Gademann, *Chem. Eur. J.* **2008**, *14*, 10579–10584.

[37] J.-Y. Wach, S. Bonazzi, K. Gademann, *Angew. Chem. Int. Ed.* **2008**, *47*, 7123–7126.

[38] J. Gomes, A. Grunau, A. K. Lawrence, L. Eberl, K. Gademann, *Chem. Commun.* **2013**, *49*, 155–157.

to act as one and regulates various mechanisms such as surface attachment or virulence factor production.[39] Based on *N*-acyl-l-homoserine lactone (AHL) autoinducers, the hybrids **30** and **31** have been developed featuring different catechol anchoring units. Titania beads coated with hybrid **31** induced QS in the GFP-based reporter strain *Pseudomonas putida* F117 proving the viability of this approach. Even though dialysis experiments with the coated beads revealed leakage of the AHL into the surrounding medium, the beads retained their activity upon extensive washing (10 cycles).

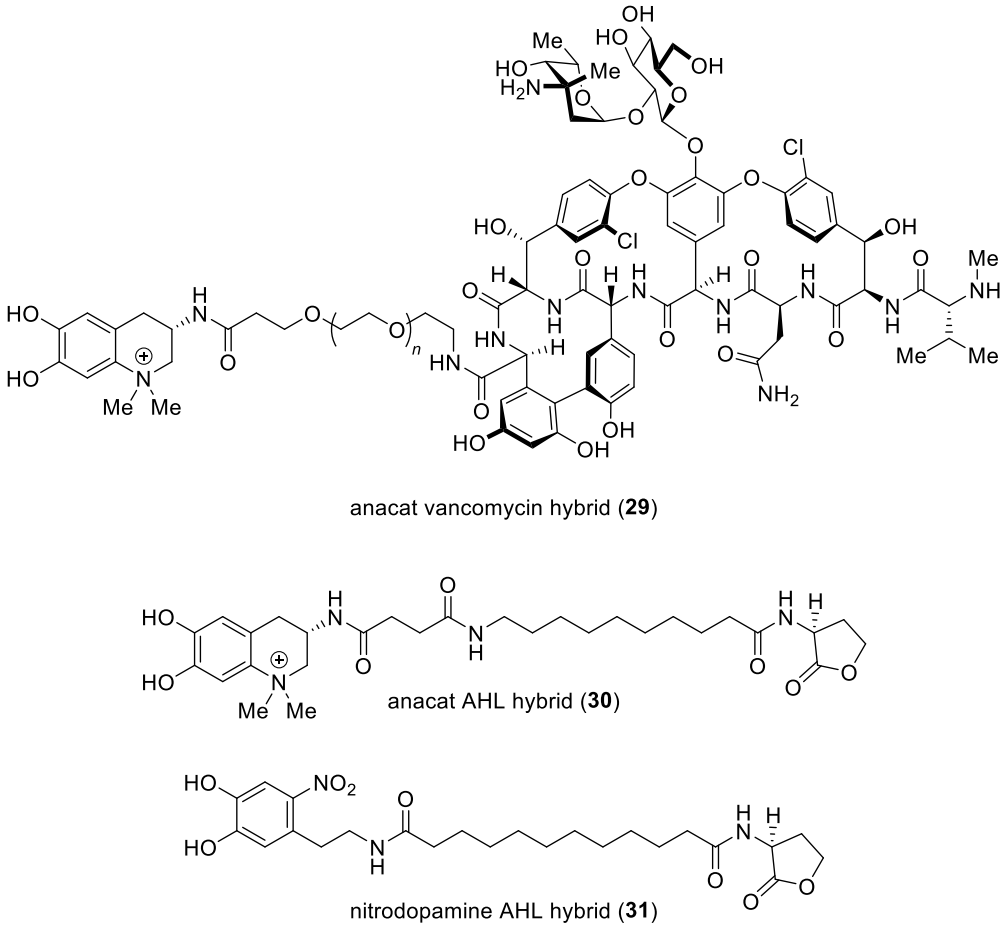

Figure 7: Natural product hybrids as surface coating agents to actively combat bacterial colonization.

[39] Reviews: (a) W.-L. Ng, B. L. Bassler, *Annu. Rev. Genet.* **2009**, *43*, 197–222; (b) S. Dobretsov, M. Teplitski, V. Paul, *Biofouling* **2009**, *25*, 413–427.

1.2 A Tractable Surface Release System[40]

After nitrodopamine (**19**) had proved to be a valuable molecular surface anchor with strong binding and high surface coverage on solid metal oxide supports, we envisioned further development of this unit by adding more functionality. It is quite evident that this anchoring moiety contains a nitro-aryl core, which has been utilized in photoremovable protecting groups (PPGs) for decades. Structurally the simplest representative of these so-called caging groups is the *o*-nitrobenzyl group, the photo-induced cleavage mechanism of which is shown in Scheme 4.[41]

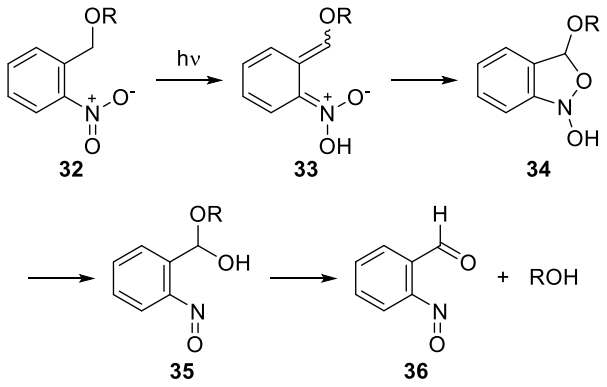

Scheme 4: Photolysis mechanism of the *o*-nitrobenzyl group.

Excitation of the 2-nitroaryl compound **32** generates the *aci*-nitro tautomer **33**. Presumably the neutral nitronic acid cyclizes irreversibly to benzisoxazoline intermediate **34**, which then opens up to give hemiacetal **35**. Fragmentation of the hemiacetal group releases the cargo molecule (ROH) along with 2-nitrosobenzaldehyde (**36**). Additional substituents on the aromatic ring allow for tuning of the excitation wavelength applied during cleavage. Furthermore, introduction of a methyl group in the benzylic position enhanced cleavage efficiency by facilitating the generation of *aci*-nitro tautomer **33**. Among the most prevalent PPGs used today, the *o*-nitrobenzyl group bears almost the entire nitrodopamine (**19**) framework in its structure. While this structural analogy is promising, removal of the methylene bridge to obtain the catechol induces electronic changes and thereby might alter cleavage efficiency of the unit. Besides the chemical changes, the whole physical setup, with the catechols being directly attached to a solid support and the resulting new physical conditions, could form additional obstacles. For instance, it was not clear whether the absorption of light by the aromatic moiety within a SAM on top of a solid surface remains as efficient as in typical solution phase. In

[40] R. Wehlauch, J. Hoecker, K. Gademann, *ChemPlusChem* **2012**, *77*, 1071–1074.

[41] A. P. Pelliccioli, J. Wirz, *Photochem. Photobiol. Sci.* **2002**, *1*, 441–458.

addition, the most common material used as solid support, titanium(IV) oxide, is photo-active itself and is commonly used as a photocatalyst, for example in the detoxification of wastewaters.[42]

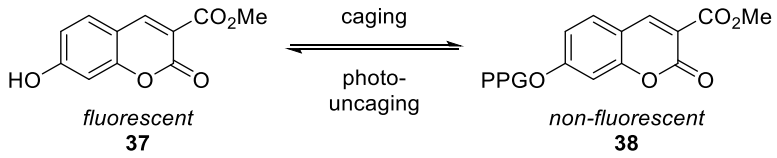

Scheme 5: Coumarin dyes as proof-of-concept cargos.

As a proof of concept, we decided to use coumarin dye **37** as a first cargo (Scheme 5). By attachment of the catechol anchor to the OH group, caged fluorophores were synthesized — non-fluorescent substances which are cleaved upon photoirradiation to yield fluorescent dyes. When we tried to synthesize caged fluorophore **38** the final deprotection of the catechol failed under various conditions and these observations can be explained as shown in Scheme 6.

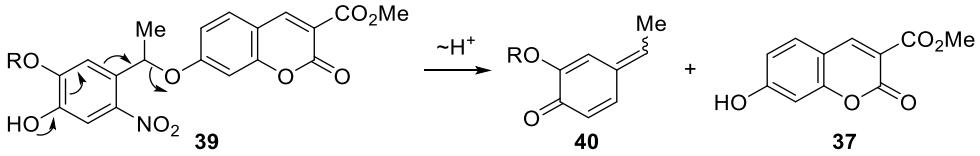

Scheme 6: Proposed decomposition of 1st generation photo-labile catechol anchors during deprotection. R = H, MOM.

The electron-withdrawing effect of the nitro group of caged fluorophore **39** results in low pK_a values of the catechol protons and facilitates the formation of *para*-quinone methide **40** and therefore the release of fluorophore **37**. Thus, we moved to another PPG as blueprint for our surface anchoring unit, the *ortho*-nitrophenethyl group **41**. This homologous structure does not allow for the formation of a quinone methide. The mechanism for cleavage of this PPG is different from the mechanism presented for the *o*-nitrobenzyl group **32** (Scheme 7).[43]

[42] I. K. Konstantinou, T. A. Albanis, *Appl. Catal., B* **2004**, *49*, 1–14.

[43] S. Walbert, W. Pfleiderer, U. E. Steiner, *Helv. Chim. Acta* **2001**, *84*, 1601–1611.

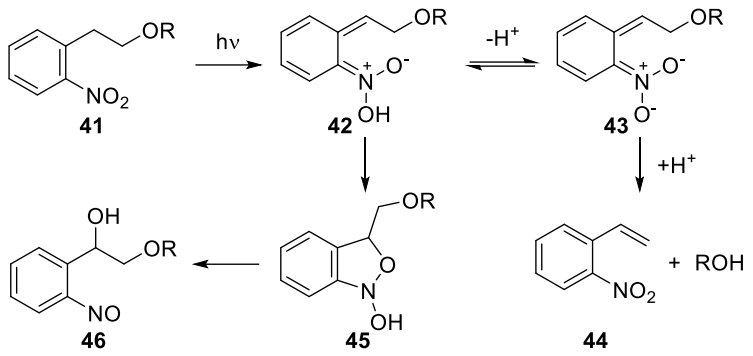

Scheme 7: Photolysis mechanism of the *o*-nitrophenethyl group.

Photoexcitation induces formation of an analogous *aci*-nitro tautomer **42** as shown above. At this point, however, two different mechanistic pathways are possible. The first and productive pathway proceeds *via* deprotonation to the nitronate anion **43** and leads to an elimination reaction and extrusion of the cargo (ROH) giving 2-nitrostyrene (**44**) as a byproduct. The undesired second pathway is unproductive. Analogous to the lower homolog **33** the nitronic acid of **42** attacks at the benzyl position to form benzisoxazoline intermediate **45**, which then opens up again. Alcohol **46** is generated, which cannot fragment to release the cargo, leading to a potential loss of material.

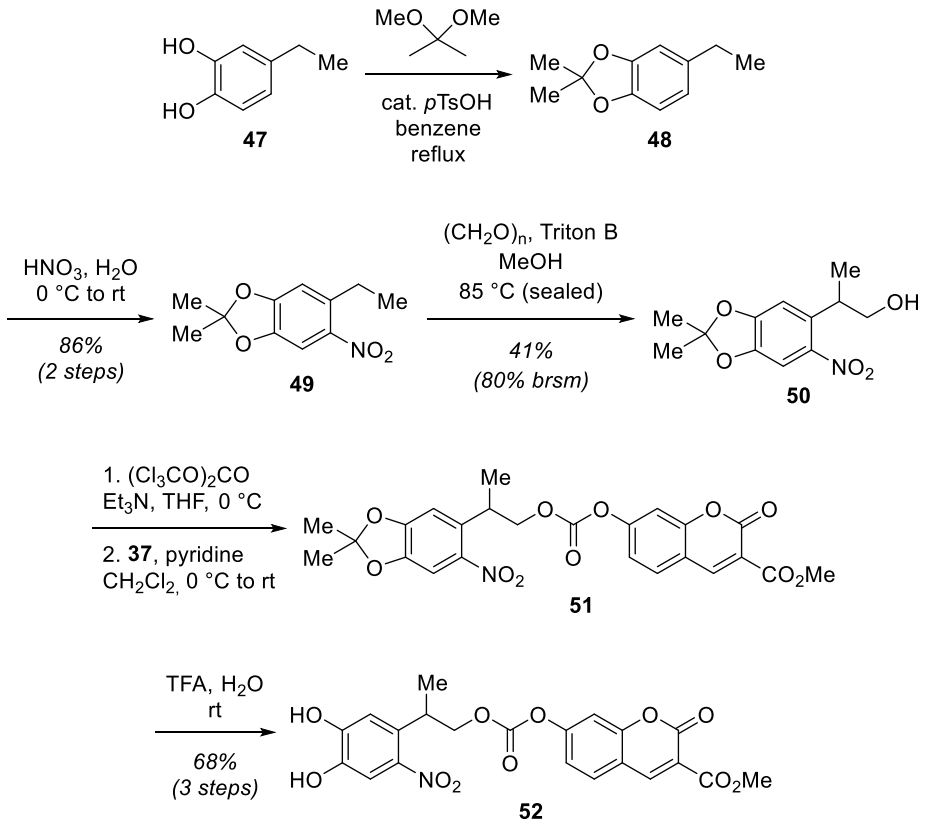

Scheme 8: Synthesis of caged fluorophore **52**.

We designed a synthetic route to caged fluorophore **52** (Scheme 8). Synthesis of the anchor commenced with protection of 4-ethylcatechol (**47**) with an acetonide group under acid catalysis. Acetonide **48** was subjected to nitration with half-concentrated nitric acid giving compound **49** in very good yield. Homologation with paraformaldehyde in methanolic Triton B (benzyltrimethylammonium hydroxide) under heating gave the final anchor precursor **50** in low yield. However, a large portion of the starting material was recovered and could be recycled in this step. Due to ease of synthesis, precursor **50** was coupled with coumarin **37** *via* a carbonate bridge using a protocol we had already developed during the synthesis of a caged retinoic acid analog.[44] Deprotection of the catechol moiety was effected by treatment with aqueous TFA and followed by purification with preparative reversed-phase HPLC giving the caged fluorophore **52** in good overall yield.

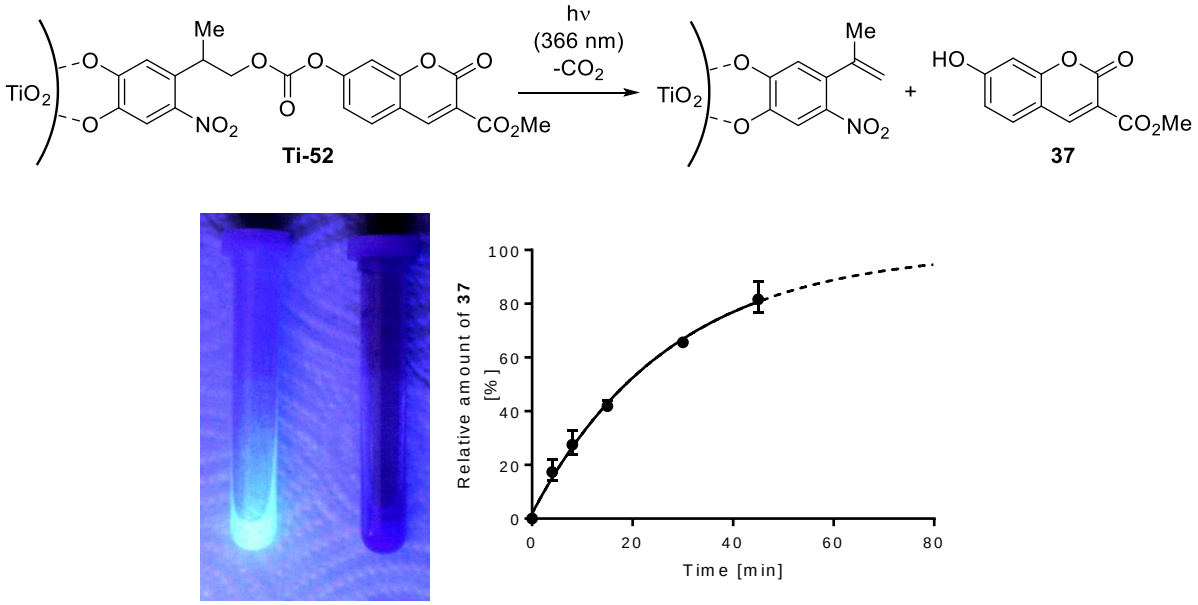

Figure 8: Photocleavage of immobilized caged fluorophore **Ti-52** under UV irradiation.

The compound **52** was then transferred into SAMs on titania microparticles (**Ti-52**) by a dip-and-rinse procedure. After washing, the particles were re-suspended in MOPS buffer medium and irradiated at 366 nm under a common laboratory UV lamp. Release of the free coumarin dye **37** was observed in terms of developing fluorescence as well as detection by reversed-phase HPLC-MS (Figure 8).

[44] J. Hoecker, R. Liffert, P. Burch, R. Wehlauch, K. Gademann, *Org. Biomol. Chem.* **2013**, *11*, 3314–3321.

1.3 Results and Discussion

1.3.1 Improved Synthesis of the Photo-Labile Anchoring Unit

After a successful proof-of-concept study, our first aim was the optimization of our synthesis of the protected anchoring unit **50**. While our original route was efficient enough to obtain the required amount of material, the synthesis had two major drawbacks. The starting material, 4-ethylcatechol (**47**), is expensive (ca. 100 CHF/g) when obtained from commercial suppliers and the low yield of the homologation at the end of the sequence required several cycles as the isolated amount of product **50** barely exceeded the amount of reisolated starting material **49** (41%/39%).

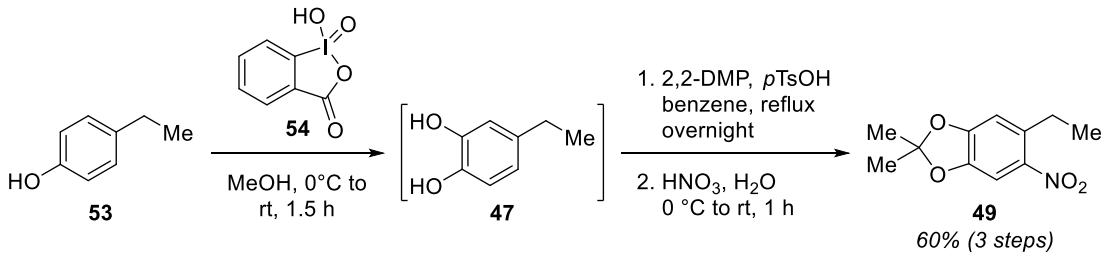

Scheme 9: Access to catechol derivatives by oxidation of 4-ethylphenol (**53**).

The direct oxidation of phenols to *ortho*-quinones using 2-iodoxybenzoic acid (IBX, **54**) as the oxidant has been reported by Pettus and coworkers in 2002[45] and a simplified procedure including *in situ* reduction to the free catechol by addition of sodium dithionite has been reported by Bernini and coworkers in 2011.[46] IBX (**54**) itself is readily available from 2-iodobenzoic acid (IBA, ca. 0.9 CHF/g) by oxidation with Oxone (2 $KHSO_5 \cdot KHSO_4 \cdot K_2SO_4$, <0.1 CHF/g).[47] When a methanolic solution of 4-ethylphenol (**53**, ca. 0.1 CHF/g) was treated with IBX (**54**) in methanol, full conversion of the starting material **53** was observed within 1.5 h (Scheme 9). Reduction of the quinone intermediate by sodium dithionite (<0.1 CHF/g) was completed within 10 min after addition and crude catechol **47** was isolated as a brown oil. Although the texture of the material obtained was contrasting from the commercial substance (grey solid), ^{1}H NMR analysis indicated high purity and any attempts of further purification either failed (crystallization, sublimation) or were inefficient (activated carbon, flash chromatography, size exclusion chromatography). The crude catechol **47** was subjected to our previously applied acetonide protection conditions and again the resulting crude product **48** was

[45] D. Magdziak, A. A. Rodriguez, R. W. Van De Water, T. R. R. Pettus, *Org. Lett.* **2002**, *4*, 285–288.

[46] R. Bernini, F. Crisante, N. Merendino, R. Molinari, M. C. Soldatelli, F. Velotti, *Eur. J. Med. Chem.* **2011**, *46*, 439–446.

[47] M. Frigerio, M. Santagostino, S. Sputore, *J. Org. Chem.* **1999**, *64*, 4537–4538.

of high purity. While purification by flash chromatography was possible without significant loss of substance, the material could simply be carried on to nitration in half-conc. nitric acid. After workup, nitroaryl compound **49** was obtained as a pure yellow solid making an additional purification step unnecessary. With this improved sequence we could drastically reduce the cost of our synthesis. However, in terms of atom economy the oxidation with IBX (**54**) was not satisfying. Even though only a small excess of reagent (1.1 eq.) was used, the oxidant **54** (280 g/mol) outweighs the substrate **53** (122 g/mol) more than twice. Therefore, IBA was recovered from the reaction mixture by acid/base extraction in a model experiment, where out of the 34 mmol of employed IBX (**54**) 63% of pure IBA were recovered.

Table 1: Optimization of the final homologation towards anchor precursor **50**.

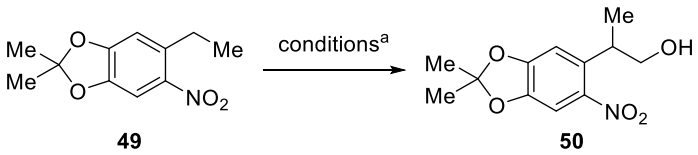

49 **50**

Entry	**$(CH_2O)_n$** [eq.]	**Base** [eq.]	**Solvent**	**Time** [h]	**Conversion** (^{1}H NMR)
1	20	Triton B, 4.5	MeOH	65	45%
2	10	Triton B, 1.05	MeOH	20	15%
3	20	KO^{t}Bu, 4.5	MeOH	22	22%
4	20	KO^{t}Bu, 5.0	^{t}BuOH (110 °C)	21	16%
5	2.0	Triton B, 0.50	DMSO/MeOH, 10:1	4.5	96%
6	2.0	Triton B, 0.25	DMSO/MeOH, 10:1	1.5	70%

[a] Reactions were performed in a sealed tube at 85 °C.

Addressing the second drawback of our original synthesis a series of experiments was conducted to optimize the reaction conditions of the final homologation step and selected results are shown in Table 1. During our earlier studies (entry 1) we could already observe that the reaction stopped at a maximum conversion of 45% and could not be forced to completion by addition of more reagents and continued heating. Beside the low yield of this transformation the very long reaction time makes recycling of recovered starting material **49** a lengthy procedure. Reducing the amount of both base and paraformaldehyde also resulted only in reduced conversion of the substrate **49** after 20 h (entry 2). When Triton B was replaced by the stronger base potassium *tert*-butanolate, again only low conversion was detected after 22 h (entry 3). In order to be able to reach higher temperatures in our sealed tube system, the solvent was switched to *tert*-butanol and the oil bath temperature was increased to 110 °C (entry 4). Despite some solubility issues conversion remained almost unaffected. As this reaction is

catalytic in base but even large excess of reagent did not lead to high conversion, we decided to boost basicity by the use of aprotic but highly polar DMSO as the solvent. Since we used Triton B as a methanolic solution, methanol could not be eliminated completely from the reaction mixture. With tremendously reduced amounts of paraformaldehyde (2.0 eq.) and a substoichiometric amount of Triton B (0.5 eq.), conversion of 96% of starting material **49** was observed by ^{1}H NMR analysis after 4.5 h reaction time (entry 5). After workup and purification by flash chromatography, an isolated yield of 85% was obtained. With further reduced amounts of base (0.25 eq.) 70% conversion were reached after only 1.5 h, however, the reaction stopped at this point and prolonged heating did not lead to completion (entry 6). With these optimized conditions in hand, synthesis of the protected anchor precursor **50** could be achieved in four synthetic steps from 4-ethylphenol (**53**) in 51% overall yield (Scheme 10).

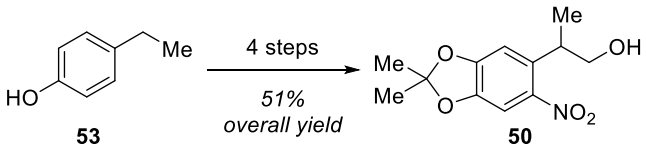

53 **50**

Scheme 10: Summary of the improved synthesis of protected anchor precursor **50**.

1.3.2 Functional Group Evaluation

In order to investigate the photo release properties of the nitrocatechol system in more detail, a series of model analogs was synthesized carrying different functional groups linking the anchoring unit with the cargo. The compounds were then photolyzed and a comparison of the cleavage efficiency of the various leaving groups was drawn.

1.3.2.1 Synthesis of Functional Group Analogs

The most relevant functional groups for caging of small organic molecules are hydroxyl, amino and carboxylic acid groups. The utilization of carbonates and carbamates for the mild coupling of hydroxyl and amino groups, respectively, has already been demonstrated above and these functional groups were also included in this study. In the field of chemical biology, phosphates are another important class of functional groups. However, the properties of phosphates and thus their chemical behavior differ strongly from the former functional groups and the synthesis of phosphate cages is not as general. Although photolysis of the cages can only be induced by UV irradiation, the proportion of which is relatively small in artificial room lighting, all reactions have been performed in the dark and exposure to light was minimized during workup and purification.

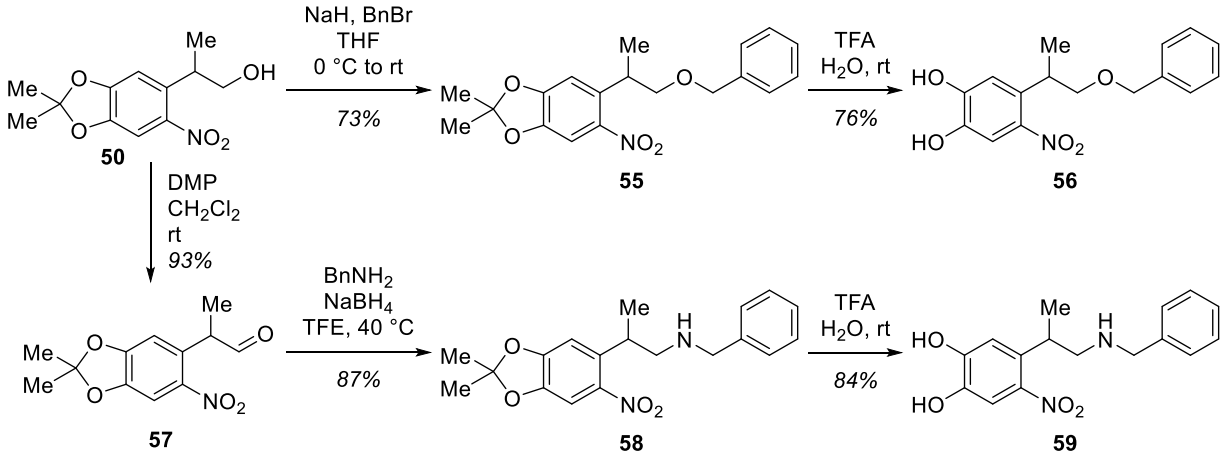

Scheme 11: Syntheses of ether and amine analogs.

Starting from protected anchor precursor **50**, ether analog **56** was synthesized *via* the Williamson ether synthesis using sodium hydride as the base and benzyl bromide as the electrophile giving the protected ether **55** in good yield (Scheme 11). In a general procedure, cleavage of the acetonide protecting group was achieved by treatment with aqueous TFA and the free catechol **56** was obtained in good yield after purification by preparative reversed-phase HPLC. Synthesis of amine analog **59** was achieved by reductive amination. Anchor precursor **50** was oxidized to the corresponding aldehyde **57** in excellent yield using Dess-Martin

periodinane as the oxidant. Following a protocol developed by Tajbakhsh and coworkers,[48] the aldehyde **57** was condensed with benzylamine in trifluoroethanol, which could be observed by the fast development of an intense red color of the reaction mixture. Reduction by sodium borohydride led to amine **58**. Final deprotection following our general procedure gave catechol **59** in very good yield.

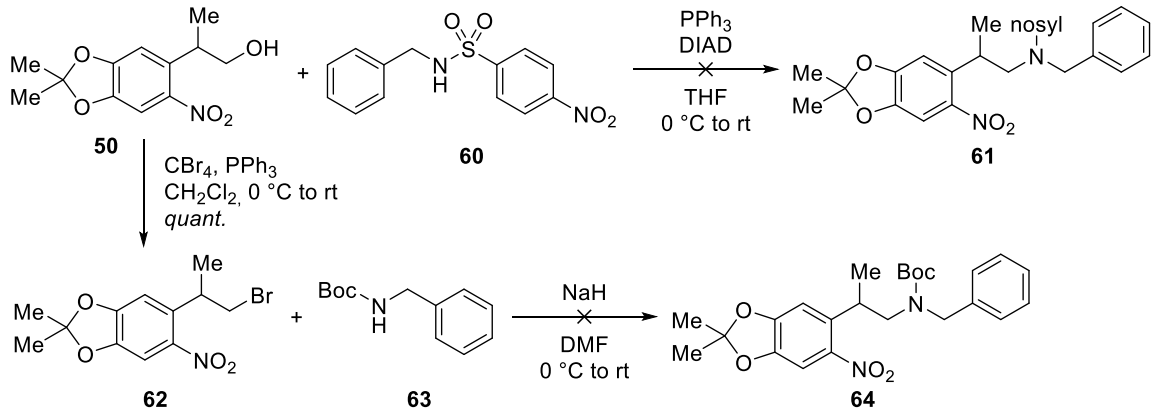

Scheme 12: Failed attempts towards acetonide **58**.

Several previous attempts to obtain acetonide **58** had failed (Scheme 12). Our first approach was based on the nosyl strategy developed by Fukuyama and coworkers[49] and benzylnosylamide **60** was obtained *via* known procedures.[50] Subsequent coupling of amide **60** with anchor precursor **50** under Mitsunobu reaction conditions was not successful in our hands. In a second approach, alcohol **50** was first converted to the corresponding bromide **62** in an Appel reaction. When known Boc-protected benzylamine **63**[51] in DMF was treated with sodium hydride followed by addition of bromide **62** the desired amine **64** could not be obtained. Instead, the bromide **62** underwent an elimination reaction to the corresponding nitrostyrene.

[48] M. Tajbakhsh, R. Hosseinzadeh, H. Alinezhad, S. Ghahari, A. Heydari, S. Khaksar, *Synthesis* **2011**, 490–496.

[49] T. Kann, T. Fukuyama, *Chem. Commun.* **2004**, 353–359.

[50] B. Nyasse, L. Grehn, U. Ragnarsson, H. L. S. Maia, L. S. Monteiro, I. Leito, I. Koppel, J. Koppel, *J. Chem. Soc., Perkin Trans. 1* **1995**, 2025–2031.

[51] S. V. Chankeshwara, A. K. Chakraborti, *Synthesis* **2006**, 2784–2788.

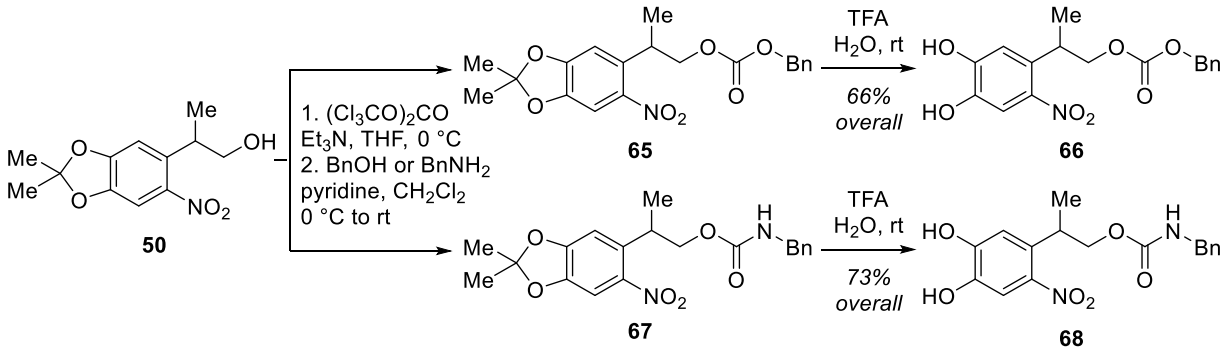

Scheme 13: Syntheses of carbonate (**66**) and carbamate (**68**) analogs.

The carbonate and carbamate model compounds **66** and **68**, respectively, were synthesized following our previously developed procedure (Scheme 13). Acetonide **50** was transformed into its chloroformate ester using triphosgene in THF in the presence of triethylamine. The mixture was evaporated under high vacuum and redissolved in dichloromethane. A solution of either benzyl alcohol or benzylamine in pyridine was added giving carbonate **65** or carbamate **67**, respectively. The crude acetonides **65** and **67** were subjected to the general deprotection method and catechols **66** and **68** were obtained in good overall yields.

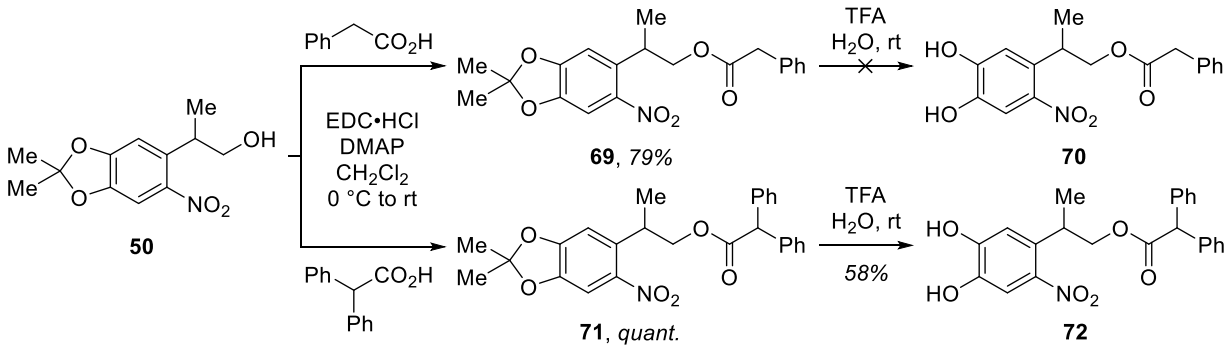

Scheme 14: Syntheses of ester analogs **70** and **72**.

Ester intermediate **69** was synthesized in good yield by coupling of phenylacetic acid with acetonide **50** using EDC·HCl and DMAP as coupling reagents (Scheme 14). When ester **69** was treated with aqueous TFA, the ester function was hydrolyzed before the acetonide protecting group and catechol **70** could not be obtained. Also, the use of weaker acids such as acetic acid or dichloroacetic acid did not lead to the desired deprotection. We therefore changed the acid coupling partner in the first step to diphenylacetic acid and intermediate **71** was produced in excellent yield. Due to the increased steric bulk in the α-position of the ester function, deprotection of ester **71** was successful using the general method resulting in an only slightly reduced yield of catechol **72** when compared to the other substrates.

1.3.2.2 Photo-Cleavage

The cleavage efficiency of the different catechols **56**, **59**, **66** and **68** was studied in a kinetic analysis by monitoring of the photo-induced decay of the substances. Aqueous solutions of the substrates were irradiated at 366 nm under a common laboratory UV lamp and analyzed by reversed-phase UPLC-MS after certain time intervals (Figure 9). The relative amount of substrate within each series was determined by integration of its respective peak in the UV traces obtained. The released cargos (BnOH, $BnNH_2$) could not be identified in the UV traces probably due to their low extinction coefficients compared to the light harvesting catechols.

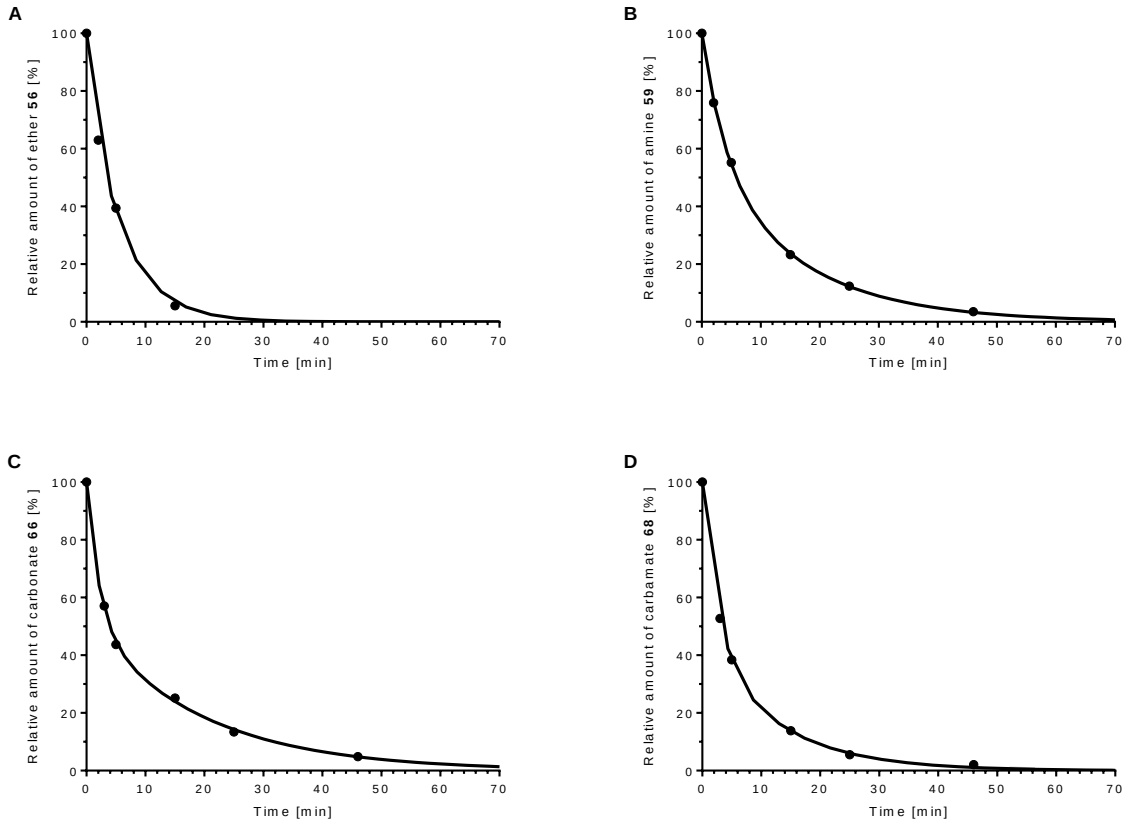

Figure 9: Decay of catechols **56** (A), **59** (B), **66** (C) and **68** (D) in solution quantified by reversed-phase UPLC-MS.

Comparing the different kinetic profiles, it became obvious that cleavage of ether **56** was most efficient with only 39% of substrate remaining after five minutes of irradiation (Figure 9A). After 25 minutes of irradiation no substrate **56** was detected anymore. Decay of amine **59** (Figure 9B) was significantly slower with more than 12% of the substance **59** intact after 25 minutes of irradiation. This observation was expected as it is in accord with the fact that amides represent worse leaving groups than alcoholates. However, cleavage of carbonate **66** (Figure 9C) and carbamate **68** (Figure 9D) was surprisingly slow. Since both functions should

be good leaving groups comparable to carboxylates, the reaction seemed to be harmed by additional factors. While photolysis of carbamate **68** was more efficient than photolysis of amine **59** and thus showed a reasonable profile, the line shape of the decrease of carbonate **66** seemed remarkable. The reaction proceeded fast in the beginning and, with 44% substrate left after five minutes, was comparable to that of ether **56**. Then, the reaction slowed down and after 25 minutes still more than 13% of the substrate remained. Since these experiments were conducted in buffered aqueous medium at low concentrations, the observed effects cannot be addressed to a change in pH. A possibility that seems unlikely but cannot be excluded is the formation of an undesired byproduct with a high extinction coefficient. Accumulation of this substance would then lead to increased light absorption and progressive inhibition of the photolysis reaction. The photocleavage of ester **72** could not be included in the present series as the substance proved to be insoluble in water. When a dilute solution of ester **72** in MeCN was added to aqueous MOPS buffer solution, the compound precipitated. The substance could be photolyzed in a mixture of MeCN/water (1:2), but the reaction proceeded significantly slower in less protic medium. This observation was expected and can be explained mechanistically (cf. Scheme 7). The *aci*-nitro tautomer, which is formed after photoexcitation of the nitrocatechol, needs to be deprotonated in order to eliminate the cargo, which is then neutralized by protonation. These proton transfer steps occur much more efficiently in aqueous medium and the reaction can be entirely shut down in an aprotic environment.

To evaluate the photorelease of cargo from solid support catechols **56**, **59**, **66** and **68** were immobilized as SAMs on titania nanoparticles using a previously developed dip-and-rinse procedure.[40] While the particles showed a slightly yellow coloration after the immobilization procedure, the respective cargos (BnOH or $BnNH_2$) could not be detected after the photolysis experiments. Different factors were considered to overcome this problem. The cargos chosen for this study were very small, which can complicate detection by UPLC-MS, and relatively apolar, which could lead to the precipitation of released molecules on the titania nanoparticles. To test these factors 3,4,5-trimethoxybenzylamine (**73**) was chosen as a cargo and catechol **74** was prepared analogously to amine **59** (Scheme 15). Unfortunately, after immobilization of catechol **74** and release of the cargo by photolysis, the latter could not be detected in the medium by means of reversed-phase UPLC-MS.

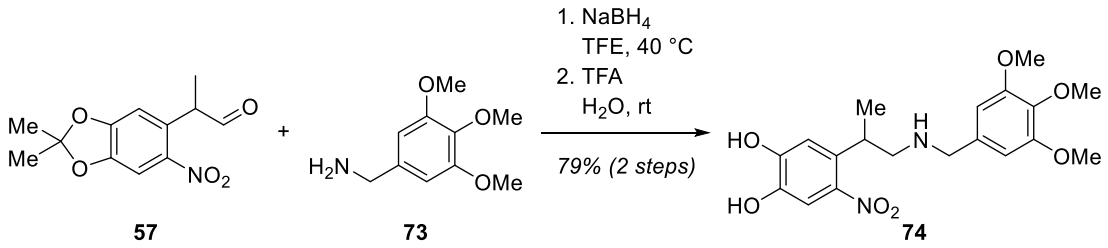

57 **73** **74**

Scheme 15: Synthesis of catechol **74** carrying a heavier and more polar cargo.

1.4 Conclusion

In summary, we have developed a cost-efficient and straightforward synthesis of our protected surface anchoring moiety yielding the target **50** in four synthetic steps from cheap 4-ethylphenol (**53**) in 51% overall yield. Furthermore, we synthesized a series of model compounds (**56**, **59**, **66** and **68**) to evaluate photocleavage efficiency with different leaving groups establishing experimental procedures that allow for the coupling of various cargo molecules. The fastest photolysis reactions were observed using ether and carbamate functions to connect the surface anchor and the cargo. While these groups allow for attachment of a broad range of amines and alcohols, the application of esters is limited. A hypothetic cargo needs sufficient steric encumbrance at the α-carbon atom to prevent hydrolysis of the ester during deprotection of the catechol anchor. Further studies need to be carried out focusing on the application of the system on solid surfaces giving detailed insights in release kinetics from solid support. Also, a determination of the actual surface coverage, that can be reached using such nitrocatechol anchors, would yield crucial information to estimate the dosage of a released substance.

2 Catecholic Binders for Dynamic Functional Systems

2.1 Dynamic Covalent Bonds in Functional Systems

The ability to selectively target one particular bond in a given substrate molecule is of vital importance for synthetic organic chemistry. The challenge of finding appropriate conditions resulting in a chemo- and site-selective reaction becomes increasingly difficult with higher structural complexity of the substrate. Especially when assembling large macro- and supramolecular architectures, classic organic transformations fail to target only one specific bond within the plethora of bonds present leading to undesired side reactions. For the preparation of such architectures, non-covalent interactions like hydrogen bonding and hydrophobic interactions are valuable tools and the exploration of less prominent molecular interactions such as halogen bonding is of current interest.[52]

Table 2: Examples of non-covalent, dynamic covalent and covalent bonds encountered in functional systems.

Non-covalent	Dynamic covalent	Covalent
Hydrogen bond	Disulfide	C-C
Hydrophobic	Hydrazone	C-H
Ionic bond	Boronate ester	C-O
π-Stacking	Imine	C-N
Cation-π	Thioester	O-S
Halogen bond	Hemiacetal/acetal	O-P
Anion-π		O-B

The so-called dynamic covalent bonds combine the properties of covalent and non-covalent interactions in a unique manner.[53] Depending on the conditions, these bonds can either be as rigid and stable as covalent bonds or as dynamic and rapidly interchanging as non-covalent bonds. A disulfide bond for example is stable under acidic conditions, but exchanges and equilibrates rapidly under basic conditions in the presence of thiolates. This definition is kind of loose in a sense that many covalent bonds become labile under specific conditions. However, for a bond to be classified as "dynamic covalent" these conditions need to be mild enough to tolerate other functional groups within the molecular scaffold. This dual nature of dynamic covalent bonds makes them very attractive for the generation of molecular structures with

[52] (a) P. Politzer, J. S. Murray, *ChemPhysChem* **2013**, *14*, 278–294; (b) T. M. Beale, M. G. Chudzinski, M. G. Sarwar, M. S. Taylor, *Chem. Soc. Rev.* **2013**, *42*, 1667–1680.

[53] (a) J.-M. Lehn, *Top. Curr. Chem.* **2012**, *322*, 1–32; (b) S. Otto, *Acc. Chem. Res.* **2012**, *45*, 2200–2210; (c) F. B. L. Cougnon, J. K. M. Sanders, *Acc. Chem. Res.* **2012**, *45*, 2211–2221.

specific functions,[54] well demonstrated by the example of dynamic covalent libraries.[55] In a combinatorial fashion a set of building blocks is linked by reversible chemical transformations and the distribution of products typically depends on the free-energy landscape presented to the system (thermodynamic control).[56] Changing the experimental conditions alters this free-energy landscape and thus product distribution can be influenced, for example by the addition of an external template which cannot participate in the reversible covalent binding events. Non-covalent interactions between library members and the template will energetically favor these binders and promote their production. After equilibration of the system, library members can be isolated under conditions that do not allow for further exchange of the dynamic covalent bonds. If library members are able to intermolecularly bind to copies of themselves, the equilibrium shifts towards these self-assembling members. This mechanism represents an example of self-replication which plays a central role in origin-of-life theories.[55,57]

Systems chemistry focuses on the interfacing of functional components to yield a chemical system with emergent properties, which were not present in the individual components and which were not necessarily deducible from the characteristics of individual components. The combination of several non-covalent interactions is very common in biological and chemical systems, for example hydrogen bonding, hydrophobic and π-π interactions in double-stranded DNA or in protein secondary and tertiary structures. Also, the combined use of dynamic covalent organic bonds with non-covalent interactions such as metal coordination chemistry has been established[58] and most recently the development of a chemical system able to store, recall and erase information has been reported.[59] However, the use of several dynamic covalent organic bonds within a system remains rare.[60] An illustrative example of such a system are small molecular walkers (Scheme 16).[61] The function of this system is to move a molecular

[54] (a) S. J. Rowan, S. J. Cantrill, G. R. L. Cousins, J. K. M. Sanders, J. F. Stoddart, *Angew. Chem. Int. Ed.* **2002**, *41*, 898–952; (b) J. N. H. Reek, S. Otto (eds.), *Dynamic Combinatorial Chemistry*, WILEY-VCH, Weinheim, **2010**; (c) Y. Jin, C. Yu, R. J. Denman, W. Zhang, *Chem. Soc. Rev.* **2013**, *42*, 6634–6654.

[55] (a) R. A. R. Hunt, S. Otto, *Chem. Commun.* **2011**, *47*, 847–858; (b) J. Li, P. Nowak, S. Otto, *J. Am. Chem. Soc.* **2013**, *135*, 9222–9239.

[56] (a) Q. Ji, R. C. Lirag, O. Š. Miljanić, *Chem. Soc. Rev.* **2014**, *43*, 1873–1884; (b) E. Mattia, S. Otto, *Nat. Nanotechnol.* **2015**, *10*, 111–119.

[57] (a) V. del Amo, D. Philp, *Chem. Eur. J.* **2010**, *16*, 13304–13318; (b) E. Moulin, N. Giuseppone, *Top. Curr. Chem.* **2012**, *322*, 87–106.

[58] M. L. Saha, S. De, S. Pramanik, M. Schmittel, *Chem. Soc. Rev.* **2013**, *42*, 6860–6909.

[59] J. Holub, G. Vantomme, J.-M. Lehn, *J. Am. Chem. Soc.* **2016**, *138*, 11783–11791.

[60] A. Wilson, G. Gasparini, S. Matile, *Chem. Soc. Rev.* **2014**, *43*, 1948–1962.

[61] M. J. Barrell, A. G. Campaña, M. von Delius, E. M. Geertsema, D. A. Leigh, *Angew. Chem. Int. Ed.* **2011**, *50*, 285–290.

fragment, the walker (shown in red), along a molecular track in a predefined direction. To achieve this directional movement a sequential combination of basic disulfide exchange, light-induced *cis–trans*-isomerization and acidic hydrazone exchange is necessary. While reversing the order of events changes the direction of movement, the sequence must remain the same to enable directionality. The key to achieving this directional movement lies in the orthogonality of the dynamic covalent bonds utilized in the system.[60,62]

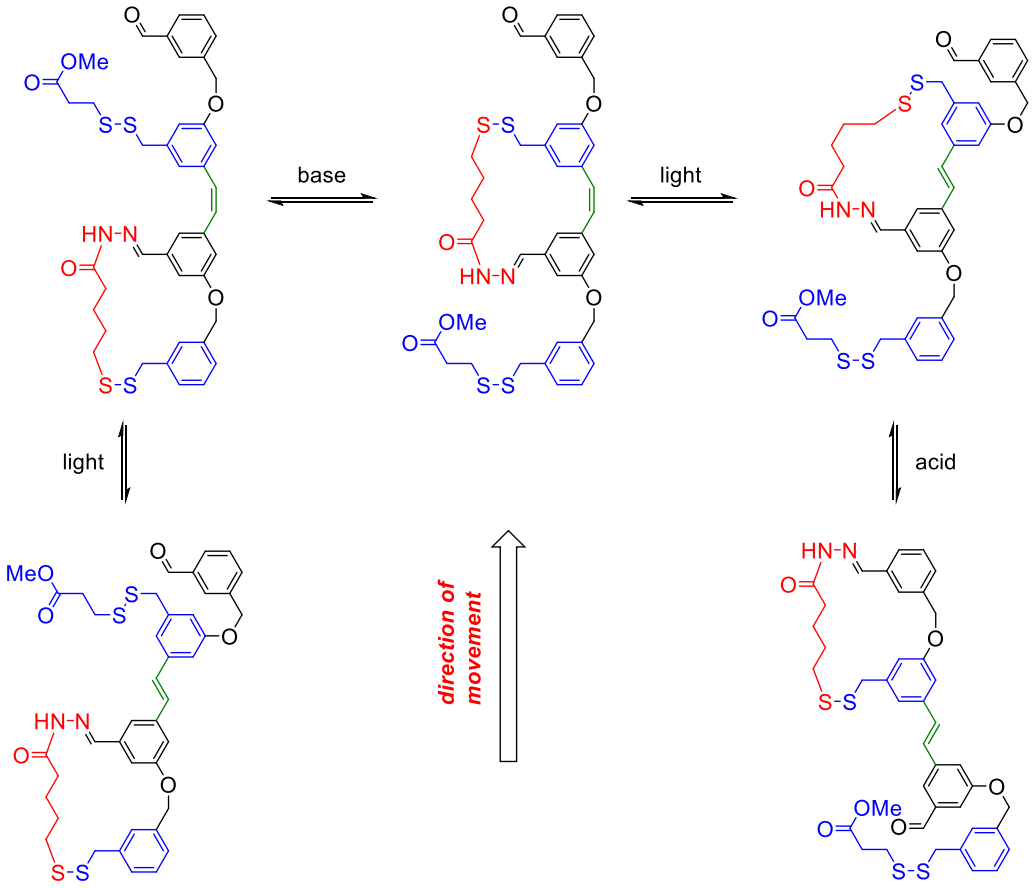

Scheme 16: A molecular walker (red) moving along a molecular track in a defined direction.

[62] M. von Delius, E. M. Geertsema, D. A. Leigh, A. M. Z. Slawin, *Org. Biomol. Chem.* **2010**, *8*, 4617–4624.

An example demonstrating the power of this methodology of orthogonal dynamic covalent bonds is the formation of double-channel photosystems,[63] functional multicomponent surface architectures for the generation of photocurrent (Figure 10). To build such architectures, an initiator precursor equipped with diphosphonate anchors was deposited onto an indium-doped tin oxide (ITO) surface (**75**). Naphthalenediimide (NDI) π-stacks were then grown on the surface using self-organizing surface-initiated polymerization (SOSIP, **76**).[64] Two thiolate groups generated by reduction of the precursor initiate a ring-opening disulfide-exchange polymerization process, which is propagated by two asparagusic acid esters flanking the NDI building blocks. Treatment with excess hydroxylamine cleaved the benzaldehyde caps leaving free hydrazide groups (**77**), which were subsequently coupled with porphyrin and phthalocyanine derivatives (**78**). This overall process is called templated stack exchange (TSE).[65] The parallel π-stacks of this architecture were demonstrated to transport electrons and holes in an antiparallel fashion. While NDI stacks transport electrons towards the surface, the porphyrin/phthalocyanine stacks move holes away from the surface. An improved system was prepared by replacing NDI and porphyrin/phthalocyanine stacks with oligothiophene and Bingel fullerene stacks, respectively.[66] By introduction of a redox gradient along the π-stacks *via* variation of the electron density of the aryl moieties charge recombination was minimized.

[63] G. Sforazzini, R. Turdean, N. Sakai, S. Matile, *Chem. Sci.* **2013**, *4*, 1847–1851.

[64] (a) N. Sakai, M. Lista, O. Kel, S. Sakurai, D. Emery, J. Mareda, E. Vauthey, S. Matile, *J. Am. Chem. Soc.* **2011**, *133*, 15224–15227; (b) M. Lista, J. Areephong, N. Sakai, S. Matile, *J. Am. Chem. Soc.* **2011**, *133*, 15228–15231.

[65] N. Sakai, S. Matile, *J. Am. Chem. Soc.* **2011**, *133*, 18542–18545.

[66] H. Hayashi, A. Sobczuk, A. Bolag, N. Sakai, S. Matile, *Chem. Sci.* **2014**, *5*, 4610–4614.

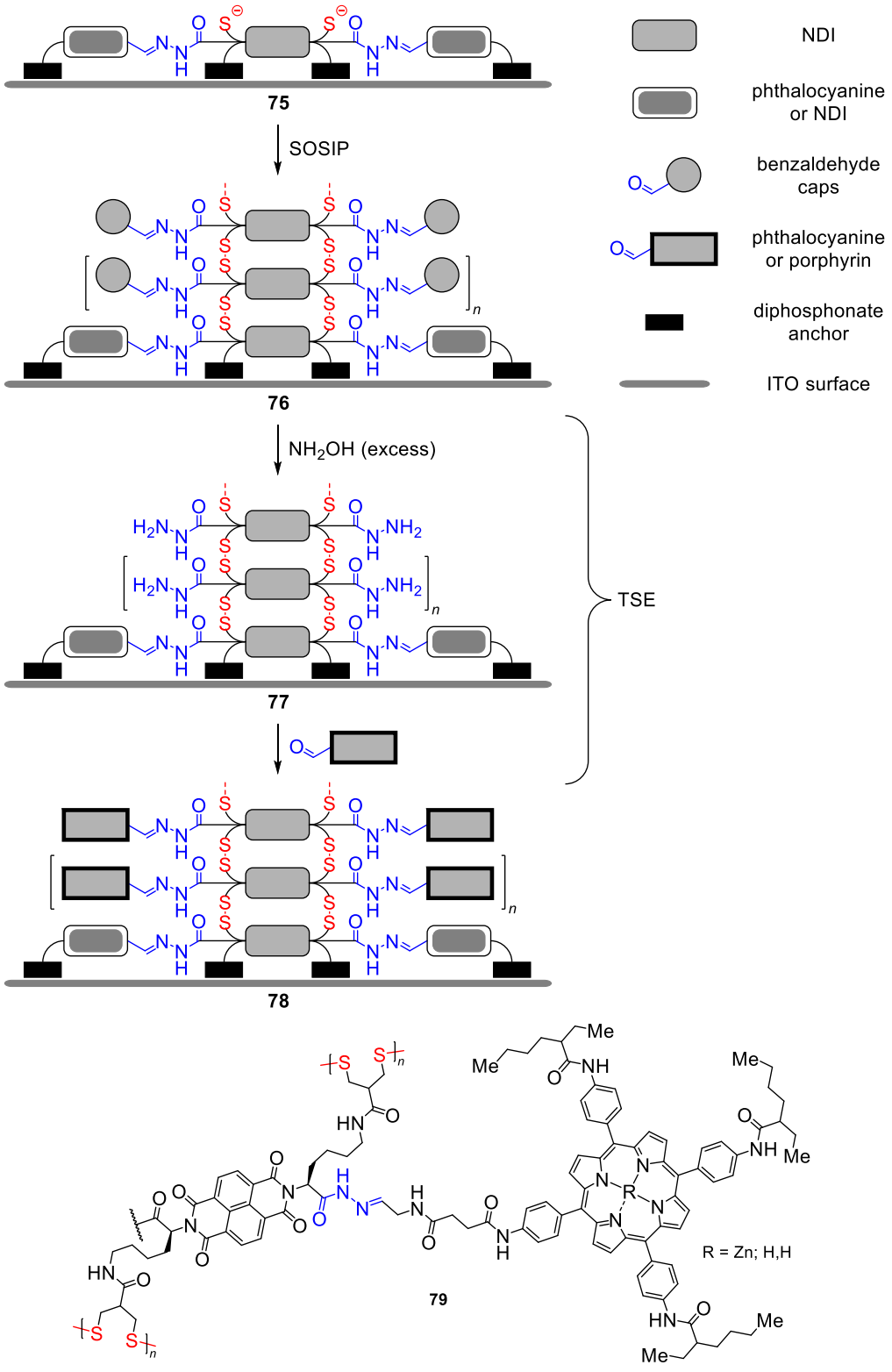

Figure 10: Schematic representation of a double-channel surface architecture produced by SOSIP and TSE and a representative structure of an NDI unit attached to a porphyrin unit (**79**).

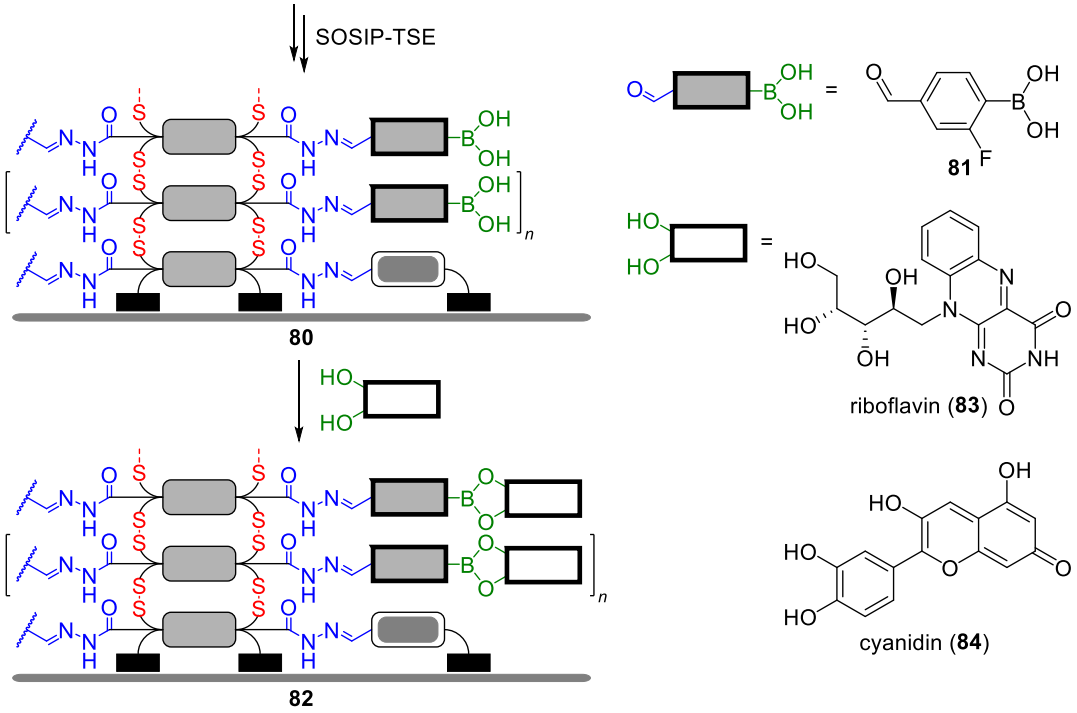

Figure 11: Schematic representation of triply dynamic surface architecture including boronate esters (left) and two natural products, which could be sensed by incorporation into the scaffold (right). For a detailed description of the symbols used, see Figure 10.

The complexity of architectures accessible by this methodology could be increased dramatically by the discovery of additional combinations of three or even more dynamic covalent bonds. A few examples have been reported adding boronate esters as a third component.[67] Using the techniques described above, NDI stacks were grown on an ITO surface using SOSIP (**80**) and different boronic acid derivatives (*e.g.* **81**) were introduced by TSE (**82**, Figure 11).[67a,b] It was shown that boronate ester formation is feasible and chemosensing of different natural catechols and vicinal diols such as riboflavins (**83**) and anthocyanins (**84**) was performed using this system. While simultaneous formation of boronate esters, hydrazones and disulfides was demonstrated,[67c] complete orthogonality could not be established. The lability of boronate esters towards hydrolysis was problematic as hydrazone exchange required strong acids. Due to the high binding affinities of electron-poor catechols to metal oxides, a series of catechol derivatives was synthesized and boronate ester formation was evaluated in functional surface architectures.

[67] (a) K.-D. Zhang, S. Matile, *Angew. Chem. Int. Ed.* **2015**, *54*, 8980–8983; (b) K.-D. Zhang, N. Sakai, S. Matile, *Org. Biomol. Chem.* **2015**, *13*, 8687–8694; (c) L. Rocard, A. Berezin, F. De Leo, D. Bonifazi, *Angew. Chem. Int. Ed.* **2015**, *54*, 15739–15743.

2.2 Results and Discussion

2.2.1 Synthesis of Catechol Derivatives

The initial synthetic studies towards new electron-poor catechol derivatives built on the synthesis we had already developed for a photolabile nitrocatechol anchor. Different halogenated catechols were expected to serve as valuable starting point, since aryl halides can be further transformed using cross-coupling reactions. Furthermore, reports on natural chlorocatechols from the cement of the sandcastle worm *Phragmatopoma californica*[68] and derived bio-inspired polymers[69] suggest, that the chloro-substituent increases the acidity and lowers the oxidation potential of the catechol. Consequently, these chlorocatechols show a higher coordination affinity for metal ions, which fueled our interest in these compounds.

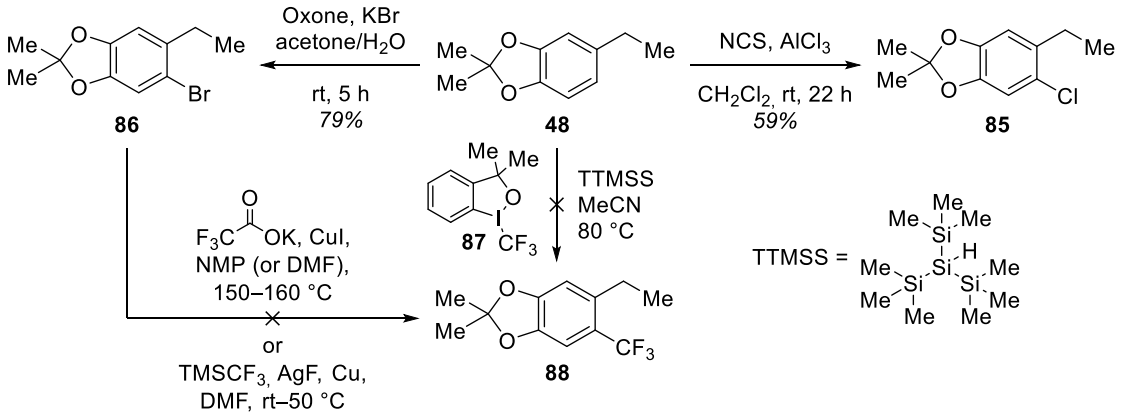

Scheme 17: Attempts to functionalize known acetonide intermediate **48**.

Acetonide **48** was prepared following our known route and functionalization of the aryl core was explored (Scheme 17). Similar transformations performed on hydroxytyrosol derivatives served as a benchmark.[70] Chlorination of acetonide **48** using *N*-chlorosuccinimide (NCS) in the presence of catalytic amounts of aluminium trichloride (10 mol%)[71] provided the desired chloride **85** in moderate yield. The loss of material was attributed to the acidic reaction conditions and the possible formation of hydrogen chloride from the catalyst and residual water in the reaction flask leading to cleavage of the protecting group. To circumvent these drawbacks, instead of simply switching the reagent NCS to *N*-bromosuccinimide, another methodology was chosen avoiding acidic reagents. Bromination of acetonide **48** was achieved

[68] C. J. Sun, A. Srivastava, J. R. Reifert, J. H. Waite, *J. Adhesion* **2009**, *85*, 126–138.

[69] L. Garcia-Fernández, J. Cui, C. Serrano, Z. Shafiq, R. A. Gropeanu, V. San Miguel, J. Iturri Ramos, M. Wang, G. K. Auernhammer, S. Ritz, A. A. Golriz, R. Berger, M. Wagner, A. del Campo, *Adv. Mater.* **2013**, *25*, 529–533.

[70] R. Bernini, S. Cacchi, G. Fabrizi, E. Filisti, *Org. Lett.* **2008**, *10*, 3457–3460.

[71] Y. Zhang, K. Shibatomi, H. Yamamoto, *Synlett* **2005**, 2837–2842.

using equimolar amounts of Oxone ($KHSO_5 \cdot 0.5\ KHSO_4 \cdot 0.5\ K_2SO_4$) and potassium bromide in aqueous acetone[72] to give the desired bromide **86** in good yield. According to the original publications Oxone oxidizes acetone to dimethyldioxirane (DMDO), which in turn oxidizes the halide anion to a "reactive species", that transfers a halogen atom to the aryl moiety of the substrate. Visual inspection of the present bromination reaction clearly point towards the *in situ* formation of elemental bromine as the reaction mixture develops an intense brown color within the first minutes slowly fading back to the initial yellow color of the mixture. In the presence of potassium sulfate from the triple salt oxidant Oxone, the reaction mixture is buffered so that the hydrogen bromide produced as a byproduct is deprotonated straight away. With the first aryl halide derivatives in hand, we immediately moved on to cross-coupling strategies and became particularly interested in the synthesis of a trifluoromethylated compound **88**. Following two procedures involving the formation of "Cu-CF_3" as active species either from a combination of potassium trifluoroacetate and copper(I) iodide[73] or a combination of the Ruppert-Prakash reagent (trifluoromethyltrimethylsilane, TMS-CF_3[74]), silver fluoride and copper,[75] conversion to the desired product **88** was not observed. After several attempts, only starting material was recovered except for a small percentage of the corresponding aryl iodide observed by UPLC-MS in the product mixture of the former protocol. This side product was formed by copper-mediated halogen exchange at the high temperatures applied (160 °C).[76] Also a direct electrophilic trifluoromethylation approach using the Togni reagent[77] (**87**, 3,3-dimethyl-1-trifluoromethyl-1,2-benziodoxole[78]) was not successful and only starting material **48** was recovered.

[72] (a) P. Bovicelli, E. Mincione, R. Antonioletti, R. Bernini, M. Colombari, *Synth. Commun.* **2001**, *31*, 2955–2963; (b) P. Bovicelli, R. Bernini, R. Antonioletti, E. Mincione, *Tetrahedron Lett.* **2002**, *43*, 5563–5567.

[73] K. Matsui, E. Tobita, M. Ando, K. Kondo, *Chem. Lett.* **1981**, 1719–1720.

[74] (a) I. Ruppert, K. Schlich, W. Volbach, *Tetrahedron Lett.* **1984**, *25*, 2195–2198; (b) G. K. S. Prakash, R. Krishnamurti, G. A. Olah, *J. Am. Chem. Soc.* **1989**, *111*, 393–395.

[75] M. M. Kremlev, A. I. Mushta, W. Tyrra, Y. L. Yagupolskii, D. Naumann, A. Möller, *J. Fluor. Chem.* **2012**, *133*, 67–71.

[76] G. E. Carr, R. D. Chambers, T. F. Holmes, *J. Chem. Soc., Perkin Trans. 1* **1988**, 921–926.

[77] M. S. Wiehn, E. V. Vinogradova, A. Togni, *J. Fluor. Chem.* **2010**, *131*, 951–957.

[78] P. Eisenberger, S. Gischig, A. Togni, *Chem. Eur. J.* **2006**, *12*, 2579–2586.

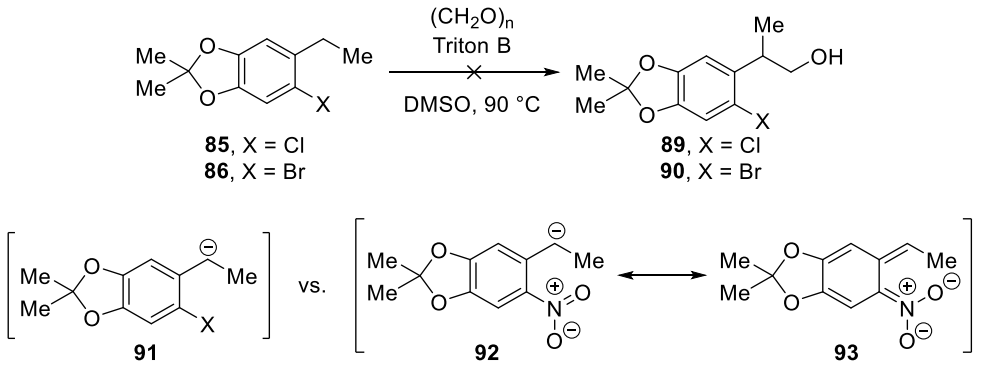

Scheme 18: Aryl halides did not undergo homologation with paraformaldehyde due to decreased acidity of the benzylic protons.

When either aryl chloride **85** or aryl bromide **86** were subjected to the homologation conditions optimized for photoactive nitro derivative **50** (Scheme 18), neither of the two substrates was converted to the desired product and only starting materials were detected by ^{1}H NMR analysis of the reaction mixtures. The acidity of the benzylic protons of halides **85** and **86** is decreased compared to their nitro analog, which can be rationalized by the resonance structures of the intermediate anion. While the aryl halide anion **91** can only delocalize the negative charge across the phenyl ring, an additional resonance form is possible for nitro anion **92** stabilizing the charge as a nitronate **93**. Not having found a way to introduce a functional handle into the catechol units, which would be essential for the future attachment of additional components, no further experiments were conducted on this synthetic approach.

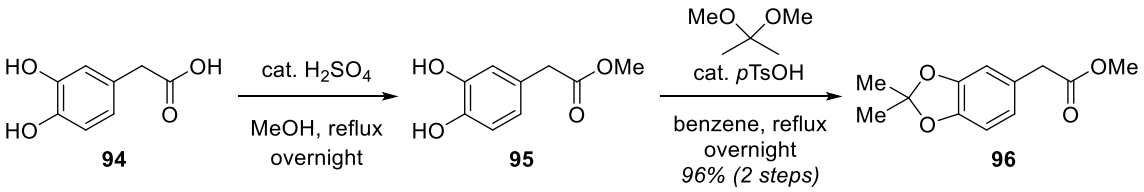

Scheme 19: Synthesis of fully protected DOPAC.

Our new approach focused on the use of commercially available 3,4-dihydroxyphenylacetic acid (DOPAC, **94**) as a common precursor, which already possesses the desired catechol function as well as the homobenzylic functional handle for attachment of another component (Scheme 19). Protection of the free acid **94** was achieved *via* Fischer esterification in refluxing methanol in the presence of a catalytic amount of sulfuric acid giving methyl ester **95** followed by acetonide formation on the catechol applying our previously developed procedure yielding fully protected DOPAC **96** in excellent yield. The preparation of this compound had been

published in the literature before and a similar two step approach applying 2,2-dimethoxypropane as the solvent in the second transformation gave only 72% yield.[79] An attractive one-pot procedure reported to produce compound **96** in 94% yield directly from DOPAC using 2,2-dimethoxypropane and *para*-toluenesulfonic acid (*p*TsOH) in refluxing toluene could not be reproduced in our laboratory.[80]

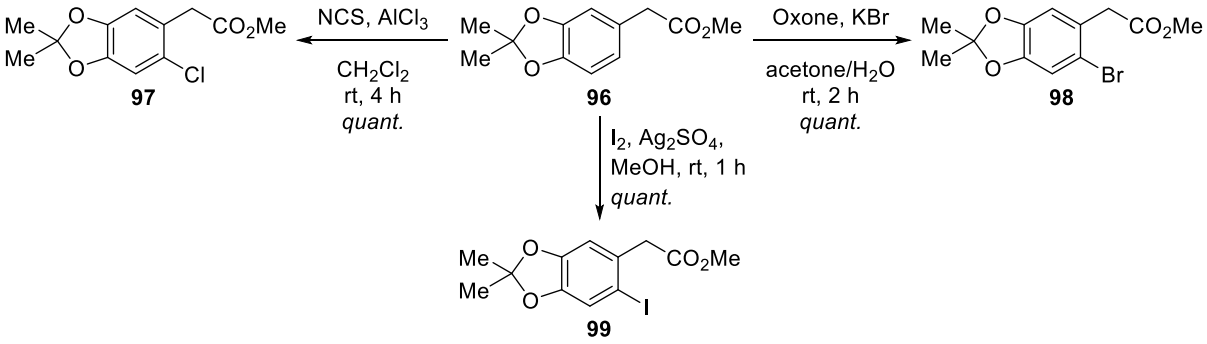

Scheme 20: Halogenation reactions of protected DOPAC.

Moving on to the functionalization of protected intermediate **96**, halogenation reactions came into focus again. Application of the procedures described above produced both aryl chloride **97** and aryl bromide **98** in excellent yields (Scheme 20). The chlorination reaction was monitored closely and full conversion of the starting material **96** was observed after only four hours allowing for a drastic reduction in reaction time, possibly reducing decomposition of the product **97** in the acidic medium. Furthermore, a positive influence of the electron-withdrawing ester substituent on both reactions cannot be excluded as both yields were increased compared to our earlier studies (cf. Scheme 17). Also, iodination of compound **96** was achieved under mild conditions using a combination of iodine and silver sulfate in methanol[81] producing the desired aryl iodide **99** in excellent yield in only one hour. When ethanol was used as the solvent in this transformation, as described in the original procedure, partial exchange of the ester group was observed, and a mixture of methyl and ethyl esters was obtained.

[79] B. Geiseler, L. Fruk, *J. Mater. Chem.* **2012**, *22*, 735–741.

[80] B. Almeida Cotrim, J. Joglar, M. J. L. Rojas, J. M. Decara del Olmo, M. Macias-González, M. R. Cuevas, M. Fitó, D. Muñoz-Aguayo, M. I. Covas Planells, M. Farré, F. R. de Fonseca, R. de la Torre, *J. Agric. Food Chem.* **2012**, *60*, 1067–1074.

[81] W.-W. Sy, B. A. Lodge, A. W. By, *Synth. Commun.* **1990**, *20*, 877–880.

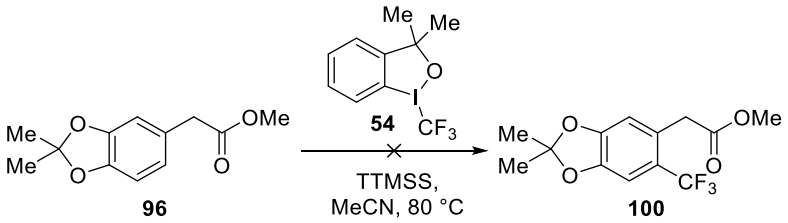

Scheme 21: Electrophilic trifluoromethylation of protected DOPAC could not be achieved.

With the three different aryl halides **97**–**99** in hand, we turned to further coupling reactions and explored the synthesis of trifluoromethyl derivative **100**. Initial experiments on the direct electrophilic trifluoromethylation of protected DOPAC **96** using the Togni reagent **87** did not lead to formation of the desired product (Scheme 21) and efforts were focused on the use of copper-mediated trifluoromethylation strategies. A classic approach using trifluoroacetate salts as the trifluoromethyl source[73] showed promising results. This method is attractive due to the low cost as well as easy handling of trifluoroacetate salts. An evaluation of different reaction conditions was performed (Table 3).

Table 3: Optimization studies on the trifluoromethylation of aryl halides **98** and **99** using potassium trifluoroacetate.

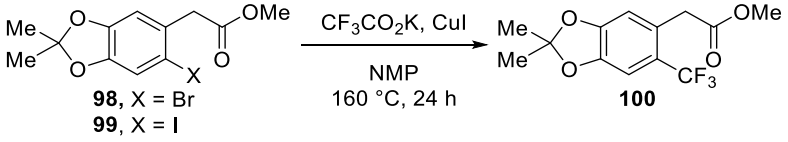

Entry	**-X**	**CF_3CO_2K** [eq.]	**CuI** [eq.]	**Yield** [%][a]
1	-Br	4	2	62
2	-Br	6	3	54
3	-Br	6	6	64
4	-I	6	6	33
5	-I	4	0.4 Cu^0, 0.4 Ag_2O	dec.

[a] Highest isolated yield obtained under the stated conditions.

Typical procedures use excess amounts of potassium trifluoroacetate as well as copper iodide in *N*-methylpyrrolidone (NMP). Applying 4 eq. of potassium trifluoroacetate and 2 eq. of copper iodide transformed aryl bromide **98** to the desired compound **100** in up to 62% yield (Entry 1). Since full conversion of the starting material **98** was not always observed within 24 h, reagent loadings were increased with no significant influence on the outcome of the reaction (Entries 2 and 3). Common side products in all cases were the reduced protected DOPAC **96** as well as a pentafluoroethyl homolog of **100**, which is formed by repeated coupling of a

trifluoromethyl group to the product **100**. While the formation of these side products was not unexpected, their yield relative to the desired product varied significantly. Attempts to create more defined reaction conditions by the use of degassed solvent and pre-dried potassium trifluoroacetate did not lead to any change in product distribution. When the substrate was changed to the more reactive aryl iodide **99**, an overall decrease in yield was observed (Entry 4). Full conversion of the starting material was observed within less than 17 h. However, ^{1}H NMR analysis indicated the formation of several unidentified side products, likely caused by the high reaction temperature (160 °C) in combination with the high reactivity of aryl iodides. A recent protocol using only catalytic amounts of elemental copper in the presence of silver(I) oxide as a promoter[82] did not yield the desired product and decomposition of the starting material was observed (Entry 5). While initial experiments on aryl bromide **98** provided the desired product **100** in acceptable yield, these results could not be reproduced reliably over several experiments rendering this approach unpredictable. Thus, the Ruppert-Prakash reagent was investigated as a trifluoromethyl source[83] generally allowing for milder reaction conditions (Table 4).

Table 4: Studies on the trifluoromethylation of aryl iodide **99** using the Ruppert-Prakash reagent.

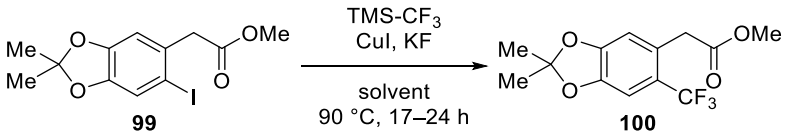

Entry	**TMS-CF$_3$** [eq.]	**CuI** [eq.]	**KF** [eq.]	**Solvent**	**Yield** [%]
1	1.4	1.8	1.4	DMF/NMP[a]	81
2	1.5	1.6	1.5	DMF/NMP	86
3	2.0	2.2	2.0	DMF/NMP	92
4	2.0	1.2	2.0	DMF/NMP	n.d.
5	1.5	1.6	1.5	EtCN	<20% conv.
6	2.0	2.1	2.0	NMP	88

[a] Solvents were always used in a 1:1 ratio.

[82] Y. Li, T. Chen, H. Wang, R. Zhang, K. Jin, X. Wang, C. Duan, *Synlett* **2011**, 1713–1716.

[83] H. Urata, T. Fuchikami, *Tetrahedron Lett.* **1991**, *32*, 91–94.

Initial experiments using 1.4 eq. of the Ruppert-Prakash reagent, 1.8 eq. copper(I) iodide and 1.4 eq. pre-dried potassium fluoride in a 1:1 mixture of DMF/NMP yielded 81% of the desired product **100** containing less than 10% of the pentafluoroethyl homolog, as quantified by ^{1}H NMR analysis (Entry 1). Gradually increasing the excess of the trifluoromethyl source and its activator slightly improved the yield to 92% without causing undesired side reactions (Entries 2 and 3). Only when the excess of copper(I) iodide was reduced below the level of the other reagents, the formation of additional side products was observed (Entry 4). Under these conditions, highly reactive trifluoromethyl anions are generated from the reagents but the amount of copper(I) present in the mixture is not sufficient to stabilize the reactive species leading to undesired side reactions. A recent report on the use of propionitrile as solvent in these transformations reducing the amount of pentafluoroethyl side product[75] could not be confirmed in our hands (Entry 5). After 48 h reaction time, we did not only observe less than 20% conversion of the starting material by ^{1}H NMR analysis, but also the presence of more of the pentafluoroethyl compound than of the desired product **100** in the mixture. The use of pure NMP as solvent turned out to have no significant influence on the reaction outcome and 88% yield were obtained on a 1.3 mmol scale (Entry 6).

Table 5: Optimization studies on the methylsulfonylation of aryl iodide **99**.

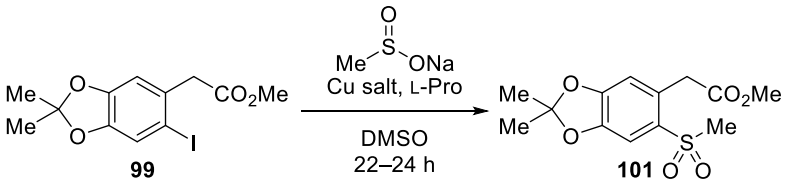

Entry	**Cu salt, eq.**	**$MeSO_2Na$** [eq.]	**L-Pro** [eq.]	**Temperature** [°C]	**Yield** [%]
1	CuI, 0.4	1.5	0.4	80	35
2	$Cu(OAc)_2$, 0.4	1.5	0.4	80	59
3	$Cu(OAc)_2$, 0.4	1.5	0.4	100	77
4	$Cu(OAc)_2$, 0.6	1.6	0.6	100	86

As a last functionalization, the synthesis of methylsulfonyl derivative **101** from iodide **99** was investigated (Table 5). Following a published procedure for the copper-catalyzed and proline-promoted sulfonylation using sodium methanesulfinate in DMSO at 80 °C[84] gave the desired product **100** in 35% yield (Entry 1). Although copper(II) acetate was reported to perform significantly worse than copper(I) iodide in the original publication, the unusual blue color of the reaction mixture indicated the formation of copper(II) during the reaction and prompted us to carry out the control experiment. Indeed, copper(II) acetate could efficiently catalyze the present transformation with a higher isolated yield of 59% (Entry 2). As the reaction proceeded slow and full conversion of the starting material **99** was not always observed after 24 h, the reaction temperature was increased to 100 °C resulting in faster conversion and slightly increased yields (Entry 3). Optimal results were achieved using 60 mol% instead of 40 mol% of proline and copper salt affording the product in 86% yield (Entry 4).

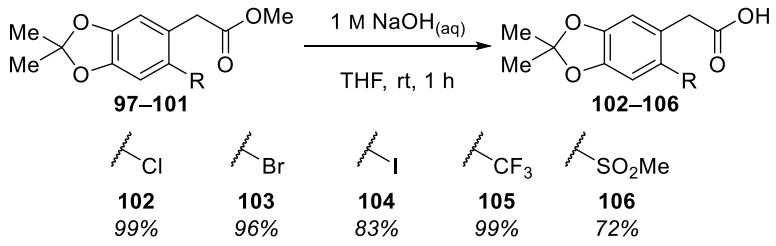

Scheme 22: Saponification of catechol precursors **97**–**101**.

In order to enable the attachment of cargos to catechol precursors **97**–**101**, saponification of the ester moiety was performed on all derivatives (Scheme 22). A solution of substrate in THF was treated with 1 M aqueous sodium hydroxide giving a turbid mixture. Within 60 min, the reaction mixture turned clear indicating full conversion of the starting material. After acidification, carboxylic acids **102**–**106** were isolated by extraction in good to excellent yields. Another strategy considered for the formation of a chemical handle for further modifications, was reduction of the ester function to a primary hydroxyl group. An exemplary reduction using lithium aluminium hydride in THF was performed on trifluoromethyl derivative **100** producing the desired alcohol **107** in excellent yield (Scheme 23).

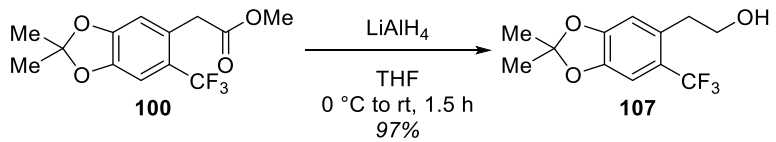

Scheme 23: Exemplary reduction of ester **100** to primary alcohol **107**.

[84] W. Zhu, D. Ma, *J. Org. Chem.* **2005**, *70*, 2696–2700.

Cleavage of the acetonide protecting group was performed on derivatives **98**–**101** to set up the free catechols for further studies (Scheme 24). Neat acetonide was treated with cold 20% aqueous TFA and after 2–3 h, a mixture of distinct dark brown color was obtained. The mixture was concentrated, and the residue was subjected to preparative reversed-phase HPLC affording the catechols **108**–**111** in moderate to good yields. Since these compounds were designed to serve as highly polar binders, flash chromatography over silica gel was not possible due to coating of the stationary phase. Catechols **108**–**110** were obtained as off-white solids, which were stable in air at 4 °C over several months. Methylsulfonylcatechol **111** was obtained as a hygroscopic orange solid illustrating the high polarity of the compound.

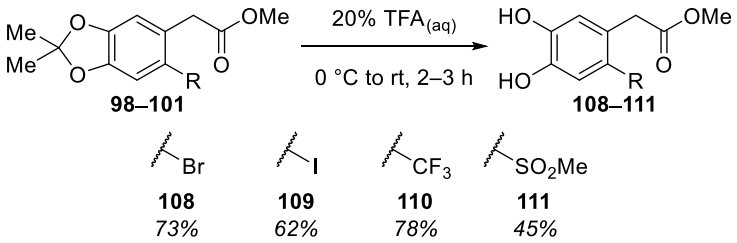

Scheme 24: Acetonide cleavage and formation of free catechols.

2.2.2 Application of Electron-Poor Catechols in Triply Dynamic Functional Systems[85]

Functional systems employing three types of dynamic covalent bonds, namely disulfides, hydrazones and boronate esters, had been reported before and simultaneous formation of these three bonds had been demonstrated.[67] A very recent study introduced even a fourth reaction, that could be run simultaneously; the 1,4-addition of thiols onto conjugated acceptors.[86] In order to assess the applicability of bio-inspired electron-poor catechols in functional systems, the stability of their corresponding boronate esters with three different phenylboronic acid derivatives was investigated. Besides our novel catechols **108**–**111**, the series included nitrodopamine (**19**) and the anachelin chromophore (**16**), since these catechols are known to strongly bind to metal oxides. Furthermore, quercetin (**113**), alizarin red (**114**) and coumarin derivative **115** were included as positive controls known to form boronate esters in functional systems.[67a] By titration of UV-active catechols with boronic acids and reverse titration of alizarin red boronate esters with UV-inactive catechols, the dissociation constants K_D were

[85] These studies have been performed by Santiago Lascano and Dr. Kang-Da Zhang in the research group of Prof. Dr. Stefan Matile at the University of Geneva and have been published: S. Lascano, K.-D. Zhang, R. Wehlauch, K. Gademann, N. Sakai, S. Matile, *Chem. Sci.* **2016**, *7*, 4720–4724.

[86] H. M. Seifert, K. Ramirez Trejo, E. V. Anslyn, *J. Am. Chem. Soc.* **2016**, *138*, 1091610924.

determined. Benzoxaborole derivative **112** was identified as the best binding partner resulting in K_D values distributed over a suitable range allowing for the formation of boronate esters of markedly different stabilities (Scheme 25). Among the compounds studied, nitrocatechol **19** and methylsulfonylcatechol **111** gave the best values in the sub-millimolar range. Anachelin chromophore **16** showed intermediate stability in between the positive control substances, which were closely followed by trifluoromethylcatechol **110** and bromocatechol **108**. Iodocatechol **109** gave a surprisingly high K_D value.

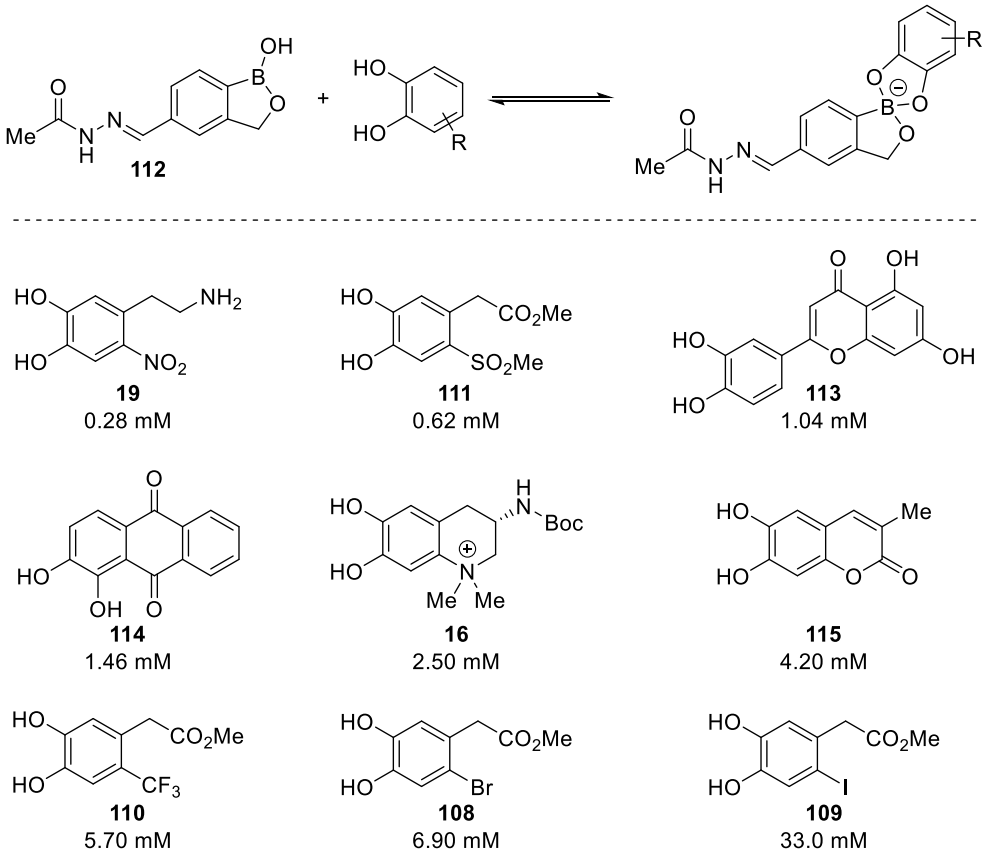

Scheme 25: Series of catechol derivatives investigated in the formation of boronate esters. Dissociation constants K_D listed below each compound were assessed by titration. Catechols are ordered by increasing K_D values.

Exchange reactions of boronate esters, hydrazones and disulfides were studied in solution to find conditions that allow for orthogonal exchange of each single function in presence of the others (Scheme 26). Boronate ester **116** and bromocatechol **108** were exposed to 2% Hünig's base and 10% D_2O in DMSO-d_6 and the reaction monitored by ^{1}H NMR spectroscopy. Equilibrium was reached with a half-life of substrates t_{50} <3 min and the mixture contained boronate esters **116** and **117** in a ratio of 1:1.1. Hydrazones and disulfides did not react under these conditions. Hydrazone exchange was the main obstacle in this study, since boronate esters tend to hydrolyze under acidic conditions. However, the use of methyl 3-amino-4-

hydroxybenzoate (**119**) as an organocatalyst[87] facilitated hydrazone exchange in only 1.5 mM TFA. Equilibration in t_{50} = 11.9 h produced hydrazones **120** and **122** in a ratio of 1.3:1. At this stage it was of key importance that boronate ester **116** remained intact under these conditions and also disulfides did not react. Finally, exchange of disulfides **124** and **125** was triggered by small amounts of benzylthiol in the presence of triethylamine (both 2.0 mM). Equilibrium was reached in t_{50} = 2.5 h with disulfides **124** and **126** present in a ratio of 1:1.6 and again hydrazones and boronate esters were not affected.

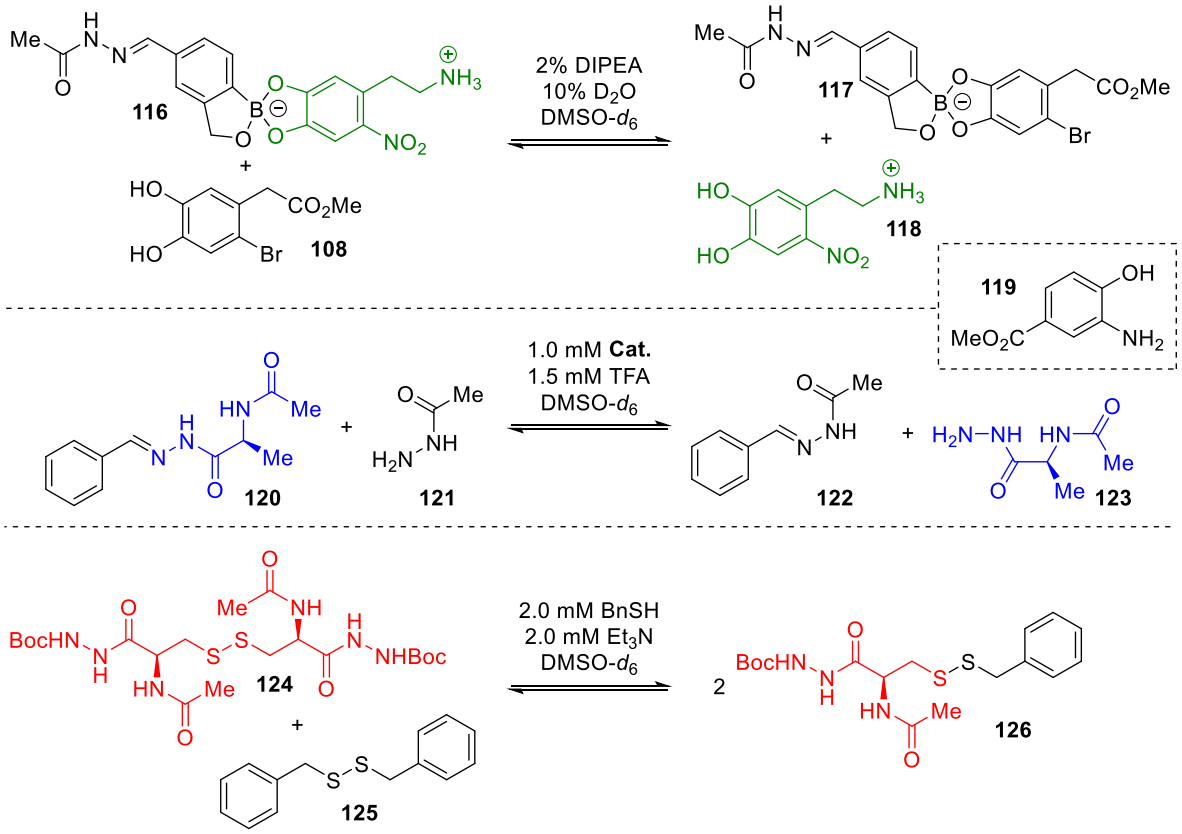

Scheme 26: Conditions for orthogonal exchange of boronate esters, hydrazones and disulfides in solution.

In order to demonstrate the applicability of three orthogonal dynamic organic covalent bonds in functional systems, the above findings were translated into a multicomponent surface architecture **128** (Scheme 27). On an ITO surface, NDI stacks were grown by the SOSIP technique (**127**). Benzoxaborole **129** was incorporated by TSE and boronate ester formation was achieved by incubation in a solution of nitrocatechol **19** and Hünig's base resulting in surface architecture **128**. While formation of all three bonds had already been achieved, the challenge was to carry out hydrazone exchange without cleaving the boronate ester groups. Due to the small amount of substance on the surface, several solid supports were incubated in the

[87] D. Larsen, M. Pittelkow, S. Karmakar, E. T. Kool, *Org. Lett.* **2015**, *17*, 274–277.

same sample of hydrazone exchange medium. The accumulated substance in the medium was then analyzed by ^{1}H NMR spectroscopy and intact boronate ester **132** was identified along with only small amounts of the hydrolyzed benzoxaborole. Additional evidence for the presence of boronate ester **132** was obtained by ESI-MS. Thus, surface architecture **128** represents the first functional system based on three orthogonal dynamic organic covalent bonds.

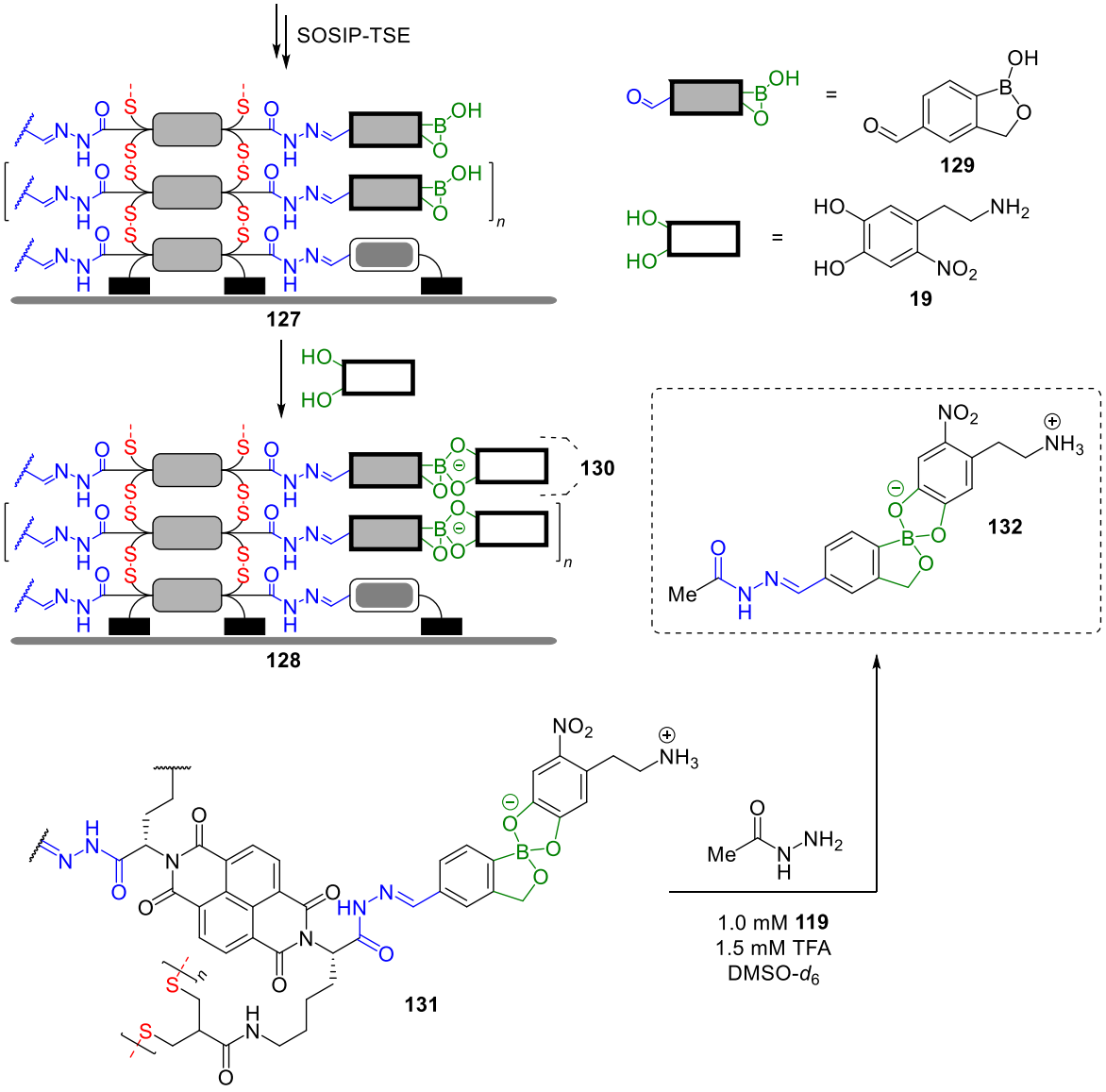

Scheme 27: Multicomponent surface architecture containing three orthogonal dynamic covalent bonds.

2.2.3 New Generation Binders

In late 2015, Wolkenstein and coworkers have reported the structures of borolithochromes,[88] natural spiroborate pigments isolated from pink-colored calcareous material of the putative Jurassic red alga *Solenopora jurassica*.[89] Microgram amounts of 13 different compounds were isolated by HPLC and their structures and absolute configurations were assigned mainly using microcryoprobe NMR analysis. The fact, that these natural products are of Jurassic age and thus survived for more than 150 million years implies a high stability of the spiroborate moiety and raises the question, whether 1,8-naphthalenediol-based binders would perform superior compared to the catechols **108**–**111** when applied in orthogonal boronate ester exchange in triply dynamic functional systems. Building on our results with nitrocatechol **19** and methylsulfonyl catechol **111** (cf. Scheme 25), we investigated the synthesis of similar naphthalene-based compounds bearing an electron-withdrawing substituent and a chemical handle in the *para*-positions relative to the hydroxyl groups.

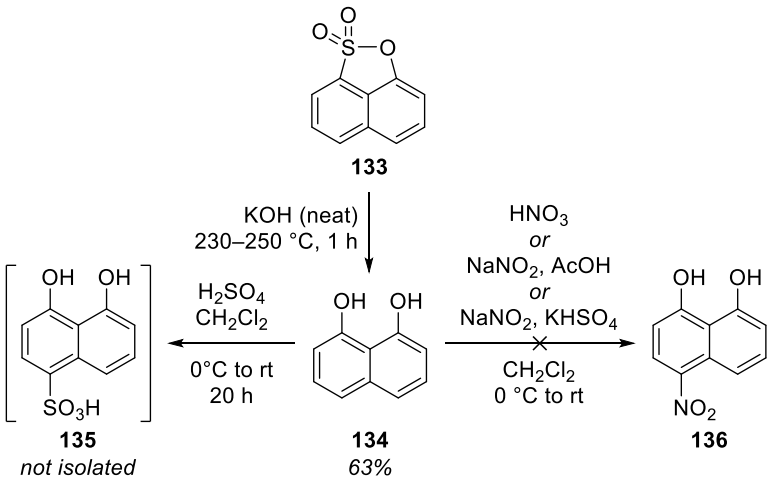

Scheme 28: Synthesis of 1,8-naphthalenediol (**134**) and direct functionalization attempts.

Commercially available 1,8-naphthosultone (**133**) was hydrolyzed under harsh basic conditions to afford 1,8-naphthalenediol (**134**)[90] in good yield after recrystallization from chloroform (Scheme 28). The possibility to introduce a sulfonic acid substituent without the need for protection of the hydroxyl groups was investigated briefly at this stage. The sulfonic acid function would be desirable as it is electron-withdrawing and could be used as a chemical handle in form of a sulfonamide at the same time. When diol **134** was treated with sulfuric acid,

[88] K. Wolkenstein, H. Sun, H. Falk, C. Griesinger, *J. Am. Chem. Soc.* **2015**, *137*, 13460–13463.

[89] K. Wolkenstein, J. H. Gross, H. Falk, *Proc. Natl. Acad. Sci. USA* **2010**, *107*, 19374–19378.

[90] (a) H. Erdmann, *Liebigs Ann.* **1888**, *247*, 306–366; (b) K. A. Parker, T. Iqbal, *J. Org. Chem.* **1980**, *45*, 1149–1151.

conversion of the starting material was observed and UPLC-MS analysis showed the expected mass (m/z = 241, $[M+H]^+$) of the main constituent of the crude product mixture. However, ^{1}H NMR analysis indicated the presence of several different aromatic compounds in the mixture and isolation of the highly polar sulfonic acid **135** was not achieved. Also, nitration of the free diol **134** was investigated using classic nitration conditions as well as milder conditions applying sodium nitrite in the presence of acid. In all cases, only a complex mixture was obtained. When the temperature was decreased below 0 °C, no reaction was observed.

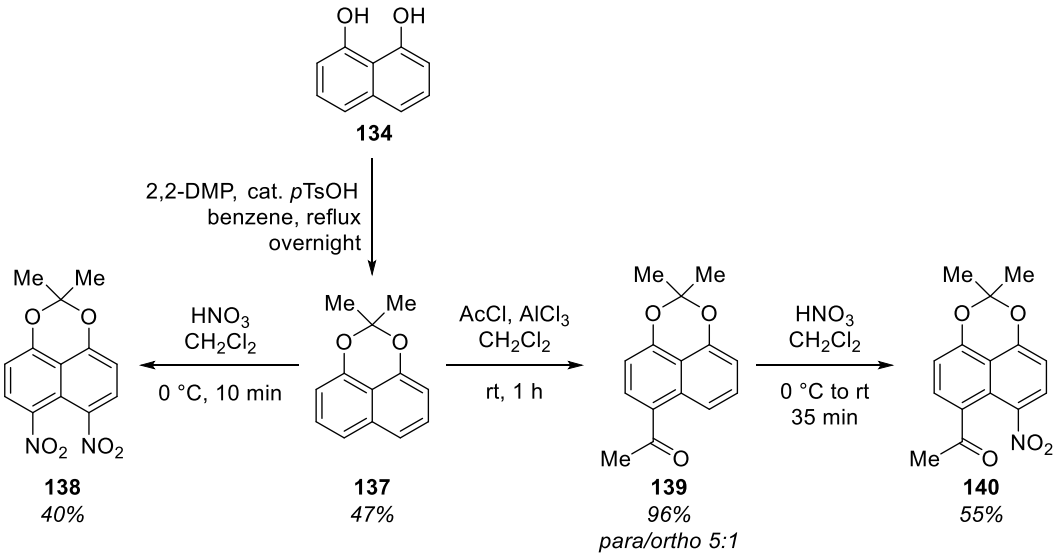

Scheme 29: Protection and functionalization of diol **134**.

Due to the complications encountered with direct functionalization, diol **134** was protected as an acetonide, a strategy that had proved successful with the catechol derivatives. Applying our previously developed conditions, acetonide **137** was obtained in a moderate yield of 47%. Introduction of the nitro group was attempted, and surprisingly TLC indicated formation of a single product in 10 minutes at 0 °C. However, after purification the material was identified as the symmetric dinitro compound **138**. Attempts to use milder nitration conditions (cf. Scheme 28) were not successful. Installation of a chemical handle could be achieved using Friedel-Crafts acylation conditions[91] and afforded ketone **139** in an excellent yield of 96% as a mixture of *para*- and *ortho*-isomers in a ratio of 5:1. While partial separation of the isomers was possible chromatographically, nitration of the mixture followed by chromatography over silica gel gave the desired nitroaryl compound **140** as a single isomer in 55% yield. Bromination and iodination of ketone **139** were attempted using the protocols applied for the synthesis of catechol derivatives (cf. Scheme 20), but ^{1}H NMR and HRMS analyses clearly pointed towards the

[91] N. P. Buu-Hoï, D. Lavit, *J. Chem. Soc.* **1956**, 2412.

formation of two regioisomers in ca. 1:1 ratio, which could not be improved when reactions were performed at low temperatures.

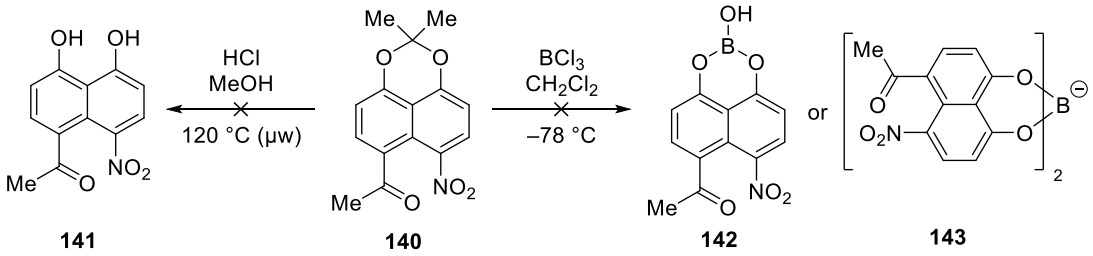

141 **140** **142** **143**

Scheme 30: Attempts to cleave the acetonide protecting group.

Efforts to cleave the acetonide protecting group to yield either the free diol **141** or a borate such as **142** or **143** were unsuccessful. While treatment with methanolic hydrogen chloride at elevated temperatures did not lead to conversion of the starting material, forcing conditions like heating to 120 °C in a microwave reactor slowly lead to darkening of the mixture without formation of a product detectable by ^{1}H NMR analysis. When acetonide **140** was treated with boron trichloride, fast conversion of the starting material was observed, but only complex mixtures were obtained even when the reaction temperature was reduced to –78 °C.

2.3 Conclusion

The development of an efficient branched synthesis of several electron deficient catechol derivatives has been achieved with the potential to use aryl halide intermediates for further synthetic studies and extend the portfolio of substrates. The synthetic catechols were used in the formation and controlled exchange of boronate esters and were subsequently applied in a triply dynamic surface architecture, which represents the first functional system employing three orthogonal dynamic organic covalent bonds. Synthetic efforts towards new naphthalene-derived aromatic diols based on spiroborate natural products have yielded an advanced nitroaryl intermediate. Further studies on the deprotection of this intermediate or the use of alternative protecting groups need to be performed in order to make the test substrate available. The investigation of additional functionalization methods could lead to a broader scope of substituents on the aryl core and thus provide a new series of diols to be tested in dynamic functional systems.

3 Rapamycin-Based Probes for the Structural Investigation of TOR Complexes

3.1 Introduction

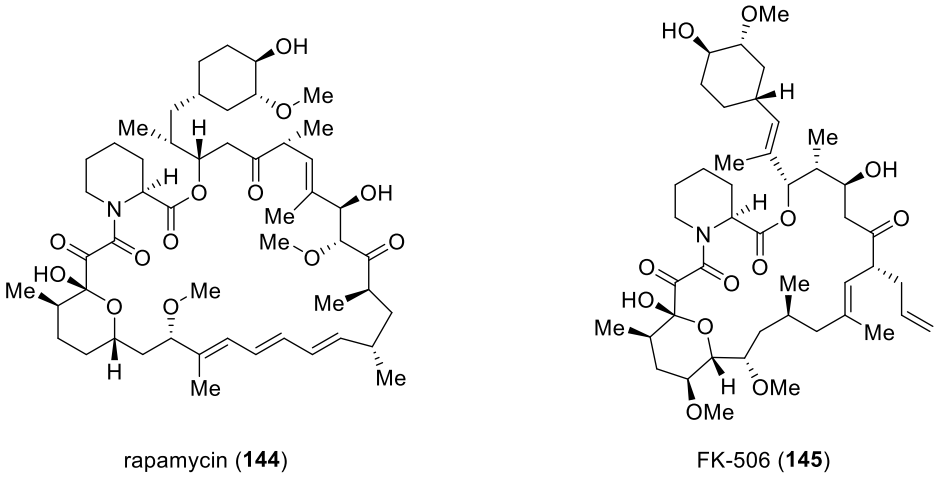

Figure 12: Structures of immunosuppressive natural products from *Streptomyces* species.

Rapamycin (**144**), also known under the generic name sirolimus, is a macrocyclic polyketide isolated from the bacterium *Streptomyces hygroscopicus* in 1975 by Sehgal and coworkers at Ayerst Pharmaceuticals (Figure 12).[92] The bacteria cultures had been isolated from a soil sample collected on Easter Island (Rapa Nui), from which the name rapamycin was derived. Initially, the compound **144** was recognized for its antifungal activity, especially against several species of the *Candida* genus,[92] and its structure was determined by single crystal X-ray crystallography[93] as well as NMR spectroscopy.[94] Although further studies reported potent immunosuppressive[95] and antitumor activities[96] of rapamycin (**144**), drug development was ceased.[97] In 1987, FK-506 (**145**) was isolated from *Streptomyces tsukubaensis* and reports on its immunosuppressive properties triggered a revival in the investigation of rapamycin.[98]

[92] (a) C. Vézina, A. Kudelski, S. N. Sehgal, *J. Antibiot.* **1975**, *28*, 721–726; (b) S. N. Sehgal, H. Baker, C. Vézina, *J. Antibiot.* **1975**, *28*, 727–732.

[93] D. C. N. Swindells, P. S. White, J. A. Findley, *Can. J. Chem.* **1978**, *56*, 2491–2492.

[94] J. A. Findlay, L. Radics, *Can. J. Chem.* **1980**, *58*, 579–590.

[95] R. R. Martel, J. Klicius, S. Galet, *Can. J. Physiol. Pharmacol.* **1977**, *55*, 48–51.

[96] (a) J. Douros, M. Suffness, *Cancer Treatment Rev.* **1981**, *8*, 63–87; (b) C. P. Eng, S. N. Sehgal, C. Vézina, *J. Antibiot.* **1984**, *37*, 1231–1237.

[97] K. Garber, *J. Natl. Cancer Inst.* **2001**, *93*, 1517–1519.

[98] (a) H. Tanaka, A. Kuroda, H. Marusawa, H. Hatanaka, T. Kino, T. Goto, M. Hashimoto, T. Taga, *J. Am. Chem. Soc.* **1987**, *109*, 5031–5033; (b) T. Kino, H. Hatanaka, M. Hashimoto, M. Nishiyama, T. Goto, M. Okuhara, M. Kosaka, H. Aoki, H. Imanaka, *J. Antibiot.* **1987**, *40*, 1249–1255; (c) T. Kino, H. Hatanaka, S. Miyata, N. Inamura, M. Nishiyama, T. Yajima, T. Goto, M. Okuhara, M. Kohsaka, H. Aoki, T. Ochiai, *J. Antibiot.* **1987**, *40*, 1256–1265.

Eventually rapamycin (**144**) was approved in 1999 for clinical use to prevent organ rejection after renal transplantation (marketed as Rapamune©). Additional rapamycin analogs (rapalogs) were developed in the following years and received clinical approval (see Section 3.2). Extensive biochemical studies led to the discovery of the cellular target or rapamycin (TOR) and subsequent investigations established TOR signaling as a central pathway, that is highly conserved among most eukaryotes. Many reviews describing TOR signaling in different organisms have been published in the past.[99]

In the early 1990s, TOR was first discovered in the yeast *Saccharomyces cerevisiae* using rapamycin-resistant mutants.[100] Two genes were identified encoding for two essential and homologous proteins, TOR1 and TOR2, which belong to the phosphatidylinositol 3-kinase-related kinase (PIKK) family. This study also showed that an intracellular cofactor, the FK-506-binding protein 12 (FKBP12), is required for the toxicity of rapamycin. Disruption of the gene encoding for FKBP12 had no effect on the viability of the yeast. On the contrary, other known inhibitors of FKBP12 were not immunosuppressive.[101] Thus, the FKBP12-rapamycin complex gained new toxic properties against a target required for viability of the organism. Further investigations provided evidence that the FKBP12-rapamycin complex binds directly to TOR1 and TOR2.[102] The yeast *S. cerevisiae* is a special case as its genome encodes for two TOR kinases, whereas most other eukaryotes have only one TOR gene.[99e] Interestingly, there are no reports on FKBP12 being a part of normal TOR signaling and the protein is thought to be hijacked by rapamycin (**144**).[99d] Investigations of the biological roles of TOR1 and TOR2 concluded that TOR2 has two essential functions; one is redundant with TOR1 (and thus TOR1 is not essential) while the other one is unique to TOR2.[103] The observation that inhibition of TOR signaling induces starvation symptoms led to the assumption that TOR actively controls cell growth. It was shown that only the shared TOR1/2 signaling branch is responsive to

[99] See for example: (a) M. Laplante, D. M. Sabatini, *Cell* **2012**, *149*, 274–293; (b) H. Pópulo, J. M. Lopes, P. Soares, *Int. J. Mol. Sci.* **2012**, *13*, 1886–1918; (c) R. Zoncu, A. Efeyan, D. M. Sabatini, *Nat. Rev. Mol. Cell Biol.* **2011**, *12*, 21–35; (d) R. Loewith, M. N. Hall, *Genetics* **2011**, *189*, 1177–1201; (e) S. Wullschleger, R. Loewith, M. N. Hall, *Cell* **2006**, *124*, 471–484.

[100] J. Heitman, N. R. Movva, M. N. Hall, *Science* **1991**, *253*, 905–909.

[101] S. L. Schreiber, *Science* **1991**, *251*, 283–287.

[102] (a) R. Stan, M. M. McLaughlin, R. Cafferkey, R. K. Johnson, M. Rosenberg, G. P. Livi, *J. Biol. Chem.* **1994**, *269*, 32027–32030; (b) M. C. Lorenz, J. Heitman, *J. Biol. Chem.* **1995**, *270*, 27531–27537; (c) Y. Zheng, Y. Jiang, *Cell* **1995**, *82*, 121–130.

[103] (a) N. C. Barbet, U. Schneider, S. B. Helliwell, I. Stansfield, M. F. Tuite, M. N. Hall, *Mol. Biol. Cell* **1996**, *7*, 25–42; (b) A. Schmidt, M. Bickle, T. Beck, M. N. Hall, *Cell* **1997**, *88*, 531–542; (c) A. Schmidt, T. Beck, A. Koller, J. Kunz, M. N. Hall, *EMBO J.* **1998**, *17*, 6924–6931; (d) S. B. Helliwell, I. Howald, N. Barbet, M. N. Hall, *Genetics* **1998**, 148, 99–112.

nutrients and sensitive to rapamycin (**144**), while the TOR2 unique branch is not. A breakthrough was accomplished in 2002, when two large multiprotein complexes, TOR complex (TORC) 1 and 2, were isolated from yeast cells.[104] Studies on the complexes established two separate TOR signaling pathways: TORC1 contains either TOR1 or TOR2, it is rapamycin-sensitive and involved in the shared TOR1/2 pathway. TORC2 contains exclusively TOR2, it is rapamycin-insensitive and involved in the TOR2 unique pathway. Furthermore, it was confirmed that not only the TOR kinases but also the TORCs are conserved among other eukaryotes.[105]

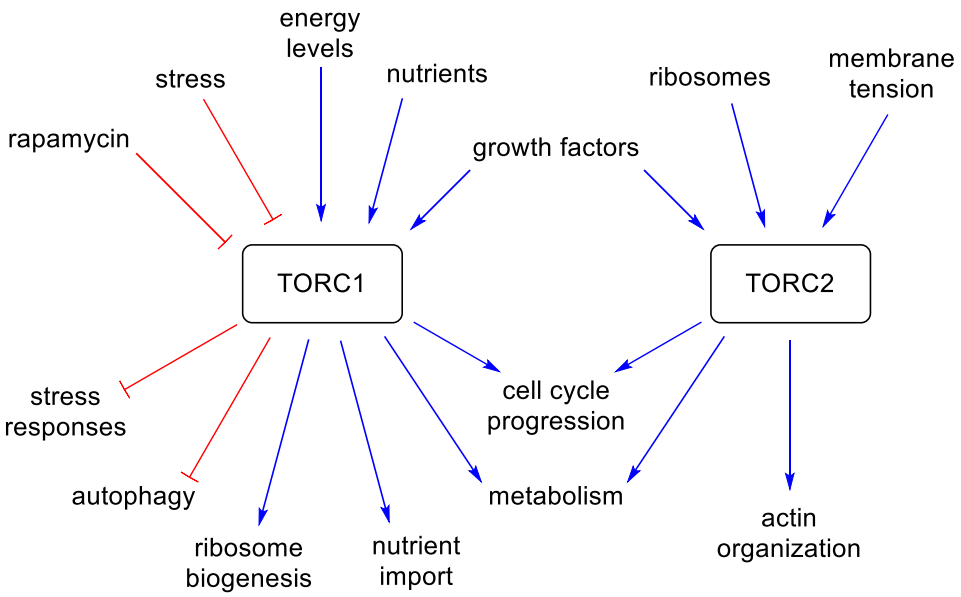

Figure 13: General functionality of the TOR complexes.

To date many upstream regulators and downstream targets of the TOR signaling network have been identified and it is recognized as a central signaling pathway.[99] TORC1 (~1.2 MDa) actively regulates the accumulation of cellular mass in response to the abundance and quality of nutrients in the environment. It controls translational processes and thus influences protein expression, especially the biogenesis of ribosomes but also permeases for the import of

[104] (a) R. Loewith, E. Jacinto, S. Wullschleger, A. Lorberg, J. L. Crespo, D. Bonenfant, W. Oppliger, P. Jenoe, M. N. Hall, *Mol. Cell* **2002**, *10*, 457–468; (b) K. P. Wedaman, A. Reinke, S. Anderson, J. Yates, III, J. M. McCaffery, T. Powers, *Mol. Biol. Cell* **2003**, *14*, 1204–1220; (c) A. Reinke, S. Anderson, J. M. McCaffery, J. Yates, III, S. Aronova, S. Chu, S. Fairclough, C. Iverson, K. P. Wedaman, T. Powers, *J. Biol. Chem.* **2004**, *279*, 14752–14762.

105 (a) K. Hara, Y. Maruki, X. Long, K. Yoshino, N. Oshiro, S. Hidayat, C. Tokunaga, J. Avruch, K. Yonezawa, *Cell* **2002**, *110*, 177–189; (b) D.-H. Kim, D. D. Sarbassov, S. M. Ali, J. E. King, R. R. Latek, H. Erdjument-Bromage, P. Tempst, D. M. Sabatini, *Cell* **2002**, *110*, 163–175; (c) E. Jacinto, R. Loewith, A. Schmidt, S. Lin, M. A. Rüegg, A. Hall, M. N. Hall, *Nat. Cell Biol.* **2004**, *6*, 1122–1128; (d) D. D. Sarbassov, S. M. Ali, D.-H. Kim, D. A. Guertin, R. R. Latek, H. Erdjument-Bromage, P. Tempst, D. M. Sabatini, *Curr. Biol.* **2004**, *14*, 1296–1304.

nutrients. In addition to promoting anabolism, TORC1 suppresses stress-responsive pathways to effect cell growth. Interestingly, TORC1 is involved in aging processes and therefore in the regulation of life span. The observation that dietary restriction increases the life span of biological systems has been linked to TORC1 and studies involving genetic or chemical downregulation of TORC1 led to an increased life span in yeast, worms, flies and mice.[106] Inhibition of TORC1 signaling by rapamycin (**144**) leads to a marked decrease of protein synthesis and induction of catabolic processes like autophagy. The cell exits from the cell cycle and enters a G0 state, also known as quiescence. TORC2 (~1.4 MDa) appears to be activated by membrane tension[107] and ribosomes.[108] Since the number of active ribosomes directly influences the growth capacity of a cell, TORC2 is only active in growing cells. It controls the organization of the actin cytoskeleton as well as endocytosis and is involved in the regulation of sphingolipid biosynthesis. In a simplified model, TORC1 regulates the temporal aspects of cell growth and TORC2 controls the spatial aspects. These central roles for cell viability make the TOR signaling network a target for disease and indeed deregulation is observed especially in cancer where rapid cell growth is often characteristic.[99a,b,109]

[106] (a) T. Vellai, K. Takacs-Vellai, Y. Zhang, A. L. Kovacs, L. Orosz, F. Müller, *Nature* **2003**, *426*, 620; (b) K. Jia, D. Chen, D. L. Riddle, *Development* **2004**, *131*, 3897–3906; (c) P. Kapahi, B. M. Zid, T. Harper, D. Koslover, V. Sapin, S. Benzer, *Curr. Biol.* **2004**, *14*, 885–890; (d) V. Wanke, E. Cameroni, A. Uotila, M. Piccolis, J. Urban, R. Loewith, C. De Virgilio, *Mol. Microbiol.* **2008**, *69*, 277–285; (e) D. E. Harrison, R. Strong, Z. D. Sharp, J. F. Nelson, C. M. Astle, K. Flurkey, N. L. Nadon, J. E. Wilkinson, K. Frenkel, C. S. Carter, M. Pahor, M. A. Javors, E. Fernandez, R. A. Miller, *Nature* **2009**, *460*, 392–395.

[107] For a recent review of TORC2, see: C. Gaubitz, M. Prouteau, B. Kusmider, R. Loewith, *Trends Biochem. Sci.* **2016**, *41*, 532–545.

[108] V. Zinzalla, D. Stracka, W. Oppliger, M. N. Hall, *Cell* **2011**, *144*, 757–768.

[109] (a) B. Seto, *Clin. Transl. Med.* **2012**, *1*, 29; (b) N. Husseinzadeh, H. D. Husseinzadeh, *Gynecol. Oncol.* **2014**, *133*, 375–381.

3.2 Concept of the Project

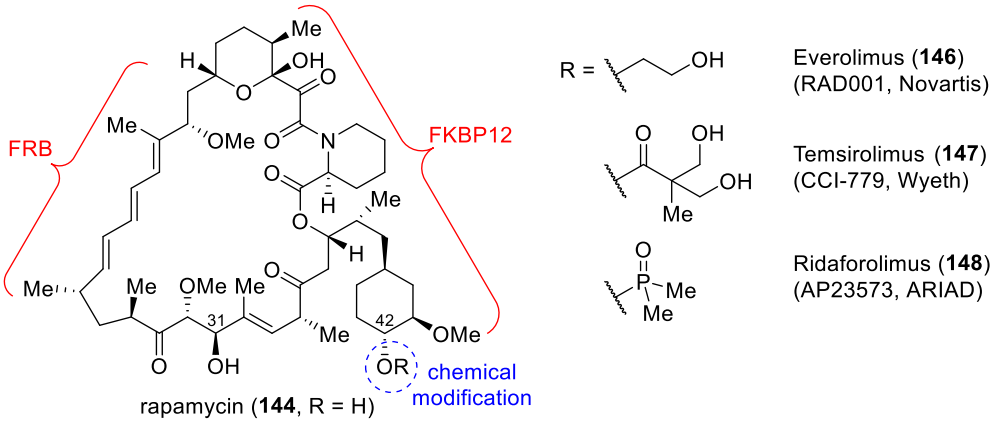

Figure 14: FRB and FKBP12 binding sites of rapamycin (**144**) and examples of derived drugs.

Although many biological aspects of TOR have been discovered and the constitutions of the multiprotein TORCs of different organisms have been reported,[99] their detailed molecular structures were largely unknown until very recently.[107] While for example the atomic structures of the FKBP12-rapamycin complex[110] as well as FKBP12-rapamycin complexed with the FKBP12-rapamycin binding domain (FRB) of human TOR[111] have been determined *via* X-ray crystallography in the 1990s, the fully assembled TORCs awaited characterization. Thus, structural features such as the exact alignment of the different proteins in the complex or the exact location of the TOR kinase pocket were uncertain. A low-resolution structure (26 Å) of human TORC1 obtained by cryo-electron microscopy (cryo-EM) was reported in 2010. The protein complex was obtained in small amounts from genetically modified cells using tandem affinity purification (TAP). A high-resolution (5.9 Å) structure of human TORC1, also obtained by cryo-EM, was eventually published in 2016 allowing for the complete assignment of the folded protein domains.[112] A low-resolution cryo-EM structure (26 Å) of yeast TORC2 was reported in 2015.[113] This study proved that the FRB of TORC2 was blocked by a protein named Avo3 and removal of a C-terminal part of Avo3 furnished rapamycin-sensitive TORC2.

[110] G. D. Van Duyne, R. F. Standaert, S. L. Schreiber, J. Clardy, *J. Am. Chem. Soc.* **1991**, *113*, 7433–7434.

[111] (a) J. Choi, J. Chen, S. L. Schreiber, J. Clardy, *Science* **1996**, *273*, 239–242; (b) J. Liang, J. Choi, J. Clardy, *Acta Crystallogr. D Biol. Crystallogr.* **1999**, *55*, 736–744.

[112] C. H. S. Aylett, E. Sauer, S. Imseng, D. Boehringer, M. N. Hall, N. Ban, T. Maier, *Science* **2016**, *351*, 48–52.

[113] C. Gaubitz, T. M. Oliveira, M. Prouteau, A. Leitner, M. Karuppasamy, G. Konstantinidou, D. Rispal, S. Eltschinger, G. C. Robinson, S. Thore, R. Aebersold, C. Schaffitzel, R. Loewith, *Mol. Cell* **2015**, *58*, 977–988.

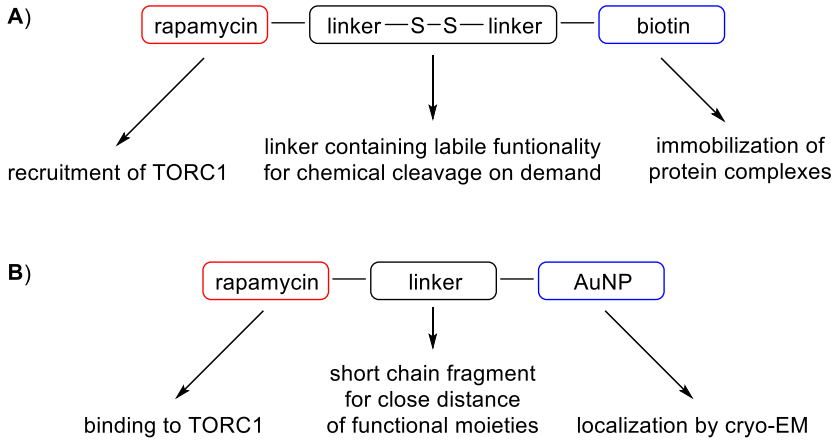

Figure 15: Schematic designs of rapamycin-based probes for the analysis of TORCs.

In 2014, we initiated our studies on the development of rapamycin-based probes which could be used for the structural analysis of TORCs. Considering the two protein binding sites of rapamycin (**144**), two hydroxyl groups at C31 and C42 seemed suitable for synthetic modifications of the macrolide (Figure 14). Reports on the deactivation of 31-*O*-alkylated compounds[114] and a comparison of commercial drugs like compounds **146**–**148** rendered the 42-hydroxyl group the function of choice for the introduction of additional molecular components. We devised two different molecular architectures for biochemical probes (Figure 15). The first design featured a rapamycin unit **144** tethered to a biotin molecule. Furthermore, the tether should contain a labile functional group, in this case a disulfide group, through which the probe could be chemically cleaved on demand. The resulting probe could be used to isolate TORC1 by pull-down experiments. The rapamycin moiety would recruit TORC1 from protein extract of genetically unmodified cells and the biotin moiety would be exploited for immobilization of the complexes *via* biotin-streptavidin binding. The purified complexes could then be collected by cleavage of the functional group in the linker. This technique might allow for the isolation of TORC1 on milligram-scale and thus enable X-ray crystallographic analysis of the complex. The second design featured a rapamycin unit **144** conjugated to gold nanoparticles (AuNPs) *via* a short linker. This assembly would allow for the tracking of FKBP12-rapamycin binding sites in TORCs by cryo-EM. A short linker between the macrolide and AuNPs would assure spatial confinement of the resulting probe and thus enable exact localization within the protein complex.

[114] R. Sedrani, S. Cottens, J. Kallen, W. Schuler, *Transplant. Proc.* **1998**, *30*, 2192–2194.

3.3 Results and Discussion

3.3.1 Synthesis of Rapamycin-Biotin Hybrids

At the onset of our studies, a technique allowing the selective modification of rapamycin (**144**) at the desired position 42 was needed. A process involving 31,42-*O*-disilylation of macrolide **144** followed by selective deprotection to yield a 31-*O*-silylated rapamycin derivative had been reported in the patent literature and this route had also been used by Wyeth in the production of temsirolimus (**147**).[115] However, this synthesis involves many steps and the monoprotected rapamycin derivative requires the need for activated coupling partners to react with the secondary 42-hydroxyl function. A more efficient procedure for the direct synthesis of rapamycin 42-*O*-esters was reported in 2005 by Wyeth researchers.[116] In an enzymatic transformation using either *Candida antarctica* lipase B or Amano lipase PS from *Burkholderia cepacia*, rapamycin (**144**) was selectively esterified in position 42 by different vinyl ester or acid anhydride precursors.

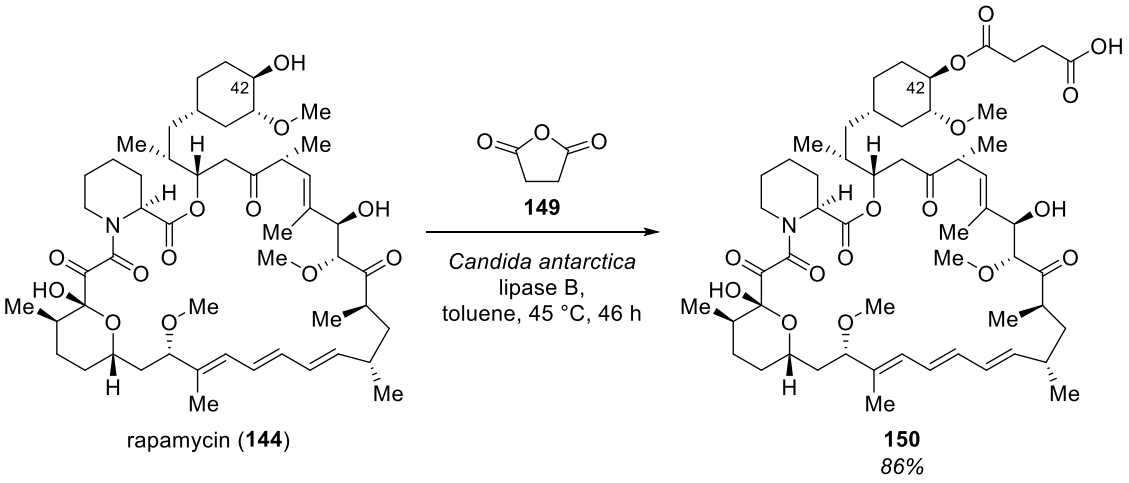

Scheme 31: Synthesis of rapamycin hemisuccinate (**150**) adopted from Gu *et al*.

Using *Candida antarctica* lipase B immobilized on polymer beads (Immobead 150) and succinic anhydride (**149**) in toluene at 45 °C for 46 h, rapamycin 42-*O*-hemisuccinate (**150**) was prepared in a single step (Scheme 31). The product **150** was isolated in 86% yield after chromatography over silica gel. This approach is very attractive as it circumvents the use of protecting groups minimizing the number of synthetic steps performed on the precious natural

[115] (a) C.-C. Shaw, J. Sellstedt, R. Noureldin, G. K. Cheal, G. Fortier (American Home Products Corporation), US 2001/0039338 A1, **2001**; (b) W. Chew, C.-C. Shaw (Wyeth), US 7153957 B2, **2004**.

[116] (a) J. Gu, M. E. Ruppen, P. Cai, *Org. Lett.* **2005**, *7*, 3945–3948; (b) J. Gu, P. Cai, M. E. Ruppen (Wyeth), US7268144 B2, **2005**.

product **144**. Furthermore, a free carboxylic acid group is introduced to the molecule providing a functional group that allows for selective targeting through amide coupling reactions.

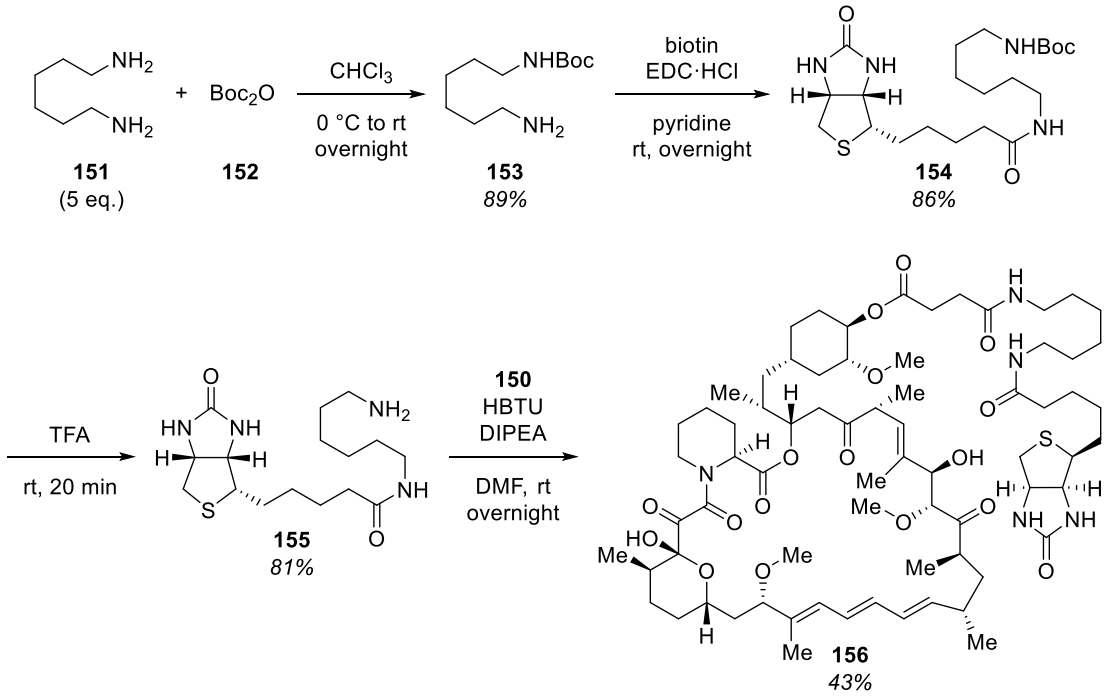

Scheme 32: Synthesis of rapamycin-biotin hybrid **156**.

With functionalized rapamycin derivative **150** in hands, we investigated the introduction of a biotin moiety (Scheme 32). Hexanediamine **151** was chosen as a preliminary test linker to investigate the synthesis of our probe architecture. Mono-Boc-protected linker **153** was obtained by treatment of excess diamine **151** (5 eq.) with di-*tert*-butyl dicarbonate (**152**) in chloroform.[117] The desired product **153** was obtained in 89% yield calculated from dicarbonate **152**. Linker **153** was then attached to biotin in an amide coupling reaction using EDC hydrochloride in pyridine providing compound **154** in 86% yield.[118] Boc-deprotection was achieved by treatment of the neat substance with TFA affording the biotin-linker fragment **155** in 81% yield.[118] A final peptide coupling reaction with rapamycin hemisuccinate **150** applying *O*-(benzotriazol-1-yl)-*N*,*N*,*N*′,*N*′-tetramethyluronium hexafluorophosphate (HBTU) in the presence of Hünig's base in DMF gave the all-carbon probe **156** in 43% yield after purification by preparative reversed-phase HPLC.

[117] C. Dardonville, C. Fernandez-Fernandez, S.-L. Gibbons, G. J. Ryan, N. Jagerovic, A. M. Gabilondo, J. J. Meana, L. F. Callado, *Bioorg. Med. Chem.* **2006**, *14*, 6570–6580.

[118] M. Collot, B. Sendid, A. Fievez, C. Savaux, A. Standaert-Vitse, M. Tabouret, A. S. Drucbert, P. M. Danzé, D. Poulain, J.-M. Mallet, *J. Med. Chem.* **2008**, *51*, 6201–6210.

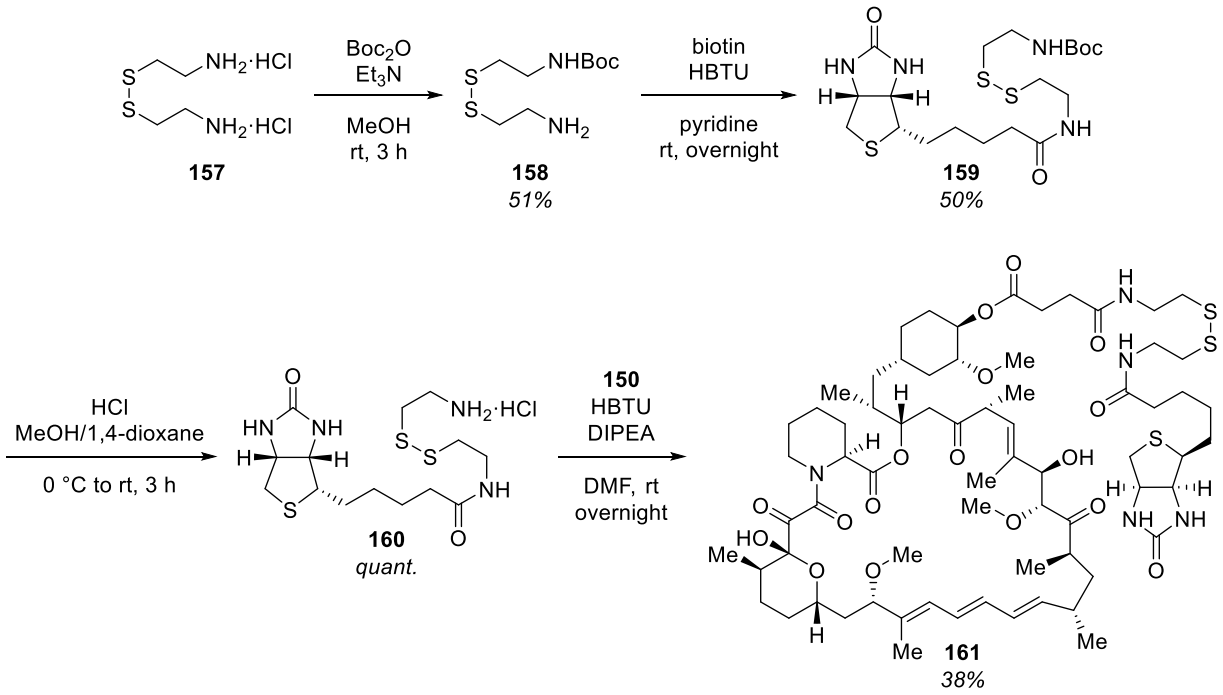

Scheme 33: Synthesis of rapamycin-biotin hybrid **161**.

For the cleavable rapamycin-based probe we exchanged the 1,6-hexanediamine fragment with cystamine. Thus, cystamine dihydrochloride (**157**) was also protected using di-*tert*-butyl dicarbonate requiring triethylamine to neutralize the starting material in this case. In a statistical reaction, mono-Boc cystamine (**158**) was produced in 51% yield. The following amide coupling with biotin was first attempted under same conditions used in the previous synthesis, but the desired product was not obtained. During the basic aqueous workup used to remove the urea byproduct of the coupling reagent the product **159** decomposed rapidly, most likely due to disulfide cleavage. When the mixture was concentrated after complete conversion of the substrates and the residue was subjected directly to purification by HPLC, the yield could be improved to 40%. The best results were obtained when HBTU was used instead of EDC hydrochloride providing compound **159** in 50% yield. Cleavage of the Boc protecting group also failed under our previous conditions using TFA and milder conditions were used instead. Treatment of compound **159** with hydrochloric acid in a methanol/1,4-dioxane (2:1) mixture afforded the desired biotin-linker fragment **160** as a hydrochloride salt in quantitative yield after HPLC purification. Peptide coupling with rapamycin hemisuccinate **150** under the same conditions used for probe **156** provided the desired rapamycin-based probe **161** in 38% yield on a 28 mg-scale following purification *via* HPLC.

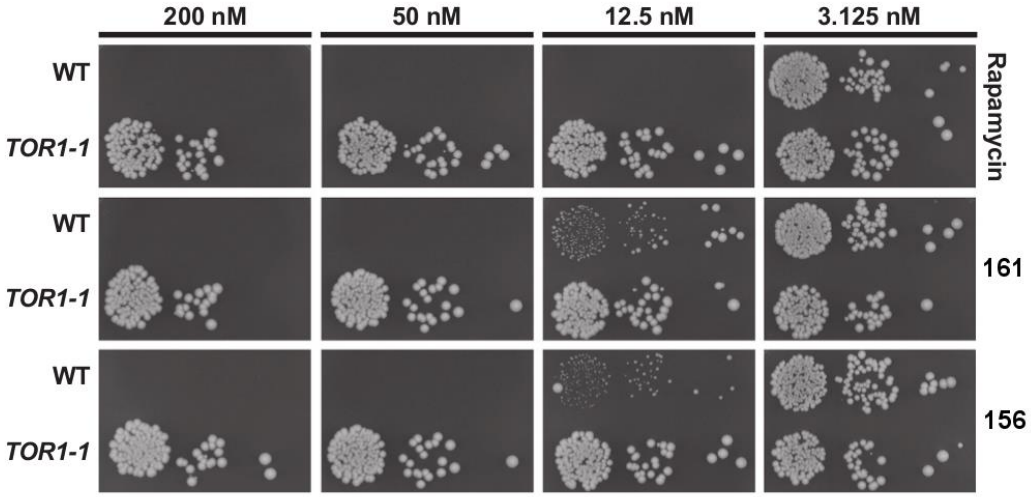

Figure 16: Toxicity test of all-carbon probe **156** (bottom) and disulfide probe **161** (middle) in four different concentrations against wild-type (WT) *Saccharomyces cerevisiae* and a rapamycin-resistant mutant (TOR1-1). Rapamycin (**144**) was used as a control (top).

Both probes **156** and **161** were then evaluated for their toxicity against two strains of *S. cerevisiae* (Figure 16).[119] Yeast cells were incubated in the presence of either probe **156** or **161** and rapamycin (**144**) was used as a control. All three compounds completely inhibited growth of wild-type (WT) *S. cerevisiae* at concentrations of 200 and 50 nM. Slow growth was observed with probes **156** and **161** at 12.5 nM concentration, whereas rapamycin (**144**) still showed complete inhibition. At 3.125 nM concentration, none of the substances displayed growth inhibitory effects. A rapamycin-resistant mutant of *S. cerevisiae* (TOR1-1) was not affected by the substances in any of the four concentrations. From these observations, we concluded that both compounds **156** and **161** were still active TOR inhibitors. While activity was slightly decreased compared to the parent compound **144** itself, the mode of action appeared to be unchanged, since rapamycin-resistant yeast was not impaired in the experiments.

The ability of probes **156** and **161** to recruit TORC1 from a yeast protein extract was evaluated next applying two different protocols.[119] In the first test, streptavidin beads were loaded with one of the probes, then saturated with biotin and washed extensively. The beads were incubated in yeast protein extract for 2.5 h at 4 °C and washed again. The isolated protein constituents were analyzed using gel electrophoresis with Coomassie brilliant blue staining or Western blot. In the second experiment, the individual probes were directly incubated in yeast protein extract, which had been partially depleted from biotinylated proteins. The probes were recovered from the extract using streptavidin beads and protein constituents were analyzed as mentioned above.

[119] Biological tests have been performed by Dr. Manoël Prouteau and Christl Gaubitz in the group of Prof. Dr. Robbie Loewith at the University of Geneva.

Unfortunately, both pull-down experiments were not successful and neither TORC1 nor any of the proteins involved in the complex were pulled down from the yeast protein extracts. Since the amount of isolated contaminants from the first experiments seemed to correlate to the amount of probe used to coat the streptavidin beads, we concluded that the probes bind to streptavidin. In combination with the toxicity observed against yeast cells, both biological functions of hybrids **156** and **161** appeared to be intact but were possibly exclusive and could not be exploited simultaneously, thus preventing the isolation of TORC1. Another reason for our observations could be fast enzyme-mediated hydrolysis of the probes.

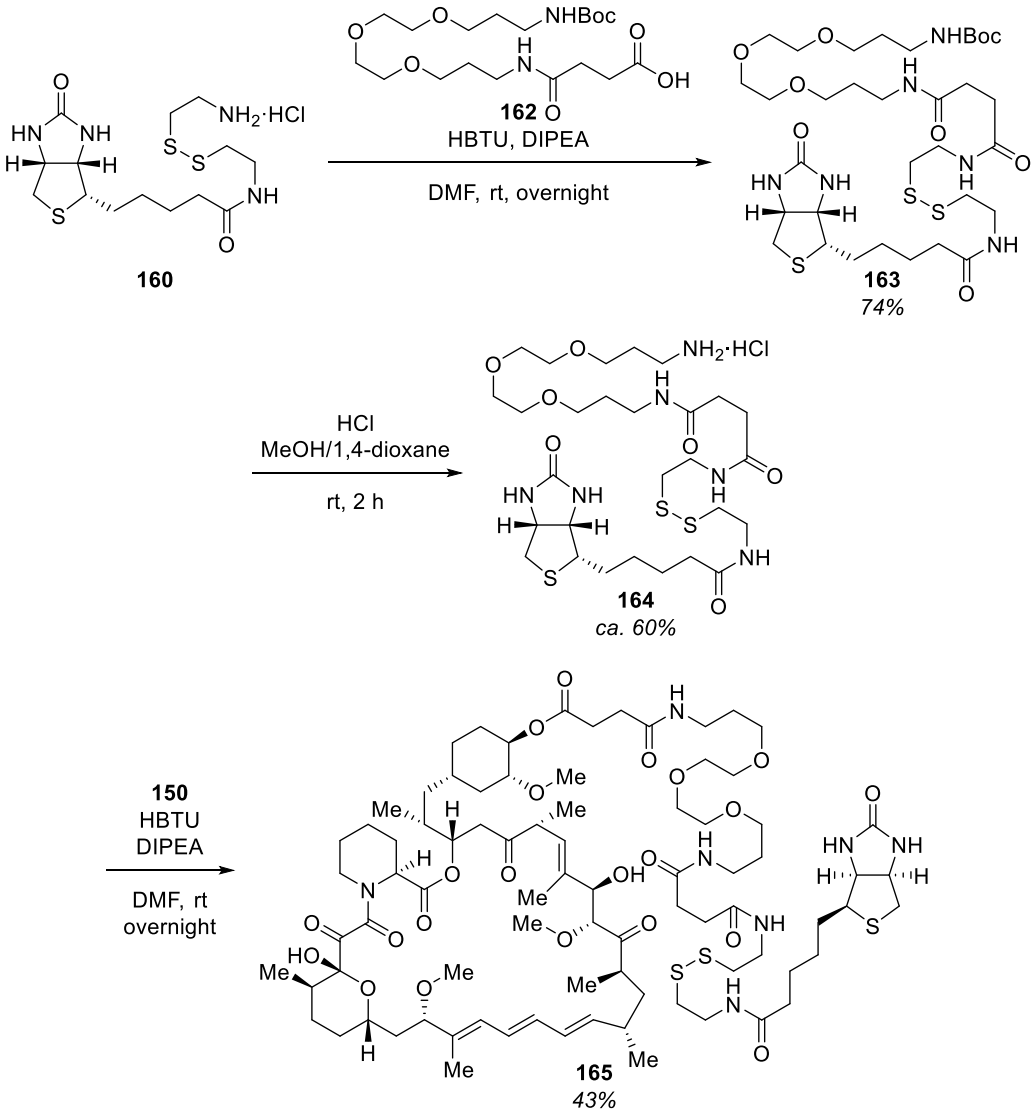

Scheme 34: Synthesis of elongated rapamycin-biotin hybrid **165**.

To test whether the short linking units used to connect the two biologically active moieties of hybrids **156** and **161** prevented simultaneous protein binding through steric encumbrance, we developed a new probe **165** featuring an extended linking unit (Scheme 34). In order not to introduce too many apolar fragments to the probe, which might result in undesired hydrohpobic effects and prevent a stretched conformation of the molecule in solution, we chose a polar chain fragment. Elongation of the linker was achieved by coupling the disulfide-containing fragment **160** with commercially available *N*-Boc-*N'*-succinyl-4,7,10-trioxa-1,13-tridecanediamine (**162**). Use of HBTU in the presence of Hünig's base provided the desired product **163** in 74% after purification by HPLC. The Boc protecting group was removed by treatment with hydrochloric acid in a mixture of methanol/1,4-dioxane (1:1) giving the crude hydrochloride salt **164** in about 60% yield. Peptide coupling with rapamycin hemisuccinate **150** under the previously developed conditions afforded extended probe **165** in 43% yield following HPLC purification. Thus, the yield of the final step assembling hybrids **156**, **161** and **165** remained very constant throughout the study. The extended rapamycin-biotin hybrid **165** awaits biological evaluation.

3.3.2 Synthetic Studies towards a Rapamycin-Gold Nanoparticle Conjugate

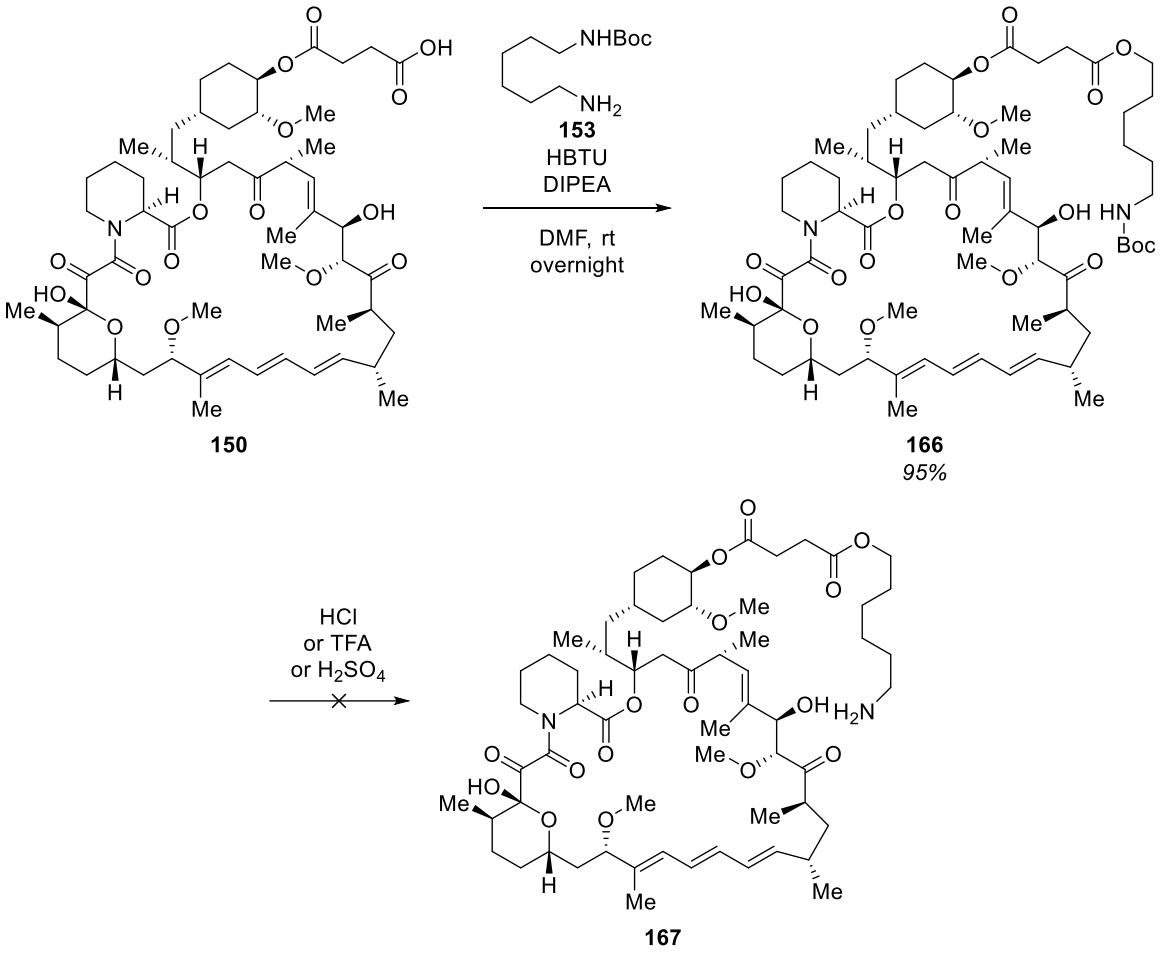

Scheme 35: Synthetic efforts towards a rapamycin derivative bearing an amino-terminated side chain.

To generate a rapamycin-AuNP conjugate, we planned to use commercially available AuNPs, which are stabilized by phosphine ligands presenting carboxylate groups to the outside of the particles. Such AuNPs enable the attachment of additional molecular fragments through peptide coupling. Therefore, the synthesis of a rapamycin derivative with a short linker chain bearing a terminal amine function was investigated (Scheme 35). Initial attempts focused on the use of mono-Boc-protected diamine **153** and peptide coupling with rapamycin hemisuccinate **150** was performed using HBTU in the presence of Hünig's base providing derivative **166** in 95% yield after flash chromatography. Unfortunately, cleavage of the Boc protecting group failed under various conditions. When solutions of hydrochloric acid in either 1,4-dioxane (commercial) or methanol (commercial or prepared by addition of AcCl to methanol) were applied at 0 °C, partial formation of a species with the correct mass was indicated by UPLC-MS analysis along with side product formation. After quenching with either aqueous sodium bicarbonate or a mild basic ion-exchange resin followed by extraction, only complex mixtures were obtained. A decrease in temperature slowed down conversion of the starting material while experiments at

room temperature resulted in fast decomposition. Treatment of compound **166** TFA in dichloromethane at 0 °C also led to decomposition of the substrate. A protocol that had been developed to synthesize temsirolimus (**147**) described a high-yielding reaction of a semisynthetic intermediate in a mixture of THF and 2 N sulfuric acid (2:1) for 88 h at 0–5 °C.[115a] When compound **166** was reacted under the same conditions, only slow decomposition was observed.

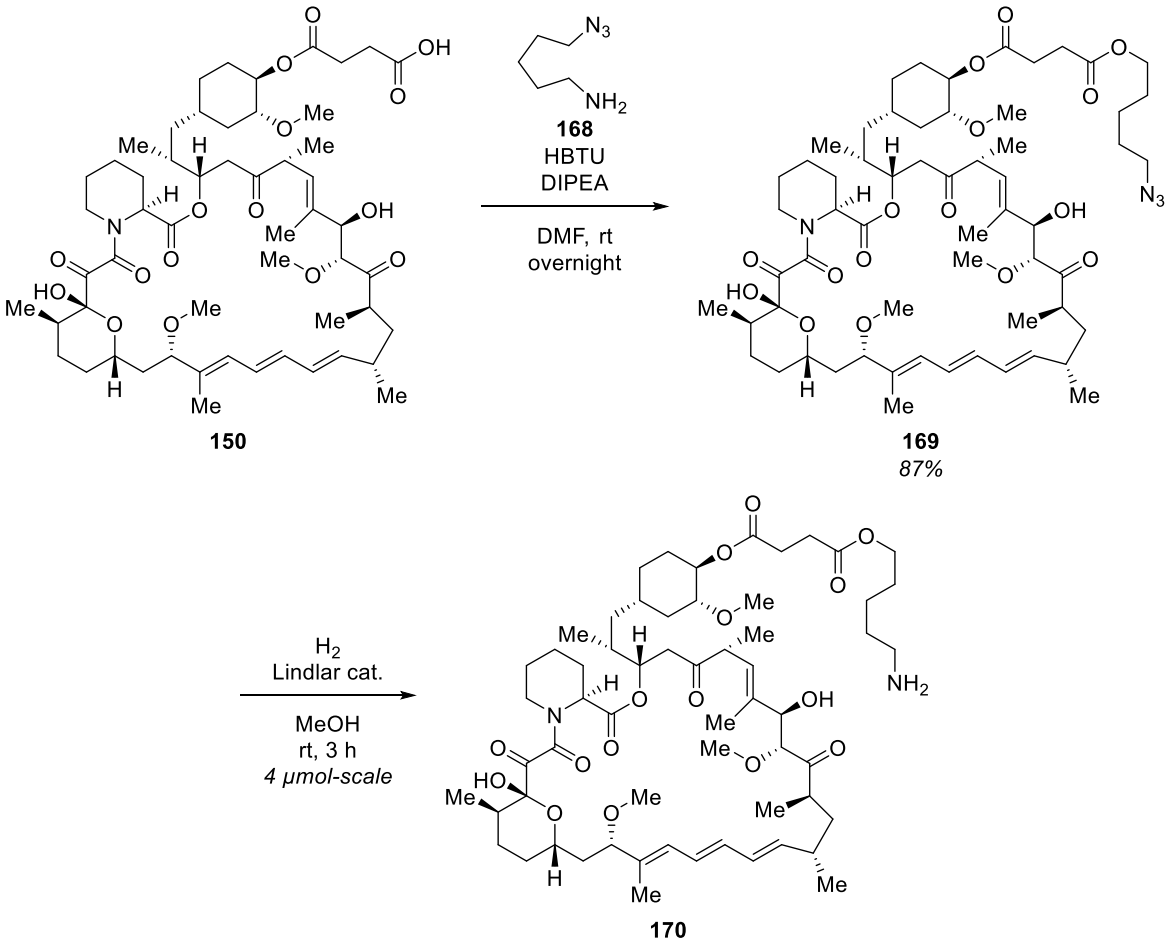

Scheme 36: Synthesis of rapamycin derivative **170** bearing an amino-terminated side chain for conjugation to AuNPs.

At this point, the synthetic strategy was changed to the use of a terminal azide instead of the Boc-protected amino group. Known 5-azidopentan-1-amine (**168**) was prepared following published procedures to serve as the linker fragment.[120] Peptide coupling with rapamycin hemi-succinate **150** using HBTU and Hünig's base afforded azido derivative **169** in 87% yield after flash chromatography. Transformation of the azide function *via* the Staudinger reduction was investigated first.[121] When compound **169** was treated with triphenylphosphine in a mixture of

[120] J. W. Lee, S. I. Jun, K. Kim, *Tetrahedron Lett.* **2001**, *42*, 2709–2711.

[121] H. Staudinger, J. Meyer, *Helv. Chim. Acta* **1919**, *2*, 635–646.

THF and water (3:1) at room temperature only very slow conversion of the substrate was observed and UPLC-MS analysis indicated decomposition. To avoid the formation of the iminophosphorane intermediate involved in the Staudinger reduction we briefly investigated hydrogenation of the azide function. A very mild procedure using the Lindlar palladium catalyst in methanol under a hydrogen atmosphere (1 atm) at room temperature[122] resulted in a clean reaction reaching full conversion after 3 h. Analysis of the crude mixture by UPLC-MS indicated formation of a single product with the correct mass. Due to the small scale, on which this reaction was performed (4 µmol), additional investigations need to be performed. The obtained substance decomposed within 48 h at 4 °C suggesting that the primary amino group possibly attacks the macrocycle.

[122] P. G. Reddy, T. V. Pratap, G. D. K. Kumar, S. K. Mohanty, S. Baskaran, *Eur. J. Org. Chem.* **2002**, 3740–3742.

3.4 Conclusion

The synthesis of three different rapamycin-biotin hybrid probes **156**, **161** and **165** was accomplished using a strategy that avoids the use of protecting groups on the macrolide natural product rapamycin (**144**) and thus minimizes the number of synthetic steps performed on this sensitive compound. While the two first generation hybrids **156** and **161** were shown to be active inhibitors of the molecular target of rapamycin (TOR), their application in the isolation of target of rapamycin complex 1 (TORC1) from a yeast protein extract of *S. cerevisiae* failed. As a rationale for these observations, we hypothesized the linking unit of the hybrids **156** and **161** might be too short. Consequently, the synthesis of an elongated rapamycin-biotin hybrid **165** was developed and the compound awaits biochemical evaluation. Investigations towards the synthesis of a rapamycin-gold nanoparticle conjugate established the synthesis of an amino-rapamycin derivative **170**. Further studies on the final formation of this compound and subsequent attachment to gold nanoparticles need to be performed.

4 Synthetic Studies on the *Securinega* Alkaloids[123]

4.1 The *Securinega* Alkaloids – A Literature Review

4.1.1 General Overview

Figure 17: *S. suffruticosa* in Bupyung, Korea (left)[124] and *F. virosa* on Maui, Hawaii (right).[125]

The *Securinega* alkaloids comprise a group of more than 60 known natural products found in plants of the Phyllanthaceae family and more precisely in the *Flueggea*, *Margaritaria*, *Phyllanthus* and *Securinega* genera.[126] These plants are commonly found in the subtropical zones of the Americas, Africa and Asia, and are broadly applied as traditional medicines in these regions. For example, the species *Securinega suffruticosa* and *Flueggea virosa* (Figure 17) — two rich and well-studied sources of *Securinega* alkaloids — have been used in Chinese folk medicine to treat a variety of symptoms such as lumbago, indigestion, impotence, rheumatism, infantile paralysis or eczema.[127] *F. virosa* was used to treat complications of the liver, kidneys, gall bladder, bladder and genitals as well as bilharzia in Senegalese medicine. In India, it was used against diabetes.[128] *Margaritaria discoidea* has been used in Guinean folk

[123] Parts of this chapter have been published: (a) R. Wehlauch, K. Gademann, *Asian J. Org. Chem.* **2017**, *6*, 1146–1159; (b) R. Wehlauch, S. M. Grendelmeier, H. Miyatake-Ondozabal, A. H. Sandtorv, M. Scherer, K. Gademann, *Org. Lett.* **2017**, *19*, 548–551.

[124] https://commons.wikimedia.org/wiki/File:Securinega_suffruticosa.JPG; Dalgial, CC BY-SA 3.0 license, accessed 05.10.2016.

[125] https://commons.wikimedia.org/wiki/File:Starr_070111-3247_Flueggea_virosa.jpg; Forest & Kim Starr, CC BY 3.0 license, accessed 05.10.2016.

[126] For a general review on *Securinega* alkaloids, see: E. Chirkin, W. Atkatlian, F.-H. Porée in *The Alkaloids, Vol. 74* (Ed.: H.-J. Knölker), Academic Press, London, **2015**, pp. 1–120.

[127] (a) B. Li, M. G. Gilbert, G. Fischer, C. A. Meyer in *Flora of China, Vol. 11* (Eds.: Z. Y. Wu, P. H. Raven, D. Y. Hong), Missouri Botanical Garden Press, St. Louis, **2008**, p. 178; (b) S. Qin, J.-Y. Liang, Y.-W. Guo, *Helv. Chim. Acta* **2009**, *92*, 399–403, and references therein.

[128] B. Oliver-Bever, *J. Ethnopharmacol.* **1983**, *7*, 1–93, and references therein.

medicine to treat malaria, diabetes and diarrhea among others.[129] *Phyllanthus niruri* has been used for the treatment of malaria and other diseases in India and China,[130] but also in Central Africa.[131] In West Africa, it was used as a stomachic.[128,132] Several groups have reported on the isolation of *Securinega* alkaloids from samples of *P. niruri* collected in India[133] and Thailand.[134] However, these alkaloids were not found in samples of the same species collected in Brazil.[135] This result might be explained by the different environmental conditions presented to the plants. Recently, it was shown that plant growth regulators influence the alkaloid content of *S. suffruticosa* callus cultures, and promotion as well as inhibition of alkaloid production was observed.[136] To date, no report has been published on the isolation of *Securinega* alkaloids from a plant sample collected in the Americas. Interestingly, *Securinega* alkaloids have been obtained from *Zygogynum pauciflorum*,[137] a species of the Winteraceae family found in New Caledonia. Since this family is not related to Phyllanthaceae, the study revealed a rare case of metabolic convergence. The Phyllanthaceae family of plants represents one of several Euphorbiaceae segregates and was classified in 2006.[138] Nevertheless, the *Securinega* alkaloids are often assigned to the Euphorbiaceae in the recent literature.

[129] M. S. T. Diallo, M. A. Baldé, A. Camara, M. S. Traoré, M. L. Bah, A. S. Diallo, A. K. Camara, S. Laurent, A. Roch, R. N. Muller, L. Maes, L. Pieters, A. M. Baldé, *J. Plant Sci.* **2015**, *3*, 40–46, and references therein.

[130] M. Zhou, H. Zhu, K. Wang, W. Wei, Y. Zhang, *Nat. Prod. Res.* **2012**, *26*, 762–764.

[131] P. Babady-Bila, T. E. Gedris, W. Herz, *Phytochemistry* **1996**, *41*, 1441–1443.

[132] For a recent review on the *Phyllanthus* genus, see: X. Mao, L.-F. Wu, H.-L. Guo, W.-J. Chen, Y.-P. Cui, Q. Qi, S. Li, W.-Y. Liang, G.-H. Yang, Y.-Y. Shao, D. Zhu, G.-M. She, Y. You, L.-Z. Zhang, *Evid. Based Complement. Alternat. Med.* **2016**, *in press*, doi:10.1155/2016/7584952.

[133] (a) N. B. Mulchandani, S. A. Hassarajani, *Planta Med.* **1984**, *50*, 104–105; (b) B. S. Joshi, D. H. Gawad, S. W. Pelletier, G. Kartha, K. Bhandary, *J. Nat. Prod.* **1986**, *49*, 614–620.

[134] P. Petchnaree, N. Bunypraphatsana, G. A. Cordell, H. J. Gowe, P. J. Cox, R. A. Howie, S. L. Patt, *J. Chem. Soc., Perkin Trans. 1* **1986**, 1551–1556.

[135] J. B. Calixto, A. R. S. Santos, V. Cechinel Filho, R. A. Yunes, *Med. Res. Rev.* **1998**, *18*, 225–258.

[136] D. Raj, A. Kokotkiewicz, A. Drys, M. Luczkiewicz, *Plant Cell Tiss. Organ Cult.* **2015**, *123*, 39–45.

[137] A. Ahond, J. Guilhem, J. Hamon, J. Hurtado, C. Poupat, J. Pusset, M. Pusset, T. Sévenet, P. Potier, *J. Nat. Prod.* **1990**, *53*, 875–881.

[138] P. Hoffmann, H. Kathriarachchi, K. J. Wurdack, *Kew Bull.* **2006**, *61*, 37–53.

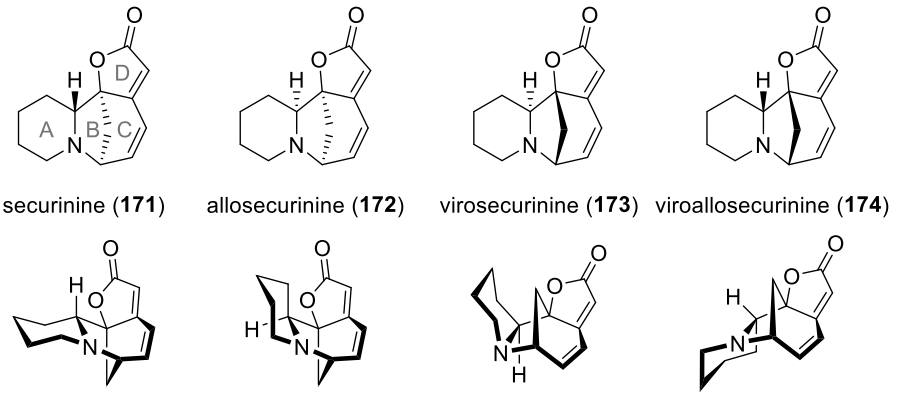

Figure 18: Two- and three-dimensional representations of securinine (**171**) and its stereoisomers.

In 1956, securinine (**171**) was isolated from *S. suffruticosa* by Murav'eva and Ban'kovskii as the first member of this alkaloid family (Figure 18).[139] Being the most abundant and best-studied *Securinega* alkaloid, it has been the major representative ever since. The tetracyclic structure of securinine (**171**) was elucidated independently by two research groups in 1962[140] and the correct absolute configuration was established by chemical degradation studies[141] and an X-ray crystal structure of securinine hydrobromide.[142] Total synthesis of the racemic natural product and chiral resolution by recrystallization with (+)-10-camphorsulfonic acid confirmed the structural and stereochemical assignments.[143] Another alkaloid isolated from *S. suffruticosa* showed great similarities to securinine (**171**)[140b] and was identified as the epimeric allosecurinine (**172**), in which the A and B rings are fused with an opposite configuration.[144] Surprisingly, the investigation of the alkaloid contents of *F. virosa* (synonymous with *S. virosa*) yielded yet another stereoisomer of securinine (**171**), which was found to be its enantiomer virosecurinine (**173**).[145] A systematic study of the two plant species and their metabolites then led to the last possible stereoisomer viroallosecurinine (**174**), the enantiomer of allosecurinine (**172**).[146] The study showed that while *S. suffruticosa* contained only securinine (**171**) and

[139] V. I. Murav'eva, A. I. Ban'kovskii, *Dokl. Akad. Nauk SSSR* **1956**, *110*, 998–1000.

[140] (a) S. Saito, K. Kotera, N. Sugimoto, Z. Horii, Y. Tamura, *Chem. Ind.* **1962**, 1652–1653; (b) I. Satoda, M. Murayama, J. Tsuji, E. Yoshii, *Tetrahedron Lett.* **1962**, *3*, 1199–1206.

[141] (a) S. Saito, K. Kotera, N. Shigematsu, A. Ide, Z. Horii, Y. Tamura, *Chem. Ind.* **1963**, 689; (b) S. Saito, K. Kotera, N. Shigematsu, A. Ide, N. Sugimoto, Z. Horii, M. Hanaoka, Y. Yamawaki, Y. Tamura, *Tetrahedron* **1963**, *19*, 2085–2099.

[142] S. Imado, M. Shiro, Z. Horii, *Chem. Pharm. Bull.* **1965**, *13*, 643–651.

[143] Z. Horii, M. Hanaoka, Y. Yamawaki, Y. Tamura, S. Saito, N. Shigematsu, K. Kotera, H. Yoshikawa, Y. Sato, H. Nakai, N. Sugimoto, *Tetrahedron* **1967**, *23*, 1165–1174.

[144] Z. Horii, Y. Yamawaki, Y. Tamura, S. Saito, H. Yoshikawa, K. Kotera, *Chem. Pharm. Bull.* **1965**, *13*, 1311–1318.

[145] T. Nakano, T. H. Yang, S. Terao, *Tetrahedron* **1963**, *19*, 609–619.

[146] S. Saito, T. Tanaka, T. Iwamoto, C. Matsumura, N. Sugimoto, Z. Horii, M. Makita, M. Ikeda, Y. Tamura, *J. Pharm. Soc. Jpn.* **1964**, *84*, 1126–1133.

allosecurinine (**172**), *S. virosa* contained exclusively their optical antipodes virosecurinine (**173**) and viroallosecurinine (**174**). However, leaves of the male plant of *S. suffruticosa* var. *amamiensis* contained both securinine (**171**) and virosecurinine (**173**) along with allosecurinine (**172**). Besides the very unusual distribution of stereoisomers, these observations also demonstrate the high diversity of alkaloid constituents in the different plants.

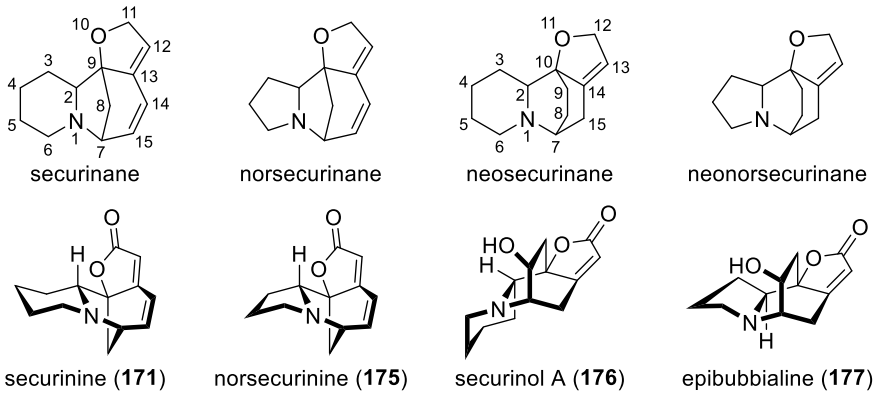

Figure 19: The *Securinega* alkaloid skeletons and representative natural products of each class.

The *Securinega* alkaloids can be divided into four groups based on their core structures (Figure 19). The compounds shown in Figure 18 share a securinane-type core, which is characterized by an azabicyclo[3.2.1]octane BC ring system with fused piperidine (A) and butenolide (D) rings. A homologous series of norsecurinane-type structure contains a pyrrolidine instead of the piperidine A ring; norsecurinine (**175**)[147] represents a member of this class. In contrast to securinine (**171**), only two natural stereoisomers of the lower homolog have been isolated, the second one being *ent*-norsecurinine.[133b] The numbering for the securinane and norsecurinane skeletons is identical except for the C6 position being omitted for norsecurinane-type alkaloids. Both groups comprise 14,15-dihydro derivatives with most of them bearing 15-hydroxy or -methoxy substituents. Also, numerous 4-hydroxy or -methoxy derivatives as well as combinations of both (*i.e.* 4,15-disubstituted 14,15-dihydro compounds) are known. The neosecurinane and neonorsecurinane skeletons are characterized by an azabicyclo[2.2.2]octane core with fused butenolide and either piperidine or pyrrolidine rings. The neosecurinane-type alkaloid securinol A (**176**) was isolated from *S. suffruticosa* in 1965 by Horii and coworkers.[148] The Japanese researchers found, that upon treatment with methanesulfonyl chloride and pyridine the compound was dehydrated to viroallosecurinine (**174**). Thus, securinol A (**176**) was assigned a 15-hydroxy-14,15-dihydrosecurinane-type structure. More than 25 years later,

[147] G. O. Iketubosin, D. W. Mathieson, *J. Pharm. Pharmacol.* **1963**, *15*, 810–815.

[148] Z. Horii, M. Ikeda, Y. Tamura, S. Saito, K. Kotera, T. Iwamoto, *Chem. Pharm. Bull.* **1965**, *13*, 1307–1311.

Arbain, Sargent and coworkers investigated the alkaloid contents of *Margaritaria indica* and revised the structure of securinol A (**176**).[149] Based on a comparison of NMR data of alkaloid **176** and other *Securinega* alkaloids, and ultimately on X-ray crystallographic analysis of securinol A hydrobromide, the neosecurinane-type structure shown in Figure 19 was established.

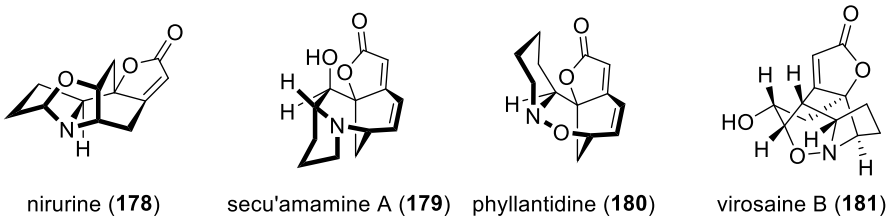

Figure 20: Examples of *Securinega* alkaloids with unusual skeletons.

Besides the four groups described so far, several alkaloids have been isolated possessing unprecedented structures, which do not fit the general motifs (Figure 20). Nirurine (**178**) was isolated from *Phyllanthus niruri* in 1986 by Cordell and coworkers, and its structure was elucidated by single crystal X-ray crystallography.[134] The pentacyclic compound has an additional oxazolidine ring formed by a C5-O-C8 bridge. Secu'amamine A (**179**), which was isolated from *S. suffruticosa* var. *amamiensis* in 2003 by Ohsaki, Kobayashi and coworkers, contains an extended B ring and thus an azabicyclo[3.3.1]nonane core with an additional carbon atom between the C2 and C9 atoms.[150] Its structure was assigned using spectroscopic methods, mainly NMR analysis, and was later confirmed by comparison with material obtained through total synthesis.[151,152] Also, isolation of the C3-OH epimer secu'amamine H from *F. suffruticosa* (synonymous with *S. suffruticosa*) was reported by Wang, Ye and coworkers in 2014.[153] An extended B ring was also observed for phyllantidine (**180**), which was isolated from *Phyllanthus discoides* in 1965 by Munavalli and Parello.[154] Structural elucidation by Munavalli, Horii and coworkers was based on spectroscopic methods as well as the characterization of chemical degradation products of phyllanthidine.[155] This alkaloid features an oxazabicyclo[3.3.1]nonane

[149] D. Arbain, A. A. Birkbeck, L. T. Byrne, M. V. Sargent, B. W. Skelton, A. H. White, *J. Chem. Soc., Perkin Trans. 1* **1991**, 1863–1869.

[150] A. Ohsaki, H. Ishiyama, K. Yoneda, J. Kobayashi, *Tetrahedron Lett.* **2003**, *44*, 3097–3099.

[151] P. Liu, S. Hong, S. M. Weinreb, *J. Am. Chem. Soc.* **2008**, *130*, 7562–7563.

[152] H. Han, A. B. Smith, III, *Org. Lett.* **2015**, *17*, 4232–4235.

[153] L. Zhou, B.-X. Zhao, R.-W. Jiang, X.-J. Huang, Z.-L. Wu, Y. Wang, W.-C. Ye, *J. Asian Nat. Prod. Res.* **2014**, *16*, 593–601.

[154] J. Parello, S. Munavalli, *C. R. Acad. Sci. Paris* **1965**, *260*, 337–340.

[155] Z. Horii, T. Imanishi, M. Yamauchi, M. Hanaoka, J. Parello, S. Munavalli, *Tetrahedron Lett.* **1972**, *19*, 1877–1880.

core with an additional oxygen atom between the N and C7 atoms. Interestingly, this compound can be obtained from allosecurinine (**172**) by oxidation with hydrogen peroxide. The structure of phyllantidine (**180**) was also confirmed by comparison with a fully synthetic sample.[156] Arguably the most complex structures among the monomeric *Securinega* alkaloids discovered so far were reported for the pseudoenantiomeric virosaines A and B (**181**), which were isolated from *F. virosa* by Zhang, Ye and coworkers in 2012.[157] The three-dimensional structures are best explained starting from a neonorsecurinane-type skeleton. The virosaines contain an additional oxygen atom between the N and C7 atoms as well as a bond between the C5 and C15 atoms. Their structures were determined using a combination of NMR spectroscopic, circular dichroism (CD) and X-ray crystallographic analyses, and were both confirmed by comparison with material obtained by total synthesis.[158,159]

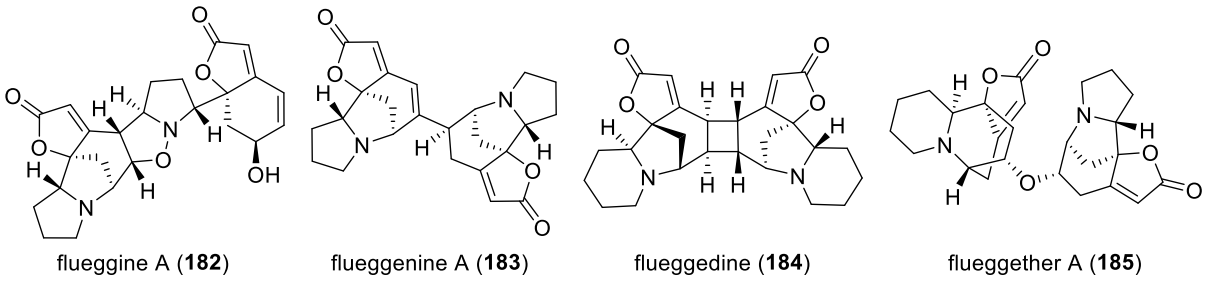

Figure 21: Examples of *Securinega* alkaloid dimers with different connectivity.

A large group within the *Securinega* alkaloids, of which many were only discovered recently, are oligomeric alkaloids. All known oligomers were isolated from *F. virosa* structurally spanning from dimeric to pentameric compounds.[126,160] The different dimers discovered so far display a large structural variety with respect to the modes of connectivity of the individual subunits (Figure 21). While most oligomers contain norsecurinane-type monomers (*e.g.* **182**

[156] C. A. Carson, M. A. Kerr, *Angew. Chem. Int. Ed.* **2006**, *45*, 6560–6563.

[157] B.-X. Zhao, Y. Wang, D.-M. Zhang, X.-J. Huang, L.-L. Bai, Y. Yan, J.-M. Chen, T.-B. Lu, Y.-T. Wang, Q.-W. Zhang, W.-C. Ye, *Org. Lett.* **2012**, *14*, 3096–3099.

[158] H. Miyatake-Ondozabal, L. M. Bannwart, K. Gademann, *Chem. Commun.* **2013**, *49*, 1921–1923.

[159] H. Wei, C. Qiao, G. Liu, Z. Yang, C. Li, *Angew. Chem. Int. Ed.* **2013**, *52*, 620–624.

[160] (a) L.-S. Gan, C.-Q. Fan, S.-P. Yang, Y. Wu, L.-P. Lin, J. Ding, J.-M. Yue, *Org. Lett.* **2006**, *8*, 2285–2288; (b) B.-X. Zhao, Y. Wang, D.-M. Zhang, R.-W. Jiang, G.-C. Wang, J.-M. Shi, X.-J. Huang, W.-M. Chen, C.-T. Che, W.-C. Ye, *Org. Lett.* **2011**, *13*, 3888–3891; (c) H. Zhang, C.-R. Zhang, K.-K. Zhu, A.-H. Gao, C. Luo, J. Li, J.-M. Yue, *Org. Lett.* **2013**, *15*, 120–123; (d) H. Zhang, W. Wei, J.-M. Yue, *Tetrahedron* **2013**, *69*, 3942–3946; (e) B.-X. Zhao, Y. Wang, C. Li, G.-C. Wang, X.-J. Huang, C.-L. Fan, Q.-M. Li, H.-J. Zhu, W.-M. Chen, W.-C. Ye, *Tetrahedron Lett.* **2013**, *54*, 4708–4711; (f) H. Zhang, Y.-S. Han, M. A. Wainberg, J.-M. Yue, *Tetrahedron* **2015**, *71*, 3671–3679; (g) H. Zhang, K.-K. Zhu, Y.-S. Han, C. Luo, M. A. Wainberg, J.-M. Yue, *Org. Lett.* **2015**, *17*, 6274–6277; (h) H. Zhang, Y.-S. Han, M. A. Wainberg, J.-M. Yue, *Tetrahedron Lett.* **2016**, *57*, 1798–1800; (i) G.-Y. Wang, A.-T. Wang, B.-X. Zhao, X.-P. Lei, D.-M. Zhang, R.-W. Jiang, Y. Wang, W.-C. Ye, *Tetrahedron Lett.* **2016**, *57*, 3810–3813.

and **183**), securinane- and neosecurinane-type subunits have been identified as well (e.g. **184** and **185**). The larger oligomers are structurally less diverse and primarily feature norsecurinane-type monomers connected *via* C-C bonds between the C12, C14 and C15 atoms (**186**–**188**, Figure 22).

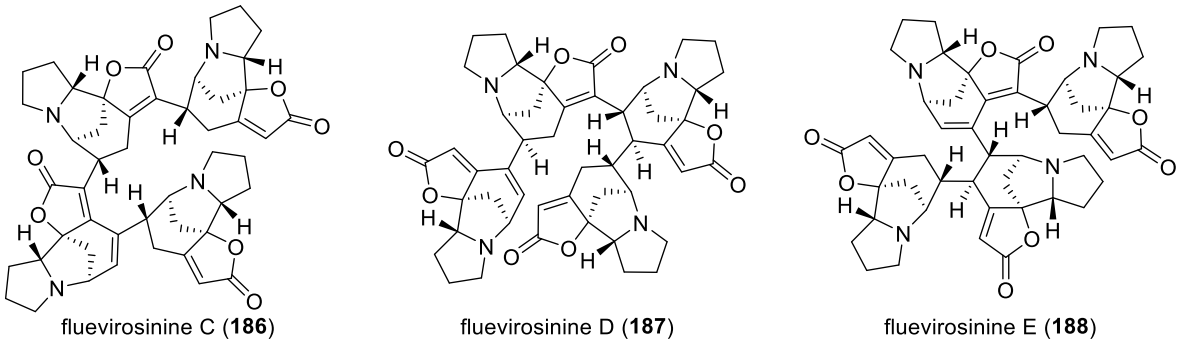

Figure 22: Examples of norsecurinine-based tetrameric *Securinega* alkaloids.

Due to the great structural analogy between the different alkaloids and the plethora of stereoisomers present, the field of *Securinega* alkaloids can be confusing and several discrepancies and errors have found their way into the literature. For example, after the structural revision of securinol A (**176**) in 1991,[149] it became obvious that several other known alkaloids like securinol B and C[148,161] or 14,15-dihydroallosecurinine-15β-ol[162] needed or still need to be reinvestigated. Also, the controversial interpretation of analytical data during the structural elucidation of different alkaloids raises questions about the integrity of the results. For example, CD spectroscopy has frequently been used to determine the absolute configuration of previously unknown compounds. The spectra of newly isolated alkaloids were compared to those of known ones to draw conclusions on the similarities and differences in absolute configuration. But whereas one study attributed the observation of an opposite Cotton effect to an inverted configuration at the AB ring fusion at C2 of neonorsecurinane-type alkaloids,[163] another study concludes inverted configurations at C7 and C10 in the bridged BC ring system of neosecurinane-type alkaloids from the same observation.[164]

[161] Z. Horii, M. Yamauchi, M. Ikeda, T. Momose, *Chem. Pharm. Bull.* **1970**, *18*, 2009–2012.

[162] J. L. Mensah, J. Gleye, C. Moulis, I. Fouraste, *J. Nat. Prod.* **1988**, *51*, 1113–1115.

[163] P. J. Houghton, T. Z. Woldemariam, S. O'Shea, S. P. Thyagarayan, *Phytochemistry* **1996**, *43*, 715–717.

[164] G.-C. Wang, Y. Wang, Q. Li, J.-P. Liang, X.-Q. Zhang, X.-S. Yao, W.-C. Ye, *Helv. Chim. Acta* **2008**. *91*, 1124–1129.

4.1.2 Biological Activities

The pharmacological value of plants from the *Flueggea*, *Margaritaria*, *Phyllanthus* and *Securinega* genera has been recognized a long time ago, which is proved by their widespread use in traditional medicine (cf. Section 4.1.1). The main alkaloid found in these plants is securinine (**171**) and thus most bioactivity studies have focused on the properties of securinine (**171**) and its stereoisomers. Over the past 60 years, many studies have investigated the effects of either crude plant extracts or pure *Securinega* alkaloids on numerous biological systems. Different compounds have shown activity on the CNS, cytotoxicity against several cancer cell lines as well as antimicrobial activity and this research area has been reviewed in 2011[165] and 2014.[126]

Soon after securinine (**171**) had been isolated in 1956, the first pharmacological studies on this alkaloid were published. Securinine (**171**) was tested in different animal models including cats and mice, and CNS stimulant activity, primarily in the spinal cord, was reported.[166] Oral and subcutaneous administration of securinine (**171**) in low doses increase reflex action, cardiac activity, and muscular tone without causing any secondary effects.[128] Overdosage of securinine (**171**) leads to heavy convulsions of all skeletal muscles and eventually death due to respiratory arrest. The biological effects of securinine (**171**) are comparable to those of strychnine,[167] but its toxicity is at least ten times lower resulting in a larger therapeutic window.[168] In the Soviet Union, securinine nitrate was approved as a substitute for strychnine and marketed as a drug until the 1990s.[126] In 1985, Beutler and coworkers reported γ-aminobutyric acid (GABA) receptor antagonism for securinine (**171**) and 14,15-dihydrosecurinine, and thus identified a molecular target of these alkaloids for the first time.[169] However, while allosecurinine (**172**) and virosecurinine (**173**) did not show any GABA receptor binding affinity, both compounds exhibit convulsant activity suggesting that other biological targets are involved. Xu and Zhang reported in 2004 that daily oral administration of securinine (**171**) restored spatial cognitive function in rats, which had been treated with a high dose of β-amyloid protein (βAP) (25-35).[170]

[165] W. Zhang, J.-Y. Li, P. Lan, P.-H. Sun, Y. Wang, W.-C. Ye, W.-M. Chen, *J. Chin. Pharm. Sci.* **2011**, *20*, 203–217.

[166] A. D. Turova, Y. A. Aleshkina, *Farmakol. Toksikol.* **1956**, *19*, 11–17.

[167] S. L. Friess, R. C. Durant, E. R. Whitcomb, L. J. Reber, W. C. Thommesen, *Tox. Appl. Pharmacol.* **1961**, *3*, 347–357.

[168] H. Chang, *Chin. Med. J.* **1974**, *54*, 65.

[169] J. A. Beutler, E. W. Karbon, A. N. Brubaker, R. Malik, D. R. Curtis, S. J. Enna, *Brain Res.* **1985**, *330*, 135–140.

[170] L. Xu, J. Zhang, *Neurol. Res.* **2004**, *26*, 792–796.

βAP deposition and accumulation play a major role in Alzheimer's disease. The authors attributed this therapeutic effect to the alkaloid's interaction with the GABA receptor. Recent studies by Magaji and coworkers on the antipsychotic effect of the aqueous fraction of root bark extract from *F. virosa* (which constitutes more than 60% of the total extract) proved an antagonistic activity on dopamine D_1 receptors.[171]

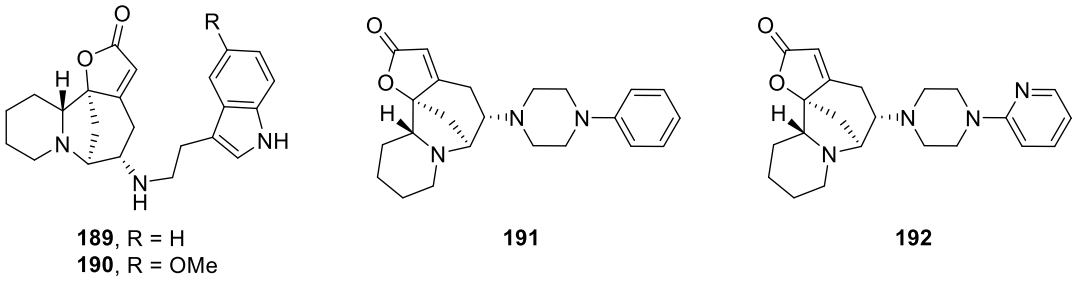

Figure 23: Semisynthetic securinine conjugates by Klochkov *et al*. showing activity on rat neurons as well as antioxidant activity. R = H, OMe.

Klochkov and coworkers investigated a series of semisynthetic securinine conjugates for their effect on kainic acid-induced currents in rat cerebellum Purkinje neurons (Figure 23).[172] It was shown that securinine (**171**) as well as the semisynthetic derivatives **189** and **191** increased currents when administered in low concentration regimes (10–100 nM), but blocked them at high concentrations (1–10 μM), confirming the CNS activity of these alkaloids. In a more recent study, the same group investigated similar compounds for their effect on Fe^{3+}-induced peroxide oxidation of lipids in rat-brain homogenates and reported antioxidant properties for derivatives **189**, **190** and **192**.[173] A group of Chinese researchers reported on the neuritogenic activity of different *Securinega* alkaloids and synthetic derivatives in 2016.[174] While the monomeric alkaloids securinine (**171**), securitinine and 15α-methoxy-14,15-dihydroallosecurinine showed only minimal effects on neurite outgrowth of mouse neuroblastoma (Neuro-2a) cells, the dimeric norsecurinamine B (**193**)[175] strongly promoted the formation and elongation of neurites

[171] (a) M. G. Magaji, J. A. Anuka, I. Abdu-Aguye, A. H. Yaro, I. M. Hussaini, *Afr. J. Tradit. Complement. Altern. Med.* **2008**, *5*, 147–153; (b) M. G. Magaji, M. Mohammed, R. A. Magaji, A. M. Musa, I. Abdu-Aguye, I. M. Hussaini, *Metab. Brain Dis.* **2014**, *29*, 161–165.

[172] S. G. Klochkov, S. V. Afanas'eva, V. V. Grigor'ev, *Chem. Nat. Compd.* **2008**, *44*, 197–202.

[173] S. G. Klochkov, M. E. Neganova, S. V. Afanas'eva, E. F. Shevtsova, *Pharm. Chem. J.* **2014**, *48*, 15–17.

[174] G. Tang, X. Liu, N. Ma, X. Huang, Z.-L. Wu, W. Zhang, Y. Wang, B.-X. Zhao, Z.-Y. Wang, F. C. F. Ip, N. Y. Ip, W.-C. Ye, L. Shi, W.-M. Chen, *ACS Chem. Neurosci.* **2016**, *7*, 1442–1451.

[175] Despite the compound being shown with a different configuration in ref. 172, the accompanying drawings and text clearly suggest that norsecurinamine B was investigated. Isolation of norsecurinamine B: G.-Y. Wang, A.-T. Wang, B.-X. Zhao, X.-P. Lei, D.-M. Zhang, R.-W. Jiang, Y. Wang, W.-C. Ye, *Tetrahedron Lett.* **2016**, *57*, 3810–3813.

(Figure 24). Several analogs have been prepared featuring different bridging units between the two alkaloid moieties and significant neuritogenic activity has been observed for compounds **194**. The percentage of differentiated cells observed after incubation with analogs **194** (25 μM) paralleled the positive control compound retinoic acid (10 μM) with a slightly reduced total neurite length. In 2007, Lubick and coworkers reported activity of securinine (**171**) against infections with *Coxiella burnetii* (Q Fever) in mice.[176] It was shown that the observed effect was not based on any bactericidal action of securinine (**171**), but due to innate immune cell stimulation resulting in enhanced macrophage clearance of phase II *C. burnetii*. A more than tenfold reduction of viable *C. burnetii* was observed in securinine-treated mice 96 hours after infection. A follow-up study together with Shipman and coworkers provided a detailed proteomic analysis of monocytes after exposure to securinine (**171**).[177] It was suggested that securinine (**171**) removed an inhibitor of monocyte immune response and thus led to the observed stimulation.

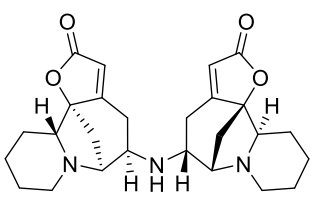

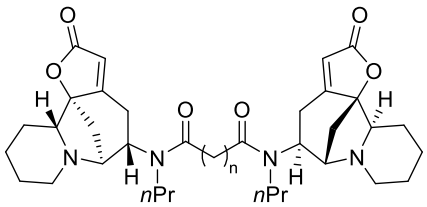

Figure 24: *Securinega* alkaloid dimers with neuritogenic activity.

The cytotoxic effects of *Securinega* alkaloids have been investigated in numerous studies and Table 6 gives an overview of the cell lines that were affected with IC_{50} values in the micromolar range. Significant growth inhibition and induction of apoptosis has been observed for various

[176] (a) K. Lubick, M. Radke, M. Jutila, *J. Leukoc. Biol.* **2007**, *82*, 1062–1069; (b) K. Lubick, M. Radke, M. Jutila, *J. Leukoc. Biol.* **2008**, *83*, 1068.

[177] M. Shipman, K. Lubick, D. Fouchard, R. Guram, P. Grieco, M. Jutila, E. A. Dratz, *PLoS ONE* **2012**, *7*, e41278.

human cancer cell lines including leukemia,[178] colon,[179,180,181] epidermoid,[181,182] lung,[181] ovarian,[183] cervical[184] and breast[160b,185] cancer cells. While the observed activities were not outstanding, the selectivity against certain cell lines is an important advantage of these agents. An example for this selectivity was reported by Wald and coworkers in 2010.[179] They investigated the effect of securinine (**171**) on human colon cancer HCT116 cells using two cell lines, one of which was protein p53-deficient ($p53^-$) while the other one was not ($p53^+$). They observed that apoptosis was induced in both cell lines, but with different efficiencies. A significantly lower IC_{50} value for the $p53^-$ cell line (17.5 μM) was observed compared to the $p53^+$ cell line (50 μM). Since protein p53 is inactivated in most human cancer cells, selective targeting of mutated cells might be possible. By knockdown experiments the authors showed that securinine (**171**) led to G2/M cell cycle arrest followed by p73-mediated apoptosis in $p53^-$ cells. While cell cycle arrest was also observed in $p53^+$ cells, induction of p21 led to recovery of the cells, which re-entered the cell cycle after 24 hours. A broad SAR study concerning the cytotoxicity of the *Securinega* alkaloids has not been published to date. However, there are also many natural congeners without any cytotoxic activity including phyllantidine (**180**),[182] secu'amamines B–D[182] and E–G,[186] virosaines A and B (**181**),[157] flueggenine B,[160a] flueggether A (**185**) and virosinine A,[160g] flueggether D,[160h] and the norsecurinine-derived tetra- and pentamers fluevirosinines B–J (*e.g.* **186**–**188**).[160f] Furthermore, the study published by Tatematsu, Lee and coworkers in 1991 included virosecurinine (**173**) and viroallosecurinine (**174**) along with five semisynthetic analogs.[181] Comparing the cytotoxic alkaloids from Table 6 to the listed non-cytotoxic compounds leads to the same conclusion, that the Japanese researchers already drew in 1991. The α,β,γ,δ-unsaturated lactone moiety is an essential

[178] (a) K. Gupta, A. Chakrabarti, S. Rana, R. Ramdeo, B. L. Roth, M. L. Agarwal, W. Tse, M. K. Agarwal, D. N. Wald, *PLoS ONE* **2011**, *6*, e21203; (b) N.-Z. Dong, Z.-L. Gu, *Acta Pharmacol. Sin.* **1999**, *20*, 267–270; (c) S. Han, G. Zhang, M. Li, D. Chen, Y. Wang, W. Ye, Z. Ji, *Oncol. Rep.* **2014**, *31*, 2245–2251.

[179] S. Rana, K. Gupta, J. Gomez, S. Matsuyama, A. Chakrabarti, M. L. Agarwal, A. Agarwal, M. K. Agarwal, D. M. Wald, *FASEB J.* **2010**, *24*, 2126–2134.

[180] (a) Y. Xia, C. Cheng, S. Yao, Q. Zhang, Y. Wang, Z. Ji, *Filotherapia* **2011**, *82*, 1258–1264; (b) C. Chen, Y. Xia, S. Yao, Q. Zhang, Y. Wang, Z. Ji, *Pharmazie* **2012**, *67*, 351–354.

[181] H. Tatematsu, M. Mori, T.-H. Yang, J.-J. Chang, T. T.-Y. Lee, K.-H Lee, *J. Pharm Sci.* **1991**, *80*, 325–327.

[182] A. Ohsaki, Y. Kobayashi, K, Yoneda, A. Kishida, H. Ishiyama, *J. Nat. Prod.* **2007**, *70*, 2003–2005.

[183] O. R. Johnson-Ajinwo, A. Richardson, W.-W. Li, *Phytomedicine* **2014**, *22*, 1–4.

[184] J. Stefanowicz-Hajduk, B. Sparzak-Stefanowska, M. Krauze-Baranowska, J. R. Ochoka, *PLoS ONE* **2016**, *11*, e0165372.

[185] M. Li, S. Han, G. Zhang, Y. Wang, Z. Yi, *Pharmazie* **2014**, *69*, 217–223.

[186] A. Ohsaki, T. Nagaoka, K. Yoneda, A. Kishida, *Tetrahedron Lett.* **2009**, *50*, 6965–6967.

structural feature for cytotoxic effects. Also, the relative configuration of the ring junction might be important, since securinine (**171**) and allosecurinine (**172**) as well as virosecurinine (**173**) and viroallosecurinine (**174**), respectively, do not exhibit similar cytotoxic effects.

Table 6: Overview of *Securinega* alkaloids and their activity against cancer cell lines.

Alkaloid	**Cell line (cancer type)**	**Ref.**
Securinine (**171**)	HCT116 (human colon cancer)	179
	SW480 (human colon cancer)	180
	KB (human epidermoid cancer)	182
	L1210 (murine lymphoma)	182
	HL60 (human leukemia)	178
	THP-1 (human leukemia)	178a
	OCI-AML3 (human leukemia)	178a
	OVCAR-8 (human ovarian cancer)	183
	A2780 (human ovarian cancer)	183
	A2780cis (human ovarian cancer)	183
	HeLa S3 (human cervical cancer)	184
	MCF-7 (human breast cancer)	185
Virosecurinine (**173**)	P-388 (murine leukemia)	181
	HCT-8 (human colon cancer)	181
	KB (human epidermoid cancer)	181
	A-549 (human lung cancer)	181
Viroallosecurinine (**174**)	P-388 (murine leukemia)	181
4-Epiphyllanthine	KB (human epidermoid cancer)	182
	L1210 (murine lymphoma)	182
Flueggine A (**182**)	MCF-7 (human breast cancer)	160b
	MDA-MD-231 (human breast cancer)	160b
	MCF-7/ADR (human breast cancer)	160b
Flueggine B	MCF-7 (human breast cancer)	160b
	MDA-MD-231 (human breast cancer)	160b
	MCF-7/ADR (human breast cancer)	160b
Flueggenine A (**183**)	P-388 (murine leukemia)	160a

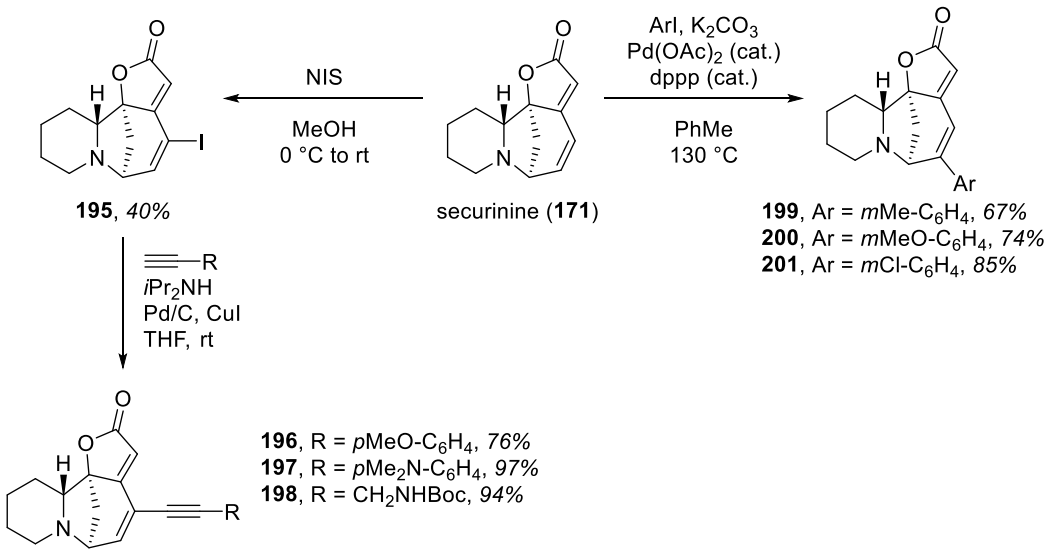

Scheme 37: Syntheses of semisynthetic securinine derivatives with cytotoxic properties reported by Fahy, Ratovelomanana-Vidal *et al*. Three of the most active compounds of each series are shown. dppp = 1,3-bis(diphenylphosphino)propane.

In early 2016, Fahy, Ratovelomanana-Vidal and coworkers published the first systematic study on the antineoplastic activity of semisynthetic securinine derivatives.[187] 14-Iodosecurinine (**195**) was synthesized in moderate yield by iodination with NIS and a series of 14-arylsecurinines was accessed through Suzuki coupling with different arylboronic acids (not shown). Cytotoxicity on human colon cancer HCT116 cells was investigated *in vitro* and while 80.9% growth inhibition was observed for iodosecurinine **195** after 72 h at a 1 µM concentration, no activity was observed for the arylated derivatives. The researchers then introduced an acetylene spacer and synthesized a second series (including compounds **196**–**198**) *via* Sonogashira coupling (Scheme 37, left). A total of 24 derivatives was generated, of which 23 compounds exhibited greatly improved growth inhibition compared to securinine (**171**). For the most active semisynthetic derivatives bearing aromatic and non-aromatic side chains, the cytotoxicity assay was expanded to also include the three human cancer cell lines A375 (melanoma), A549 (lung) and HL60 (leukemia). IC_{50} values in the nanomolar range were observed for all cell lines (Table 7). The same group reported a second study in early 2016 focusing on semisynthetic 15-arylsecurinine derivatives generated by Heck coupling of securinine (**171**) with different aryl iodides (Scheme 37, right).[188] While *ortho*-substituted aryl iodides did not react even under optimized conditions, 18 derivatives with *meta*- and *para*-substituents (including compounds **199**–**201**) as well as the unsubstituted phenyl derivative were synthesized. This series was

[187] M. Perez, T. Ayad, T. Maillos, V. Poughon, J. Fahy, V. Ratovelomanana-Vidal, *ACS Med. Chem. Lett.* **2016**, *7*, 403–407.

[188] M. Perez, T. Ayad, T. Maillos, V. Poughon, J. Fahy, V. Ratovelomanana-Vidal, *Eur. J. Med. Chem.* **2016**, *109*, 287–293.

evaluated for cytotoxicity against the HCT116 cell line and efficient growth inhibition was observed for *meta*-substituted 15-aryl derivatives. In the expanded assay including four cell lines, the most active compounds displayed IC_{50} values in the nanomolar range, thus even outperforming the compounds tested in the first study.

Table 7: IC_{50} values of the most active semisynthetic securinine derivatives against four human cancer cell lines reported by Fahy, Ratovelomanana-Vidal *et al*.

Compound	**IC_{50} [µM]**			
	HCT116	A375	A549	HL60
196	0.34	0.06	0.29	0.66
197	0.42	0.17	0.60	0.42
198	1.66	0.36	2.64	5.00
199	0.28	0.07	0.14	0.13
200	0.26	0.08	0.12	0.14
201	0.23	0.08	0.11	0.14
Securinine (**171**)	>10	6.1	>10	>10

Securinine (**171**) and related *Securinega* alkaloids have also been reported to show antimicrobial activity. In 1990, Fouraste and coworkers reported mild antibacterial activity of securinine (**171**) against *Escherichia coli*, *Enterococcus faecium*, *Mycobacterium smegmatis*, *Pseudomonas aeruginosa* and *Staphylococcus aureus* with minimal inhibitory concentrations of 500 µg/mL for all species except *E. faecium* where 1 mg/mL was necessary.[189] Antiprotozoal activity against *Plasmodium falciparum* (causative agent of malaria) was reported in the same year by Weenen, Nkunya and coworkers for extracts[190a] as well as pure securinine (**171**)[190b] isolated from *M. discoidea*. Quinn and coworkers have screened a natural product-based library using electrospray ionization Fourier transform ion cyclotron resonance mass spectrometry (ESI-FTICR-MS) and have recently identified *P. falciparum* deoxyuridine 5′-triphosphate nucleotidohydrolase (*Pf*dUTPase) as the molecular target of securinine-type natural products. Strong binding was observed for securinine (**171**), its three stereoisomers **172**–**174** and norsecurinine (**175**). IC_{50} values in the range of 17.1–82.4 µM were found for these compounds during the asexual- and gametocyte-stages of the parasite. Antiprotozoal activity of securinine (**171**) against *Toxoplasma gondii* (causative agent of toxoplasmosis) was reported by

[189] J. L. Mensah, I. Lagarde, C. Ceschin, G. Michel, J. Gleye, I. Fouraste, *J. Ethnopharmacol.* **1990**, *28*, 129–133.

[190] (a) H. Weenen, M. H. H. Nkunya, D. H. Bray, L. B. Mwasumbi, L. S. Kinabo, V. A. E. B. Kilimali, L. B. P. A. Wijnberg, *Planta Med.* **1990**, *56*, 368–370; H. Weenen, M. H. H. Nkunya, D. H. Bray, L. B. Mwasumbi, L. S. Kinabo, V. A. E. B. Kilimali, L. B. P. A. Wijnberg, *Planta Med.* **1990**, *56*, 371–373.

Ananvoranich and coworkers in 2011.[191] In this study, not only was an antiproliferative activity of securinine (**171**) with an IC_{50} of 9.8 µM observed, but also its ability to induce parasite differentiation from the actively replicating tachyzoite stage to the dormant encysted bradyzoite stage. Furthermore, Diallo, Baldé and coworkers reported on the activity of *Securinega* alkaloids in extracts from *M. discoidea* against *Trypanosoma brucei brucei* (causative agent of African trypanosomiasis, sleeping sickness) and *Trypanosoma cruzi* (causative agent of American trypanosomiasis, Chagas disease).[129,192] Interestingly, these authors did not observe any antibacterial activity against *S. aureus* and *E. coli* with concentrations up to 64 µg/mL. Also, no activity against *P. falciparum* was observed in this concentration range.

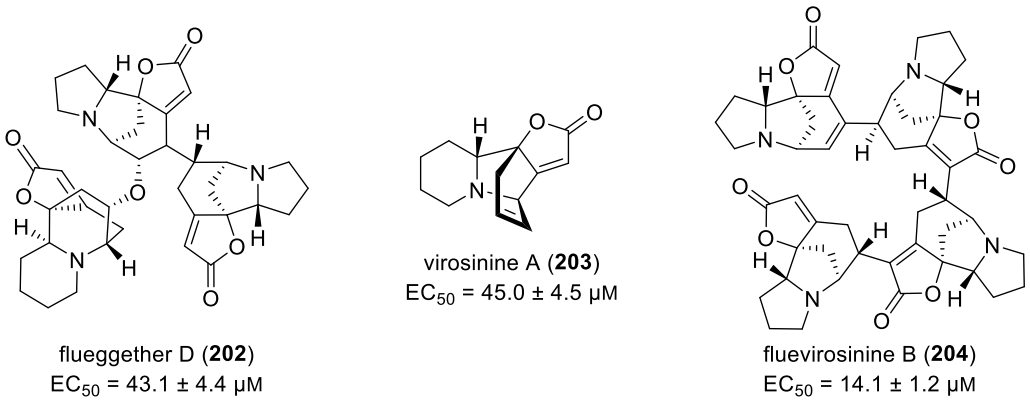

Figure 25: Examples of *Securinega* alkaloids with anti-HIV activity reported by Yue *et al*.

The team of Yue and coworkers reported the isolation of several *Securinega* alkaloids. Since 2015, they systematically tested these newly discovered natural products for their antiviral activity on HIV-1 NL 4-3 infected human T-lymphoblastoid MT-4 cells.[160f–h] Mild anti-HIV activity was observed for flueggethers A (**185**) and D (**202**), the structurally unusual virosinine A (**203**) and several of the norsecurinine-based tetra- and pentameric fluevirosinines (Figure 25). The observed half maximal effective concentrations (EC_{50}) typically ranged from 43.1 µM for flueggether D (**202**) to 139 µM for fluevirosinine I with the exception of fluevirosinine B (**204**) showing an EC_{50} of 14.1 µM. These compounds generally exhibited no or only marginal cytotoxicity with IC_{50} values >100 µM. From 2002 to 2008, Singh and coworkers investigated the antifungal activities of *ent*-norsecurinine,[193a] norsecurinine (**175**),[193b] allosecurinine

[191] M. Holmes, A. K. Crater, B. Dhudshia, A. N. Thadani, S. Ananvoranich, *Exp. Parasitol.* **2011**, *127*, 370–375.

[192] M. S. Traore, S. Diane, M. S. T. Diallo, E. S. Balde, M. A. Balde, A. Camara, A. Diallo, A. Keita, P. Cos, L. Maes, L. Pieters, A. M. Balde, *Planta Med.* **2014**, *80*, 1340–1344.

[193] (a) M. Goel, S. Maurya, V. B. Pandey, V. P. Singh, A. K. Singh, U. P. Singh, *Mycobiology* **2002**, *30*, 225–227; (b) S. Sahni, S. Maurya, U. P. Singh, A. K. Singh, V. P. Singh, V. B. Pandey, *Mycobiology*

(**172**)[193c] and securinine (**171**).[193d] These alkaloids were evaluated for their activities against spore germination of different plant pathogenic and saprophytic fungi including species from the *Alternaria*, *Curvularia*, *Colletotrichum* and *Helminthosporium* genera among others. Also, *Erysiphe pisi*, a causative agent of the pea powdery mildew, was tested. While all compounds were active, the best results were obtained with securinine (**171**) and allosecurinine (**172**). Complete inhibition of spore germination of some species was observed at concentrations as low as 200 ppm and strong growth inhibition of all investigated species was observed at 1000 ppm.

4.1.3 Biosynthesis

The biosynthesis of *Securinega* alkaloids was investigated by three different groups in the 1970s. Extensive feeding experiments of *S. suffruticosa* plants with radio-labeled compounds followed by extraction and chemical degradation of (mainly) securinine (**171**) established the biosynthetic origin of the *Securinega* alkaloids and led to the formulation of a plausible biogenetic pathway. Since the 1990s, several groups contributed to this area with refined proposals, many of which focused on the biogenesis of structurally unusual members.

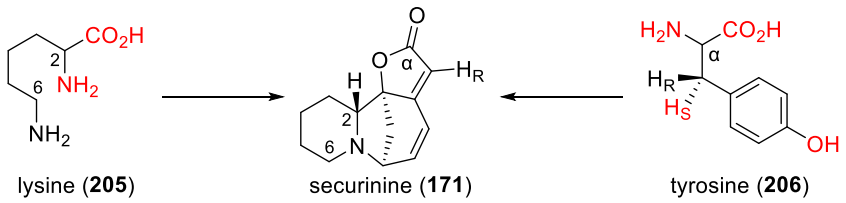

Scheme 38: Biogenetic origin of securinine. Only atoms shown in black were incorporated in the natural product.

The biosynthesis of the tetracyclic alkaloid core was first investigated in 1974. Parry investigated the origin of the CD ring fragment and feeding experiments using racemic [2-^{14}C]-tyrosine (**206**) yielded radioactive securinine (**171**, Scheme 38).[194] Administration of radio-labeled phenylalanine did not yield radioactive securinine (**171**) and suggested that *S. suffruticosa* is not able to convert phenylalanine into tyrosine (**206**). Furthermore, Parry predicted that, in analogy to other piperidine alkaloids, the piperidine A ring of securinine (**171**) is naturally derived from lysine (**205**). A study by Yamasaki and coworkers proved that this

2005, *33*, 97–103; (c) A. K. Singh, M. B. Pandey, U. P. Singh, *Mycobiology* **2007**, *35*, 62–64; (d) A. K. Singh, M. B. Pandey, S. Singh, A. K. Singh, U. P. Singh, *Mycobiology* **2008**, *36*, 99–101.

[194] R. J. Parry, *Tetrahedron Lett.* **1974**, *15*, 307–310.

was indeed the case.[195] Feeding experiments with racemic [2-^{14}C]-lysine, L-[U-^{14}C]-lysine (**205**) and [1,5-^{14}C]-cadaverine (**207**) gave radioactive securinine (**171**), whereas the administration of other radio-labeled compounds like DOPA (**1**) and tyramine did not lead to incorporation of the labels. The authors also noted that similar results were obtained for allosecurinine (**172**) suggesting that both alkaloids are formed *via* similar pathways. In 1975, Parry reported the administration of (3*R*)-[3-^{3}H]- and (3*S*)-[3-^{3}H]-tyrosine (**206**) to *S. suffruticosa* plants.[196] Securinine (**171**), that was biosynthetically derived from the (3*S*)-tritiated compound **206**, showed only 6% incorporation of tritium while the (3*R*)-tritiated compound **206** was incorporated in 72%. Since both chirally tritiated tyrosine (**206**) versions were only ca. 85% stereochemically pure, these results demonstrated the stereospecific abstraction of hydrogen from the *si* face during biosynthesis. A study by Spenser and coworkers followed in 1976 showing that the incorporation of lysine (**205**) was also proceeding in a non-symmetrical fashion.[197] When racemic [2-^{14}C]-lysine (**205**) or [2-^{14}C]-Δ^1-piperideine (**208**) were fed to the plants, the radio-label was specifically incorporated in the C2 position of securinine (**171**). Further experiments using [*RS*-6-^{3}H;6-^{14}C]-DL-lysine (**205**) indicated incorporation of the ε-nitrogen of lysine (**205**) into securinine (**171**) as loss of the ε-nitrogen would have been accompanied by at least partial loss of tritium, which was not observed.

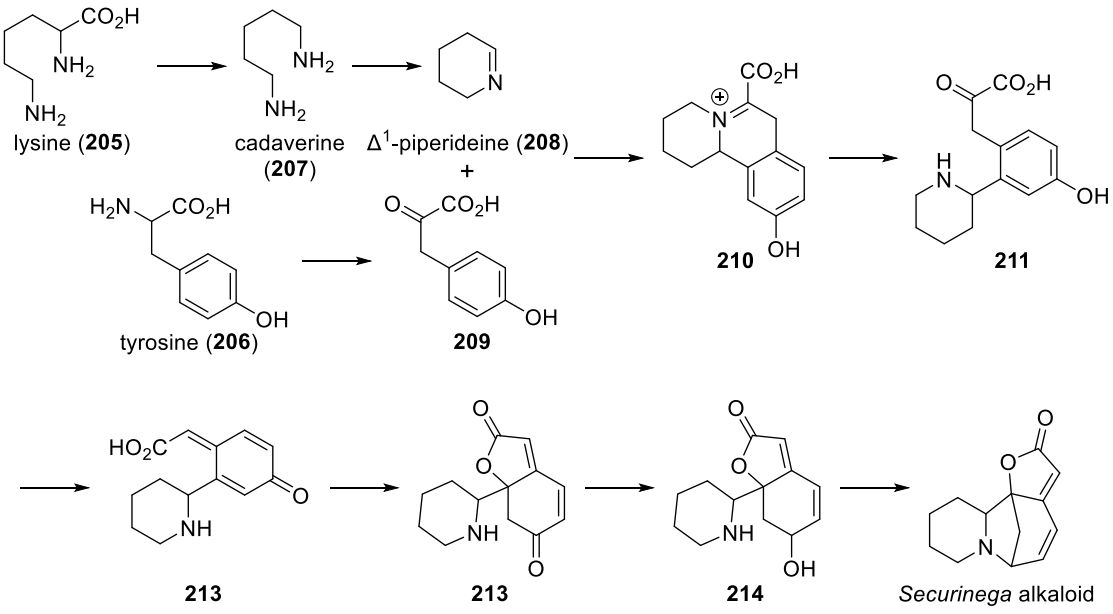

Scheme 39: General biogenetic pathway for *Securinega* alkaloids proposed in the 1970s.

[195] (a) U. Sankawa, K. Yamasaki, Y. Ebizuka, *Tetrahedron Lett.* **1974**, *15*, 1867–1868; (b) U. Sankawa, Y. Ebizuka, K. Yamasaki, *Phytochemistry* **1977**, *16*, 561–563.

[196] (a) R. J. Parry, *J. Chem. Soc., Chem. Commun.* **1975**, 144–145; (b) R. J. Parry, *Bioorg. Chem.* **1978**, *7*, 277–288.

[197] W. M. Golebiewski, P. Horsewood, I. D. Spenser, *J. Chem. Soc., Chem. Commun.* **1976**, 217–218.

Based on these results, a general biosynthetic pathway was formulated.[196,197] A similar biogenesis was expected for norsecurinine (**175**) involving ornithine instead of lysine (**205**). However, this pathway remains speculative and the detailed synthetic steps are still unknown. Since the neosecurinane-type alkaloids had not been discovered at the time, they were not considered in the investigations outlined above. Observations by Magnus and coworkers in the early 1990s provided some new insights on how securinane- and neosecurinane-type alkaloids might be linked biosynthetically.[198] During the total synthesis of nirurine (**178**), an unusual rearrangement of a synthetic intermediate was observed under Mitsunobu reaction conditions. Starting from an azabicyclo[2.2.2]octane substrate, an azabicyclo[3.2.1]octane product was obtained in high yield. The authors investigated this transformation and optimized it for use in the total synthesis of racemic norsecurinine ((±)-**175**, Scheme 40A). When intermediate (±)-**215** was treated with methanesulfonyl chloride in the presence of triethylamine, clean rearrangement was observed giving racemic norsecurinine ((±)-**175**) in 91% yield. This observation refuels speculation about the biogenesis of such compounds. From previously proposed biosynthetic intermediate **213**, two pathways become possible (Scheme 40B). The first scenario is a branched pathway leading to either neo(nor)securinane-type alkaloids *via* 1,6-addition of the amine and reduction of the carbonyl or (nor)securinane-type alkaloids by reduction and amination. The second possibility is a linear pathway, where intermediate **213** only forms neo(nor)securinane-type alkaloids, which are then rearranged to norsecurinane-type compounds through an aziridinium intermediate **216**. Although a possible biogenetic relevance of the transformation was noted by Magnus and coworkers, the resulting significance for the biogenesis of *Securinega* alkaloids was not pointed out. In the literature, only one report by Ye, Jiang and coworkers took note of this rearrangement and reproduced the earlier findings.[199]

Busqué, de March and coworkers suggested an alternative biosynthesis of intermediate **214** of the original proposal in 2008.[200] The isomeric natural products (–)-menisdaurilide ((–)-**217**) and (–)-aquilegiolide ((–)-**218**, Scheme 41A), originally isolated from *Aquilegia atrata* in 1984,[201]

[198] (a) P. Magnus, J. Ródriguez-López, K. Mulholland, I. Matthews, *J. Am. Chem. Soc.* **1992**, *114*, 383–385; (b) P. Magnus, J. Ródriguez-López, K. Mulholland, I Matthews, *Tetrahedron* **1993**, *49*, 8059–8072.

[199] N. Ma, Y. Yao, B.-X. Zhao, Y. Wang, W.-C. Ye, S. Jiang, *Chem. Commun.* **2014**, *50*, 9284–9287.

[200] G. G. Bardají, M. Cantó, R. Alibés, P. Bayón, F. Busqué, P. de March, M. Figueredo, J. Font, *J. Org. Chem.* **2008**, *73*, 7657–7662.

[201] A. Guerriero, F. Pietra, *Phytochemistry* **1984**, *23*, 2394–2396.

have also been isolated from plants of the genus *Phyllanthus*.[202] In 2006, the isolation of (+)-menisdaurilide ((+)-**217**) and (+)-aquilegiolide ((+)-**218**) along with securinine (**171**) and other alkaloids from *S. suffruticosa* was reported for the first time.[203] This study prompted the Spanish team to suggest these bicyclic lactones as biosynthetic intermediates of the *Securinega* alkaloids (Scheme 41B). The alternative route proposes formation of a CD ring subunit (**217** or **218**) from tyrosine (**206**). Vinylogous Mannich addition of either butenolide **217** or **218** with Δ^1-piperideine (**208**) or an equivalent C_5N unit would lead to formation of the previously proposed intermediate **214**. This strategy was realized in the total syntheses of allosecurinine (**172**) and viroallosecurinine (**174**, see Section 4.1.4).

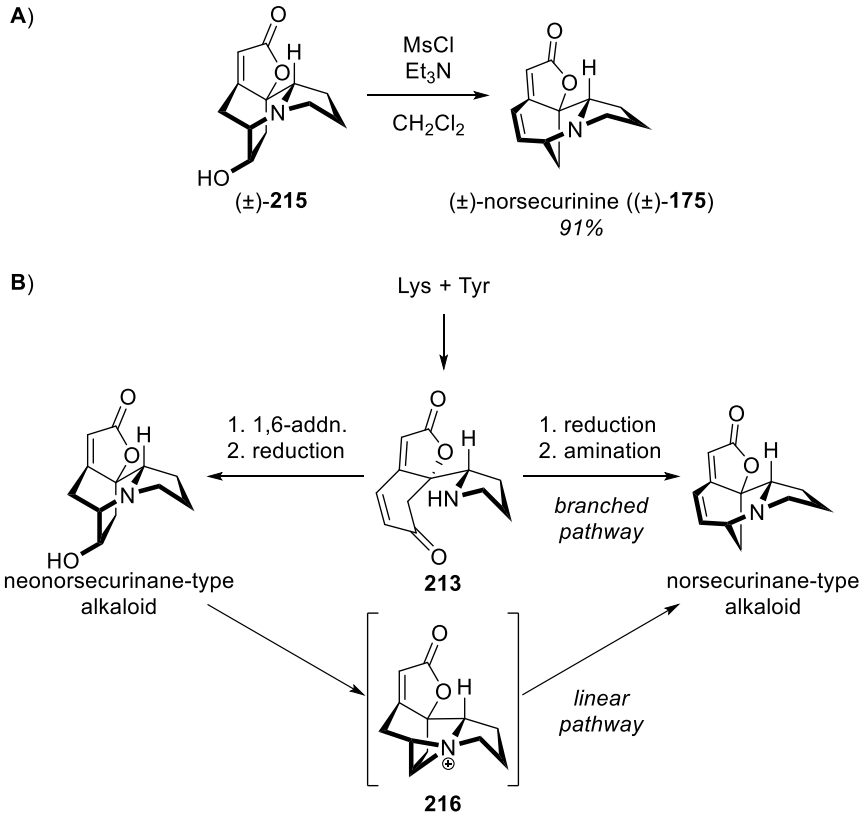

Scheme 40: A) Direct rearrangement of neonorsecurinane-type intermediate ((±)-**215**) to norsecurinane-type (±)-norsecurinine ((±)-**175**) reported by Magnus *et al*.; B) Possible biogenetic pathways for *Securinega* alkaloids. Similar pathways are expected for homologous alkaloids.

[202] (a) T. L. Bachmann, F. Ghia, K. B. G. Torssel, *Phytochemistry* **1993**, *33*, 189–191; (b) R. M. Kuster, W. B. Mors, H. Wagner, *Biochem. Syst. Ecol.* **1997**, *25*, 675; (c) J. Youkwan, P. Srisomphot, S. Sutthivaiyakit, *J. Nat. Prod.* **2005**, *68*, 1006–1009.

[203] Y. Wang, Q. Li, W.-C. Ye, F. Ip, N. Ip, S.-X. Zhao, *Zhongguo Tianran Yaowu* **2006**, *4*, 260–263; *Chem. Abstr.* **2006**, *146*, 518050.

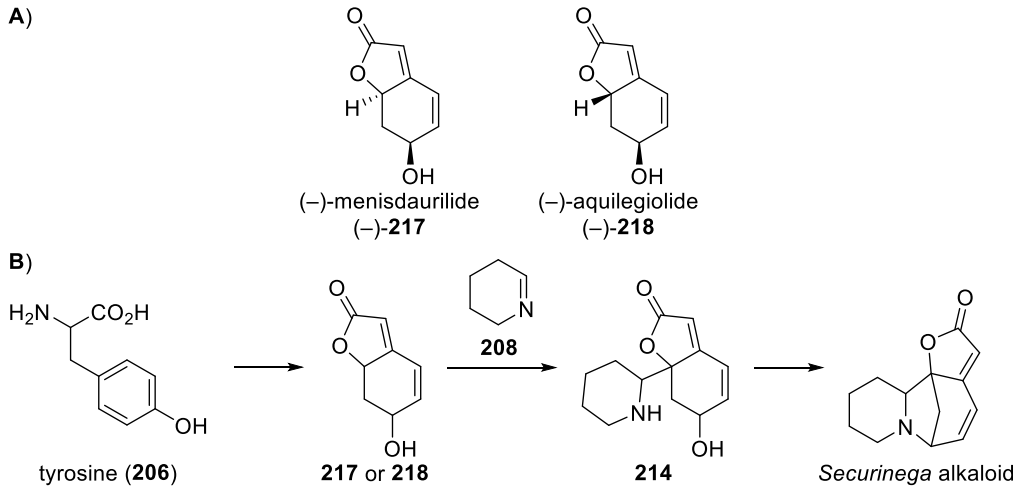

Scheme 41: A) Structures of natural lactones menisdaurilide (**217**) and aquilegiolide (**218**). B) Biosynthesis of *Securinega* alkaloids proposed by Busqué, de March *et al*.

Further biogenetic investigations and speculations concerned the structurally unusual *Securinega* alkaloids. Cordell and coworkers isolated nirurine (**178**) in 1986 and proposed a biosynthesis for the compound (Scheme 42A).[134] The authors suggested an intermediate **219** derived from ornithine and dopamine. Cyclization to prenirurine (**177**) followed by oxidative oxazolidine formation possibly *via* an additional iminium ion intermediate (not shown) would lead to the formation of nirurine (**178**). Prenirurine (**177**) was isolated from *Phyllanthus amarus* in 1996 and named epibubbialine.[163] Magnus and coworkers investigated the last cyclization step during their total synthesis of nirurine (**178**, Scheme 42B).[198a] When epibubbialine (**177**) was treated with *m*CPBA, nirurine (**178**) was formed but only in ca. 10% yield. The main product of this transformation was the tetracyclic compound **220** and it was concluded that the oxazolidine ring is probably formed earlier in the biosynthesis.

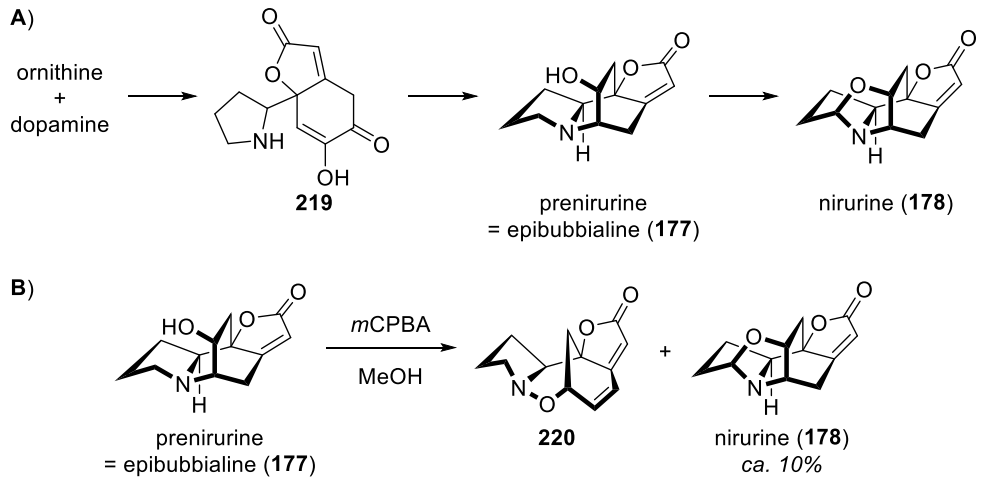

Scheme 42: A) Biogenesis of nirurine (**178**) proposed by Cordell *et al*. B) Experimental observations by Magnus *et al*.

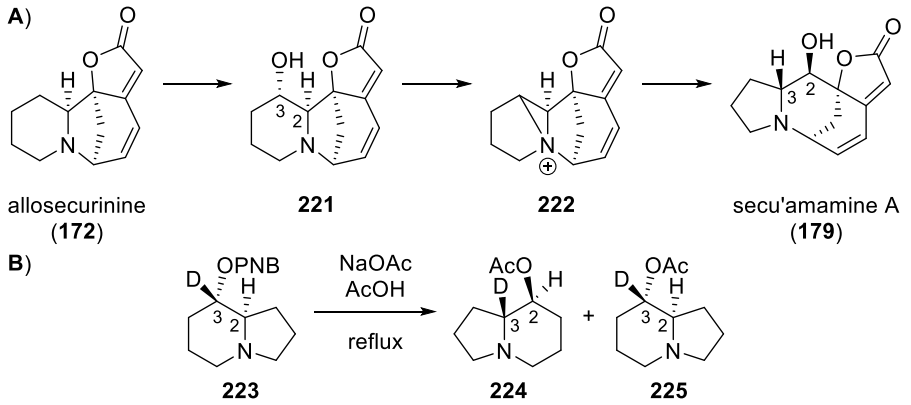

Scheme 43: A) Biosynthesis of secu'amamine A (**179**) proposed by Magnus *et al*. B) Model study providing evidence for an aziridinium ion intermediate. PNB = *para*-nitrobenzoyl.

In 2006, Magnus and coworkers proposed a biosynthesis for secu'amamine A (**179**, Scheme 43A).[204] Starting from allosecurinine (**172**), the authors hypothesized that oxidation to 3β-hydroxyallosecurinine (**221**) would give rise to a possible rearrangement. Formation of aziridinium intermediate **222** followed by the attack of water in the tertiary C2 position. Evidence for the existence of the putative aziridinium intermediate **222** was provided through a model system (Scheme 43B). When the deuterated ester **223** was treated with sodium acetate in refluxing acetic acid, two products were observed by ^{1}H NMR analysis. The desired rearranged product **224** along with the transesterified compound **225** was identified proving the possibility of this transformation in the less-strained bicyclic system.

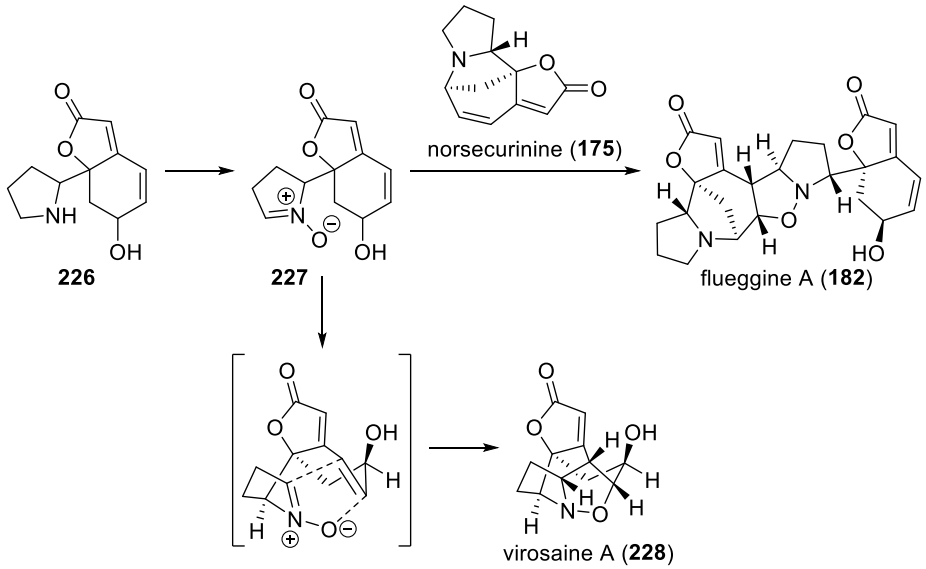

Scheme 44: Biosyntheses of virosaine A (**228**) and flueggine A (**182**) proposed by Wang, Ye *et al*.

[204] P. Magnus, A. I. Padilla, *Org. Lett.* **2006**, *8*, 3569–3571.

Along with the isolation of flueggine A (**182**)[160b] as well as virosaines A (**228**) and B (**181**),[157] Wang, Ye and coworkers provided a biosynthetic proposal for these compounds (Scheme 44). The authors speculated that the common intermediate **226** could be oxidized to nitrone **227**, which could either react with norsecurinine (**175**) in an intermolecular 1,3-dipolar cycloaddition or perform an intramolecular 1,3-dipolar cycloaddition to give virosaine A (**228**) or B (**181**). Viability of both transformations was indicated by DFT calculations[205] and all three natural products were synthesized using this strategy.[158,159,199]

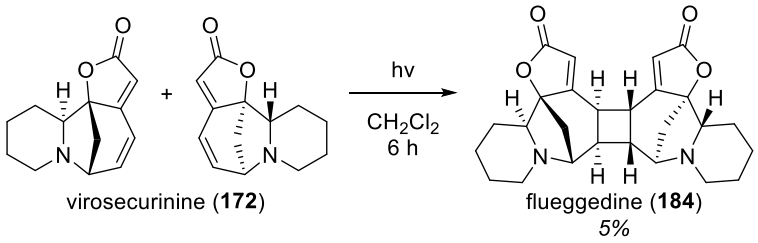

Scheme 45: The photodimerization of virosecurinine to flueggedine reported by Zhu, Chen, Ye *et al*.

After the isolation of flueggedine (**184**), Zhu, Chen, Ye and coworkers deduced the compound was formed from virosecurinine (**172**) by a [2+2] cycloaddition (Scheme 45). When a solution of virosecurinine (**172**) in dichloromethane was irradiated with UV light, the formation of flueggedine (**184**) was observed. Even though dimer **184** was obtained in only 5% yield, it was the only photodimer formed in the reaction and 90% of starting material **172** were recovered.

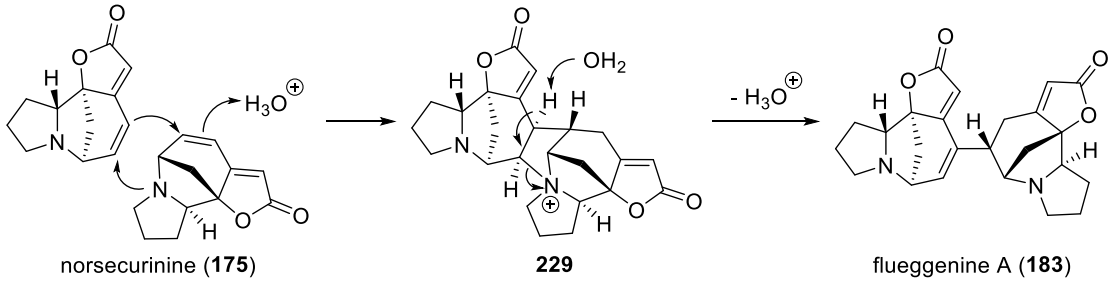

Scheme 46: Biosynthesis of flueggenine A (**183**) proposed by Yue *et al*.

Biosyntheses of other *Securinega* alkaloid oligomers were proposed by Yue and coworkers. For example, biosynthetic dimerization of norsecurinine (**175**) could proceed *via* an acid-catalyzed cycloaddition/ring-opening sequence involving an ammonium ion intermediate **229** to give flueggenine A (**183**, Scheme 46).[160c] Using different monomer units or performing a similar transformation on the D ring double bond would explain the different connectivity observed among the oligomers.[160f]

[205] P. P. Painter, R. P. Pemberton, B. M. Wong, K. C. Ho, D. J. Tantillo, *J. Org. Chem.* **2014**, *79*, 432–435.

4.1.4 Total Synthesis of *Securinega* Alkaloids

Numerous synthetic studies on the *Securinega* alkaloids have been published and more than 20 papers have reported the total synthesis of one or several members of the compound family (Table 8).[206] Most approaches targeted the azabicyclo[3.2.1]octane-based alkaloids securinine (**171**), norsecurinine (**175**) and their stereoisomers. But also different members featuring an azabicyclo[2.2.2]octane core such as nirurine (**178**),[198] virosine A[207] and bubbialidine[158] as well as compounds with an unusual structure like virosaines A (**228**)[158] and B (**181**)[159] or flueggine A (**182**)[159,199] have been synthesized. While a number of innovative strategies have been developed for the construction of the tetracyclic *Securinega* alkaloid core, different motifs have reoccurred over time and certain transformations have proven exceptionally useful.

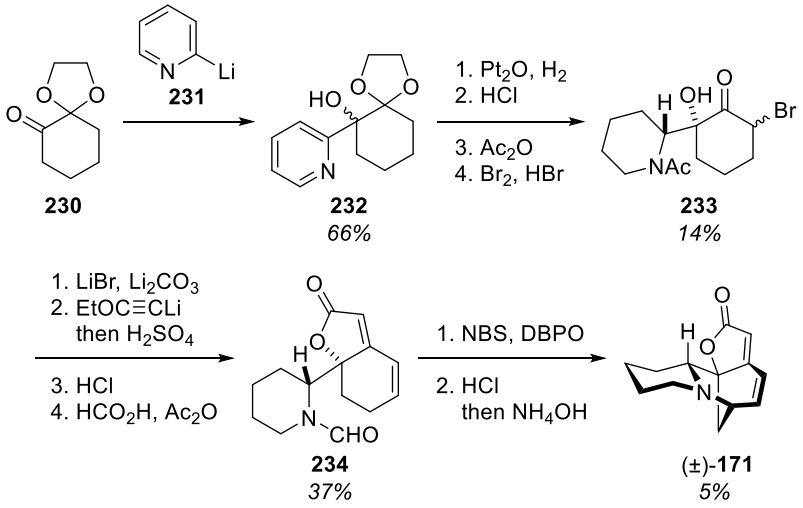

Scheme 47: The first total synthesis of racemic securinine (**171**) reported by Horii *et al*. in 1967. DBPO = dibenzoyl peroxide.

The first total synthesis focused on securinine (**171**) and has been reported by Horii and coworkers in 1967,[143] right after their structural determination of the compound. The synthesis started with ketal **230**, which was reacted with 2-pyridinyllithium (**231**), the two fragments representing rings C and A of the final natural product, respectively (Scheme 47). The pyridine **232** was reduced by hydrogenation affording diastereomers and the ketal group was cleaved using hydrochloric acid. The amine was protected with acetic anhydride and diastereomers were separated at this stage. By comparison with a degradation product of securinine (**171**) the major isomer was identified to possess the correct relative configuration and bromination afforded intermediate **233** in 14% yield. The unsaturation in the C ring was achieved by elimination of hydrogen bromide and the D ring was installed by addition of lithium ethoxyacetylide followed by acidic hydrolysis. The acyl protecting group on the amine had to be

[206] Review: S. M. Weinreb, *Nat. Prod. Rep.* **2009**, *26*, 758–775.

[207] G. Bélanger, M. Dupuis, R. Larouche-Gauthier, *J. Org. Chem.* **2012**, *77*, 3215–3221.

exchanged to a more labile formyl group at this point affording the tricyclic intermediate **234**. Final formation of the B ring was achieved applying an allylic bromination/deprotection/nucleophilic substitution sequence producing racemic securinine ((±)-**171**), although in low yield. Resolution of the enantiomers afforded pure securinine (**171**) and virosecurinine (**173**).

Table 8: Previously published total syntheses of *Securinega* alkaloids in chronological order.

Entry	Author(s)	Year	*Securinega* Alkaloid(s)	Ref.
1	Horii *et al.*	1967	securinine (rac.)	143
2	Heathcock *et al.*	1987	norsecurinine (rac.)	208
3	Jacobi *et al.*	1991	(–)-, (+)-norsecurinine	209
4	Magnus *et al.*	1992	norsecurinine (rac.), nirurine (rac.)	198
5	Weinreb *et al.*	2000	(–)-norsecurinine, (+)-14,15-dihydronorsecurinine, phyllanthine	223
6	Honda *et al.*	2000	securinine (rac., formal)	220
7	Liras *et al.*	2001	securinine (rac.)	210
8	Honda *et al.*	2004	viroallosecurinine	219
9	Alibes, de March *et al.*	2004	securinine, (–)-allonorsecurinine	216
10	Honda *et al.*	2004	securinine	218
11	Figueredo *et al.*	2005	(–)-norsecurinine	213
12	Kerr *et al.*	2006	(+)-phyllanthidine	156
13	Weinreb *et al.*	2008	secu'amamine A	151
14	Busqué, de March *et al.*	2008	allosecurinine, viroallosecurinine	200
15	Kerr *et al.*	2008	allosecurinine	212
16	Thadani *et al.*	2009	securinine	217
17	Bayón, Figueredo *et al.*	2009	securinine, (–)-norsecurinine	214
18	Wood *et al.*	2010	(+)-norsecurinine, (+)-allonorsecurinine	211
19	Srihari *et al.*	2012	(–)-allonorsecurinine	221
20	Bélanger *et al.*	2012	virosine A	207
21	Wood *et al.*	2012	securinine (rac.), allosecurinine (rac.)	215
22	Yang, Li *et al.*	2013	virosaine B, flueggine A	159
23	Gademann *et al.*	2013	bubbialidine, virosaine A	158
24	Ye, Jiang *et al.*	2014	(–)-norsecurinine, (–)-niruroidine, flueggine A	199
25	Zheng *et al.*	2015	14,15-dihydrosecurinine, securinine (formal)	224
26	Smith *et al.*	2015	secu'amamine A	152

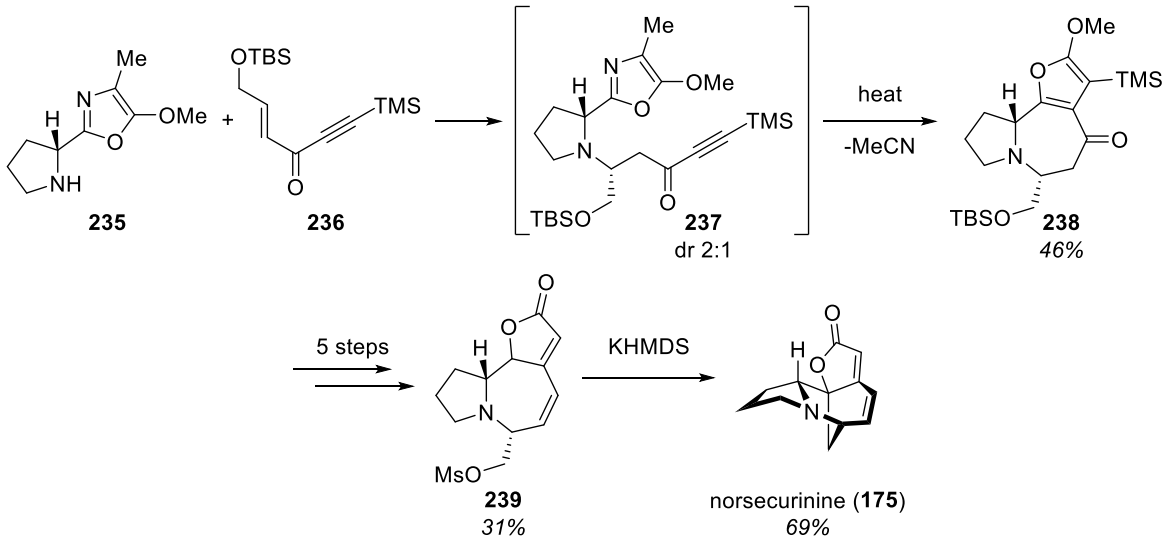

Scheme 48: The first enantiospecific total synthesis of norsecurinine (**175**) reported by Jacobi *et al*. in 1991.

After this seminal work, it took 20 years before the second total synthesis of a *Securinega* alkaloid was published by Heathcock and coworkers in 1987.[208] Starting from proline representing the A ring fragment, the B, C and D rings were constructed in this sequence in 12 linear steps affording racemic norsecurinine ((±)-**175**) in 2% overall yield. The first enantioselective synthesis of norsecurinine (**175**) was reported by Jacobi and coworkers in 1991,[209] who also utilized proline as a starting material (Scheme 48). Starting from either L- or D-proline afforded the enantiomerically pure (+)- or (–)-norsecurinine (**175**), respectively. In this approach, proline served as the A ring fragment and was converted to oxazole **235**, which underwent spontaneous Michael addition with enone **236** to generate labile intermediate **237**. Upon attempted chromatography of intermediate **237**, retro-Michael addition was observed. Tricycle **238** was obtained in 46% yield by heating of the crude substance leading to a Diels-Alder reaction between the oxazole and acetylene moieties under release of acetonitrile. The minor diastereomer could be separated and recycled by retro-Michael addition. Reduction of the keto function followed by dehydration formed the C ring double bond. The D ring was set up by desilylation and subsequent demethylation. Mesylation of the primary hydroxyl group gave intermediate **239**. Final formation of the B ring was achieved by treatment with KHMDS leading to an intramolecular substitution reaction giving the natural product **175** in 69% yield.

[208] C. H. Heathcock, T. W. von Geldern, *Heterocycles* **1987**, *25*, 75–78.

[209] P. A. Jacobi, C. A. Blum, R. W. DeSimone, U. E. S. Udodong, *J. Am. Chem. Soc.* **1991**, *113*, 5384–5392.

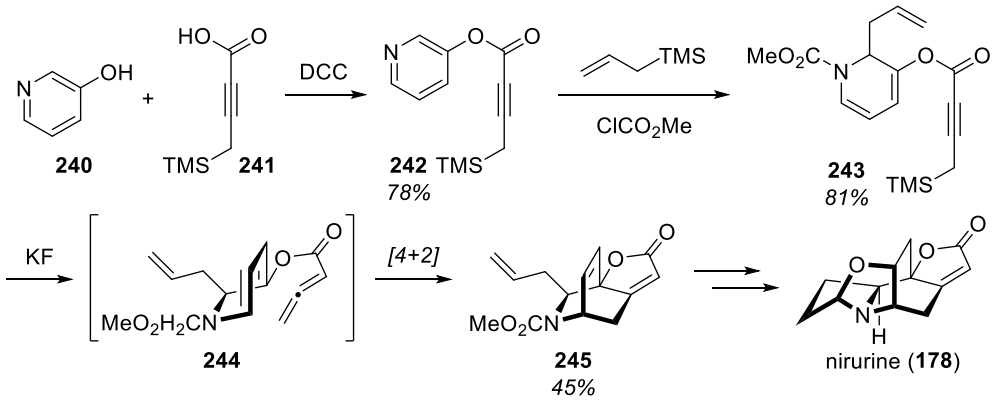

Scheme 49: Key cycloaddition step in the total synthesis of nirurine (**178**) reported by Magnus *et al*. in 1992.

One year later, Magnus and coworkers reported the total synthesis of nirurine (**178**), the first synthetic study on a *Securinega* alkaloid with an azabicyclo[2.2.2]octane core (Scheme 49).[198] This synthesis also relies on a key Diels-Alder reaction to form the tetracyclic core skeleton. Ester **242** was derived from 3-hydroxypyridine (**240**) and transformed into diene **243** in one step. Desilylation using potassium fluoride in aqueous acetic acid presumably led to formation of allene **244**. An intramolecular [4+2] cycloaddition produced intermediate **245** in 45% yield, which was further transformed into nirurine (**178**).

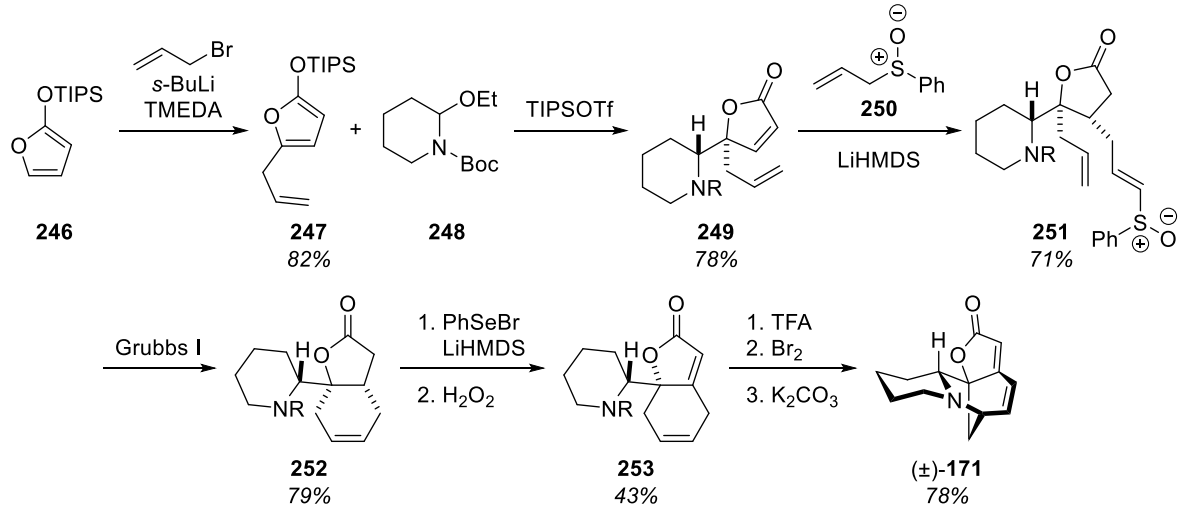

Scheme 50: The total synthesis of racemic securinine ((±)-**171**) reported by Liras *et al*. in 2001.

Within the first four decades after their discovery, only four studies on the total synthesis of *Securinega* alkaloids have been published. Since 2000, however, interest in the synthesis of these challenging natural products has increased tremendously and a variety of synthetic strategies have been developed. The total synthesis of racemic securinine ((±)-**171**) reported by

Liras and coworkers in 2001 (Scheme 50)[210] was pioneering in a sense, that it combined several methodologies, which frequently reoccurred in the syntheses published afterwards. Starting from silyloxyfuran **246**, serving as the D ring precursor, addition to allyl bromide gave allylfuran **247** in good yield. Vinylogous Mannich reaction with an iminium species generated *in situ* from protected piperidine derivative **248** introduced the A ring. Addition of allyl phenyl sulfoxide (**250**) produced the intermediate **251**, which was cyclized in a ring-closing metathesis (RCM) reaction using Grubbs' first generation catalyst providing tricyclic intermediate **252**. The double bond in the D ring was introduced by addition to phenylselenyl bromide and subsequent oxidation/elimination (**253**). Final formation of the B ring was achieved *via* acidic Boc deprotection followed by a dibromination/nucleophilic substitution/elimination sequence furnishing racemic securinine ((±)-**171**). This strategy is reminiscent of the allylic bromination/nucleophilic substitution sequence in the synthesis by Horii and coworkers (cf. Scheme 47) but distinct as it also leads to a net double bond isomerization. The same strategy has been used by Wood and coworkers in their 2010 total synthesis of (+)-allonorsecurinine.[211]

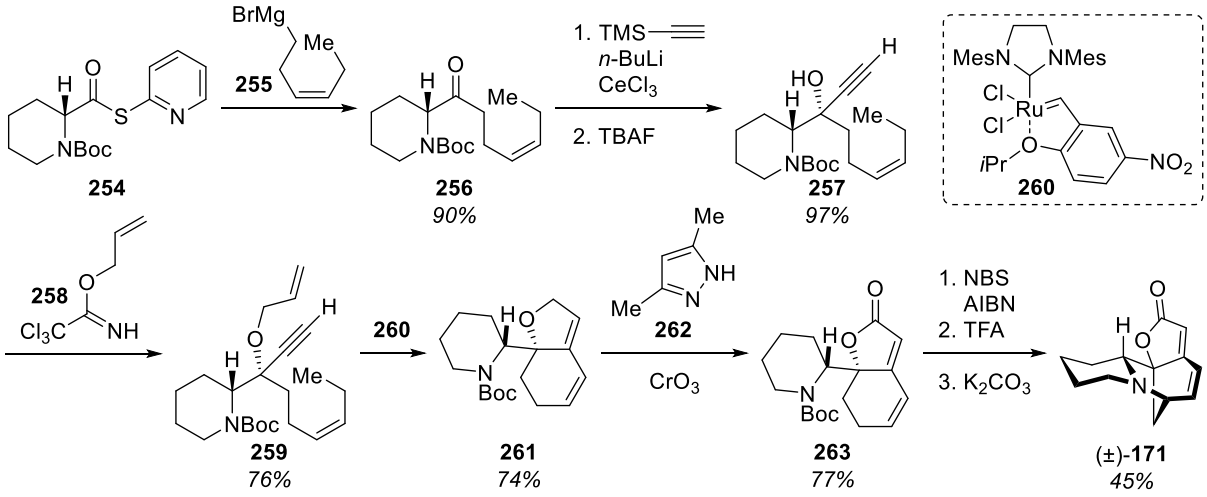

Scheme 51: Diastereoselective total synthesis of securinine (**171**) reported by Honda *et al*. in 2004.

The synthesis by Liras and coworkers exemplified the utility of RCM in the construction of the tetracyclic *Securinega* alkaloid frameworks and several other groups have used this transformation in their syntheses. While several approaches have adopted RCM for the

[210] S. Liras, J. E. Davoren, J. Bordner, *Org. Lett.* **2001**, *3*, 703–706.

[211] M. R. Medeiros, J. L. Wood, *Tetrahedron* **2010**, *66*, 4701–4709.

formation of the C ring as seen above,[156,198,212,213,214,215] there are also examples of D ring formations accomplished by this technique.[216,217] An impressive one-step C/D ring formation approach *via* tandem RCM in the first stereoselective total synthesis of securinine has been reported by Honda and coworkers in 2004 (Scheme 51).[218] Starting from known *R*-pipecolic acid-derived thioester **254** unsaturated side-chains were introduced sequentially by addition of (*Z*)-3-hexenylmagnesium bromide (**255**) to the thioester followed by addition of TMS acetylene to the ketone and desilylation to give enyne **257** in excellent yield. Alkylation of the hydroxyl function using allyl trichloroacetimidate (**258**) affording dienyne **259** set up the stage for the key tandem RCM reaction using the ruthenium catalyst **260** to construct the C/D ring system in one step and high yield. Attempts to use an acrylate ester instead of allyl ether **259** in this transformation were unsuccessful and thus allylic oxidation with chromium trioxide and 3,5-dimethylpyrazole (**262**) was applied to form the butenolide **263**. Final B ring formation was accomplished using the bromination/deprotection/substitution sequence originally developed by Horii and coworkers. A very similar strategy has been applied in the total synthesis of viroallosecurinine (**174**) reported in a follow-up publication by Honda and coworkers in 2004.[219]

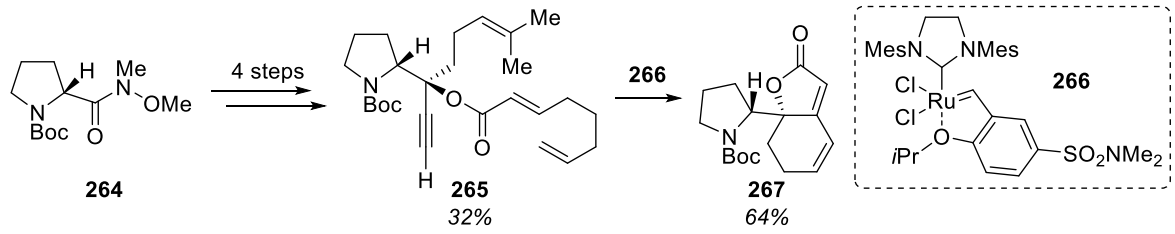

Scheme 52: Tandem RCM in the synthesis of norsecurinine (**175**) reported by Yang, Li *et al*. in 2013.

[212] A. B. Leduc, M. A. Kerr, *Angew. Chem. Int. Ed.* **2008**, *47*, 7945–7948.

[213] R. Alibés, P. Bayón, P. de March, M. Figueredo, J. Font, E. García-García, D. González-Gálvez, *Org. Lett.* **2005**, *7*, 5107–5109.

[214] D. González-Gálvez, E. García-García, R. Alibés, P. Bayón, P. de March, M. Figueredo, J. Font, *J. Org. Chem.* **2009**, *74*, 6199–6211.

[215] J.-H. Chen, S. R. Levine, J. F. Buergler, T. C. McMahon, M. R. Medeiros, J. L. Wood, *Org. Lett.* **2012**, *14*, 4531–4533.

[216] R. Alibés, M. Ballbé, F. Busqué, P. de March, L. Elias, M. Figueredo, J. Font, *Org. Lett.* **2004**, *6*, 1813–1816.

[217] B. Dhudshia, B. F. T. Cooper, C. L. B. Macdonald, A. N. Thadani, *Chem. Commun.* **2009**, 463–465.

[218] T. Honda, H. Namiki, K. Kaneda, H. Mizutani, *Org. Lett.* **2004**, *6*, 87–89.

[219] T. Honda, H. Namiki, M. Watanabe, H. Mizutani, *Tetrahedron Lett.* **2004**, *45*, 5211–5213.

This tandem RCM strategy was later picked up by Yang, Li and coworkers in their total syntheses of virosaine B (**181**) and flueggine A (**182**) published in 2013,[159] which proceeded *via* norsecurinine (**175**) and (+)-allonorsecurinine as intermediates. In this report, commercially available Weinreb amide **264** was converted into intermediate **265** in an alkylation sequence very similar to the one described above (Scheme 52). The use of relay RCM facilitated tandem enyne metathesis on the α,β-unsaturated ester **265** allowing for the direct formation of the butenolide moiety obviating an additional oxidation step. Again, B ring formation of tricyclic intermediate **267** was accomplished using the sequence by Horii and coworkers affording norsecurinine (**175**) in this case. Interestingly, this sequence became increasingly popular and many groups reported on its use in the recent years.[199,216,220,221]

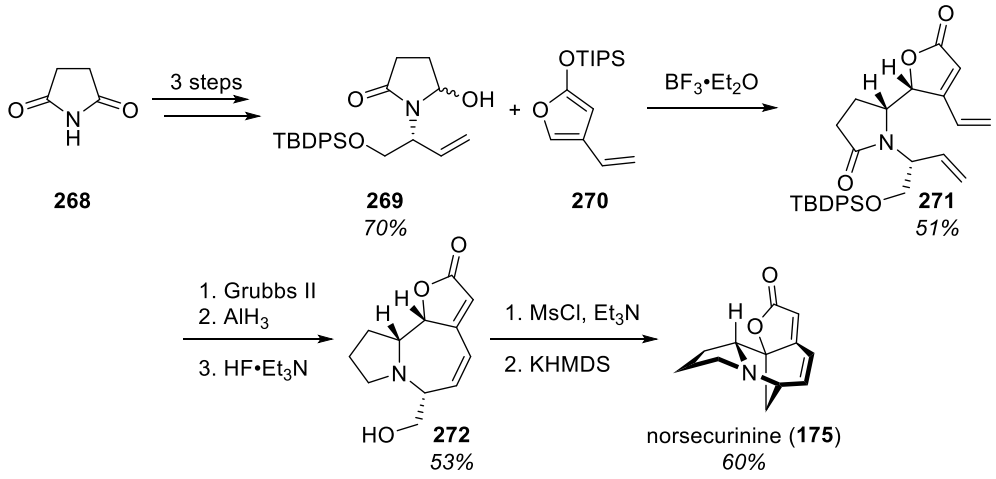

Scheme 53: Total synthesis of norsecurinine (**175**) reported by Figueredo *et al*. in 2005.

Application of the vinylogous Mannich reaction to connect A and D ring fragments, which was pioneered by Liras and coworkers (cf. Scheme 50), was also implemented by other research groups. In the total synthesis of norsecurinine (**175**) reported by Figueredo and coworkers in 2005 (Scheme 53),[213] this transformation was used to prepare RCM precursor **271**. Hydroxy-lactam **269** was synthesized from succinimide (**268**) in three steps. Exposure to boron trifluoride etherate lead to formation of the corresponding *N*-acyliminium ion, which was captured with silyloxyfuran **270** to form product **271**. Cyclization by RCM followed by reduction of the lactam and desilylation gave known intermediate **272**. Following the mesylation/nucleophilic substitution sequence developed by Jacobi and coworkers (cf. Scheme 48) yielded

[220] T. Honda, H. Namiki, M. Kudoh, N. Watanabe, H. Nagase, H. Mizutani, *Tetrahedron Lett.* **2000**, *41*, 5927–5930.

[221] A. S. Reddy, P. Srihari, *Tetrahedron Lett.* **2012**, *53*, 5926–5928.

norsecurinine (**175**). This approach has also been applied in the total synthesis of securinine (**171**) reported by the same group in 2009.[214]

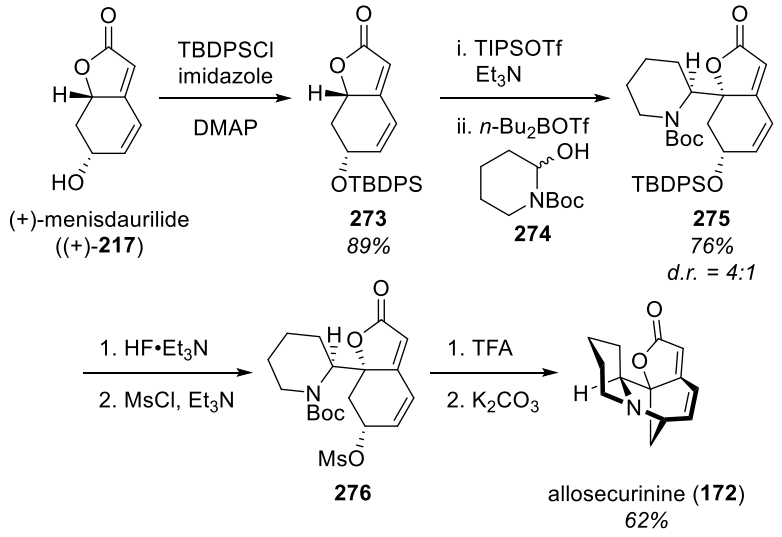

Scheme 54: Total synthesis of allosecurinine (**172**) starting from the natural product (+)-menisdaurilide ((+)-**217**) reported by Busqué, de March *et al*. in 2008.

The same group reported another strategy involving a key vinylogous Mannich reaction in 2008.[200] Their synthesis commenced from the natural product (+)-menisdaurilide ((+)-**217**), the synthesis of which they had reported before,[222] and a possible biogenetic relevance of the key transformation was suggested (Scheme 54). After protection of (+)-menisdaurilide ((+)-**217**), a one-pot procedure including formation of a silyloxyfuran from butenolide **273** followed by vinylogous Mannich reaction with an *N*-acyliminium ion afforded intermediate **275**. The *N*-acyliminium ion was generated *in situ* from lactamol **274** by Lewis acid activation using dibutylboron triflate. Only two chromatographically separable diastereomers were formed in this transformation in a ratio of 4:1 with the major isomer **275** possessing the desired absolute configuration. The synthesis was completed by desilylation followed by mesylation to create a leaving group. Acidic Boc cleavage and subsequent intramolecular substitution furnished allosecurinine (**172**). The same synthetic route was applied using (–)-menisdaurilide ((–)-**217**) providing viroallosecurinine (**174**).

[222] F. Busqué, M. Cantó, P. de March, M. Figueredo, J. Font, S. Rodríguez, *Tetrahedron: Asymmetry* **2003**, *14*, 2021–2032.

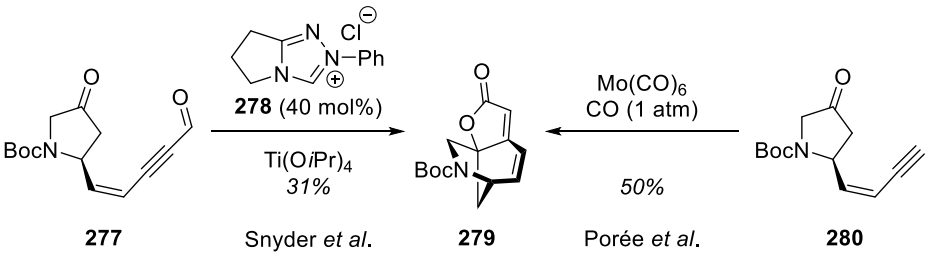

Scheme 55: Recent approach to the tricyclic core of Securinega alkaloids using NHC catalysis by Snyder *et al*. and an extension of the methodology employing a hetero-Pauson-Khand reaction by Porée *et al*.

Beside the frequently reoccurring synthetic motifs described so far other unique methods have enriched the diversity of *Securinega* alkaloid total synthesis. For example, the studies on butenolide D ring formation by Horner-Wadsworth-Emmons reaction or a related one-pot procedure applying the Bestmann ylide during the total syntheses of norsecurinine (**175**), (+)-14,15-dihydronorsecurinine and phyllanthine by Weinreb and coworkers,[223] which have been picked up during the recent total synthesis of 14,15-dihydrosecurinine by Zheng and coworkers.[224] Also the aza-Michael addition/aldol addition/lactonization sequence developed by Weinreb and coworkers for the construction of secu'amamine A should be mentioned at this point.[151] Another unique approach toward the bridged B/C/D ring system of securinine (**171**) was recently reported by Snyder and coworkers (Scheme 55).[225] By an intramolecular *N*-heterocyclic carbene (NHC)-catalyzed [3+2] cycloaddition using catalyst precursor **278** in the presence of titanium isopropoxide, the ynal and keto functions of compound **277** were cyclized in a single step to yield the protected *Securinega* alkaloid core **279** in 31%. Inspired by this work, Porée and coworkers have developed a [2+2+1] cycloaddition approach featuring a hetero-Pauson-Khand reaction.[226] Thus, the precursor **280** carries a terminal alkyne and the missing C_1 unit is introduced by metal-bound carbon monoxide. Although the product **279** was obtained in only 50% yield, this transformation seems highly valuable for the development of further synthetic strategies toward the *Securinega* alkaloid family.

[223] (a) G. Han, M. G. LaPorte, J. J. Folmer, K. M. Werner, S. M. Weinreb, *Angew. Chem. Int. Ed.* **2000**, *39*, 237–240; (b) G. Han, M. G. LaPorte, J. J. Folmer, K. M. Werner, S. M. Weinreb, *J. Org. Chem.* **2000**, *65*, 6293–6306.

[224] X. Zheng, J. Liu, C.-X. Ye, A. Wang, A.-E. Wang, P.-Q. Huang, *J. Org. Chem.* **2015**, *80*, 1034–1041.

[225] A. M. ElSohly, D. A. Wespe, T. J. Poore, S. A. Snyder, *Angew. Chem. Int. Ed.* **2013**, *52*, 5789–5794.

[226] E. Chirkin, S. Michel, F.-H. Porée, *J. Org. Chem.* **2015**, *80*, 6525–6528.

4.1.5 The Total Syntheses of Bubbialidine and Virosaine A

In 2013, our research group has published the first enantioselective total syntheses of the neosecurinane-type alkaloid bubbialidine (**292**) and the unusual birdcage-shaped virosaine A (**228**),[158] which were both accessed by the synthetic route outlined in the following. A key intermediate of the synthesis is the butenolide **288**, which represents the C and D rings in the final natural product and is the TBDPS-protected form of the natural product (+)-aquilegiolide ((+)-**218**). The route to compound **288** was based on related synthetic studies reported in the literature.[200,227] Initially the synthesis was designed to yield virosaine A (**228**), which had been isolated from *F. virosa* in 2012 by Wang, Zhang, Ye and coworkers.[157] Bubbialidine (**292**) was obtained by deprotection of an intermediate *en route*.

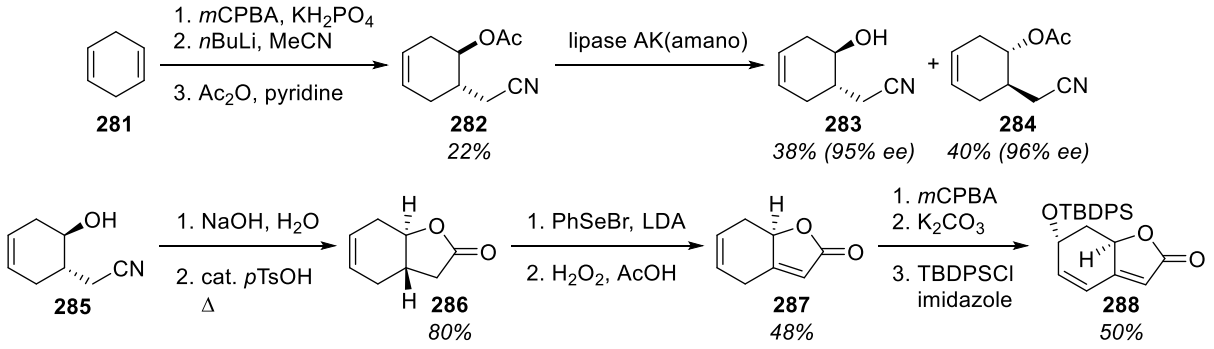

Scheme 56: Synthesis of the bicyclic key intermediate **288**.

The synthesis commenced with a mono-epoxidation of commercially available 1,4-cyclohexadiene (**281**) with *meta*-chloroperbenzoic acid (*m*CPBA) followed by epoxide opening using cyanomethyllithium (Scheme 56). The resulting secondary alcohol was acetylated with acetic anhydride giving the racemic acetate **282** in 22% yield. Enzymatic kinetic resolution was applied as the source of chirality in the synthesis and alcohol **283** was obtained in 95% enantiomeric excess. Basic hydrolysis of the nitrile function and subsequent acid-catalyzed lactone formation gave compound **286** in 80% yield.[227a] The D ring double bond was introduced by an α-selenation/oxidative elimination sequence affording the butenolide **287** in a moderate yield of 48%. Diastereoselective introduction of the hydroxyl group and concomitant isomerization of the C-C double bond into conjugation with the butenolide moiety was achieved through epoxidation using *m*CPBA followed by regioselective epoxide opening using potassium carbonate. Protection with TBDPSCl afforded the intermediate **288** in 50% yield.

[227] (a) N. Kato, M. Inada, H. Sato, S. Ito, M. Shoji, M. Ueda, *Tetrahedron Lett.* **2007**, *48*, 7702–7705; (b) G. Audran, K. Mori, *Eur. J. Org. Chem.* **1998**, 57–62.

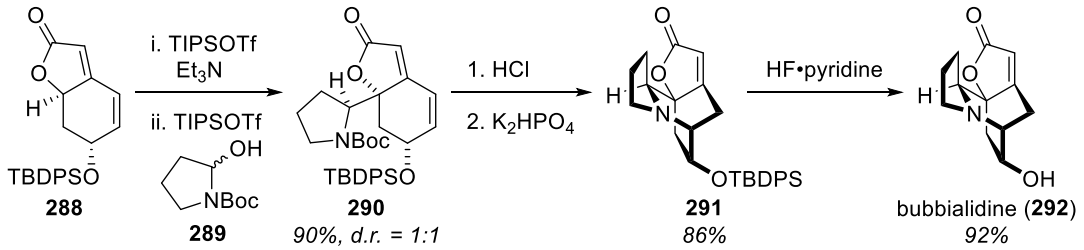

Scheme 57: Construction of the bridged tetracyclic framework and synthesis of bubbialidine (**292**).

The A ring pyrrolidine fragment was introduced by a vinylogous Mannich reaction applying the one-pot procedure developed by Busqué, de March and coworkers.[200] The reaction afforded an excellent yield of 90% and only two out of four possible diastereomers were formed and could be separated chromatographically (**290**, Scheme 57). Rather surprisingly a diastereomeric ratio of only 1:1 was observed diminishing the high yield. In contrast, the original publication reported a diastereomeric ratio of 4:1 in favor of the desired isomer using a homologous 6-membered lactamol. The secondary amine of diastereomer **290** was deprotected under acidic conditions affording the corresponding hydrochloride salt. Under extremely mild conditions using dipotassium hydrogen phosphate as a base, intramolecular vinylogous aza-Michael addition occurred affording the bridged tetracycle **291** in an excellent yield of 86% over the two steps. Desilylation of this intermediate using Olah's reagent led to the natural product bubbialidine (**292**) in 92% yield.

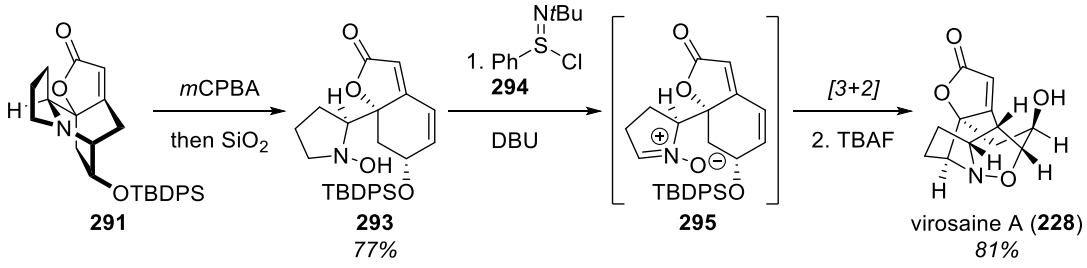

Scheme 58: Final steps in the total synthesis of virosaine A (**228**).

Moving on toward the second natural product intermediate **291** was oxidized to the corresponding *N*-oxide using *m*CPBA (Scheme 58). Cope elimination was observed upon exposure to silica opening up the B ring to give hydroxylamine **293**. Oxidation to the nitrone **295** with *N*-*tert*-butylbenzenesulfinimidoyl chloride (**294**) in the presence of 1,8-diazabicyclo-[5.4.0]undec-7-en (DBU) proceeded regioselectively and a spontaneous intramolecular 1,3-dipolar cycloaddition furnished the unusual alkaloid framework. Final desilylation using tetrabutylammonium fluoride (TBAF) produced the natural product virosaine A (**228**) in 81% yield.

4.1.6 Secu'amamine E and its Enantiomer Virosine A

In continuation of the synthetic program on *Securinega* alkaloids within our research group, we turned our focus on neosecurinane-type alkaloid secu'amamine E (**296**, Figure 26), which was isolated alongside secu'amamines F and G from *Securinega suffruticosa* var. *amamiensis* by Ohsaki and coworkers in 2009.[186] Their structures were elucidated by spectroscopic means (mainly NMR spectroscopy) and the absolute configuration of their BC ring systems was determined to be opposite to securinol A (**176**) by a comparison of the respective circular dichroism (CD) spectra showing an opposite Cotton effect. Thus, secu'amamine E (**296**) is the higher homolog of bubbialidine (**292**) and represents an attractive target for total synthesis, as it should be obtainable using a similar synthetic strategy. No detailed investigations concerning the bioactivity of secu'amamine E (**296**) have been reported. The isolation paper states that no cytotoxicity on P388 leukemia cells was observed, in a short comment at the end of the publication. Also, no synthetic studies by other research groups towards this alkaloid have been reported to date.

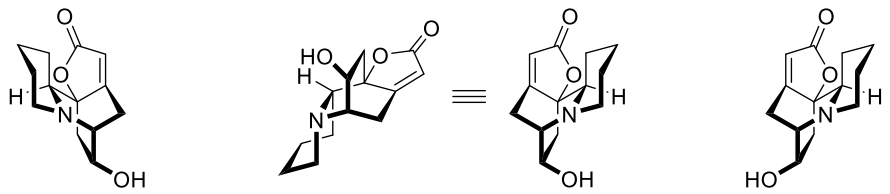

Figure 26: Structures of different neosecurinane-type alkaloids.

Another neosecurinane-type alkaloid isolated from *Flueggea virosa* by Ye and coworkers in 2008 is virosine A (**297**), the optical antipode of secu'amamine E (**296**).[164] Its structure and absolute configuration were determined using the same techniques mentioned above, namely NMR and CD spectroscopy. Again, no investigations concerning the bioactivity of this alkaloid have been reported. The structure of virosine A (**297**) was confirmed *via* total synthesis of the natural product by Bélanger and coworkers in 2012.[207] Due to the enantiomeric relationship between virosine A (**297**) and secu'amamine E (**296**), which has not been pointed out in any of the mentioned literature reports, the key features of the synthesis by Bélanger and coworkers shall be presented at this point.

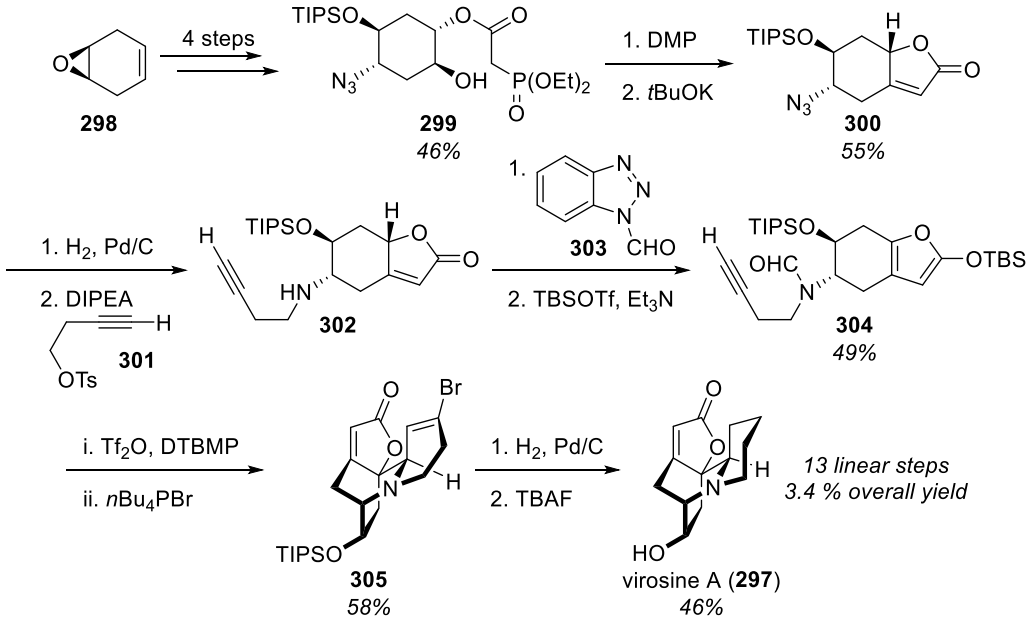

Scheme 59: Enantioselective total synthesis of virosine A (**297**) reported by Bélanger *et al*. in 2012.

The synthesis started from *meso*-epoxide **298**, which was elaborated into intermediate **299** in 46% overall yield *via* chromium-catalyzed desymmetrization using azidotrimethylsilane, hydroxyl-directed epoxidation followed by silyl protection and subsequent epoxide opening with diethylphosphonoacetic acid (Scheme 59). The hydroxyl function was oxidized using Dess-Martin periodinane (DMP) and treatment with potassium *tert*-butoxide triggered an intramolecular Horner-Wadsworth-Emmons reaction to obtain butenolide **300** representing the C/D ring system of the final natural product. The azide group was then reduced and the resulting amine was alkylated and formylated sequentially using 3-butynyl tosylate (**301**) and *N*-formyl-benzotriazole (**303**), respectively. Silylation of the butenolide moiety afforded silyloxyfuran **304** in 49% yield from azide **300**. The key transformation of the synthesis was a Vilsmeier-Haack/Mannich cyclization cascade leading to the bridged tetracyclic core structure, a method that had been reported by the same group in 2008.[228] Activation of the formyl group using triflic anhydride and 2,6-di-*tert*-butyl-4-methylpyridine (DTBMP) led to Vilsmeier-Haack reaction with the silyloxyfuran moiety. The resulting iminium species then reacted with the terminal alkyne function in a Mannich reaction upon addition of tetrabutylphosphonium bromide giving tetracycle **305** in 58% yield. Cleavage of the bromide, reduction of the A ring by hydrogenation and final desilylation of the hydroxyl group provided virosine A (**297**) in 46% yield. In summary, the natural product **297** was obtained by a sequence of 13 linear steps in 3.4% overall yield from *meso*-epoxide **298**.

[228] R. Larouche-Gauthier, G. Bélanger, *Org. Lett.* **2008**, *10*, 4501–4504.

4.2 The First Enantioselective Total Synthesis of Secu'amamine E[229]

4.2.1 Synthetic Outline

After the total syntheses of bubbialidine (**292**) and virosaine A (**228**) had been accomplished in our group, focus turned toward secu'amamine E (**296**). Structurally the two alkaloids only differ in the A ring. While bubbialidine (**292**) is characterized as a neonorsecurinane-type alkaloid containing a pyrrolidine unit, secu'amamine E (**296**) belongs to the neosecurinane group containing a piperidine unit instead and thus it represents the higher homolog of bubbialidine (**292**). We therefore envisioned that secu'amamine E (**296**) could be constructed using a strategy based on the synthetic route developed for bubbialidine (**292**) and virosaine A (**228**, cf. Section 4.1.5).

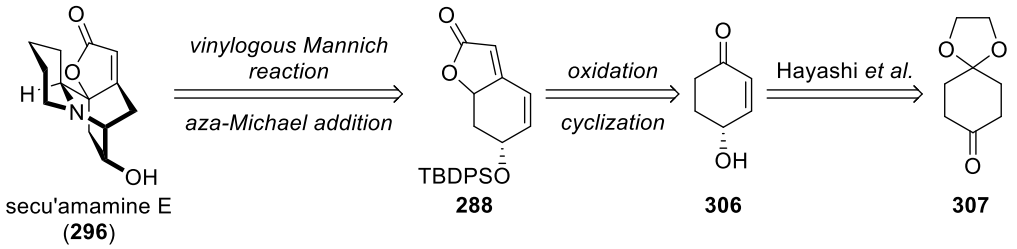

Scheme 60: Retrosynthetic analysis of secu'amamine E (**296**).

The vinylogous Mannich/aza-Michael reaction sequence was very efficient in the construction of the bridged tetracycle and should be adopted for the present project leading back to the known intermediate **288**. In our earlier work, this intermediate was synthesized in 11 linear steps. Due to some low yielding transformations as well as an enzymatic kinetic resolution, intermediate **288** was obtained in only 1.6% overall yield from 1,4-cyclohexadiene (**281**). A more convenient approach to access this compound is desirable, as it could serve as a general intermediate on the way to several *Securinega* alkaloids considering that both configurations of the silyl ether might be obtainable through the same route. The configuration of the butenolide moiety is of no concern at this point, as the following vinylogous Mannich reaction proceeds *via* the corresponding planar silyloxyfuran. We planned to synthesize butenolide **288** by α-hydroxylation of enone **306** and cyclization either through intramolecular aldol condensation or Horner-Wadsworth-Emmons olefination of a suitable ester precursor would furnish the butenolide moiety. An efficient synthesis of enone **306** from mono-ketal **307** was described by Hayashi and coworkers during the total synthesis of (+)-panepophenanthrin.[230]

[229] Simone M. Grendelmeier has contributed to this work during her Master's thesis, Basel, 2015.

[230] M. Matsuzawa, H. Kakeya, J. Yamaguchi, M. Shoji, R. Onose, H. Osada, Y. Hayashi, *Chem. Asian J.* **2006**, *1*, 845–851.

4.2.2 Synthesis of the C Ring Fragment

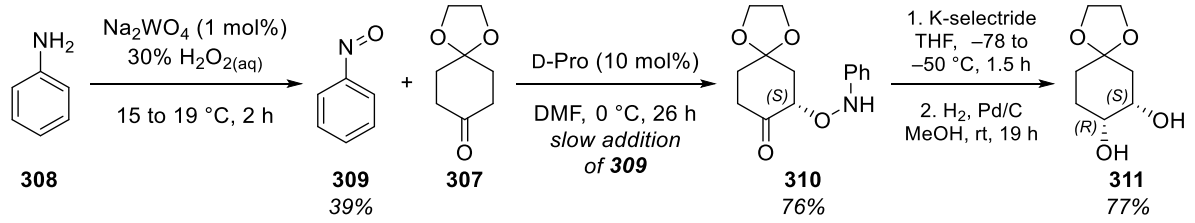

Scheme 61: Introduction of chirality *via* organocatalysis and stereoselective reduction.

Our synthetic efforts commenced with the synthesis of enone **306** *via* the route developed by Hayashi and coworkers (Scheme 61).[230] Nitrosobenzene (**309**) was obtained in 39% yield by oxidation of aniline (**308**) with sodium tungstate and hydrogen peroxide following a known procedure.[231] Mono-ketal **307** was then subjected to an organocatalyzed α-aminoxylation reaction using nitrosobenzene as the electrophile and D-proline as the catalyst affording the (*S*)-configured ketal **310** in 76% yield after flash chromatography on an 84-mmol scale. The keto function was then reduced in a stereoselective fashion using K-selectride (potassium tri-*sec*-butylborohydride) to afford exclusively the *syn*-product. After workup, the crude material was hydrogenated overnight using palladium on charcoal under a hydrogen atmosphere. The *syn*-diol **311** was obtained in 77% yield from ketone **310**. An alternative method for reductive N-O bond cleavage reported in the literature using catalytic amounts of copper(II) sulfate[232] (and thus avoiding the use of hydrogen gas) was not successful leading to decomposition of the substrate.

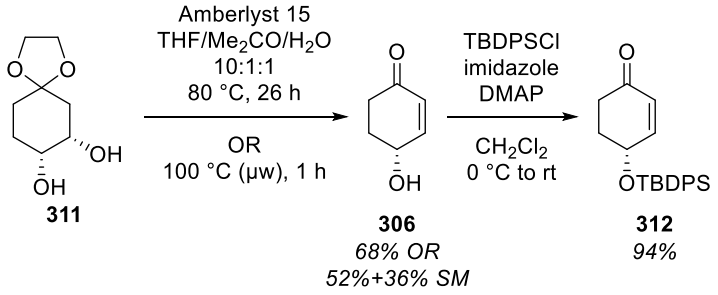

Scheme 62: Synthesis of silyl-protected enone **311**.

Acidic treatment of diol **311** with Amberlyst 15 in a refluxing mixture of THF, acetone and water led to cleavage of the ketal moiety followed by elimination of water to give the enone **306** in 68% yield (Scheme 62). While thorough washing of the acidic resin with THF had to be performed in all cases to obtain workable amounts of product, the mode of heating had a large

[231] S. M. Opalka, A. R. Longstreet, D. T. McQuade, *Beilstein J. Org. Chem.* **2011**, *7*, 1671–1679.
[232] N. Momiyama, H. Yamamoto, *J. Am. Chem. Soc.* **2003**, *125*, 6038–6039.

impact on the composition of the reaction mixture after different reaction times. When this transformation was performed conventionally by heating on an oil bath at 80 °C, slow conversion of starting material was observed (>24 h) and only the desired product **306** could be identified in the reaction mixture by means of ^{1}H NMR spectroscopy. The rest of the material seemed to have decomposed, possibly by polymerization of the enone function or elimination of the second hydroxyl group. When performed in a sealed tube in a microwave reactor at 100 °C, only the desired enone **306** and the starting material **311** were observed by ^{1}H NMR analysis of the mixture after 1 h reaction time. Further heating of the mixture did not lead to further conversion of substrate **311**. In both cases the enone **306** was usually isolated in ca. 50% yield with the latter procedure providing an additional amount of 36% of the starting material **311**. While enone **306** could be obtained by the route of Hayashi and coworkers, on large scale only 30% overall yield from ketal **307** could be achieved, as microwave reactions were limited to small scale. It should be mentioned at this point, that even though all four transformations (**307** to **306**) were performed several times independently by two experimenters using different substrate and reagent batches, the high yields reported in the literature could not be reproduced in our hands (76%/77%/68% vs. 93%/85%/85%).[230]

The hydroxyl group of enone **306** was protected as a silyl ether using TBDPS chloride in the presence of imidazole and DMAP. Initially this transformation was performed following a procedure reported by Busqué, de March and coworkers for the silylation of menisdaurilide (**217**, cf. Scheme 54),[200] which used an excess of imidazole (3.1 eq.). Employing the same amount of reagent in the present transformation led to a low isolated yield of the desired product **312**. In one case, an undesired compound was isolated in large amount. HRMS analysis confirmed that the compound was formed by addition of imidazole onto the desired enone **312**. Most probably 1,4-addition of imidazole gave the *trans*-Michael adduct as indicated by ^{1}H NMR analysis. When a smaller amount of only 1.02 eq. of imidazole was applied together with 1.02 eq. of TBDPSCl and 0.1 eq. DMAP, the desired silyl ether **312** was obtained in 94% yield on a 13-mmol scale.

4.2.3 Construction of the D Ring Butenolide

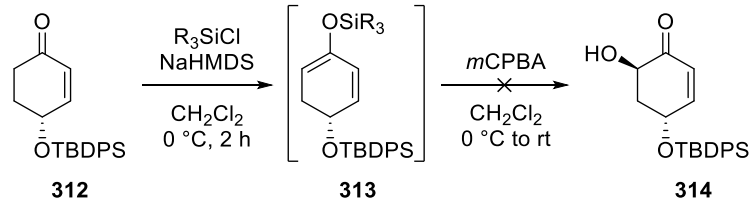

Scheme 63: Rubottom oxidation was not successful in the synthesis of the α-hydroxy enone **314**. R = Me, Et.

For the formation of the D ring we planned to perform α-hydroxylation on the enone **312** followed by esterification with a C_2 building block suitable for an intramolecular olefination to forge the butenolide moiety. Initial attempts to synthesize the α-hydroxy ketone **314** focused on the Rubottom oxidation (Scheme 63). Treatment with either TMSCl or TESCl in dichloromethane at 0 °C and NaHMDS as a base produced silyl ethers **313** from enone **312**. After extraction and evaporation, the successful formation of both silyl ethers **313** was confirmed by ^{1}H NMR analysis of the crude substances. Intermediate **313** was then redissolved in dichloromethane and *m*CPBA was added at 0 °C. Unfortunately, the desired product **314** was not formed and only decomposition of the starting material was observed. The outcome of this transformation is likely due to the presence of a second double bond in the substrate leading to undesired side reactions.

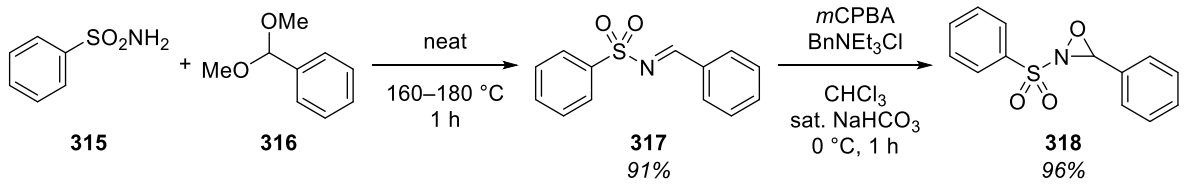

Scheme 64: Preparation of Davis oxaziridine **318**.

To avoid possible side reactions of the second double bond, we switched to the use *N*-sulfonyl-oxaziridines (Davis oxaziridines) as an electrophilic oxygen source. Following the original procedures developed by Davis and coworkers,[233] benzenesulfonamide (**315**) and benzaldehyde dimethyl acetal (**316**) were condensed to obtain the sulfonimine **317** and oxidation with *m*CPBA gave the Davis oxaziridine **318** in excellent yield (Scheme 64).

[233] (a) F. A. Davis, J. Lamendola, Jr., U. Nadir, E. W. Kluger, T. C. Sedergran, T. W. Panunto, R. Billmers, R. Jenkins, Jr., I. J. Turchi, W. H. Watson, J. S. Chen, M. Kimura, *J. Am. Chem. Soc.* **1980**, *102*, 2000–2005; (b) F. A. Davis, O. D. Stringer, *J. Org. Chem.* **1982**, *47*, 1774–1775.

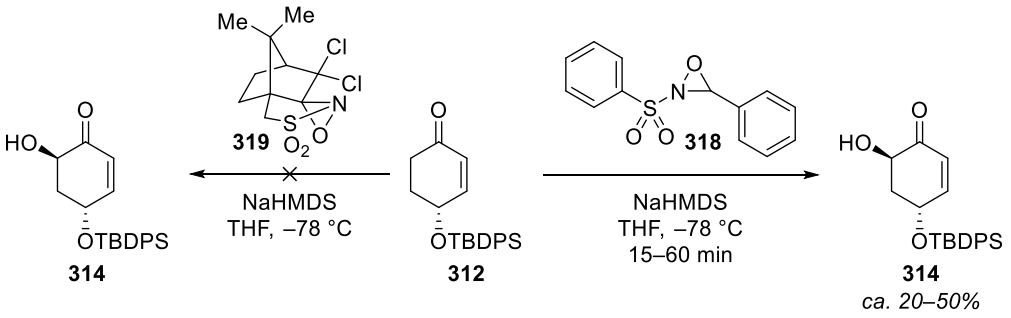

Scheme 65: α-Hydroxylation efforts using Davis oxaziridines.

When enone **312** was reacted with NaHMDS in THF at –78 °C followed by the addition of Davis oxaziridine **318**, clean formation of the desired α-hydroxy ketone **314** as a single diastereomer was observed (Scheme 65). In the reaction mixture, only the desired product **314** along with sulfonimine **317**, the oxaziridine-derived byproduct, was detected by ^{1}H NMR analysis after quenching with an aqueous ammonium chloride solution. The same reaction outcome was observed when a mixture of enone **312** and oxaziridine **318** in THF at –78 °C was directly treated with NaHMDS simplifying the experimental procedure. However, purification of product **314** proved to be difficult. Not only was the compound decomposing slowly during chromatography over silica, also an identical R_f value of the similarly decomposing sulfonimine **317** was observed. Chromatography over alumina resulted in complete decomposition of the product **314**. Addition of 1 M aqueous hydrogen chloride solution to the reaction mixture after quenching led to hydrolysis of the sulfonimine **317** but only <50% yield of the desired product **314** was obtained after chromatography over a short silica column. Also, experiments using powdered active charcoal to remove the byproduct **317** were not successful. The best results were obtained when after extraction of the reaction mixture with diethyl ether, the combined organic layers were washed several times with a 10% aqueous solution of sodium hydrogen sulfite. This procedure removed most of the imine and aldehyde (from hydrolysis of sulfonimine **317**) contents and, after drying and evaporation, gave crude α-hydroxy ketone **314** as a yellow oil, which was not purified further. Attempts to avoid byproduct **317** by the use of oxaziridine **319** failed as formation of compound **314** was not observed.

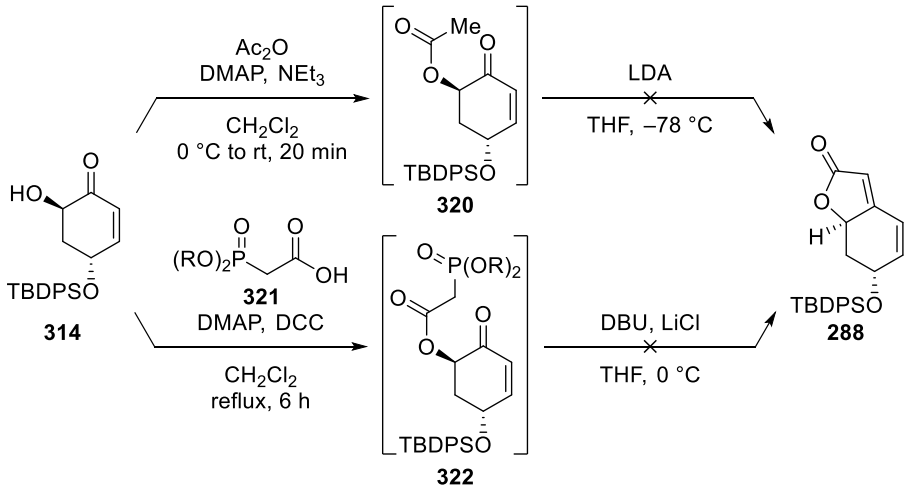

Scheme 66: Two-step esterification/olefination approaches towards butenolide **288**. R = Me, Et.

Esterification of α-hydroxy ketone **314** was performed using either acetic anhydride to generate acetate **320** or a 2-(dialkylphosphoryl)acetic acid (**321**) to generate the dimethyl- as wells as the diethylphosphonate **322** (Scheme 66). While TLC and ^{1}H NMR analyses indicated clean formation of each of the three esters, cyclization efforts to obtain butenolide **288** failed in all cases and only decomposition of the substrates was observed.

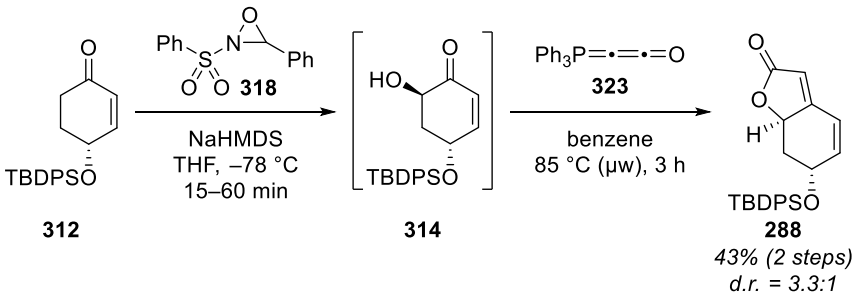

Scheme 67: Optimized synthesis of intermediate **288** by α-hydroxylation with Davis oxaziridine **318** and butenolide formation with the Bestmann ylide (**323**).

A very attractive approach Weinreb and coworkers had used for the late stage D ring formation in their synthesis of (+)-14,15-dihydronorsecurinine[223] is the use of the Bestmann ylide (**323**).[234] In a one-pot procedure, nucleophilic addition of alcohol **314** to the ketene carbonyl and subsequent intramolecular Wittig olefination gave the desired silyl-protected (+)-aquilegiolide **288** (Scheme 67). The highest yields were obtained when a mixture of crude α-hydroxy ketone **314** (as described above) and ylide **323** in benzene were heated at 85 °C in a microwave reactor giving 43% yield of the key intermediate **288** over two steps in a diastereomeric ratio 3.3:1 estimated by ^{1}H NMR analysis. The outcome of this transformation was highly dependent on the quality of the starting materials used. The moisture sensitive ylide **323** was best prepared

[234] H. J. Bestmann, D. Sandmeier, *Chem. Ber.* **1980**, *113*, 274–277.

by elimination of ethanol from the corresponding ester, ethyl (triphenylphosphanylidene)-acetate,[235] and used within a few days. But also, the purity of the α-hydroxy ketone **314** was crucial and yields for this sequence varied substantially. The addition of triethylamine had no influence on the transformation. In contrast to our earlier work, where the intermediate **288** was obtained as a colorless solid,[158] material produced *via* the present route was always obtained as a yellowish oil, which could not be purified further by repeated flash chromatography. Although ^{1}H NMR analysis indicated high purity of the butenolide **288**, further investigations on the identity and origin of the impurities might lead to improved results in the D ring formation.

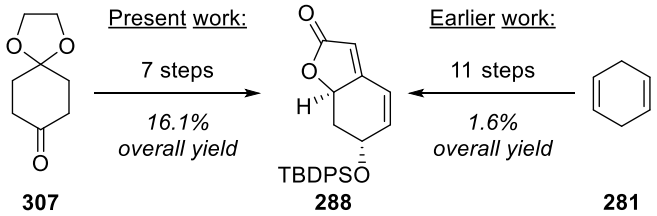

Scheme 68: Comparison of the two syntheses of intermediate **288** developed by our group.

Compared to our old synthesis we could shorten the route from 11 linear synthetic steps to only 7 steps and we could significantly improve the overall yield from 1.6% to 16.1% (Scheme 68). Considering the moderate yield of 43% for the last two steps of the sequence, further improvements of these transformations would boost the overall results of the present synthesis.

4.2.4 Final Assembly of Secu'amamine E

In order to set up the carbon skeleton of secu'amamine E (**296**) from the butenolide key intermediate **288**, the piperidine A ring had to be introduced and the bridging B ring needed to be closed. Due to the structural similarity between secu'amamine E (**296**) and bubbialidine (**292**) we planned to adopt the remaining steps from our total synthesis of the latter alkaloid. Thus, the A ring fragment was introduced using the vinylogous Mannich reaction described by Busqué, de March and coworkers.[200]

[235] I. S. Marcos, A. Benéitez, R. F. Moro, P. Basabe, D. Dìez, J. G. Urones, *Tetrahedron* **2010**, *66*, 8605–8614.

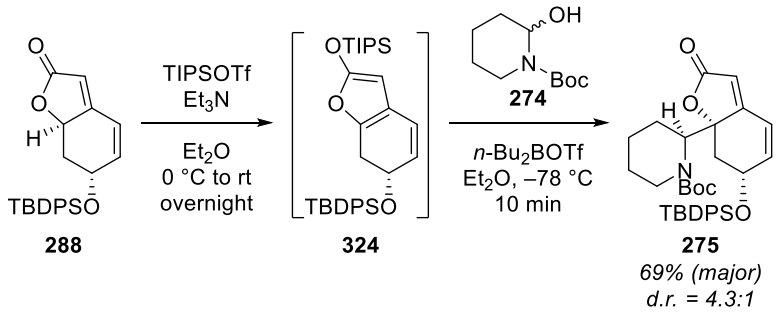

Scheme 69: Introduction of the piperidine A ring by a vinylogous Mannich reaction.

Butenolide **288** was converted into the silyloxyfuran **324** using triisopropylsilyl triflate in the presence of triethylamine and TLC indicated a clean spot-to-spot transformation (Scheme 69). Since stereo information of the butenolide moiety is erased during this step, the starting material could be utilized as a diastereomeric mixture. The Boc-protected δ-lactamol **274** served as the A ring precursor and was prepared from the corresponding lactam by reduction with lithium triethylborohydride.[236] Addition of dibutylboron triflate to a mixture of silyloxyfuran **324** and lactamol **274** in diethyl ether at –78 °C triggered formation of an *N*-acyliminium ion. Subsequent attack of the silyloxyfuran **324** gave the Mannich addition product as a mixture of two diastereomers in a ratio of 4.3:1 and a combined yield of 85%. The diastereomers were separated by repeated flash chromatography affording the pure major isomer **275** in 69% yield. In contrast to our earlier work, where the five-membered γ-lactamol **289** had been used instead of δ-lactamol **274** and the two diastereomers were obtained in a 1:1 ratio (cf. Scheme 57), the present transformation proceeded with good diastereoselectivity reproducing the values reported in the original publication. Furthermore, the pure diastereomer **275** displayed two sets of signals in the ^{1}H NMR spectrum corresponding to rotamers as described by Busqué, de March and coworkers.[200]

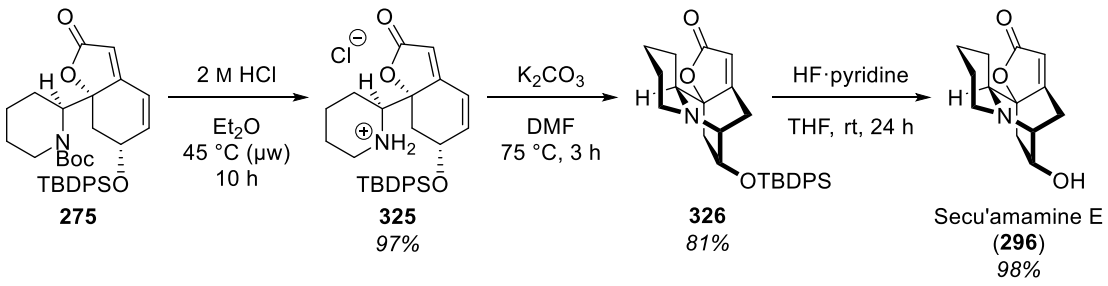

Scheme 70: B ring formation and synthesis of secu'amamine E (**296**).

The Boc protecting group was removed from the piperidine ring by heating of intermediate **275** in a 2 M ethereal hydrogen chloride solution giving the hydrochloride salt **325** in an excellent

[236] R. K. Dieter, R. R. Sharma, *J. Org. Chem.* **1996**, *61*, 4180–4184.

yield of 97% after dilution with dichloromethane, filtration, and evaporation of the reaction mixture (Scheme 70). This transformation was also performed in a 1 M solution of acid requiring approximately double reaction time. When the reaction was carried out by conventional heating on an oil bath, small amounts of the starting material **275** were detected even after 40 h reaction time. Hydrochloride **325** was then subjected to an intramolecular vinylogous aza-Michael addition to close the bridging B ring and form the azabicyclo[2.2.2]-octane core of the natural product. When the reaction was performed under our original conditions using dipotassium hydrogen phosphate in DMF at 75 °C, only partial conversion to the desired tetracycle **326** was observed. The transformation required long reaction times of more than 24 h and strongly varying yields of the product were isolated after flash chromatography (ca. 20–73%). Upon switching to more basic potassium carbonate instead of the phosphate base, a reproducible yield of 81% of tetracycle **326** was obtained after only 3 h reaction time. Final desilylation was achieved by treatment with an excess of Olah's reagent in THF at room temperature affording the natural product secu'amamine E (**296**) in an excellent yield of 98% after flash chromatography. Analytical data collected from the synthetic material matched those reported by Ohsaki and coworkers for the authentic natural product (Table 9). While optical rotation values were almost identical for natural and synthetic samples, also the NMR data were in good agreement. In the ^{1}H NMR spectrum, chemical shifts of synthetic secu'amamine E (**296**) did not deviate more than 0.02 ppm from the values of the natural sample except for three overlapping signals, which were not resolved in the spectrum of the synthetic material and were therefore averaged as one signal. Chemical shifts in the ^{13}C NMR spectrum showed a small general deviation of –0.04 to –0.06 ppm for all signals, possibly due to slight differences in pH of the deuterated solvents. Furthermore, FTIR and HRMS data were collected supporting the identity of the synthetic natural product. Thus, we have achieved the first enantioselective total synthesis of secu'amamine E (**296**) in 12 synthetic steps from commercially available ketal **307** in an overall yield of 8.5%.

We investigated the toxicity of secu'amamine E (**296**) in an assay against *Thamnocephalus platyurus* (beaver-tail fairy shrimp).[237] After 24 h of incubation, no toxic effects were observed in concentrations up to 100 µM confirming the findings by Ohsaki and coworkers.[186]

[237] The assay was conducted in cooperation with Manuel Scherer at the University of Zurich.

Table 9: Comparison of analytical data for natural and synthetic secu'amamine E (**296**). Data for natural secu'amamine E were adopted from Ohsaki et al.[186] All NMR data were collected using CD_3OD as the solvent.

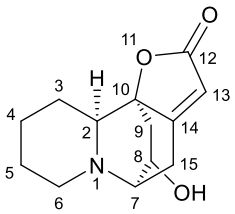

secu'amamine E (**296**)

Natural: $[\alpha]_D$ = –43.8° (c = 0.08 in MeOH)
Synthetic: $[\alpha]_D$ = –45.7° (c = 0.10 in MeOH)

Atom No.	**δ_H(natural)** [ppm], **multiplicity**, ***J*** [Hz]	**δ_H(synthetic)** [ppm], **multiplicity**, ***J*** [Hz]	**δ_C(natural)** [ppm]	**δ_C(synthetic)** [ppm]
2	2.79, dd, 12.0, 1.8	2.78, m[a]	66.50	66.46
3	1.50, m	1.50, m	26.80	26.75
	0.86, qd, 12.0, 4.0	0.87, qd, 11.8, 4.0		
4	1.35, m	1.34, m	25.11	25.07
	1.81, m	1.82, m		
5	1.56, m	1.58, m	27.71	27.66
6	2.75, td, 11.0, 3.2	2.78, m[a]	53.55	53.51
	2.94, m	2.96, m		
7	2.88, ddd, 5.7, 1.4, 1.3	2.88, m	60.39	60.33
8	4.30, dddd, 9.5, 5.0, 3.0, 1.4	4.31, m	65.37	65.30
9	2.66, dd, 12.2, 9.5	2.67, dd, 12.2, 9.6	41.57	41.50
	1.38, dd, 12.2, 5.0	1.38, dd, 12.2, 4.9		
10			86.29	86.23
12			176.31	176.25
13	5.74, t, 1.9	5.74, t, 1.9	112.04	111.99
14			177.25	177.20
15	2.82, m	2.78, m[a]	30.32	30.28
	2.97, ddd, 18.4, 1.9, 1.3	2.96, m		

[a] Signals were not resolved and averaged as a single multiplet.

4.3 Rearrangements of Neo(nor)securinane- to (Nor)securinane-type Alkaloids

The transformation of an azabicyclo[2.2.2]octane core into an azabicyclo[3.2.1]octane core observed by Magnus and coworkers during the total synthesis of nirurine (**178**) might be of great significance for the biosynthesis of the *Securinega* alkaloids (see Scheme 40).[198] Although Horii and coworkers also reported similar transformations for securinol A (**176**),[148] B and C,[161] the correct structural foundation had not been established at the time. As a consequence, these observations have not been considered during the development of the general biosynthetic pathway formulated in the 1970s (see Scheme 39). Also, the observations by Magnus and coworkers did not receive much attention in the literature. The only similar transformation reported to date is the rearrangement of niruroidine ((–)-**215**) to norsecurinine (**175**, Scheme 71).[199] However, a closer look at the reported substrates reveals that niruroidine ((–)-**215**) represents the (–)-enantiomer of the racemic synthetic intermediate **215** reported by Magnus and coworkers.

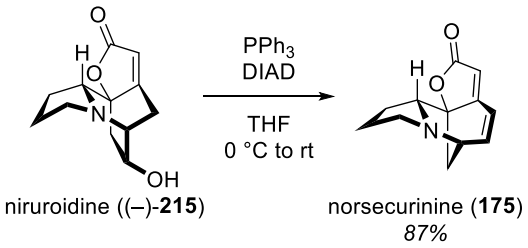

Scheme 71: Rearrangement reported by Ye, Jiang *et al.*

With synthetic access to secu'amamine E (**296**) we decided to investigate the generality of the dehydrative rearrangement of neonorsecurinane- to norsecurinane-type alkaloids. Synthetic bubbialidine (**292**) was obtained through the previously published route and also bubbialine (**327**) was prepared from the other diastereomer of intermediate **290** (Scheme 57).[158] Thus, three different alkaloids were tested (Figure 27).

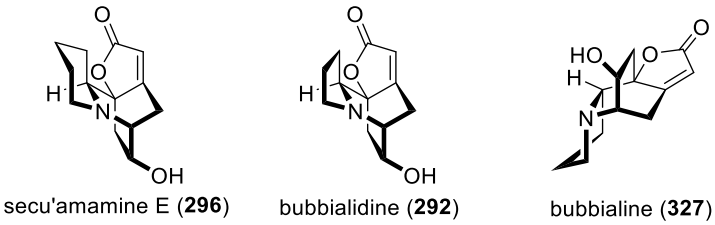

Figure 27: The three *Securinega* alkaloids investigated in the present study.

Structurally, all three candidates were distinct from the substrates of the earlier reports. The present alkaloids have an inverted configuration at the AB ring junction at C2 relative to niruroidine ((–)-**215**). Secu'amamine E (**296**) and bubbialidine (**292**) are homologous featuring a piperidine and a pyrrolidine A ring, respectively. Furthermore, both feature an *antiperiplanar* configuration of the tertiary amine and hydroxyl functions, whereas bubbialine (**327**) features a *synperiplanar* configuration.

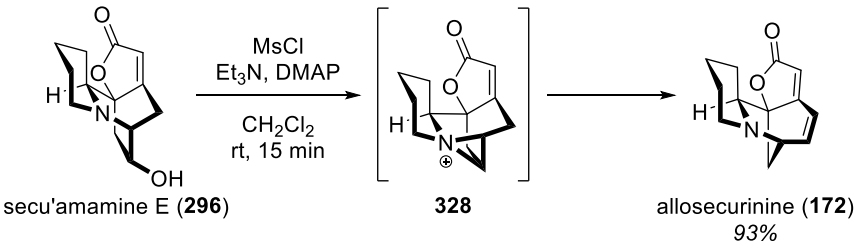

Scheme 72: Dehydrative rearrangement of secu'amamine E (**296**) to allosecurinine (**172**).

When a mixture of secu'amamine E (**296**), DMAP and triethylamine in dichloromethane was treated with methanesulfonyl chloride at room temperature, very fast conversion of the substrate was observed (Scheme 72). The mixture turned yellow and a colorless solid precipitated. Although reactions were typically run for 10–15 min, complete consumption of the alkaloid **296** was observed by TLC, even when the sample was taken from the reaction mixture within 1 min after addition of the reagent. The mixture was then concentrated under high vacuum and subjected to flash chromatography giving allosecurinine (**172**) in an excellent yield of 93%. Very similar results were obtained with the homologous bubbialidine (**292**, Scheme 73). A fast spot-to-spot transformation proceeded upon the same experimental treatment described above and (–)-allonorsecurinine (**329**) was isolated, albeit in a somewhat lower yield of only 63%.

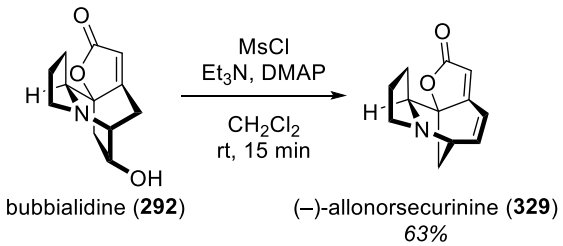

Scheme 73: Dehydrative rearrangement of bubbialidine (**292**) to (–)-allonorsecurinine (**329**).

When bubbialine (**327**) was treated under same conditions, again, fast spot-to-spot transformation was observed (Scheme 74). However, after separation of the crude mixture, bubbialine mesylate **330** was obtained in almost quantitative yield. Also, prolonged stirring of the reaction mixture did not trigger the rearrangement. Only under forcing conditions transformation of this intermediate was observed. A mixture of mesylate **330** and triethylamine in dichloromethane

was prepared in a pressure tube and heated in a microwave reactor at 100 °C for 6 h. During this time the mixture developed a dark brown color and TLC indicated the formation of side products. Purification by flash chromatography afforded (+)-allonorsecurinine (**331**) in a low yield of 21% and only in moderate purity as judged by ^{1}H NMR analysis.

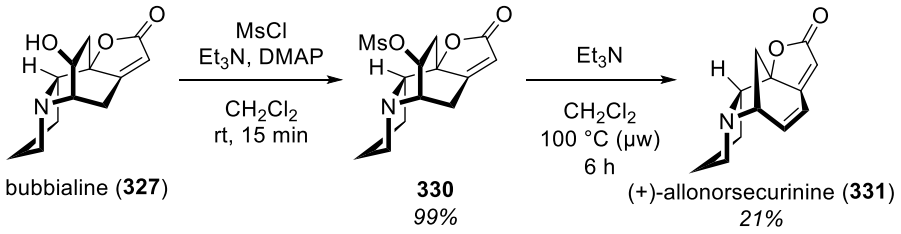

Scheme 74: Dehydrative rearrangement of bubbialine (**327**) to (+)-allonorsecurinine (**331**).

The three (nor)securinane-type products **172**, **329** and **331** obtained from the above transformations were identified by comparison of their NMR and optical rotation data with those reported in the literature.[211,212,221] The results of these experiments are in agreement with the proposed mechanism of the rearrangement process. The configuration at C2 apparently has no influence on the transformation and short reaction times in combination with good yields were observed. For the decreased yield of (–)-allonorsecurinine (**329**) compared to allosecurinine (**172**) two reasons were considered. On one hand, a loss of material during flash chromatography cannot be excluded, as these alkaloid compounds are polar and tend to stick to silica gel. Possibly, the amount of triethylamine added to the eluent used for separation was not sufficient. On the other hand, norsecurinine (**175**) is known to be a reactive compound and the large variety of known norsecurinine-based oligomers is a result and testimony thereof. While decomposition of the synthetic allosecurinine (**172**) upon storage at 4 °C was observed within several days to a few weeks, the decomposition of both allonorsecurinine enantiomers **329** and **331** appeared to be faster. Also, the clean transformation observed by TLC analysis of the reaction mixture did not indicate undesired side reactions. The stability of the mesylate intermediate **330** obtained from bubbialine (**327**) can be explained by the *synperiplanar* configuration of the amine and ester groups. While the *antiperiplanar* configuration of the other two alkaloids allows for an intramolecular S_N2 reaction leading to the aziridinium intermediate, this is not possible with mesylate **330**. The lone pair of the nucleophilic amine group cannot reach into the σ* orbital of the C-O bond and thus the mesylate needs to be extruded *via* an S_N1 mechanism. The high temperatures required for the S_N1 reaction probably led to undesired side reactions as well as decomposition of (+)-allonorsecurinine (**331**). Hence, a low yield of impure product **331** was obtained.

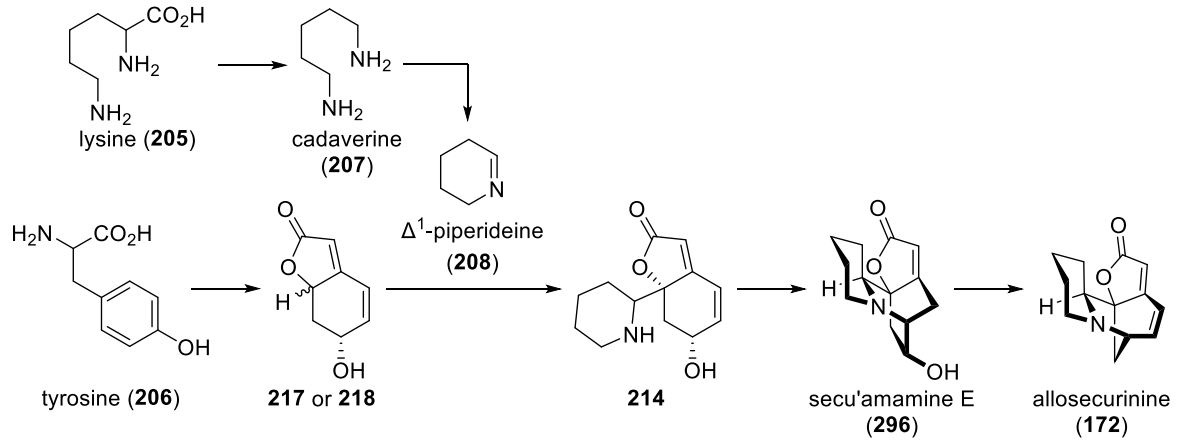

Scheme 75: Linear biogenetic hypothesis for allosecurinine (**172**).

These results support the hypothesis that the dehydrative rearrangement of neo(nor)securinane-type alkaloids with an azabicyclo[2.2.2]octane core to (nor)securinane-type alkaloids featuring an azabicyclo[3.2.1]octane core is involved in the biogenesis of *Securinega* alkaloids. Thus, we support a linear biosynthetic pathway for these compounds (Scheme 75). In the case of allosecurinine (**172**), a CD ring fragment represented by (+)-menisdaurilide ((+)-**217**) or (+)-aquilegiolide ((+)-**218**) would be generated from tyrosine (**206**). Lysine-derived Δ^1-piperideine (**208**) would be introduced and intramolecular 1,6-addition would furnish the neosecurinane-type secu'amamine E (**296**). Dehydrative rearrangement would then forge the securinane-type allosecurinine (**172**). However, this hypothesis raises new questions about the family of *Securinega* alkaloids, some of which might be addressed through further phytochemical investigations of the plants producing these compounds. Since the rearrangement only proceeds with alkaloids featuring an *antiperiplanar* configuration of the amine and hydroxyl groups, the fate of the *syn*-configured congeners remains unclear. These alkaloids were not reported to accumulate in plants and isomerization at the C15 position to invert the orientation of the hydroxyl function might occur in nature. A linear biogenesis implies a connection between certain alkaloid members and allows for a prediction, which compounds should occur in the same plant. For example, every plant, that contains secu'amamine E (**296**), should also contain allosecurinine (**172**) due to their stereochemical relationship. Accordingly, every plant, that contains bubbialidine (**292**), should also contain (–)-allonorsecurinine (**329**). In fact, both enantiomers of allonorsecurinine (**329** and **331**) have not been isolated from a natural source and remain putative natural products to date. Therefore, isolation of either compound would corroborate the linear biogenetic hypothesis. Furthermore, a general detailed mapping of the occurrence of the different alkaloids and their relative amounts would help in understanding their interrelationships.

4.4 Conclusion

We have achieved the first enantioselective total synthesis of secu'amamine E (**296**) in 12 linear synthetic steps from commercially available 1,4-cyclohexanedione monoethylene acetal (**307**) in an overall yield of 8.5%. Introduction of chirality *via* proline-catalyzed α-aminoxylation allows for modulation of the synthesis and gives access to virosine A (**297**), the enantiomer of secu'amamine E (**296**). An improved synthesis of known bicyclic lactone **288** has been developed affording the compound in 16.1% yield in only seven synthetic steps. Key steps in the assembly of secu'amamine E (**296**) include D ring formation using the Bestmann ylide, a vinylogous Mannich reaction to introduce the A ring fragment and an intramolecular vinylogous aza-Michael addition to generate the bicyclic core structure.

The dehydrative rearrangement reactions of neosecurinane-type secu'amamine E (**296**) and neonorsecurinane-type bubbialidine (**292**) and bubbialine (**327**) to securinane-type allosecurinine (**172**) and norsecurinane-type (–)- and (+)-allonorsecurinine (**329** and **331**), respectively, have been investigated. The fast and high-yielding transformation of the azabicyclo[2.2.2]-octane core to the azabicyclo[3.2.1]octane core observed with alkaloids **296** an **327** featuring an *antiperiplanar* configuration of the involved amine and hydroxyl groups confirms a possible biogenetic relevance of this process. These results support a linear biogenetic hypothesis classifying the neo(nor)securinane-type alkaloids as biogenetic precursors of the (nor)securinane-type alkaloids. Further evidence to support this hypothesis might be gained through detailed phytochemical investigations involving more species from the Phyllanthaceae plant family.

5 Conclusion

The present thesis entitled "*Design of Bio-Inspired Materials and Total Synthesis of Securinega Alkaloids*" demonstrates the versatility of modern organic chemistry and its immeasurable importance for fundamental research. The four projects presented throughout this work have yielded novel synthetic approaches contributing to the generation of complex chemical systems, the investigation of essential cellular processes and the study of plant natural products.

The first chapter described the development a of nitrocatechol-based surface anchoring unit for the immobilization and controlled release of small molecular cargos. An operationally simple dip-and-rinse procedure allowed for the formation of self-assembled monolayers on bare titanium dioxide surfaces and UV irradiation induced cleavage of the deposited substances from the solid support. Protocols for the straightforward production and modification of the coating agent were established. The potential to employ cargos exploiting different functional groups, especially amino and hydroxyl groups, was shown. The technique holds potential for drug delivery and uncaging of bioactive substances under temporal as well as spatial control.

In the second chapter, the synthesis of new catechol derivatives and their application in systems chemistry was presented. A modular branched synthesis was elaborated providing valuable intermediates for the introduction of further structural diversity. The compounds feature electron-withdrawing substituents on the aryl moiety, which have not been investigated in related materials. The novel catechol binders were utilized in the formation and dynamic exchange of boronate esters and led to the discovery of the third orthogonal dynamic covalent bond. Complementing the use of hydrazones and disulfides this additional component could potentiate the complexity achieved with dynamic functional systems. The use of naphthalenediol derivatives for boronate ester formation was suggested and first efforts towards their preparation were reported.

The third chapter documented the design of biochemical probes based on the immuno-suppressive natural product rapamycin. The bacterial macrolide was combined with biotin in three natural product hybrids for the isolation and structural characterization of the cellular target of rapamycin. While the two first-generation compounds exhibited antiproliferative activity against *S. cerevisiae* and allowed for binding to streptavidin, these functions appeared to be exclusive and an extended rapamycin-biotin hybrid was synthesized. Efforts on the assembly of a rapamycin-gold nanoparticle conjugate established the first steps towards a crucial amino rapamycin intermediate. Further development into fully functional biochemical probes might enable the isolation of the large multiprotein target of rapamycin complex 1 from

cell protein extracts and facilitate its characterization by single-crystal X-ray diffraction. Attachment of a gold nanoparticle would install a tag, which can be visualized by cryo-electron microscopy for additional structural investigations.

The fourth chapter provided a comprehensive introduction into the fascinating realm of the *Securinega* alkaloids. The first enantioselective total synthesis of secu'amamine E was achieved in 12 linear synthetic steps and 8.5% overall yield. The synthetic strategy was based on a previous synthesis of related alkaloids developed in our group and a new route to a common intermediate was devised. Key transformations on the way to secu'amamine E included butenolide formation using the Bestmann ylide, introduction of the piperidine moiety by a vinylogous Mannich reaction and an intramolecular vinylogous aza-Michael addition to forge the bridged structure of the natural product. Experiments on the rearrangement reactions of three different alkaloids, which were synthesized in our laboratories, afforded three additional known compounds through direct interconversion of the tetracyclic core structures. These results suggested a linear biogenetic hypothesis for the different subtypes of the *Securinega* alkaloids.

6 Experimental

6.1 General Information

All chemicals have been purchased from Sigma-Aldrich, Acros, Alfa Aesar, TCI or Fluorochem and were used without further purification (except for Et_3N which was freshly distilled before use). All reactions have been carried out in heat gun-dried glassware (unless aqueous reagents were used) and reactions involving air sensitive compounds have been performed under an argon atmosphere. Solvents applied for chemical transformations were either puriss quality or HPLC grade solvents, which have been dried by filtration through activated aluminium oxide under nitrogen (water content <10 ppm, *Karl-Fischer* titration). For workup and purification solvents have been distilled from technical grade. All synthetic transformations have been monitored by either thin layer chromatography (TLC), UPLC-MS or ^{1}H NMR spectroscopy.

Microwave heating (µw) was performed in sealed glass vials using a Biotage Initiator+ microwave synthesizer.

TLC was performed on Merck silica gel 60 F_{254} plates (0.25 mm thickness) precoated with fluorescent indicator. The developed plates were examined under UV light and stained with ceric ammonium molybdate or potassium permanganate followed by heating.

Concentration under reduced pressure was performed by rotary evaporation at 40 °C (unless stated otherwise).

Flash chromatography was performed using silica gel 60 (230-400 mesh) from Sigma-Aldrich with a forced flow eluent at 0.3–0.5 bar pressure.

^{1}H and ^{13}C NMR spectra were recorded using Bruker 300 MHz (^{1}H) or Bruker 400 MHz (^{1}H) & 101 MHz (^{13}C) or Bruker 500 MHz (^{1}H) & 126 MHz (^{13}C) spectrometers at room temperature. Chemical shifts (δ-values) are reported in ppm, spectra were calibrated related to solvents' residual proton chemical shifts ($CDCl_3$, δ = 7.26; CD_3OD, δ = 3.31; C_6D_6, δ = 7.16; DMSO-*d*$_6$, δ = 2.50) and solvents' residual carbon chemical shifts ($CDCl_3$, δ = 77.16; CD_3OD, δ = 49.00; C_6D_6, δ = 128.06; DMSO-*d*$_6$, δ = 39.52), multiplicity is reported as follows: s = singlet, br s = broad singlet, d = doublet, t = triplet, q = quartet, p = pentet, h = hextet, m = multiplet or unresolved and coupling constant *J* in Hz.

IR spectra were recorded on a Varian 800 FT-IR ATR Spectrophotometer or a PerkinElmer Spectrum Two IR Spectrometer both equipped with a diamond ATR unit. The absorptions are reported in cm^{-1}.

Optical rotations were determined on a Jasco P-2000 digital polarimeter at the 589.3 nm sodium D line using a 1 ml cell with a length of 10 cm and concentrations (c) are stated in g/100 mL.

High resolution mass spectra (HRMS-ESI) were recorded by Dr. Heinz Nadig at the University of Basel on a Bruker maXis 4G QTOF ESI mass spectrometer or by the mass spectrometry service at the University of Zürich on a Finnigan MAT95 mass spectrometer.

Melting points (M.p.) were determined using a Büchi B-545 apparatus in open capillaries and are uncorrected.

Preparative, reversed-phase HPLC was performed with a Varian 218 pump, a Dionex VWD-3400 detector and a Dionex AFC-3000 fraction collector on a Phenomenex Gemini-NX 10µ C18 110A (250 x 21.2 mm) column eluting with a constant gradient of MeCN in water from 5–100% over 30 min at a flow rate of 20 mL min^{-1}.

Semi-preparative, reversed-phase HPLC was performed on a Dionex HPLC system equipped with a P680 pump, an ASI-100 automated sample injector, a TCC-100 thermostatic column compartment, and a PDA-100 photodiode array detector on a Phenomenex Gemini 10µ C18 (150 x 10 mm) column eluting with stated gradients of MeCN in H_2O at a flow rate of 5 mL min^{-1}.

Analytical, reversed-phase UPLC was performed with an Agilent 1290 Infinity LC system on a Zorbax SB-C18 (1.8 µm, 50 x 2.1 mm) column eluting with a linear gradient of MeCN in H_2O containing 0.1% formic acid at a flow rate of 0.8 mL min^{-1}.

For the acute toxicity assay "Thamnotoxkit F" was purchased from MicroBioTests Inc., Kleimoer 15, 9030 Mariakerke/Ghent, Belgium, and the assay was conducted as described in the operating procedure.

IBX (**54**),[47] rapamycin hemisuccinate (**150**),[116] 5-azidopentan-1-amine (**168**),[120] Davis oxaziridine **318**,[233] the Bestmann ylide (**323**)[234] and δ-lactamol **274**[236] were obtained following known literature procedures.

Samples of bubbialidine (**292**) and bubbialine (**327**) were synthesized by Dr. Hideki Miyatake-Ondozabal and Linda Bannwart following the published route.[158]

6.2 UV-Labile Nitrocatechol Derivatives

Ethyl catechol (47):

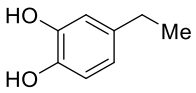

To a solution of 4-ethyl phenol (**53**, 1.00 g, 8.10 mmol, 1.0 eq.) in MeOH (80 mL) at 0 °C was added IBX (**54**, 2.50 g, 8.91 mmol, 1.1 eq.) and the mixture was stirred for 1.5 h at room temperature. Sodium dithionite was added and stirring continued for 10 min. The solvent was removed under reduced pressure. Sat. aq. $NaHCO_3$ was added and the mixture extracted with EtOAc. The combined organic layers were washed with water, dried over Na_2SO_4 and evaporated to afford crude ethyl catechol (**47**, 953 mg) as a red oil, which was used without further purification.

5-Ethyl-2,2-dimethylbenzo[*d*][1,3]dioxole (48):

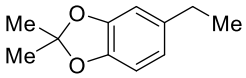

A solution of crude ethyl catechol (947 mg), 2,2-dimethoxypropane (1.68 mL, 13.7 mmol) and *p*TsOH (13.0 mg, 68.5 µmol) in benzene (25 mL) was refluxed overnight. After cooling to room temperature, the mixture was poured into sat. aq. $NaHCO_3$ followed by extraction with Et_2O. The combined organic layers were washed with water, dried over Na_2SO_4 and evaporated to afford crude acetonide **48** (1.10 g) as a yellow oil, which was used without further purification.

To obtain analytically pure **48**, the crude product could be subjected to flash chromatography (pentane, 1% Et_3N). $\mathbf{R_f}$ = 0.6 (pentane); **FTIR** (neat): $\tilde{\nu}$ = 2965, 2934, 2873, 1496, 1445, 1377, 1228, 1156, 982, 837, 808 cm^{-1}; **^{1}H NMR** (400 MHz, $CDCl_3$) δ 6.65–6.58 (m, 3H), 2.56 (q, *J* = 7.6 Hz, 2H), 1.66 (s, 6H), 1.20 (t, *J* = 7.6 Hz, 3H); **^{13}C NMR** (101 MHz, $CDCl_3$) δ 147.49, 145.43, 137.68, 119.87, 117.56, 108.36, 108.01, 28.80, 25.99, 16.14.

5-Ethyl-2,2-dimethyl-6-nitrobenzo[*d*][1,3]dioxole (49):

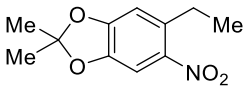

Neat, crude acetonide **48** (1.10 g) was cooled to 0 °C, a cold solution of HNO_3 (2.7 mL) in water (2.7 mL) was added and the mixture was stirred for 1 h at room temperature. The mixture was slowly poured into sat. aq. $NaHCO_3$ followed by extraction with Et_2O. The combined organic layers were washed with water dried over Na_2SO_4 and evaporated to afford **49** (1.08 g, 60% over three steps) as a yellow solid.

M.p. = 56–59 °C; $\mathbf{R_f}$ = 0.3 (pentane); **FTIR** (neat): $\tilde{\nu}$ = 2988, 2938, 2877, 1615, 1519, 1492, 1416, 1379, 1331, 1250, 1215, 981, 876 cm^{-1}; **^{1}H NMR** (400 MHz, $CDCl_3$) δ 7.39 (s, 1H), 6.64 (s, 1H), 2.88 (q, *J* = 7.4 Hz, 2H), 1.71 (s, 6H), 1.26 (t, *J* = 7.4 Hz, 3H); **^{13}C NMR** (101 MHz, $CDCl_3$) δ 151.76, 145.98, 142.30, 136.26, 120.81, 109.72, 105.59, 27.23, 26.03, 15.18; **HRMS** (ESI) Exact mass calcd. for $C_{11}H_{13}O_4NNa^+$ $[M+Na]^+$: 246.0737, found: 246.0738.

2-(2,2-Dimethyl-6-nitrobenzo[*d*][1,3]dioxol-5-yl)propan-1-ol (50):

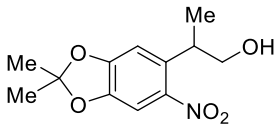

A solution of **49** (700 mg, 3.13 mmol, 1.0 eq.) and paraformaldehyde (188 mg, 6.26 mmol, 2.0 eq.) in DMSO (3.0 mL) was added methanolic benzyltrimethylammonium hydroxide solution (Triton B, 40 wt%, 0.66 mL, 1.57 mmol, 0.5 eq.) and the mixture was stirred at 90 °C for 4.5 h in a sealed tube. After cooling to room temperature, the mixture was diluted with water and neutralized using 1 M aq. HCl followed by extraction with Et_2O. The combined organic layers were washed with water, dried over Na_2SO_4 and evaporated. The residue was subjected to flash chromatography (pentane/Et_2O, 1:1, 1% Et_3N) and product fractions were first concentrated, washed with water (to remove Et_3N, which was not possible by evaporation), dried over Na_2SO_4 and then evaporated to afford **50** (675 mg, 85%) as a yellow oil, which eventually solidified at 4 °C.

$\mathbf{R_f}$ = 0.3 (pentane/EtOAc, 3:2); **FTIR** (neat): $\tilde{\nu}$ = 3335, 2988, 2927, 2878, 1519, 1493, 1379, 1335, 1256, 1214, 1033, 978, 872, 822, 759 cm^{-1}; **^{1}H NMR** (400 MHz, $CDCl_3$) δ 7.24 (s, 1H), 6.77 (s, 1H), 3.81–3.70 (m, 2H), 3.67–3.59 (m, 1H), 1.71 (s, 6H), 1.27 (d, *J* = 6.8 Hz, 3H); **^{13}C NMR** (101 MHz, $CDCl_3$) δ 151.68, 146.12, 143.94, 134.86, 121.03, 106.67, 105.31, 68.20, 36.55, 26.10, 17.84; **HRMS** (ESI) Exact mass calcd. for $C_{12}H_{15}NNaO_5^+$ $[M+Na]^+$: 276.0842, found: 276.0842.

5-(1-(Benzyloxy)propan-2-yl)-2,2-dimethyl-6-nitrobenzo[*d*][1,3]dioxole (55):

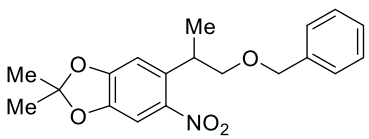

A solution of **50** (69.0 mg, 272 µmol, 1.0 eq.) in THF (0.5 mL) was cooled to 0 °C and sodium hydride (60% dispersion in mineral oil, 16.3 mg, 409 µmol, 1.5 eq.) was added. After stirring for 30 min, benzyl bromide (69.9 mg, 409 µmol, 1.5 eq.) was added dropwise and the mixture was stirred at room temperature for 24 h in the dark. The reaction mixture was cooled to 0 °C and quenched by the slow addition of water. The mixture was extracted with CH_2Cl_2 and the combined organic layers were washed with water, dried over Na_2SO_4 and evaporated. The

residue was subjected to flash chromatography (pentane/Et_2O, 7:1, 1% Et_3N) to yield **55** (68 mg, 73%) as a yellow oil.

R_f = 0.5 (pentane/Et_2O, 7:1); **FTIR** (neat): $\tilde{\nu}$ = 2890, 2853, 1522, 1496, 1338, 1262, 1219 cm^{-1}; **^{1}H NMR** (400 MHz, $CDCl_3$) δ 7.35–7.26 (m, 5H), 7.24 (s, 1H), 6.77 (s, 1H), 4.50 (s, 2H), 3.78 (h, *J* = 6.7 Hz, 1H), 3.60 (dd, *J* = 9.5, 6.3 Hz, 1H), 3.52 (dd, *J* = 9.5, 6.4 Hz, 1H), 1.71 (s, 3H), 1.71 (s, 3H), 1.30 (d, *J* = 6.9 Hz, 3H); **^{13}C NMR** (101 MHz, $CDCl_3$) δ 151.39, 145.92, 143.58, 138.45, 135.27, 128.46, 127.66, 120.77, 107.14, 105.25, 74.80, 72.96, 34.26, 26.06, 18.38; **HRMS** (ESI) Exact mass calcd. for $C_{19}H_{21}NNaO_5^+$ $[M+Na]^+$: 366.1312, found: 366.1310.

4-(1-(Benzyloxy)propan-2-yl)-5-nitrobenzene-1,2-diol (56):

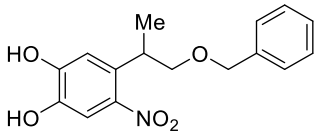

Neat **55** (54 mg, 157 µmol) was mixed with TFA (1.0 mL) and water (0.4 mL) and the mixture was stirred at room temperature for 72 h in the dark. Volatiles were removed under reduced pressure and the residue was separated by preparative reversed-phase HPLC to obtain **56** (36 mg, 76%) as a yellow semisolid.

FTIR (neat): $\tilde{\nu}$ = 3600–3100, 2873, 1522, 1329, 1283, 1217, 1189, 1061, 882, 805, 749, 698 cm^{-1}; **^{1}H NMR** (400 MHz, CD_3OD) δ 7.36 (s, 1H), 7.31–7.20 (m, 5H), 6.84 (s, 1H), 4.45 (s, 2H), 3.75 (h, *J* = 6.8 Hz, 1H), 3.58 (dd, *J* = 9.3, 6.4 Hz, 1H), 3.49 (dd, *J* = 9.3, 6.7 Hz, 1H), 1.26 (d, *J* = 6.9 Hz, 3H); **^{13}C NMR** (101 MHz, CD_3OD) δ 151.77, 144.72, 142.79, 139.61, 133.50, 129.27, 128.68, 128.53, 115.01, 112.81, 76.11, 73.83, 34.81, 18.43; **HRMS** (ESI) Exact mass calcd. for $C_{16}H_{17}NNaO_5^+$ $[M+Na]^+$: 326.0999, found: 326.1001.

2-(2,2-Dimethyl-6-nitrobenzo[*d*][1,3]dioxol-5-yl)propanal (57):

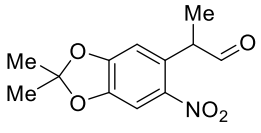

To a solution of **50** (100 mg, 395 µmol, 1.0 eq.) in CH_2Cl_2 (2.0 mL) Dess-Martin periodinane (1,1,1-triacetoxy-1,1-dihydro-1,2-benziodoxol-3(1*H*)-one, 251 mg, 592 µmol, 1.5 eq.) was added and the mixture was stirred at room temperature for 1.5 h. The mixture was poured into sat. aq. $NaHCO_3$ followed by extraction with CH_2Cl_2. The combined organic layers were dried over Na_2SO_4 and evaporated, and the residue was subjected to flash chromatography (pentane/Et_2O, 4:1, 1% Et_3N) to yield **57** (92 mg, 93%) as a yellow oil.

R_f = 0.5 (pentane/Et_2O, 4:1); **FTIR** (neat): $\tilde{\nu}$ = 2991, 1725, 1493, 1379, 1332, 1259, 1211, 978, 823 cm^{-1}; **^{1}H NMR** (400 MHz, $CDCl_3$) δ 9.74 (s, 1H), 7.46 (s, 1H), 6.58 (s, 1H), 4.32 (q, *J* = 7.1 Hz, 1H), 1.72 (s, 6H), 1.48 (d, *J* = 7.1 Hz, 3H); **^{13}C NMR** (101 MHz, $CDCl_3$) δ 199.65, 152.23, 147.09, 142.95, 129.83, 121.70, 108.78, 106.10, 48.61, 26.09, 14.58; **HRMS** (ESI) Exact mass calcd. for $C_{12}H_{13}NNaO_5^+$ $[M+Na]^+$: 274.0686, found 274.0684.

***N*-Benzyl-2-(2,2-dimethyl-6-nitrobenzo[*d*][1,3]dioxol-5-yl)propan-1-amine (58):**

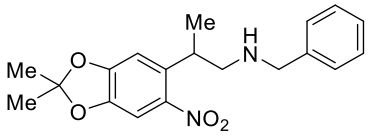

To a solution of **57** (80.0 mg, 318 µmol, 1.0 eq.) in 2,2,2-trifluoroethanol (1.5 mL) benzylamine (39 µL, 350 µmol, 1.1 eq.) was added and the mixture was stirred at 40 °C for 10 min during which the mixture turned deep red. $NaBH_4$ (14.8 mg, 382 µmol, 1.2 eq.) was added and stirring continued for 75 min in the dark. The mixture was slowly poured into sat. aq. $NaHCO_3$ followed by extraction with CH_2Cl_2. The combined organic layers were washed with sat. aq. $NaHCO_3$, dried over Na_2SO_4 and evaporated to yield **58** (95 mg, 87%) as a yellow oil, which was used without further purification.

R_f = 0.3 (pentane/EtOAc, 1:1); **FTIR** (neat): $\tilde{\nu}$ = 2988, 1520, 1494, 1338, 1260, 1219, 979 cm^{-1}; **^{1}H NMR** (400 MHz, $CDCl_3$) δ 7.35–7.21 (m, 5H), 7.22 (s, 1H), 6.69 (s, 1H), 3.76 (s, 2H), 3.67–3.58 (m, 1H), 2.81 (dd, *J* = 11.9, 7.6 Hz, 1H), 2.75 (dd, *J* = 11.9, 6.6 Hz, 1H), 1.72 (s, 3H), 1.70 (s, 3H), 1.26 (d, *J* = 6.9 Hz, 3H); **^{13}C NMR** (101 MHz, $CDCl_3$) δ 151.54, 145.84, 143.75, 140.49, 136.40, 128.46, 128.12, 126.99, 120.80, 106.35, 105.19, 55.69, 53.69, 34.23, 26.08, 20.01; **HRMS** (ESI) Exact mass calcd. for $C_{19}H_{23}N_2O_4^+$ $[M+H]^+$: 343.1652, found: 343.1655.

4-(1-(Benzylamino)propan-2-yl)-5-nitrobenzene-1,2-diol (59):

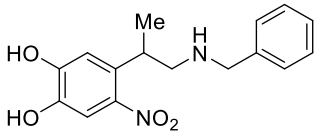

Deprotection of **58** (67.0 mg, 196 µmol) was performed analogously to **56** yielding **59** (50.0 mg, 84%) as a red oil.

FTIR (neat): $\tilde{\nu}$ = 3094, 2984, 2828, 1669, 1530, 1332, 1289, 1183, 1135, 801, 722, 698 cm^{-1}; **^{1}H NMR** (400 MHz, CD_3OD) δ 7.47–7.43 (m, 5H), 7.42 (s, 1H), 6.85 (s, 1H), 4.21–4.16 (m, 2H), 3.90–3.81 (m, 1H), 3.35–3.30 (m, 1H), 3.22 (dd, *J* = 12.6, 6.8 Hz, 1H), 1.34 (d, *J* = 6.9 Hz, 3H); **^{13}C NMR** (101 MHz, CD_3OD) δ 152.72, 145.85, 142.49,

132.10, 131.07, 131.02, 130.77, 130.28, 114.70, 113.21, 54.39, 52.86, 32.55, 20.07; **HRMS** (ESI) Exact mass calcd. for $C_{16}H_{19}N_2O_4^+$ $[M+H]^+$: 303.1339, found: 303.1340.

5-(1-Bromopropan-2-yl)-2,2-dimethyl-6-nitrobenzo[*d*][1,3]dioxole (62):

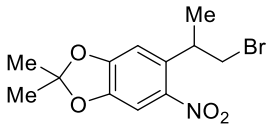

To a solution of **50** (100 mg, 0.395 mmol, 1.0 eq.) in CH_2Cl_2 (2.0 mL) at 0 °C, CBr_4 (164 mg, 0.494 mmol, 1.25 eq.) and PPh_3 (129 mg, 0.494 mmol, 1.25 eq.) were added. After 20 min the cooling bath was removed and stirring continued at room temperature for 90 min. The mixture was evaporated under reduced pressure, the residue taken up in Et_2O and filtered. The filtrate was evaporated and the residue subjected to flash chromatography (pentane/Et_2O, 5:1, 1% Et_3N) to give **62** (127 mg, quant.) as a yellow oil.

$\mathbf{R_f}$ = 0.7 (pentane/Et_2O, 5:1); **FTIR** (neat): $\tilde{\nu}$ = 3069, 2991, 1496, 1379, 1336, 1264, 1214, 979, 882, 821, 685 cm^{-1}; **^{1}H NMR** (400 MHz, $CDCl_3$) δ 7.28 (s, 1H), 6.73 (s, 1H), 3.84 (h, *J* = 6.7 Hz, 1H), 3.62 (dd, *J* = 10.0, 6.0 Hz, 1H), 3.54 (dd, *J* = 10.0, 6.8 Hz, 1H), 1.72 (d, *J* = 5.7 Hz, 6H), 1.41 (d, *J* = 6.8 Hz, 3H); **^{13}C NMR** (101 MHz, $CDCl_3$) δ 151.60, 146.47, 143.38, 134.30, 121.25, 106.70, 105.51, 39.07, 36.23, 26.09, 20.08.

Benzyl (2-(2,2-dimethyl-6-nitrobenzo[*d*][1,3]dioxol-5-yl)propyl)carbonate (65):

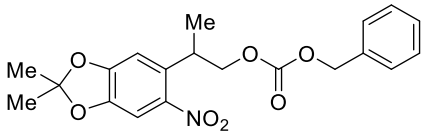

A solution of **50** (100 mg, 395 µmol, 1.2 eq.) and Et_3N (56 µL, 395 µmol, 1.2 eq.) in THF (0.6 mL) was added dropwise to a solution of triphosgene (137 mg, 461 µmol, 1.4 eq.) at 0 °C. The mixture was stirred for 30 min at 0 °C, after which volatiles were removed *in vacuo* without heating. The residue was taken up in CH_2Cl_2 (1.0 mL), added slowly to a solution of benzyl alcohol (34 µL, 329 µmol, 1.0 eq.) in pyridine (1.0 mL) at 0 °C. The resulting mixture was stirred for 20 min at 0 °C followed by another 60 min at room temperature. The mixture was poured into water and extracted with CH_2Cl_2. The combined organic layers were dried over Na_2SO_4 and evaporated to yield crude **65** (152 mg), which was used without further purification.

^{1}H NMR (400 MHz, $CDCl_3$) δ 7.42–7.28 (m, 5H), 7.26 (s, 1H), 6.75 (s, 1H), 5.14 (s, 2H), 4.34–4.22 (m, 2H), 3.84 (h, *J* = 6.8 Hz, 1H), 1.71 (s, 6H), 1.31 (d, *J* = 6.9 Hz, 3H); **^{13}C NMR** (101 MHz, $CDCl_3$) δ 155.16, 151.63, 146.35, 143.53, 135.29, 133.53, 128.74, 128.68, 128.49,

121.12, 106.87, 105.52, 71.86, 69.85, 33.55, 26.08, 18.06; **HRMS** (ESI) Exact mass calcd. for $C_{20}H_{25}N_2O_7^+$ $[M+NH_4]^+$: 405.1656, found: 405.1661.

Benzyl (2-(4,5-dihydroxy-2-nitrophenyl)propyl) carbonate (66):

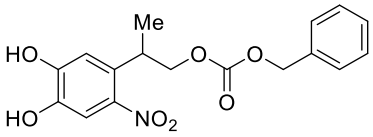

Deprotection of crude **65** (134 mg) was performed analogously to **56** yielding **66** (66.5 mg, 66% over two steps) as a yellow oil.

FTIR (neat): $\tilde{\nu}$ = 3395, 2974, 1719, 1523, 1401, 1380, 1331, 1269, 950, 884, 755, 696 cm^{-1}; **^{1}H NMR** (400 MHz, CD_3OD) δ 7.38 (s, 1H), 7.35–7.26 (m, 5H), 6.86 (s, 1H), 5.08 (s, 2H), 4.30–4.22 (m, 2H), 3.85–3.77 (m, 1H), 1.27 (d, *J* = 7.0 Hz, 3H); **^{13}C NMR** (101 MHz, CD_3OD) δ 156.47, 151.89, 145.08, 142.64, 136.96, 131.93, 129.51, 129.35, 129.07, 114.96, 113.04, 72.93, 70.50, 34.20, 17.98; **HRMS** (ESI) Exact mass calcd. for $C_{17}H_{17}NNaO_7^+$ $[M+Na]^+$: 370.0897, found: 370.0894.

2-(2,2-Dimethyl-6-nitrobenzo[*d*][1,3]dioxol-5-yl)propyl benzylcarbamate (67):

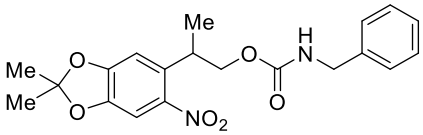

Coupling of **50** (100 mg, 395 µmol, 1.2 eq.) with benzylamine (36 µL, 329 µmol, 1.0 eq.) was performed analogously to **65** yielding crude carbamate **67** (137 mg) as a yellow oil.

FTIR (neat): $\tilde{\nu}$ = 3414, 3397, 2989, 1707, 1518, 1494, 1253, 1214, 979, 823 cm^{-1}; **^{1}H NMR** (400 MHz, $CDCl_3$) δ 7.34–7.24 (m, 5H), 7.21 (s, 1H), 6.74 (s, 1H), 4.94 (s, 1H), 4.34–4.09 (m, 4H), 3.85–3.77 (m, 1H), 1.71 (s, 3H), 1.71 (s, 3H), 1.29 (d, *J* = 6.9 Hz, 3H); **^{13}C NMR** (101 MHz, $CDCl_3$) δ 156.35, 151.49, 146.17, 143.81, 138.49, 133.91, 128.80, 127.64, 127.62, 121.01, 106.60, 105.31, 69.13, 45.20, 33.51, 26.08, 17.74; **HRMS** (ESI) Exact mass calcd. for $C_{20}H_{22}N_2NaO_6^+$ $[M+Na]^+$: 409.1370, found: 409.1373.

2-(4,5-Dihydroxy-2-nitrophenyl)propyl benzylcarbamate (68):

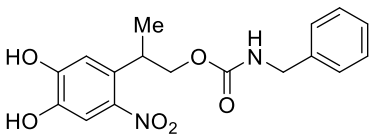

Deprotection of crude **67** (131 mg) was performed analogously to **56** yielding **68** (79.7 mg, 73% over two steps) as a yellow oil.

FTIR (neat): $\tilde{\nu}$ = 3398, 2973, 1682, 1593, 1520, 1453, 1433, 1331, 1284, 1198, 1151, 883, 804, 698 cm^{-1}; **^{1}H NMR** (400 MHz, CD_3OD) δ 7.38 (s, 1H),

7.28–7.07 (m, 5H), 6.87 (s, 1H), 4.22 (s, 2H), 4.20–4.07 (m, 2H), 3.82–3.73 (m, 1H), 1.27 (d, *J* = 6.9 Hz, 3H); **^{13}C NMR** (101 MHz, CD_3OD) δ 158.94, 151.85, 144.93, 142.78, 140.42, 132.54, 129.40, 128.03, 127.97, 114.82, 112.95, 69.77, 45.29, 34.52, 18.28; **HRMS** (ESI) Exact mass calcd. for $C_{17}H_{18}N_2NaO_6^+$ $[M+Na]^+$: 369.1057, found: 369.1053.

2-(2,2-Dimethyl-6-nitrobenzo[*d*][1,3]dioxol-5-yl)propyl 2-phenylacetate (69):

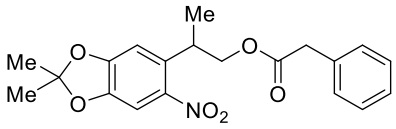

To a solution of **50** (92 mg, 363 µmol, 1.0 eq.) and phenylacetic acid (64.9 mg, 472 µmol, 1.3 eq.) in CH_2Cl_2 (1.8 mL) at 0 °C were added EDC·HCl (90.5 mg, 472 µmol, 1.3 eq.) and DMAP (22.2 mg, 182 µmol, 0.5 eq.) and the mixture was stirred overnight at room temperature in the dark. The mixture was concentrated under reduced pressure and the residue directly subjected to flash chromatography (pentane/Et_2O, 5:1, 1% Et_3N) to yield **69** (107 mg, 79%) as a yellow oil.

R_f = 0.3 (pentane/Et_2O, 5:1); **FTIR** (neat): $\tilde{\nu}$ = 2990, 1737, 1522, 1497, 1339, 1263, 1218, 980, 874, 835 cm^{-1}; **^{1}H NMR** (400 MHz, $CDCl_3$) δ 7.25 (m, 5H), 7.23 (s, 1H), 6.63 (s, 1H), 4.21 (dd, *J* = 10.9, 6.2 Hz, 1H), 4.17 (dd, *J* = 10.9, 6.9 Hz, 1H), 3.87–3.74 (m, 1H), 3.57 (s, 2H), 1.72 (s, 3H), 1.71 (s, 3H), 1.24 (d, *J* = 6.9 Hz, 3H); **^{13}C NMR** (101 MHz, $CDCl_3$) δ 171.40, 151.47, 146.20, 143.67, 133.98, 133.78, 129.38, 128.67, 127.19, 121.01, 106.73, 105.34, 68.79, 41.53, 33.26, 26.07, 17.87; **HRMS** (ESI) Exact mass calcd. for $C_{20}H_{25}N_2O_6^+$ $[M+NH_4]^+$: 389.1707, found: 389.1712.

2-(2,2-Dimethyl-6-nitrobenzo[*d*][1,3]dioxol-5-yl)propyl 2,2-diphenylacetate (71):

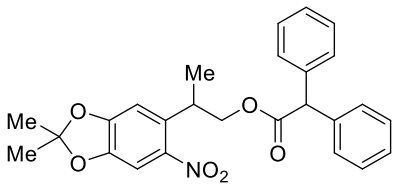

Coupling of **50** (100 mg, 0.395 µmol, 1.0 eq.) with diphenylacetic acid (101 mg, 474 µmol, 1.2 eq.) was performed analogously to **69** yielding **71** (178 mg, quant.) as a yellow oil.

R_f = 0.4 (pentane/Et_2O, 5:1); **FTIR** (neat): $\tilde{\nu}$ = 3063, 3030, 2999, 1736, 1520, 1494, 1380, 1336, 1260, 1215, 1145, 979, 874, 743, 699 cm^{-1}; **^{1}H NMR** (400 MHz, $CDCl_3$) δ 7.31–7.22 (m, 10H), 7.21 (s, 1H), 6.59 (s, 1H), 4.97 (s, 1H), 4.30 (dd, *J* = 10.9, 7.2 Hz, 1H), 4.24 (dd, *J* = 10.9, 5.9 Hz, 1H), 3.85–3.77 (m, 1H), 1.71 (s, 3H), 1.70 (s, 3H), 1.21 (d, *J* = 7.0 Hz, 3H); **^{13}C NMR** (101 MHz, $CDCl_3$) δ 172.27, 151.46, 146.17, 143.59, 138.56, 133.74, 128.71, 128.67, 127.36,

127.35, 120.98, 106.78, 105.37, 68.96, 57.30, 33.33, 26.08, 26.06, 17.89; **HRMS** (ESI) Exact mass calcd. for $C_{26}H_{25}NNaO_6^+$ $[M+Na]^+$: 470.1574, found: 470.1577.

2-(4,5-Dihydroxy-2-nitrophenyl)propyl 2,2-diphenylacetate (72):

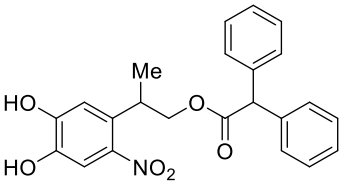

Deprotection of **71** (40.0 mg, 89.4 µmol) was performed analogously to **56** yielding **72** (21 mg, 58%) as a yellow oil.

FTIR (neat): $\tilde{\nu}$ = 3448, 3168, 3029, 2978, 1709, 1601, 1522, 1452, 1374, 1346, 1292, 1203, 1010, 879, 800, 738, 695 cm^{-1}; **^{1}H NMR** (400 MHz, CD_3OD) δ 7.34 (s, 1H), 7.30–7.11 (m, 10H), 6.79 (s, 1H), 4.96 (s, 1H), 4.31 (dd, *J* = 10.8, 8.0 Hz, 1H), 4.22 (dd, *J* = 10.8, 6.0 Hz, 1H), 3.85–3.76 (m, 1H), 1.20 (d, *J* = 6.9 Hz, 3H); **^{13}C NMR** (101 MHz, CD_3OD) δ 173.87, 151.93, 145.03, 142.80, 140.02, 139.98, 132.20, 129.63, 129.58, 129.46, 129.44, 128.13, 128.11, 114.76, 113.06, 70.01, 58.37, 34.01, 18.07; **HRMS** (ESI) Exact mass calcd. for $C_{23}H_{21}NNaO_6^+$ $[M+Na]^+$: 430.1261, found: 430.1267.

6.3 New Electron-Poor Catechol Derivatives

5-Bromo-6-ethyl-2,2-dimethylbenzo[*d*][1,3]dioxole (86):

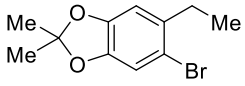

To a solution of acetonide **48** (50 mg, 0.281 mmol, 1.0 eq.) in acetone/water (4:3, 3.5 mL) KBr (38 mg, 0.323 mmol, 1.15 eq.) and Oxone (172 mg, 281 mmol, 1.0 eq.) were added and the mixture was stirred at room temperature for 5 h. Volatiles were removed under reduced pressure and the mixture extracted with CH_2Cl_2. The combined organic layers were washed with sat. aq. $Na_2S_2O_3$, dried over Na_2SO_4 and evaporated. The residue was subjected to flash chromatography (pentane, 1% Et_3N) to give aryl bromide **86** (57 mg, 79%) as a yellowish oil.

R_f = 0.5 (pentane); **^{1}H NMR** (250 MHz, $CDCl_3$) δ 6.89 (s, 1H), 6.63 (s, 1H), 2.64 (q, *J* = 7.5 Hz, 2H), 1.66 (s, 6H), 1.17 (t, *J* = 7.5 Hz, 3H); **^{13}C NMR** (101 MHz, $CDCl_3$) δ 147.35, 146.40, 135.83, 118.87, 113.42, 112.53, 109.18, 29.41, 25.95, 14.68.

Methyl 2-(2,2-dimethylbenzo[*d*][1,3]dioxol-5-yl)acetate (96):

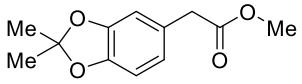

A solution of 3,4-dihydroxyphenylacetic acid (**94**, 500 mg, 2.97 mmol) in MeOH (50 mL) containing a few drops of conc. H_2SO_4 was refluxed overnight. The mixture was concentrated under reduced pressure and the residue taken up in EtOAc. The mixture was washed with sat. aq. $NaHCO_3$, dried over Na_2SO_4 and evaporated to give essentially pure methyl 3,4-dihydroxyphenylacetate (**95**, 540 mg) as a yellow oil.

R_f = 0.5 (pentane/EtOAc, 1:1); **^{1}H NMR** (400 MHz, $CDCl_3$) δ 6.82–6.74 (m, 2H), 6.72–6.64 (m, 1H), 5.52 (s, 1H), 5.36 (s, 1H), 3.70 (s, 3H), 3.52 (s, 2H).

A solution of methyl 3,4-dihydroxyphenylacetate (**95**, 540 mg, 2.97 mmol, 1.0 eq.), 2,2-dimethoxypropane (0.73 mL, 5.93 mmol, 2.0 eq.) and a catalytic amount of *p*TsOH in benzene (11 mL) was refluxed overnight. The mixture was poured in water and extracted with CH_2Cl_2. The combined organic layers were dried over Na_2SO_4 and evaporated to yield crude **96** (678 mg) which could be used in the next step without further purification. To obtain an analytically pure sample the batch was subjected to flash chromatography (pentane, 1% Et_3N) and **96** (631 mg, 96% over two steps) was obtained as a yellow oil.

R_f = 0.6 (pentane); **^{1}H NMR** (400 MHz, $CDCl_3$) δ 6.69–6.67 (m, 1H), 6.67–6.65 (m, 2H), 3.69 (s, 3H), 3.52 (s, 2H), 1.66 (s, 6H).

Analytical data are in agreement with the literature: (a) B. Geiseler, L. Fruk, *J. Mater. Chem.* **2012**, *22*, 735–741; (b) B. Almeida Cotrim, J. Joglar, M. J. L. Rojas, J. M. Decara del Olmo, M. Macias-González, M. R. Cuevas, M. Fitó, D. Muñoz-Aguayo, M. I. Covas Planells, M. Farré, F. R. de Fonseca, R. de la Torre, *J. Agric. Food Chem.* **2012**, *60*, 1067–1074.

Methyl 2-(6-chloro-2,2-dimethylbenzo[*d*][1,3]dioxol-5-yl)acetate (97):

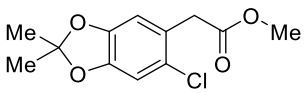

To a solution of **96** (700 mg, 3.15 mmol, 1.0 eq.) in CH_2Cl_2 (15 mL) were added NCS (607 mg, 4.41 mmol, 1.4 eq.) and $AlCl_3$ (63 mg, 473 µmol, 0.15 eq.) at room temperature and the mixture stirred for 4 h. EtOAc was added and the mixture washed with brine, dried over Na_2SO_4 and evaporated. The residue was eluted through a short silica column (pentane/Et_2O, 1:1, 1% Et_3N, no fractionation) to yield **97** (804 mg, 99%) as a yellow oil.

R_f = 0.7 (pentane/Et_2O, 1:1); **M.p.:** 55–57 °C; **FTIR** (neat): $\tilde{\nu}$ = 2985, 2957, 1744, 1490, 1380, 1338, 1259, 1198, 1164, 1151, 975, 856, 781 cm^{-1}; **^{1}H NMR** (400 MHz, $CDCl_3$) δ 6.75 (s, 1H), 6.65 (s, 1H), 3.71 (s, 3H), 3.66 (s, 2H), 1.66 (s, 6H); **^{13}C NMR** (101 MHz, $CDCl_3$) δ 171.48, 147.53, 146.71, 125.70, 124.45, 119.42, 110.69, 109.75, 52.28, 38.80, 25.99; **HRMS** (ESI) Exact mass calcd. for $C_{12}H_{13}ClNaO_4^+$ $[M+Na]^+$: 279.0395, found: 279.0394.

Methyl 2-(6-bromo-2,2-dimethylbenzo[*d*][1,3]dioxol-5-yl)acetate (98):

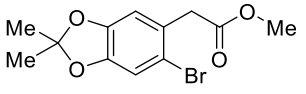

To a solution of **96** (300 mg, 1.35 mmol, 1.0 eq.) in acetone (14 mL) and water (8.0 mL) were added Oxone (873 mg, 1.42 mmol, 1.05 eq.) and KBr (193 mg, 1.62 mmol, 1.2 eq.) and the mixture was stirred at room temperature for 1 h. The mixture was filtered and acetone was removed under reduced pressure. Sat. aq. $Na_2S_2O_3$ was added and the mixture extracted with CH_2Cl_2. The combined organic layers were dried over Na_2SO_4 and evaporated to give **98** (409 mg, quant.) as a yellow oil.

R_f = 0.4 (pentane/Et_2O, 10:1); **M.p.:** 49–50 °C; **FTIR** (neat): $\tilde{\nu}$ = 2991, 2952, 1738, 1489, 1380, 1215, 1149, 980, 855, 783 cm^{-1}; **^{1}H NMR** (400 MHz, $CDCl_3$) δ 6.92 (s, 1H), 6.67 (s, 1H), 3.72 (s, 3H), 3.68 (s, 2H), 1.66 (s, 6H); **^{13}C NMR** (101 MHz, $CDCl_3$) δ 171.41, 147.69, 147.38,

126.32, 119.46, 114.81, 112.63, 110.90, 52.29, 41.36, 26.00; **HRMS** (ESI) Exact mass calcd. for $C_{12}H_{13}BrNaO_4^+$ $[M+Na]^+$: 322.9889, found: 322.9888.

Methyl 2-(6-iodo-2,2-dimethylbenzo[*d*][1,3]dioxol-5-yl)acetate (99):

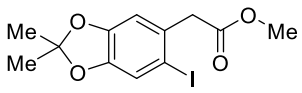

To a solution of **96** (302 mg, 1.36 mmol, 1.0 eq.) in MeOH (8.0 mL) were added Ag_2SO_4 (636 mg, 2.04 mmol, 1.5 eq.) and iodine (517 mg, 2.04 mmol, 1.5 eq.) and the brown mixture was stirred at room temperature for 1 h during which the brown color faded. The mixture was filtered, diluted with water and extracted with Et_2O. The combined organic layers were dried over Na_2SO_4 and evaporated. The residue was eluted through a short silica column (pentane/Et_2O, 5:1, 1% Et_3N, no fractionation) to yield **99** (468 mg, 99%) as an orange oil that solidified overnight at 4 °C.

R_f = 0.5–0.6 (pentane/Et_2O, 5:1); **M.p.:** 68–69 °C; **FTIR** (neat): $\tilde{\nu}$ = 2988, 2956, 1728, 1489, 1458, 1380, 1335, 1224, 1189, 1151, 981, 836 cm^{-1}; **^{1}H NMR** (400 MHz, $CDCl_3$) δ 7.15 (s, 1H), 6.71 (s, 1H), 3.72 (s, 3H), 3.70 (s, 2H), 1.66 (s, 6H); **^{13}C NMR** (101 MHz, $CDCl_3$) δ 171.41, 148.45, 147.69, 130.13, 119.38, 118.55, 110.43, 88.18, 52.30, 45.98, 26.03; **HRMS** (ESI) Exact mass calcd. for $C_{12}H_{13}INaO_4^+$ $[M+Na]^+$: 370.9751, found: 370.9750.

Methyl 2-(2,2-dimethyl-6-(trifluoromethyl)benzo[*d*][1,3]dioxol-5-yl)acetate (100):

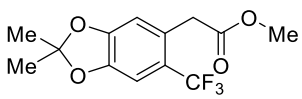

A mixture of **99** (468 mg, 1.34 mmol, 1.0 eq.), KF (156 mg, 2.69 mmol, 2.0 eq.; predried at 100 °C under high vacuum) and CuI (538 mg, 2.82 mmol, 2.1 eq.) was suspended in NMP (3.7 mL). TMS-CF_3 (0.40 mL, 2.69 mmol, 2.0 eq.) was added and the mixture was heated to 80 °C for 22 h in a sealed tube. The mixture was poured in water and some solid NaCl was added followed by extraction with CH_2Cl_2. The combined organic layers were washed with water, dried over Na_2SO_4 and evaporated. The residue was subjected to flash chromatography (pentane/Et_2O, 5:1, 1% Et_3N) to yield **100** (341 mg, 88%) as a yellow oil.

R_f = 0.7 (pentane/Et_2O, 5:1); **FTIR** (neat): $\tilde{\nu}$ = 2995, 2956, 1743, 1504, 1386, 1295, 1218, 1144, 1109, 979, 870 cm^{-1}; **^{1}H NMR** (400 MHz, $CDCl_3$) δ 6.99 (s, 1H), 6.72 (s, 1H), 3.71 (s, 5H), 1.69 (s, 6H); **^{13}C NMR** (101 MHz, $CDCl_3$) δ 171.38, 149.93, 146.60, 126.60 (q, *J* = 2.1 Hz), 124.22 (q *J* = 273.2 Hz), 121.79 (q, *J* = 30.7 Hz), 119.79, 112.08, 106.21 (q, *J* = 6.0 Hz), 52.17,

37.73 (q, *J* = 1.8 Hz), 25.91; **HRMS** (ESI) Exact mass calcd. for $C_{13}H_{13}F_3NaO_4^+$ $[M+Na]^+$: 313.0658, found: 313.0658.

Methyl 2-(2,2-dimethyl-6-(methylsulfonyl)benzo[*d*][1,3]dioxol-5-yl)acetate (101):

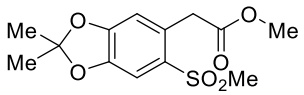

A mixture of **99** (153 mg, 439 µmol, 1.0 eq.), sodium methanesulfinate (67.3 mg, 659 µmol, 1.5 eq.), L-proline (20.4 mg, 176 µmol, 0.4 eq.) and $Cu(OAc)_2$ (31.9 mg, 176 µmol, 0.4 eq.) was suspended in DMSO and the mixture was heated to 100 °C for 24 h in a sealed tube. The reaction mixture was cooled to room temperature and quenched with sat. aq. NH_4Cl, diluted with water and extracted with EtOAc. The combined organic layers were washed with water and brine, and dried over Na_2SO_4. The residue was subjected to flash chromatography (pentane/Et_2O, 1:1, 1% Et_3N) to yield **101** (102 mg, 77%) as a yellowish solid.

R_f = 0.4 (pentane/Et_2O, 1:1); **M.p.:** 117–119 °C; **FTIR** (neat): $\tilde{\nu}$ = 3019, 2988, 2966, 2923, 1727, 1496, 1300, 1244, 1196, 1136, 983, 830, 764 cm^{-1}; **^{1}H NMR** (400 MHz, $CDCl_3$) δ 7.38 (s, 1H), 6.68 (s, 1H), 4.11 (s, 2H), 3.73 (s, 3H), 3.10 (s, 3H), 1.70 (s, 6H); **^{13}C NMR** (101 MHz, $CDCl_3$) δ 171.94, 151.84, 147.40, 131.72, 129.05, 120.79, 112.30, 109.72, 52.42, 45.08, 38.22, 26.12; **HRMS** (ESI) Exact mass calcd. for $C_{13}H_{16}NaO_6S^+$ $[M+Na]^+$: 323.0560, found: 323.0561.

2-(6-Chloro-2,2-dimethylbenzo[*d*][1,3]dioxol-5-yl)acetic acid (102):

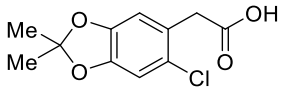

To a solution of **97** (773 mg, 3.01 mmol) in THF (15 mL) was added 1 M aq. NaOH (12 mL) and the resulting turbid mixture was stirred at room temperature for 1 h during which the mixture turned clear. Volatiles were removed under reduced pressure and the residue was acidified to pH 5 using 1 M aq. HCl. The mixture was extracted with EtOAc and the combined organic layers were washed with water, dried over Na_2SO_4 and evaporated to yield **102** (726 mg, 99%) as an off-white solid.

M.p.: 150–152 °C (dec.); **FTIR** (neat): $\tilde{\nu}$ = 2992, 2937, 1704, 1496, 1378, 1262, 1223, 1155, 975, 861, 830 cm^{-1}; **^{1}H NMR** (400 MHz, $CDCl_3$) δ 6.76 (s, 1H), 6.65 (s, 1H), 3.70 (s, 2H), 1.66 (s, 6H); **^{13}C NMR** (101 MHz, $CDCl_3$) δ 176.71, 147.73, 146.75, 125.86, 123.72, 119.55, 110.73, 109.79, 38.59, 25.98; **HRMS** (ESI) Exact mass calcd. for $C_{11}H_{11}ClNaO_4^+$ $[M+Na]^+$: 265.0238, found: 265.0241.

2-(6-Bromo-2,2-dimethylbenzo[*d*][1,3]dioxol-5-yl)acetic acid (103):

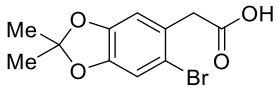

Saponification of **98** (593 mg, 1.97 mmol) was performed analogously to **102** yielding **103** (543 mg, 96%) as an off-white solid.

M.p.: 158–160 °C (dec.); **FTIR** (neat): $\tilde{\nu}$ = 2995, 2935, 1704, 1492, 1378, 1222, 1153, 972, 858, 829 cm^{-1}; **^{1}H NMR** (400 MHz, $CDCl_3$) δ 6.93 (s, 1H), 6.68 (s, 1H), 3.73 (s, 2H), 1.66 (s, 7H); **^{13}C NMR** (101 MHz, $CDCl_3$) δ 176.40, 147.88, 147.43, 125.60, 119.59, 114.94, 112.68, 110.95, 41.11, 26.01; **HRMS** (ESI) Exact mass calcd. for $C_{11}H_{11}BrNaO_4^+$ $[M+Na]^+$: 308.9733, found: 308.9737.

2-(6-Iodo-2,2-dimethylbenzo[*d*][1,3]dioxol-5-yl)acetic acid (104):

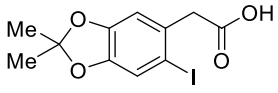

Saponification of **99** (613 mg, 1.76 mmol) was performed analogously to **102** yielding **104** (488 mg, 83%) as a yellow solid.

M.p.: 170–172 °C (dec.); **FTIR** (neat): $\tilde{\nu}$ = 2994, 2933, 1704, 1490, 1378, 1218, 1153, 965, 854, 829, 782 cm^{-1}; **^{1}H NMR** (400 MHz, $CDCl_3$) δ 7.16 (s, 1H), 6.72 (s, 1H), 3.75 (s, 2H), 1.66 (s, 6H); **^{13}C NMR** (101 MHz, $CDCl_3$) δ 176.05, 148.50, 147.88, 129.44, 119.51, 118.60, 110.48, 88.29, 45.68, 26.05; **HRMS** (ESI) Exact mass calcd. for $C_{11}H_{11}INaO_4^+$ $[M+Na]^+$: 356.9594, found: 356.9600.

2-(2,2-Dimethyl-6-(trifluoromethyl)benzo[*d*][1,3]dioxol-5-yl)acetic acid (105):

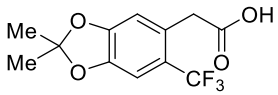

Saponification of **100** (327 mg, 1.13 mmol) was performed analogously to **102** yielding **105** (315 mg, quant.) as a yellowish solid.

M.p.: 133–135 °C; **FTIR** (neat): $\tilde{\nu}$ = 3001, 2927, 1711, 1504, 1389, 1297, 1249, 1217, 1145, 1109, 979, 872, 835 cm^{-1}; **^{1}H NMR** (250 MHz, $CDCl_3$) δ 6.99 (s, 1H), 6.71 (s, 1H), 3.78–3.73 (m, 2H), 1.69 (s, 6H); **HRMS** (ESI) Exact mass calcd. for $C_{12}H_{11}F_3NaO_4^+$ $[M+Na]^+$: 299.0502, found: 299.0506.

2-(2,2-Dimethyl-6-(methylsulfonyl)benzo[*d*][1,3]dioxol-5-yl)acetic acid (106):

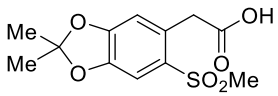

Saponification of **101** (50.0 mg, 166 µmol) was performed analogously to **102** yielding **106** (34.4 mg, 72%) as a colorless solid.

M.p.: 185–187 °C; **FTIR** (neat): $\tilde{\nu}$ = 2993, 2929, 2361, 1714, 1495, 1379, 1301, 1250, 1218, 1138, 766 cm^{-1}; **^{1}H NMR** (400 MHz, CD_3OD) δ 7.33 (s, 1H), 6.83 (s, 1H), 4.07 (s, 2H), 3.10 (s, 3H), 1.71 (s, 6H); **^{13}C NMR** (101 MHz, CD_3OD) δ 174.79, 153.05, 148.41, 132.84, 131.36, 121.90, 113.67, 110.08, 45.00, 39.05, 25.92; **HRMS** (ESI) Exact mass calcd. for $C_{12}H_{14}NaO_6S^+$ $[M+Na]^+$: 309.0403, found: 309.0408.

Methyl 2-(2-bromo-4,5-dihydroxyphenyl)acetate (108):

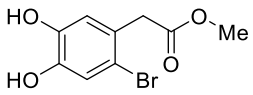

Compound **98** (161 mg, 535 µmol) was cooled to 0 °C and precooled 20% aq. TFA (1 mL) was added. After 5 min the ice bath was removed and stirring continued at room temperature for 2.5 h. Volatiles were removed under reduced pressure and the residue was separated by preparative reversed-phase HPLC to yield **108** (102 mg, 73%) as an off-white solid.

M.p.: 106–108 °C; **FTIR** (neat): $\tilde{\nu}$ = 3370, 2955, 2364, 1712, 1510, 1436, 1339, 1282, 1221, 1162, 1011, 870, 821 cm^{-1}; **^{1}H NMR** (400 MHz, CD_3OD) δ 6.94 (s, 1H), 6.75 (s, 1H), 3.68 (s, 3H), 3.63 (s, 2H); **^{13}C NMR** (101 MHz, CD_3OD) δ 173.51, 146.76, 146.15, 126.22, 119.93, 119.12, 114.06, 52.48, 41.37; **HRMS** (ESI) Exact mass calcd. for $C_9H_9BrNaO_4^+$ $[M+Na]^+$: 282.9576, found: 282.9576.

Methyl 2-(4,5-dihydroxy-2-iodophenyl)acetate (109):

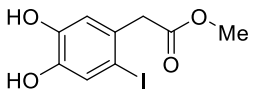

Deprotection of **99** (120 mg, 345 µmol) was performed analogously to **108**, yielding **109** (66 mg, 62%) as an off-white solid.

M.p.: 112–114 °C; **FTIR** (neat): $\tilde{\nu}$ = 3385, 2952, 2360, 2338, 1711, 1504, 1437, 1335, 1279, 1224, 1162 cm^{-1}; **^{1}H NMR** (400 MHz, CD_3OD) δ 7.18 (s, 1H), 6.76 (s, 1H), 3.68 (s, 3H), 3.64 (s, 2H); **^{13}C NMR** (101 MHz, CD_3OD) δ 173.52, 147.06, 146.71, 130.12, 126.32, 118.58, 87.46, 52.48, 45.89; **HRMS** (ESI) Exact mass calcd. for $C_9H_9INaO_4^+$ $[M+Na]^+$: 330.9438, found: 330.9438.

Methyl 2-(4,5-dihydroxy-2-(trifluoromethyl)phenyl)acetate (110):

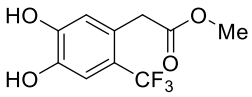

Deprotection of **100** (200 mg, 689 µmol) was performed analogously to **108**, yielding **110** (134 mg, 78%) as an off-white solid.

M.p.: 131–133 °C; **FTIR** (neat): $\tilde{\nu}$ = 3507, 3293, 1712, 1459, 1344, 1310, 1281, 1234, 1159, 1114, 1018, 841 cm^{-1}; **^{1}H NMR** (400 MHz, CD_3OD) δ 7.03 (s, 1H), 6.80 (s, 1H), 3.67 (s, 3H), 3.66 (s, 2H); **^{13}C NMR** (101 MHz, CD_3OD) δ 173.57, 149.47, 145.43, 126.09 (q, *J* = 271.5 Hz), 125.42 (q, *J* = 1.8 Hz), 120.86 (q, *J* = 30.2 Hz), 120.60, 114.08 (q, *J* = 5.5 Hz), 52.51, 38.13 (q, *J* = 2.2 Hz); **HRMS** (ESI) Exact mass calcd. for $C_{10}H_9F_3NaO_4^+$ $[M+Na]^+$: 273.0345, found: 273.0346.

Methyl 2-(4,5-dihydroxy-2-(methylsulfonyl)phenyl)acetate (111):

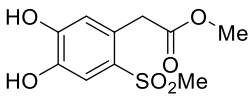

Deprotection of **101** (96.0 mg, 320 µmol) was performed analogously to **108**, yielding **111** (37.3 mg, 45%) as a hygroscopic, orange solid.

FTIR (neat): $\tilde{\nu}$ = 3362, 3027, 2957, 1721, 1595, 1520, 1440, 1293, 1208, 1128, 764 cm^{-1}; **^{1}H NMR** (400 MHz, CD_3OD) δ 7.38 (s, 1H), 6.78 (s, 1H), 3.99 (s, 2H), 3.69 (s, 3H), 3.06 (s, 3H); **^{13}C NMR** (101 MHz, CD_3OD) δ 173.82, 151.65, 146.02, 130.28, 127.51, 120.72, 117.58, 52.51, 45.16, 38.59; **HRMS** (ESI) Exact mass calcd. for $C_{10}H_{12}NaO_6S^+$ $[M+Na]^+$: 283.0247, found: 283.0249.

Naphthalene-1,8-diol (134):

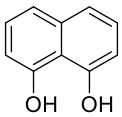

KOH pellets (50 g) were molten at 230–250 °C. To the melt 1,8-naphthosultone (**133**, 10.0 g, 48.5 mmol) was added in small portions reacting violently to give a black slurry. Addition took around 45 min and heating to 250 °C was continued for an additional 20 min. The mixture was allowed to cool to 100–150 °C (and not allowed to solidify!) and carefully diluted with water. After cooling to 0 °C, conc. HCl was added until pH 1 and the mixture was extracted with CH_2Cl_2. The combined organic layers were dried over Na_2SO_4 and filtered repeatedly through cotton wool to remove all fine black suspended solids. Volatiles were removed under reduced pressure and the residue was crystallized from $CHCl_3$ several times to obtain **134** (4.86 g, 63%) as grey to grey-brown needles.

R_f = 0.4 (pentane/Et_2O, 1:1); **M.p.:** 140–142 °C; **^{1}H NMR** (400 MHz, $CDCl_3$) δ 7.78 (s, 2H), 7.36 (dd, *J* = 8.4, 1.0 Hz, 2H), 7.29 (dd, *J* = 8.2, 7.5 Hz, 2H), 6.79 (dd, *J* = 7.5, 1.1 Hz, 2H); **^{13}C NMR** (101 MHz, $CDCl_3$) δ 152.81, 137.17, 126.85, 120.67, 114.67, 109.54.

Analytical data are in agreement with the literature: K. A. Parker, T. Iqbal, *J. Org. Chem.* **1980**, *45*, 1149–1151.

2,2-Dimethylnaphtho[1,8-*de*][1,3]dioxine (137):

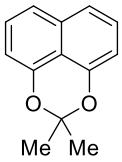

A solution of diol **134** (820 mg, 5.12 mmol, 1.0 eq.), 2,2-dimethoxypropane (1.26 mL, 10.2 mmol, 2.0 eq.) and *p*TsOH monohydrate (9.7 mg, 51.2 µmol, 1 mol-%) in benzene (15 mL) was heated to reflux overnight. After cooling to room temperature, the mixture was poured into sat. aq. $NaHCO_3$ followed by extraction with Et_2O. The combined organic layers were dried over Na_2SO_4 and evaporated under reduced pressure. The residue was subjected to flash chromatography (petroleum ether) to give **137** (482 mg, 47%) as a colorless oil which eventually solidified at 4 °C.

R_f = 0.3 (petroleum ether); **M.p.:** 59–61 °C; **^{1}H NMR** (400 MHz, $CDCl_3$) δ 7.44 (dd, *J* = 8.4, 1.2 Hz, 2H), 7.39 (dd, *J* = 8.4, 7.2 Hz, 2H), 6.85 (dd, *J* = 7.2, 1.2 Hz, 2H), 1.67 (s, 6H); **^{13}C NMR** (126 MHz, $CDCl_3$) δ 148.11, 134.35, 127.46, 120.12, 113.69, 108.90, 101.82, 25.41.

2,2-Dimethyl-6,7-dinitronaphtho[1,8-*de*][1,3]dioxine (138):

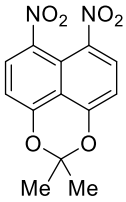

A solution of acetonide **137** (20 mg, 99.9 µmol, 1.0 eq.) in CH_2Cl_2 (0.3 mL) was cooled to 0 °C and conc. HNO_3 (0.999 mmol, 69 µL, 10 eq.) was added. After stirring for 10 min the mixture was poured into half-sat. aq. $NaHCO_3$ followed by extraction with CH_2Cl_2. The combined organic layers were dried over Na_2SO_4 and evaporated under reduced pressure. The residue was subjected to flash chromatography (pentane/EtOAc, 10:1) to obtain dinitro compound **138** (11.5 mg, 40%) as an orange-brown solid.

R_f = 0.1 (pentane/EtOAc, 10:1); **FTIR** (neat): $\tilde{\nu}$ = 3003, 2922, 2852, 1604, 1580, 1518, 1502, 1332, 1263, 1092, 852, 735 cm^{-1}; **^{1}H NMR** (400 MHz, $CDCl_3$) δ 8.30 (d, *J* = 8.5 Hz, 2H), 7.04 (d, *J* = 8.5 Hz, 2H), 1.75 (s, 6H); **^{13}C NMR** (101 MHz, $CDCl_3$) δ 152.44, 139.49, 129.86, 118.73, 113.44, 110.07, 104.23, 25.14; **HRMS** (ESI) Exact mass calcd. for $C_{13}H_{11}N_2O_6^+$ $[M+H]^+$: 291.06116, found: 291.06110.

1-(2,2-Dimethylnaphtho[1,8-*de*][1,3]dioxin-6-yl)ethan-1-one (139):

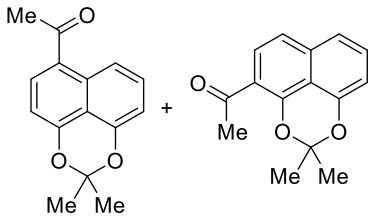

To a solution of acetonide **137** (50 mg, 0.250 mmol, 1.0 eq.) and AcCl (19 µL, 0.263 mmol, 1.05 eq.) in CH_2Cl_2 (1.0 mL) at rt $AlCl_3$ (37 mg, 0.275 mmol, 1.1 eq.) was added and the mixture immediately turned deep red. After 1 h the mixture was diluted with Et_2O, filtered and washed with sat. aq. $NaHCO_3$. The aqueous layer was back-extracted once with Et_2O and the combined organic layers were dried over Na_2SO_4 and evaporated under reduced pressure. The residue was subjected to flash chromatography (pentane/Et_2O, 15:1, 1% Et_3N) to give an isomeric mixture of ketone **139** (58 mg, 96%; *para*/*ortho*: 5:1 by ^{1}H NMR) as a yellow oil. Isomers could partially be separated by flash chromatography (pentane/Et_2O, 30:1, 1% Et_3N).

R_f = 0.2 (pentane/Et_2O, 9:1); **FTIR** (neat): $\tilde{\nu}$ = 2997, 2924, 1662, 1600, 1582, 1506, 1403, 1262, 1245, 1194, 1076, 954, 828, 763, 577 cm^{-1}; **^{1}H NMR** (400 MHz, $CDCl_3$, *para*-isomer) δ 8.63 (dd, *J* = 8.8, 0.8 Hz, 1H), 8.05 (d, *J* = 8.1 Hz, 1H), 7.55 (dd, *J* = 8.8, 7.6 Hz, 1H), 6.93 (dd, *J* = 7.6, 0.9 Hz, 1H), 6.84 (d, *J* = 8.1 Hz, 1H), 2.71 (s, 3H), 1.67 (s, 6H); **^{1}H NMR** (400 MHz, $CCDl_3$, *ortho*-isomer) δ 7.92 (d, *J* = 8.8 Hz, 1H), 7.50 (dd, *J* = 8.2, 7.5 Hz, 1H), 7.42 (dd, *J* = 8.2, 0.8 Hz, 1H), 7.41 (d, *J* = 8.8 Hz, 1H), 6.91 (dd, *J* = 7.6, 1.0 Hz, 1H), 2.71 (s, 3H), 1.74 (s, 6H); **^{13}C NMR** (126 MHz, $CDCl_3$, *para*-isomer) δ 199.81, 152.45, 147.91, 133.02, 132.13, 130.23, 127.41, 119.88, 113.76, 110.27, 107.70, 102.24, 29.26, 25.27; **HRMS** (ESI) Exact mass calcd. for $C_{15}H_{15}O_3^+$ $[M+H]^+$: 243.10157, found: 243.10153.

1-(2,2-Dimethyl-7-nitronaphtho[1,8-*de*][1,3]dioxin-6-yl)ethan-1-one (140):

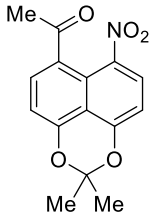

A solution of ketone **139** (isomeric mixture described above, 139 mg, 0.574 mmol, 1.0 eq.) in CH_2Cl_2 (2.5 mL) was cooled to 0 °C and conc. HNO_3 (78 µL, 1.72 mmol, 3.0 eq.) was added. After 5 min the cooling bath was removed and stirring continued at rt for 30 min. The mixture was diluted with Et_2O and poured into sat. aq. $NaHCO_3$. Layers were separated and the aq. layer was extracted with Et_2O. The combined organic layers were dried over Na_2SO_4 and evaporated under reduced pressure. The residue was subjected to flash chromatography (pentane/Et_2O, 5:1, 1% Et_3N) to give **140** (single isomer, 90 mg, 0.313 mmol, 55%) as a yellow oil.

R_f = 0.2 (pentane/Et_2O, 5:1); **FTIR** (neat): $\tilde{\nu}$ = 2920, 2850 1683, 1604, 1522, 1337, 1263, 1248, 1197, 1096, 842, 751 cm^{-1}; **^{1}H NMR** (400 MHz, $CDCl_3$) δ 8.14 (d, *J* = 8.4 Hz, 1H), 7.88 (d,

J = 8.0 Hz, 1H), 6.99 (d, *J* = 8.0 Hz, 1H), 6.93 (d, *J* = 8.4 Hz, 1H), 2.68 (s, 3H), 1.70 (s, 6H); **^{13}C NMR** (101 MHz, $CDCl_3$) δ 200.03, 152.58, 150.62, 141.30, 131.19, 130.37, 128.21, 123.12, 114.00, 109.73, 109.12, 103.39, 28.48, 25.19; **HRMS** (ESI) Exact mass calcd. for $C_{15}H_{14}NO_5^+$ $[M+H]^+$: 288.08665, found: 288.08664.

Surface Modifications:

Test tubes (5 mL) were cleaned with piranha solution (conc. H_2SO_4/30% H_2O_2, 3:1), rinsed with millipore water and oven-dried (120 °C). Portions of TiO_2 particles (10 mg, rutile, 1.0–2.0 μm) were suspended in toluene (3 mL), ultrasonicated for 20 min at 35 °C, centrifuged (4500 rpm, 10 min) and the solvent was decanted. This washing was repeated with *i*PrOH and the particles were oven-dried (120 °C) overnight.

To the TiO_2 particles (10 mg) catechol (2.0 mg) dissolved in a few drops of DMSO and MOPS buffer (3 mL) were added followed by ultrasonication for 2 min and subsequent incubation at 50 °C for 4 h under exclusion of light. During incubation TiO2 particles were re-suspended with a syringe several times. The mixture was centrifuged (4500 rpm, 10 min), the particles were washed with millipore water (2 x 3 mL) and MeOH (3 x 3 mL) with centrifugation after each washing and dried under a stream of nitrogen.

Photolysis Experiments

Applying a Falcon® Multiwell™ 24-well plate, wells were loaded with millipore water (1 mL) and a 1 mM solution of catechol in MeCN (50 μL) was added. On a sheet of aluminum foil the plate was positioned under a common laboratory UV lamp and irradiation at 366 nm was performed with a distance of approximately 3.5 cm between the lamp and the sample solutions. After certain time intervals, the entire solution of one well at a time was filtered and subjected to UPLC-MS analysis. Substance ratios were determined by integration of their respective peaks in the UV trace recorded at 254 nm.

6.4 Rapamycin-Based Probes

tert-Butyl (6-aminohexyl)carbamate (153):

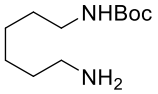

A solution of Boc_2O (**152**, 1.52 g, 6.84 mmol, 1.0 eq.) in $CHCl_3$ (14 mL) was slowly added to a solution of 1,6-hexanediamine (**151**, 5.04 g, 34.2 mmol, 5.0 eq.) in $CHCl_3$ (180 mL) at 0 °C during 100 min *via* syringe pump. After stirring over night at room temperature the mixture was filtered and evaporated. The residue was dissolved in EtOAc, washed with half-sat. aq. NaCl, dried over Na_2SO_4 and the solvent was evaporated. The residue was subjected to flash chromatography (CH_2Cl_2/MeOH 10:1, 1% Et_3N). The yellow semisolid obtained was suspended in a small amount of EtOAc. Solids were collected by filtration, recovered from the filter with MeOH, and after evaporation **153** (1.32 g, 89%) was obtained as a colorless solid.

R_f = 0.2 (CH_2Cl_2/MeOH, 10:1); **^{1}H NMR** (400 MHz, $CDCl_3$) δ 4.54 (s, 1H), 3.10 (q, *J* = 6.7 Hz, 2H), 2.69 (t, *J* = 7.0 Hz, 2H), 1.80 (br s, 2H), 1.43 (s, 9H), 1.27–1.37 (m, 4H).

Analytical data are in agreement with the literature: C. Dardonville, C. Fernandez-Fernandez, S.-L. Gibbons, G. J. Ryan, N. Jagerovic, A. M. Gabilondo, J. J. Meana, L. F. Callado, *Bioorg. Med. Chem.* **2006**, *14*, 6570–6580.

tert-Butyl (6-(5-((3a*S*,4*S*,6a*R*)-2-oxohexahydro-1*H*-thieno[3,4-*d*]imidazol-4-yl)pentanamido)hexyl) carbamate (154):

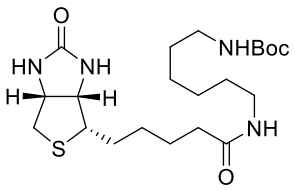

To a solution of D-biotin (250 mg, 1.02 mmol, 1.0 eq.) and **153** (221 mg, 1.02 mmol, 1.0 eq.) in pyridine (8.4 mL) was added EDC·HCl (235 mg, 1.23 mmol, 1.2 eq.) and the mixture was stirred overnight at room temperature. The mixture was concentrated under reduced pressure and solids were collected by filtration. After washing with aq. NaOH (1 M) and Et_2O, and drying **154** (392 mg, 86%) was obtained as a colorless solid.

^{1}H NMR (400 MHz, CD_3OD) δ 4.49 (ddd, *J* = 7.9, 5.0, 1.0 Hz, 1H), 4.30 (dd, *J* = 7.9, 4.4 Hz, 1H), 3.24–3.10 (m, 3H), 3.02 (t, *J* = 7.0 Hz, 2H), 2.93 (dd, *J* = 12.8, 5.0 Hz, 1H), 2.71 (d, *J* = 12.7 Hz, 1H), 2.19 (t, *J* = 7.3 Hz, 2H), 1.81–1.23 (m, 14H), 1.43 (s, 9H); **^{13}C NMR** (101 MHz, CD_3OD) δ 175.94, 166.10, 158.56, 79.78, 63.38, 61.62, 57.02, 41.24, 41.04, 40.27, 36.82, 30.90, 30.36, 29.79, 29.51, 28.80, 27.65, 27.51, 26.94.

Analytical data are in agreement with the literature: M. Collot, B. Sendid, A. Fievez, C. Savaux, A. Standaert-Vitse, M. Tabouret, A. S. Drucbert, P. M. Danzé, D. Poulain, J.-M. Mallet, *J. Med. Chem.* **2008**, *51*, 6201–6210.

_N_-Biotinyl-1,6-hexanediamine (155):

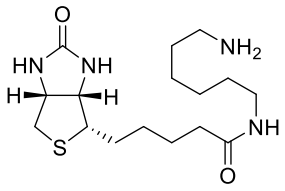

To neat **154** (100 mg, 0.226 mmol) TFA (0.6 mL) was added at room temperature and the yellow mixture was stirred for 20 min. Volatiles were removed under reduced pressure and the residue was taken up in MeOH. The mixture was neutralized using Dowex Marathon WBA ion-exchange resin and the solvent was evaporated to yield **155** (63 mg, 81%) as a yellow oil.

^{1}H NMR (400 MHz, D_2O) δ 4.60 (ddd, *J* = 8.0, 5.0, 0.9 Hz, 1H), 4.42 (dd, *J* = 8.0, 4.5 Hz, 1H), 3.36–3.30 (m, 1H), 3.26–3.10 (m, 2H), 3.04–2.93 (m, 3H), 2.78 (d, *J* = 13.0 Hz, 1H), 2.24 (t, *J* = 7.2 Hz, 2H), 1.83–1.22 (m, 14H).

Analytical data are in agreement with the literature: M. Collot, B. Sendid, A. Fievez, C. Savaux, A. Standaert-Vitse, M. Tabouret, A. S. Drucbert, P. M. Danzé, D. Poulain, J.-M. Mallet, *J. Med. Chem.* **2008**, *51*, 6201–6210.

Probe 1 (156):

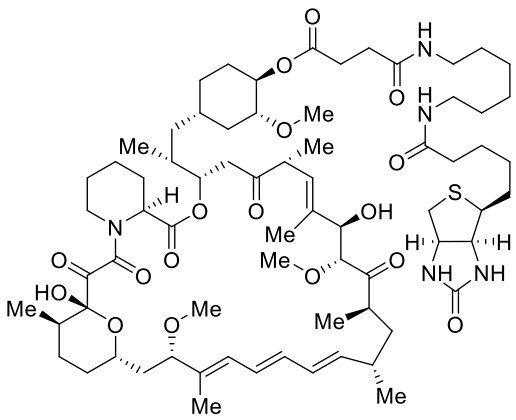

To a solution of rapamycin hemisuccinate (**150**, 25.4 mg, 25.0 µmol, 1.0 eq.) in DMF (0.2 mL) amine **155** (10.3 mg, 30.0 µmol, 1.2 eq.), HBTU (12.3 mg, 32.0 µmol, 1.3 eq.) and DIPEA (10 µL, 60.0 µmol, 2.4 eq.) were added and the mixture was stirred overnight at room temperature. The mixture was eluted through a small C_{18} SPE column using MeCN and evaporated. Separation by preparative reversed-phase HPLC gave **156** (14.3 mg, 43%) as a colorless solid.

HRMS (ESI) calcd. for $C_{71}H_{111}N_5NaO_{17}S^+$ $[M+Na]^+$: 1360.7588, found: 1360.7580.

mono-Boc cystamine (158):

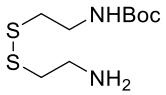

A solution of Boc_2O (1.90 g, 8.53 mmol, 1.0 eq.) and Et_3N (3.59 mL, 25.6 mmol, 3.0 eq.) in MeOH (15 mL) was added to a solution of cystamine dihydrochloride (**157**, 2.00 g 12.8 mmol, 1.0 eq.) in MeOH (100 mL) at room temperature during 20 min and the resulting mixture was stirred for another 2.5 h. Volatiles were removed under reduced pressure and the residue was taken up in aq. NaH_2PO_4 (1 M, 50 mL). The mixture was extracted with Et_2O to remove any doubly protected compound and the aqueous layer was basified to pH 9 using 1 M aq. NaOH. The mixture was extracted with EtOAc and the combined organic layers were dried over Na_2SO_4 and evaporated to yield **158** (1.09 g, 51%) as a yellow semisolid.

^{1}H NMR (250 MHz, $CDCl_3$) δ 4.93 (s, 1H), 3.45 (q, *J* = 6.3 Hz, 2H), 3.01 (t, *J* = 6.1 Hz, 2H), 2.77 (td, *J* = 6.2, 3.7 Hz, 4H), 1.44 (s, 9H).

Analytical data are in agreement with the literature: J. Niu, Z. Liu, L. Fu, F. Shi, H. Ma, Y. Ozaki, X. Zhang, *Langmuir* **2008**, *24*, 11988–11994.

***N*-Biotinyl-*N'*-Boc-cystamine (159):**

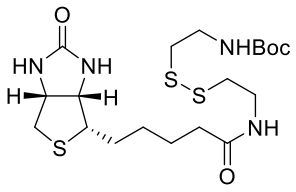

A solution of D-biotin (48.4 mg, 198 µmol, 1.0 eq.) and amine **158** (50.0 mg, 198 µmol, 1.0 eq.) in pyridine (1.7 mL) was added HBTU (90.2 mg, 238 µmol, 1.2 eq.) and the mixture was stirred overnight at room temperature. Volatiles were removed under reduced pressure and the residue was separated by preparative reversed-phase HPLC to yield **159** (47.0 mg, 50%) as a colorless solid.

R_f = 0.3 (CH_2Cl_2/MeOH, 15:1); **^{1}H NMR** (400 MHz, DMSO-d_6) δ 7.95 (t, *J* = 5.7 Hz, 1H), 6.97 (t, *J* = 5.7 Hz, 1H), 6.40 (s, 1H), 6.34 (s, 1H), 4.34–4.26 (m, 1H), 4.19–4.07 (m, 1H), 3.36–3.26 (m, 2H), 3.20 (q, *J* = 6.5 Hz, 2H), 3.14–3.03 (m, 1H), 2.82 (dd, *J* = 12.4, 5.1 Hz, 1H), 2.80–2.70 (m, 3H), 2.57 (d, *J* = 12.4 Hz, 1H), 2.06 (t, *J* = 7.4 Hz, 2H), 1.69–1.18 (m, 6H), 1.38 (s, 9H).

Analytical data are in agreement with the literature: C. Gnaccarini, W. Ben-Tahar, W. D. Lubell, J. N. Pelletier, J. W. Keillor, *Bioorg. Med. Chem.* **2009**, *17*, 6354–6359.

Cystaminyl biotinate hydrochloride (160):

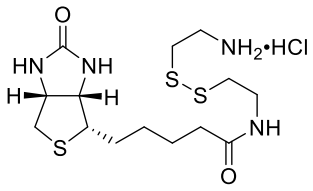

A solution of **159** (40.0 mg 83.4 µmol) in MeOH (0.8 mL) at 0 °C was added a solution of HCl in dioxane (4 M, 0.4 mL) and the mixture was stirred at room temperature for 3 h. The mixture was concentrated under reduced pressure and the residue separated by preparative reversed-phase HPLC to yield **160** (35.0 mg, quant.) as a colorless solid.

^{1}H NMR (400 MHz, DMSO-d_6) δ 7.98 (t, J = 5.7 Hz, 1H), 7.91 (s, 3H), 6.34 (s, 1H), 6.30 (s, 1H), 4.24 (dd, J = 7.8, 5.1 Hz, 1H), 4.10–4.02 (m, 1H), 3.32–3.23 (m, 2H), 3.08–2.96 (m, 3H), 2.91–2.81 (m, 2H), 2.80–2.69 (m, 3H), 2.51 (d, J = 12.4 Hz, 1H), 2.01 (t, J = 7.4 Hz, 2H), 1.62–1.15 (m, 6H).

Analytical data are in agreement with the literature: C. Gnaccarini, W. Ben-Tahar, W. D. Lubell, J. N. Pelletier, J. W. Keillor, *Bioorg. Med. Chem.* **2009**, *17*, 6354–6359.

Probe 2 (161):

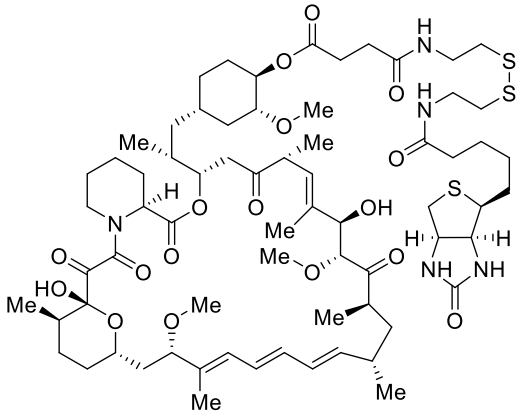

To a solution of rapamycin hemisuccinate (**150**, 54.5 mg, 53.7 µmol, 1.0 eq.) in DMF (0.2 mL) amine **160** (23.4 mg, 56.4 µmol, 1.05 eq.), HBTU (24.5 mg, 64.5 µmol, 1.2 eq.) and DIPEA (33 µL, 188 µmol, 3.5 eq.) were added and the mixture was stirred overnight at room temperature. The mixture was eluted through a small C_{18} SPE column using MeCN and evaporated. Separation by preparative reversed-phase HPLC gave **161** (28.0 mg, 38%) as a colorless solid.

HRMS (ESI) calcd. for $C_{69}H_{107}N_5NaO_{17}S_3^+$ $[M+Na]^+$: 1396.6716, found: 1396.6711.

Boc-linker 3 (163):

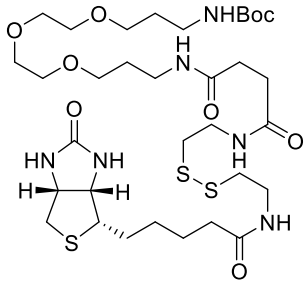

A solution of **160** (30.0 mg, 72.3 µmol, 1.0 eq.) in DMF (0.4 mL) was added *N*-boc-*N'*-succinyl-4,7,10-trioxa-1,13-tridecanediamine (**162**, 32.0 mg, 72.3 µmol, 1.0 eq.), HBTU (30.2 mg, 79.5 µmol, 1.1 eq.) and DIPEA (38 µL, 217 µmol, 3.0 eq.) and the mixture was stirred overnight at room temperature. The mixture was eluted through a small C_{18} SPE column using MeCN and evaporated. Separation by preparative reversed-phase HPLC gave **163** (41.5 mg, 74%) as a colorless solid.

^{1}H NMR (400 MHz, DMSO-d_6) δ 8.03 (t, *J* = 5.6 Hz, 1H), 7.99 (t, *J* = 5.6 Hz, 1H), 7.79 (t, *J* = 5.6 Hz, 1H), 6.76 (t, *J* = 5.7 Hz, 1H), 6.42 (s, 1H), 6.36 (s, 1H), 4.34–4.26 (m, 1H), 4.16–4.08 (m, 0H), 3.54–3.43 (m, 8H), 3.37 (td, *J* = 6.4, 3.1 Hz, 4H), 3.34–3.26 (m, 3H), 3.14–3.01 (m, 3H), 2.95 (q, *J* = 6.8 Hz, 2H), 2.82 (dd, *J* = 12.4, 5.1 Hz, 1H), 2.75 (td, *J* = 6.7, 4.1 Hz, 4H), 2.57 (d, *J* = 12.4 Hz, 1H), 2.33–2.23 (m, 4H), 2.06 (t, *J* = 7.4 Hz, 2H), 1.71–1.14 (m, 12H), 1.37 (s, 9H); **^{13}C NMR** (101 MHz, DMSO-d_6) δ 172.20, 171.52, 171.12, 162.70, 155.55, 77.39, 69.76 (2C), 69.54 (2C), 68.08, 68.06 (2C), 61.03, 59.19, 55.41, 37.98, 37.88, 37.31, 37.22, 35.79, 35.14, 30.78, 30.74, 29.72, 29.37, 28.26 (3C), 28.18, 28.03, 25.23; **HRMS** (ESI) calcd. for $C_{33}H_{60}N_6NaO_9S_3^+$ $[M+Na]^+$: 803.3476, found: 803.3486.

Linker 3 (164):

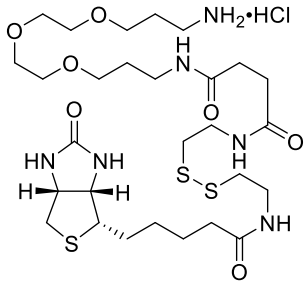

A solution of **163** (22.0 mg 28.2 µmol) in MeOH (1.0 mL) was added a solution of HCl in dioxane (4 M, 1.0 mL) and the mixture was stirred at room temperature for 2 h. The mixture was concentrated under reduced pressure and the residue eluted through a small C_{18} SPE column using 60% aq. MeCN and evaporated to yield crude hydrochloride **164** (13.0 mg, 64%) as a colorless solid, which was used without further purification.

HRMS (ESI) calcd. for $C_{28}H_{53}N_6O_7S_3^+$ $[M+H]^+$: 681.3132, found: 681.3137.

Probe 3 (165):

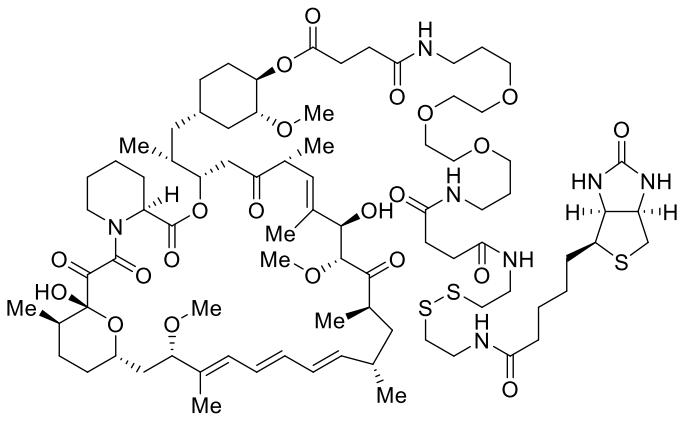

To a solution of rapamycin hemi-succinate (**150**, 18.4 mg, 18.1 µmol, 1.0 eq.) in DMF (0.2 mL) was added amine **164** (13.0 mg, 18.1 µmol, 1.0 eq.), HBTU (8.24 mg, 21.7 µmol, 1.2 eq.) and DIPEA (11 µL, 63.4 µmol, 3.5 eq.) and the mixture was stirred overnight at room temperature. The mixture was eluted through a small C_{18} SPE column using MeCN and evaporated. Separation by preparative reversed-phase HPLC gave **165** (13.0 mg, 43%) as a colorless solid.

HRMS (ESI) calcd. for $C_{83}H_{133}N_7NaO_{22}S_3^+$ $[M+Na]^+$: 1698.8558, found: 1698.8570.

Boc-protected amino rapamycin 166:

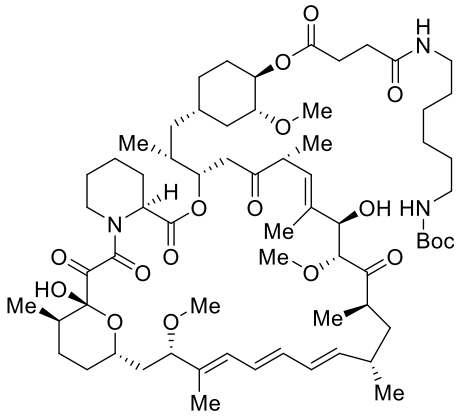

To a solution of rapamycin hemisuccinate (**150**, 30.4 mg, 30.0 µmol, 1.0 eq.) in DMF (0.2 mL) amine **153** (9.73 mg, 45.0 µmol, 1.5 eq.), HBTU (17.1 mg, 45.0 µmol, 1.5 eq.) and DIPEA (9.69 mg, 75.0 µmol, 2.5 eq.) were added and the resulting mixture was stirred overnight at room temperature. The mixture was subjected to flash chromatography (CH_2Cl_2/MeOH, 30:1) to afford **166** (34.5 mg, 95%) as an off-white foam.

$\mathbf{R_f}$ = 0.4 (CH_2Cl_2/MeOH, 20:1); **HRMS** (ESI) calcd. for $C_{66}H_{105}N_3NaO_{17}^+$ $[M+Na]^+$: 1234.7336, found: 1234.7330.

Azido rapamycin 169:

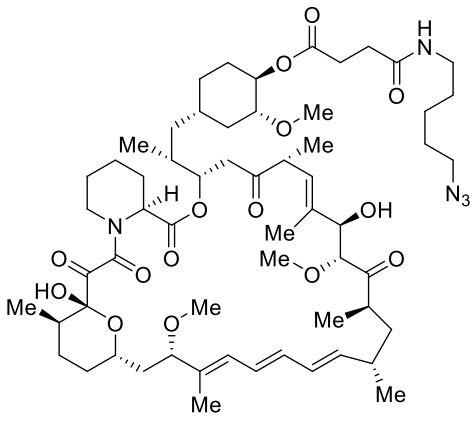

A solution of rapamycin hemisuccinate (**155**, 17.0 mg, 16.8 µmol, 1.0 eq.) in DMF (0.4 mL) was added 5-azidopentan-1-amine (**168**, 3.01 mg, 23.5 µmol, 1.4 eq.), HBTU (9.56 mg, 25.2 µmol, 1.5 eq.) and DIPEA (5.43 mg, 42.0 µmol, 2.5 eq.) and the mixture was stirred overnight at room temperature. The mixture was poured into sat. aq. $NaHCO_3$ and extracted with CH_2Cl_2. The combined organic layers were washed with water, dried over Na_2SO_4 and evaporated. The residue was subjected to flash chromatography (CH_2Cl_2/MeOH, 20:1) to afford azide **169** (16.5 mg, 87%) as a colorless foam.

R_f = 0.4 (CH_2Cl_2/MeOH, 20:1); **HRMS** (ESI) calcd. for $C_{60}H_{93}N_5NaO_{15}^+$ $[M+Na]^+$: 1146.6560, found: 1146.6553.

6.5 *Securinega* Alkaloids

Nitrosobenzene (309):

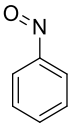

A solution of sodium tungstate (2.02 g, 6.12 mmol, 0.01 eq.) in aqueous hydrogen peroxide (30%, 40 mL) was cooled to 15–19 °C in an ice bath. Aniline (**308**, 40.8 g, 40.0 mL, 438 mmol, 1.0 eq) was added over 2 h at a constant flow rate of 0.33 mL/min using a syringe pump. During the reaction, three more portions of hydrogen peroxide (10.0 mL each) were added. The brown precipitate that had formed was filtered off and stirred in 300 mL water for 15 min. The solid was filtered again and washed with water and cold ethanol. The solid was recrystallized from ethanol to obtain colorless crystals of **309** (18.4 g, 39%).

^{1}H NMR (250 MHz, $CDCl_3$) δ 7.94–7.85 (m, 2H), 7.76–7.66 (m, 1H), 7.66–7.57 (m, 2H); **^{13}C NMR** (101 MHz, $CDCl_3$) δ 165.93, 135.68, 129.39, 121.02; **M.p.:** 65–67 °C.

Analytical data are in agreement with the literature: S. M. Opalka, A. R. Longstreet, D. T. McQuade, *Beilstein J. Org. Chem.* **2011**, *7*, 1671–1679.

(*S*)-7-Anilinoxy-1,4-dioxaspiro[4.5]decan-8-one (310):

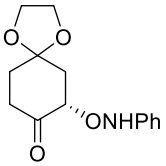

A solution of **309** (9.00 g, 84.0 mmol, 1.1 eq.) in DMF (100 mL) was added to a solution of 1,4-dioxaspiro[4.5]decan-8-one (**307**, 11.9 g, 76.4 mmol, 1.0 eq.) and D-proline (0.880 g, 7.64 mmol, 0.1 eq.) in DMF (150 mL) using a syringe pump over 26 h at 0 °C. Then the mixture was stirred for another 30 min at room temperature and quenched with pH 7 phosphate buffer solution. The mixture diluted with EtOAc and brine. Layers were separated and the aqueous layer was extracted with EtOAc. The combined organic layers were washed with brine, dried over Na_2SO_4 and the solvent was evaporated under reduced pressure. The residue was purified by flash chromatography (pentane/EtOAc, 4:1–0:1) to obtain **310** as a yellow solid (15.2 g, 76%).

$[\alpha]_D^{25}$ = −45.1 (c = 0.48 in $CHCl_3$); **^{1}H NMR** (400 MHz, $CDCl_3$) δ 7.22–7.12 (m, 2H), 6.92–6.78 (m, 3H), 4.57 (dd, *J* = 12.9, 6.5 Hz, 1H), 4.16–3.77 (m, 4H), 2.68–2.52 (m, 1H), 2.48–2.26 (m, 2H), 2.12 (t, *J* = 12.8 Hz, 1H), 2.02–1.79 (m, 2H); **^{13}C NMR** (101 MHz, $CDCl_3$) δ 208.87, 148.11, 128.99, 122.26, 114.60, 107.70, 82.82, 65.00, 64.93, 39.78, 36.12, 34.49; **M.p.:** 60–64 °C.

Analytical data are in agreement with the literature: M. Matsuzawa, H. Kakeya, J. Yamaguchi, M. Shoji, R. Onose, H. Osada, Y. Hayashi, *Chem. Asian J.* **2006**, *1*, 845–851.

(7*S*,8*R*)-7-((Phenylamino)oxy)-1,4-dioxaspiro[4.5]decan-8-ol (S311):

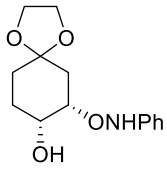

A solution of K-selectride (1 M in THF, 49.4 mL, 49.4 mmol, 2.0 eq.) was added to a solution of **310** (6.50 g, 24.7 mmol, 1.0 eq.) in THF (177 mL) at −78 °C and the reaction temperature was increased to −50 °C over 1.5 h. Sodium perborate tetrahydrate (12.2 g, 124 mmol, 5.0 eq.) and water (30 mL) were added and the reaction mixture was stirred for 30 min at room temperature. The organic layer was separated and the aqueous layer was extracted with Et_2O. The combined organic layers were washed with brine, dried over Na_2SO_4 and the solvent was evaporated to obtain crude **S311** (9.60 g) as a brown oil, which was used without further purification.

(7*S*,8*R*)-1,4-Dioxaspiro[4.5]decane-7,8-diol (311):

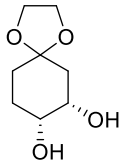

Crude **S311** (1.00 g) was dissolved in methanol (8.3 mL) under argon atmosphere. Pd/C (10 wt% Pd, 7.4 mg, 69.4 µmol) was added. The reaction mixture was stirred under an H_2 atmosphere (1 bar) at room temperature overnight. The mixture was filtered through diatomaceous earth and the solvent was evaporated. The residue was purified by flash chromatography (pentane/EtOAc, 3:1–1:3) to obtain **311** (425 mg, 72% over two steps) as a dark-red oil.

$[\alpha]_D^{25}$ = +4.4 (c = 0.39 in $CHCl_3$); **^{1}H NMR** (250 MHz, $CDCl_3$) δ 4.04–3.84 (m, 4H), 3.76–3.57 (m, 1H), 2.68 (s, 2H), 2.05–1.89 (m, 1H), 1.88–1.68 (m, 4H), 1.63–1.47 (m, 1H); **^{13}C NMR** (63 MHz, $CDCl_3$) δ 108.75, 70.40, 69.71, 64.36, 63.79, 37.92, 31.03, 26.86.

Analytical data are in agreement with the literature: M. Matsuzawa, H. Kakeya, J. Yamaguchi, M. Shoji, R. Onose, H. Osada, Y. Hayashi, *Chem. Asian J.* **2006**, *1*, 845–851.

(*R*)-4-Hydroxycyclohex-2-en-1-one (306):

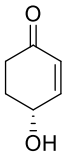

Amberlyst 15 (40.0 mg, 20 wt%, previously washed with THF) was added to a solution of **311** (200 mg, 1.05 mmol, 1.0 eq.) in THF (165 mL), H_2O (16.5 mL) and acetone (16.5 mL), and the reaction mixture was stirred at 80 °C for 21 h. Amberlyst 15 was filtered off and washed with acetone. The filtrate was dried over Na_2SO_4 and the solvent was evaporated under reduced pressure. The crude product was purified by flash chromatography (pentane/EtOAc, 1:4) to obtain **306** (103 mg, 68%) as a brown oil.

$[\alpha]_D^{25}$ = +108.1 (c = 0.26 in $CHCl_3$); **^{1}H NMR** (250 MHz, $CDCl_3$) δ 6.93 (ddd, *J* = 10.2, 2.4, 1.6 Hz, 1H), 5.97 (ddd, *J* = 10.2, 2.0, 1.0 Hz, 1H), 4.64–4.52 (m, 1H), 2.65–2.51 (m, 1H), 2.46–2.28 (m, 2H), 2.15 (s, 1H), 2.07–1.91 (m, 1H); **^{13}C NMR** (63 MHz, $CDCl_3$) δ 198.88, 152.81, 129.41, 66.51, 35.48, 32.63.

Analytical data are in agreement with the literature: M. Matsuzawa, H. Kakeya, J. Yamaguchi, M. Shoji, R. Onose, H. Osada, Y. Hayashi, *Chem. Asian J.* **2006**, *1*, 845–851.

(*R*)-4-((*tert*-Butyldiphenylsilyl)oxy)cyclohex-2-en-1-one (312):

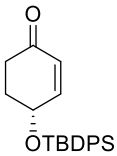

To a solution of **306** (1.49 g, 13.3 mmol, 1.0 eq.) in CH_2Cl_2 (135 mL), imidazole (924 mg, 13.6 mmol, 1.02 eq.) and DMAP (162 mg, 1.33 mmol, 0.1 eq.) were added at 0 °C. TBDPSCl (3.52 mL, 3.73 g, 13.6 mmol, 1.02 eq.) was added dropwise at 0 °C and the resulting mixture was stirred at room temperature for 2.5 h. The mixture was quenched with sat. aq. NH_4Cl, extracted with CH_2Cl_2 and the combined organic layers were dried over Na_2SO_4. The solvent was evaporated under reduced pressure. The crude product was purified by flash chromatography (pentane/EtOAc, 10:1–5:1) to obtain **312** (4.38 g, 94%) as a colorless oil.

R_f = 0.1 (pentane/EtOAc, 10:1); **$[\alpha]_D^{25}$** = +63.7 (c = 0.12 in $CHCl_3$); **FTIR** (neat): $\tilde{\nu}$ = 3070, 2957, 2857, 1686, 1589, 1427, 1383, 1348, 1250, 1104, 987, 843 cm^{-1}; **^{1}H NMR** (400 MHz, $CDCl_3$) δ 7.67–7.56 (m, 4H), 7.45–7.26 (m, 6H), 6.71 (ddd, *J* = 10.3, 2.5, 1.2 Hz, 1H), 5.79 (ddd, *J* = 10.3, 1.8, 1.0 Hz, 1H), 4.48–4.36 (m, 1H), 2.52–2.38 (m, 1H), 2.20–2.05 (m, 1H), 2.05–1.91 (m, 2H), 1.01 (s, 9H); **^{13}C NMR** (101 MHz, $CDCl_3$) δ 199.05, 153.36, 135.89, 135.87, 133.55, 133.52, 130.15, 130.13, 128.88, 127.98, 127.94, 67.71, 35.47, 32.73, 27.01, 19.29; **HRMS** (ESI) calcd. for $C_{22}H_{29}O_2Si^+$ $[M+Na]^+$: 351.1775, found: 351.1776.

(4*R*,6*R*)-4-((*tert*-Butyldiphenylsilyl)oxy)-6-hydroxycyclohex-2-en-1-one (314):

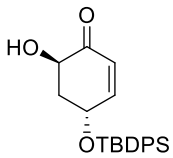

To a solution of **312** (380 mg, 1.08 mmol, 1.0 eq.) and Davis' oxaziridine **318** (339 mg, 1.30 mmol, 1.2 eq.) in THF (5.6 mL) at −78 °C a solution of NaHMDS (1 M in THF, 1.3 mL, 1.30 mmol, 1.2 eq.) was added and the resulting yellow mixture was stirred at −78 °C for 1 h. The reaction mixture was quenched with sat. aq. NH_4Cl and allowed to warm to room temperature. More sat. aq. NH_4Cl was added and the mixture extracted with Et_2O. The combined organic layers were thoroughly washed with 10% aq. $NaHSO_3$, dried over Na_2SO_4 and evaporated under reduced pressure to give crude alcohol **314** (524 mg) as a yellowish oil, which was used without further purification.

$\mathbf{R_f}$ = 0.4 (pentane/Et_2O, 3:1); **^{1}H NMR** (400 MHz, $CDCl_3$) δ 7.72–7.62 (m, 4H), 7.51–7.35 (m, 6H), 6.54 (ddd, *J* = 9.9, 5.2, 1.8 Hz, 1H), 5.98 (d, *J* = 9.9 Hz, 1H), 4.82 (dd, *J* = 12.3, 5.3 Hz, 1H), 4.47 (ddd, *J* = 5.2, 3.8, 2.4 Hz, 1H), 3.39 (br s, 1H), 2.51 (ddt, *J* = 13.3, 5.4, 2.1 Hz, 1H), 1.89 (ddd, *J* = 13.2, 12.3, 3.8 Hz, 1H), 1.08 (s, 9H); **HRMS** (ESI) Exact mass calcd. for $C_{22}H_{26}NaO_3Si^+$ $[M+Na]^+$: 389.1549, found: 389.1543.

(6*R*,7a*R*)-6-((*tert*-Butyldiphenylsilyl)oxy)-7,7a-dihydrobenzofuran-2(6*H*)-one (288):

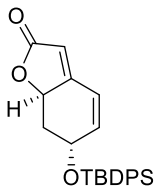

The Bestmann ylide (**323**, 53.4 mg, 0.177 mmol, 1.3 eq.) was added to a solution of α-hydroxy ketone **314** (49.8 mg, 0.136 mmol, 1.0 eq.) in benzene (3.0 mL) and the mixture was heated to 85 °C for 3 h in a microwave reactor. The mixture was diluted with Et_2O, washed with water, dried over Na_2SO_4 and solvents were removed under reduced pressure. The residue was purified by flash chromatography (pentane/Et_2O, 10:1–3:1, 1% Et_3N) to afford a diastereomeric mixture of the bicyclic product **288** (17.0 mg, 43.5 μmol, 43% over two steps; d.r. = 3.3:1, calculated by NMR) as a yellow oil.

$\mathbf{R_f}$ = 0.4 (pentane/Et_2O, 3:1); **FTIR** (neat): $\tilde{\nu}$ = 3728, 3630, 2928, 2857, 1762, 1111, 1069, 703 cm^{-1}; **^{1}H NMR** (400 MHz, $CDCl_3$, major isomer) δ 7.70–7.64 (m, 4H), 7.45–7.37 (m, 6H), 6.48 (d, *J* = 9.6 Hz, 1H), 5.96 (ddd, *J* = 9.7, 5.2, 1.0 Hz, 1H), 5.78 (s, 1H), 5.46 (ddd, *J* = 12.5, 5.0, 1.9 Hz, 1H), 4.50 (ddd, *J* = 5.6, 3.7, 2.2 Hz, 1H), 2.55 (dddt, *J* = 12.5, 5.0, 2.2, 1.0 Hz, 1H), 1.61 (td, *J* = 12.5, 3.8 Hz, 1H), 1.08 (s, 9H); **^{13}C NMR** (101 MHz, $CDCl_3$, major isomer) δ 173.47, 163.15, 144.40, 135.86, 135.83, 133.55, 133.03, 130.29, 130.17, 128.08, 127.93, 121.18, 112.29, 76.80, 65.82, 37.83, 27.01, 19.33.

Analytical data are in agreement with the literature: H. Miyatake-Ondozabal, L. M. Bannwart, K. Gademann, *Chem. Commun.* **2013**, *49*, 1921–1923.

***tert*-Butyl (*S*)-2-((6*R*,7a*S*)-6-((*tert*-butyldiphenylsilyl)oxy)-2-oxo-6,7-dihydro-benzofuran-7a(2*H*)- yl)piperidine-1-carboxylate (275):**

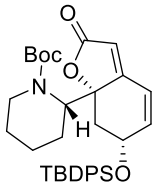

To a solution of the bicyclic compound **288** (139 mg, 0.356 mmol, 1.0 eq.) in Et_2O (3.4 mL) at 0 °C, Et_3N (0.10 mL, 0.712 mmol, 2.0 eq.) was added and the reaction mixture was stirred at 0 °C for 45 min. TIPSOTf (0.11 mL, 0.409 mmol, 1.15 eq.) was added, and the reaction mixture stirred overnight at room temperature. A solution of *tert*-butyl 2-hydroxypiperidine-1-carboxylate (**274**, 161 mg, 0.801 mmol, 2.25 eq.) in Et_2O (3.4 mL) was added and the mixture was cooled to −78 °C. Then, *n*-Bu_2BOTf (0.28 mL, 0.801 mmol, 2.25 eq.) was added dropwise during 5 min, and the mixture stirred at −78 °C for 5 min. The mixture was quenched with sat. aq. NH_4Cl, allowed to warm to room temperature and extracted with Et_2O. The combined organic layers were dried over Na_2SO_4 and the solvent was removed under reduced pressure. The crude material was purified by repeated flash chromatography (pentane/EtOAc, 6:1) to afford two diastereomers of **275** ((−)-**275**, 140 mg, 69%; (+)-**275**, 33 mg, 16%) as colorless oils. As previously reported in the literature, each isomer showed two sets of signals in the NMR spectra corresponding to rotamers.

(−)-**275:** $\mathbf{R_f}$ = 0.15 (pentane/EtOAc, 10:1); $\mathbf{[\alpha]_D^{25}}$ = −59.4 (c = 1.0 in $CHCl_3$); **^{1}H NMR** (400 MHz, $CDCl_3$, major rotamer) δ 7.73–7.60 (m, 4H), 7.51–7.34 (m, 6H), 6.51 (dd, *J* = 10.0, 2.2 Hz, 1H), 6.24 (dt, *J* = 10.0, 1.6 Hz, 1H), 5.63 (s, 1H), 4.47–4.39 (m, 1H), 3.87–3.80 (m, 1H), 3.74 (dd, *J* = 14.2, 5.7 Hz, 1H), 2.92 (td, *J* = 13.3, 4.7 Hz, 1H), 2.39 (dd, *J* = 12.1, 5.3 Hz, 1H), 1.80 (dd, *J* = 12.3, 10.3 Hz, 1H), 1.66–0.80 (m, 6H), 1.31 (s, 9H), 1.07 (s, 9H); **^{13}C NMR** (101 MHz, $CDCl_3$) δ 172.48, 166.11, 155.61, 139.86, 136.00, 135.95, 133.41, 133.03, 130.22, 128.07, 128.04, 121.81, 111.11, 89.69, 79.75, 67.21, 52.40, 41.60, 40.87, 28.26, 27.04, 23.74, 23.34, 19.24, 18.62.

Analytical data are in agreement with the literature: G. G. Bardají, M. Cantó, R. Alibés, P. Bayón, F. Busqué, P. de March, M. Figueredo, J. Font, *J. Org. Chem.* **2008**, *73*, 7657–7662.

(*S*)-2-((6*R*,7a*S*)-6-((*tert*-Butyldiphenylsilyl)oxy)-2-oxo-6,7-dihydrobenzofuran-7a(2*H*)-yl)piperidin-1- ium chloride (325):

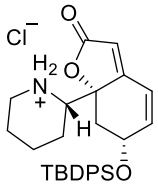

Protected amine (−)-**275** (72.0 mg, 0.125 mmol, 1.0 eq.) was dissolved in 2 M HCl in Et_2O (5.0 mL) and stirred in a microwave reactor at 45 °C for 10 h. The reaction mixture was diluted with CH_2Cl_2 and filtered. Solvents were removed under reduced pressure giving hydrochloride **325** (62.0 mg, 97%) as a colorless solid.

R_f = 0.0 (pentane/EtOAc, 2:1); **M.p.** = 179–181 °C (dec.); **$[\alpha]_D^{25}$** = −56.2 (c = 0.10 in $CHCl_3$); **FTIR** (neat): $\tilde{\nu}$ = 3376, 3050, 2932, 2858, 1753, 1640, 1428, 1112, 1084, 1064, 1003, 849, 703 cm^{-1}; **^{1}H NMR** (400 MHz, CD_3OD) δ 7.78–7.68 (m, 4H), 7.58–7.38 (m, 6H), 6.69 (dd, *J* = 10.2, 2.2 Hz, 1H), 6.46 (d, *J* = 10.2 Hz, 1H), 6.07 (s, 1H), 4.48 (dq, *J* = 7.8, 2.7 Hz, 1H), 3.25–3.07 (m, 2H), 2.85 (td, *J* = 13.4, 3.1 Hz, 1H), 2.37 (dd, *J* = 12.6, 5.0 Hz, 1H), 1.82–1.67 (m, 3H), 1.59–1.44 (m, 1H), 1.41–1.16 (m, 4H), 1.09 (s, 9H); **^{13}C NMR** (101 MHz, CD_3OD) δ 171.48, 164.41, 143.86, 137.14, 137.01, 134.13, 133.95, 131.54, 131.45, 129.19, 129.15, 120.89, 114.97, 86.22, 68.16, 58.00, 47.05, 42.52, 27.34, 24.46, 22.95, 22.80, 19.84. **HRMS** (ESI) Exact mass calcd. for $C_{29}H_{36}NO_3Si^+$ $[M-Cl]^+$: 474.2459, found: 474.2465.

(5*R*,10a*S*,12*R*)-12-((*tert*-Butyldiphenylsilyl)oxy)-4,5,8,9,10,10a-hexahydro-2*H*,7*H*-5,10b-ethanofuro[2,3-a]quinolizin-2-one (326):

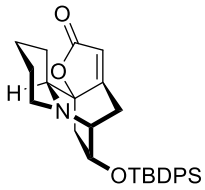

Hydrochloride **325** (92.8 mg, 0.182 mmol, 1.0 eq.) was dissolved in DMF (10 mL) and K_2CO_3 (126 mg, 0.910 mmol, 5.0 eq.) was added. The reaction mixture was heated to 75 °C and stirred for 3 h. Water was added and the mixture was extracted with EtOAc. The combined organic layers were washed with sat. aq. $NaHCO_3$ and water, dried over Na_2SO_4 and the solvent was removed under reduced pressure. The residue was purified by flash chromatography (pentane/Et_2O, 4:1) to yield tetracycle **326** (69.5 mg, 81%) as a colorless semisolid.

R_f = 0.4 (pentane/Et_2O, 4:1); **$[\alpha]_D^{25}$** = −48.8 (c = 0.10 in $CHCl_3$); **FTIR** (neat): $\tilde{\nu}$ = 3072, 2932, 2856, 1762, 1653, 1428, 1113, 1059, 1013, 840, 702 cm^{-1}; **^{1}H NMR** (400 MHz, C_6D_6) δ 7.68–7.54 (m, 4H), 7.26–7.17 (m, 6H), 5.42 (t, *J* = 1.8 Hz, 1H), 4.05 (dddd, *J* = 9.4, 4.7, 3.0, 1.5 Hz, 1H), 2.77 (dt, *J* = 18.8, 2.2 Hz, 1H), 2.41–2.24 (m, 3H), 2.18–2.07 (m, 2H), 1.92 (td, *J* = 11.1, 3.0 Hz, 1H), 1.50 (dd, *J* = 12.3, 4.8 Hz, 1H), 1.45 (d, *J* = 9.0 Hz, 2H), 1.43–0.98 (m, 4H), 1.10 (s, 9H), 0.92–0.80 (m, 1H), 0.78–0.65 (m, 1H); **^{13}C NMR** (101 MHz, C_6D_6) δ 172.79, 172.52,

136.03, 135.99, 134.04, 133.76, 130.39, 130.33, 128.59, 112.07, 83.51, 66.55, 65.28, 59.17, 52.35, 41.81, 29.31, 27.07, 26.90, 25.95, 24.24, 19.13; **HRMS** (ESI) Exact mass calcd. for $C_{29}H_{36}NO_3Si^+$ $[M+H]^+$: 474.2459, found: 474.2453.

Secu'amamine E (296):

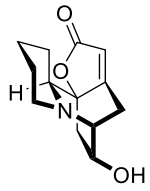

In a centrifuge tube (polypropylene) silyl ether **326** (32.0 mg, 67.6 µmol, 1.0 eq.) was dissolved in THF (3.0 mL) and HF·pyridine (200 µL, excess) was added dropwise. The yellow mixture was stirred at room temperature for 24 h. The mixture was carefully quenched with sat. aq. $NaHCO_3$ and extracted with EtOAc. The combined organic layers were washed with water, dried over Na_2SO_4 and the solvent was removed under reduced pressure. The residue was separated by flash chromatography (CH_2Cl_2/MeOH, 30:1) giving **296** (15.6 mg, 98%) as a colorless oil.

R_f = 0.2 (CH_2Cl_2/MeOH, 30:1); **$[\alpha]_D^{25}$** = −45.7 (c = 0.10 in MeOH); **FTIR** (neat): $\tilde{\nu}$ = 3446, 2936, 2852, 1756, 1737, 1651, 1150, 1000 cm^{-1}; **^{1}H NMR** (500 MHz, CD_3OD) δ 5.74 (t, *J* = 1.9 Hz, 1H), 4.42–4.20 (m, 1H), 3.05–2.91 (m, 2H), 2.90–2.86 (m, 1H), 2.84–2.72 (m, 3H), 2.67 (dd, *J* = 12.2, 9.6 Hz, 2H), 1.86–1.76 (m, 1H), 1.61–1.54 (m, 1H), 1.54–1.46 (m, 2H), 1.38 (dd, *J* = 12.2, 4.9 Hz, 1H), 1.39–1.28 (m, 1H), 0.87 (qd, *J* = 11.8, 4.0 Hz, 1H); **^{13}C NMR** (101 MHz, CD_3OD) δ 177.20, 176.25, 111.99, 86.23, 66.46, 65.30, 60.33, 53.51, 41.50, 30.28, 27.66, 26.75, 25.07; **HRMS** (ESI) Exact mass calcd. for $C_{13}H_{18}NO_3^+$ $[M+H]^+$: 236.12812, found: 236.12750.

Analytical data are in agreement with those reported for the authentic natural product: A. Ohsaki, T. Nagaoka, K. Yoneda, A. Kishida, *Tetrahedron Lett.* **2009**, *50*, 6965–6967.

General Procedure 1 (GP1):

Alkaloid (1.0 eq.) was dissolved in CH_2Cl_2 (30–40 mm). Et_3N (2.0 eq.), DMAP (2.0 eq.) and MsCl (1.8 eq.) were added in this sequence and the mixture was stirred at rt. After 15 min volatiles were evaporated under high vacuum without heating. The residue was subjected to flash chromatography.

Allosecurinine (172):

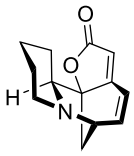

Secu'amamine E (**296**, 5 mg, 21.3 µmol) was reacted according to **GP1** giving **172** (4.3 mg, 93%) as a yellow semisolid.

R_f = 0.5 (CH_2Cl_2/MeOH, 10:1); **$[\alpha]_D^{25}$** = −487.0 (c = 0.10 in EtOH); **^{1}H NMR** (300 MHz, $CDCl_3$) δ 6.81 (dd, *J* = 9.1, 5.3 Hz, 1H), 6.65 (dd, *J* = 9.1, 1.1 Hz, 1H), 5.73 (s, 1H), 3.92 (t, *J* = 4.9 Hz, 1H), 3.67 (dd, *J* = 13.1, 3.4 Hz, 1H), 2.81–2.72 (m, 2H), 2.69 (dd, *J* = 9.9, 4.4 Hz, 1H), 1.92 (d, *J* = 9.8 Hz, 1H), 1.76–1.61 (m, 3H), 1.52–1.05 (m, 3H); **^{13}C NMR** (101 MHz, $CDCl_3$) δ 172.72, 167.48, 148.44, 122.97, 109.31, 91.78, 60.89, 58.98, 43.78, 42.75, 22.19, 21.20, 18.55.

Analytical data are in agreement with the literature: A. B. Leduc, M. A. Kerr, *Angew. Chem. Int. Ed.* **2008**, *47*, 7945–7948.

(−)-Allonorsecurinine (329):

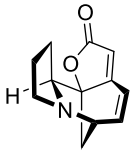

Bubbialidine (**292**, 4.0 mg, 18.1 µmol) was reacted according to **GP1** giving **329** (2.3 mg, 63%) as a yellow semisolid.

R_f = 0.4 (CH_2Cl_2/MeOH, 10:1); **$[\alpha]_D^{25}$** = −618.6 (c = 0.10 in EtOH); **^{1}H NMR** (400 MHz, $CDCl_3$) δ 6.85 (dd, *J* = 9.1, 5.4 Hz, 1H), 6.71 (dd, *J* = 9.1, 1.1 Hz, 1H), 5.79 (s, 1H), 4.16 (t, *J* = 7.4 Hz, 1H), 3.99 (t, *J* = 4.8 Hz, 1H), 2.96–2.81 (m, 3H), 2.03 (d, *J* = 10.0 Hz, 1H), 1.95–1.72 (m, 2H), 1.72–1.61 (m, 1H), 1.33–1.20 (m, 1H); **^{13}C NMR** (101 MHz, $CDCl_3$) δ 172.34, 166.99, 148.92, 124.09, 110.20, 90.80, 69.18, 57.89, 49.39, 46.95, 27.94, 25.52.

Analytical data are in agreement with the literature: A. S. Reddy, P. Srihari, *Tetrahedron Lett.* **2012**, *53*, 5926–5928.

Bubbialine mesylate (330):

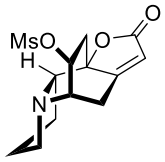

Bubbialine (**327**, 10.5 mg, 47.5 µmol) was reacted according to **GP1** giving **330** (14.0 mg, 99%) as a pale yellow solid.

R_f = 0.3 (CH_2Cl_2/MeOH, 30:1); **$[\alpha]_D^{25}$** = +141.3 (c = 0.10 in $CHCl_3$); **FTIR** (neat): $\tilde{\nu}$ = 2931, 2844, 1765, 1657, 1366, 1169, 967, 952, 899, 848, 532, 498 cm^{-1}; **^{1}H NMR** (400 MHz, $CDCl_3$) δ 5.85 (t, *J* = 2.1 Hz, 1H), 5.02 (ddd, *J* = 10.1, 3.5, 2.8 Hz, 1H), 3.74 (dd, *J* = 9.4, 6.3 Hz, 1H), 3.52 (p, *J* = 1.8 Hz, 1H), 3.21 (ddd, *J* = 20.2, 3.6, 2.0 Hz, 1H), 3.15–3.09

(m, 1H), 3.13 (s, 3H), 2.68 (td, *J* = 9.3, 7.6 Hz, 1H), 2.44 (dt, *J* = 20.2, 1.8 Hz, 1H), 2.37 (dd, *J* = 13.7, 3.5 Hz, 1H), 2.23 (dd, *J* = 13.7, 10.1 Hz, 1H), 1.91–1.74 (m, 3H), 1.16–1.03 (m, 1H); **^{13}C NMR** (126 MHz, $CDCl_3$) δ 172.73, 168.29, 114.39, 83.54, 75.89, 63.70, 54.34, 51.13, 39.35, 37.66, 27.29, 24.64, 24.24; **HRMS** (ESI) Exact mass calcd. for $C_{13}H_{18}NO_5S$ $[M+H]^+$: 300.09002, found: 300.08945.

(+)-Allonorsecurinine (331):

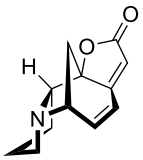

Mesylate **330** (9.0 mg, 30.1 µmol, 1.0 eq.) was dissolved in CH_2Cl_2 (0.8 mL) and Et_3N (6 µL, 42.1 µmol, 1.4 eq.) was added. The mixture was heated to 100 °C for 6 h in a microwave reactor. Volatiles were removed under high vacuum and the residue was subjected to flash chromatography and preparative TLC (CH_2Cl_2/MeOH, 20:1, 1% Et_3N) to obtain **331** (1.3 mg, 6.40 µmol, 21%) of moderate purity as an orange oil.

R_f = 0.2 (CH_2Cl_2/MeOH, 20:1); **$[\alpha]_D^{25}$** = +365.6 (c = 0.064 in EtOH); **^{1}H NMR** (500 MHz, $CDCl_3$) δ 6.81 (dd, *J* = 9.0, 5.4 Hz, 1H), 6.75 (d, *J* = 9.0 Hz, 1H), 5.83 (s, 1H), 4.27–4.22 (m, 1H), 4.09 (s, 1H), 3.08–2.93 (m, 2H), 2.87 (dt, *J* = 10.5, 7.4 Hz, 1H), 2.07 (d, *J* = 10.2 Hz, 1H), 1.96–1.79 (m, 2H), 1.77–1.67 (m, 1H), 1.37–1.16 (m, 1H); **^{13}C NMR** (126 MHz, $CDCl_3$) δ 172.17, 166.90, 148.74, 124.14, 110.33, 90.81, 69.22, 57.96, 49.40, 46.97, 27.93, 25.56.

Analytical data are in agreement with the literature: M. R. Medeiros, J. L. Wood, *Tetrahedron* **2010**, *66*, 4701–4709.

7 Appendix

NMR Spectra

5-Ethyl-2,2-dimethylbenzo[*d*][1,3]dioxole (**48**)

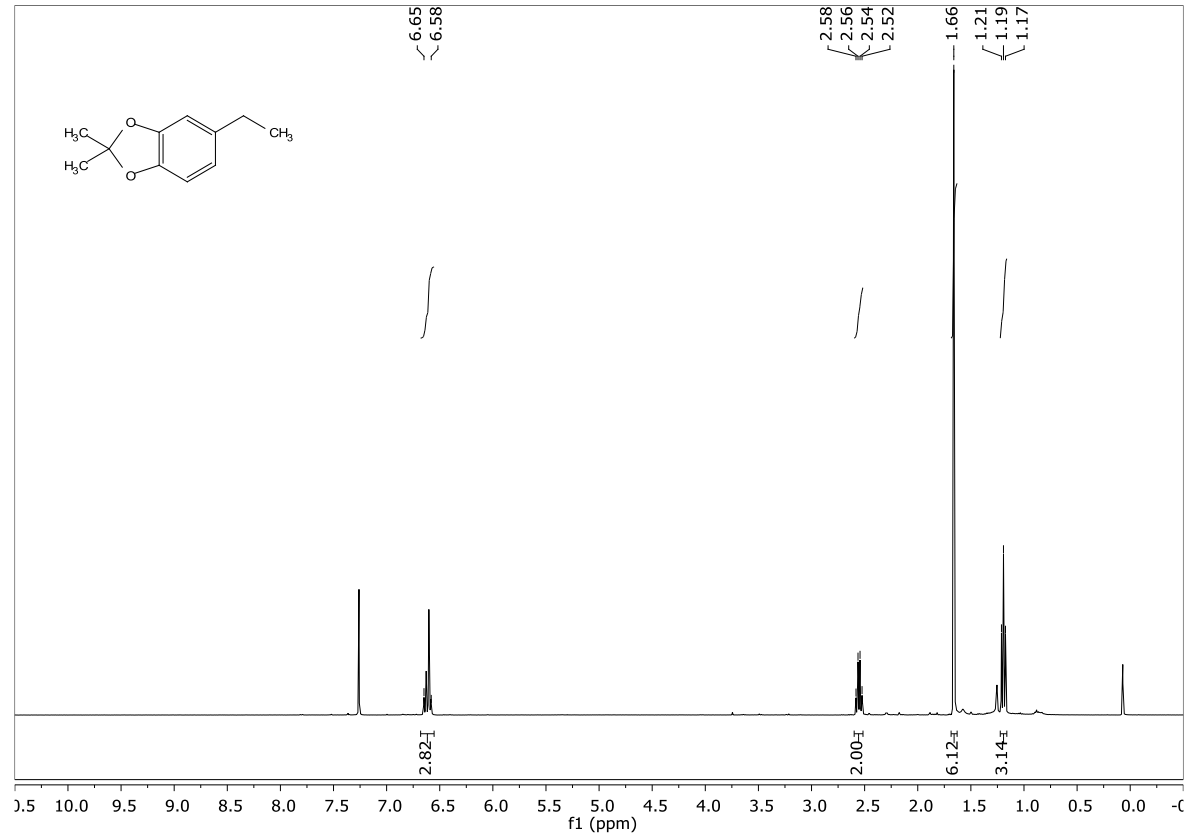

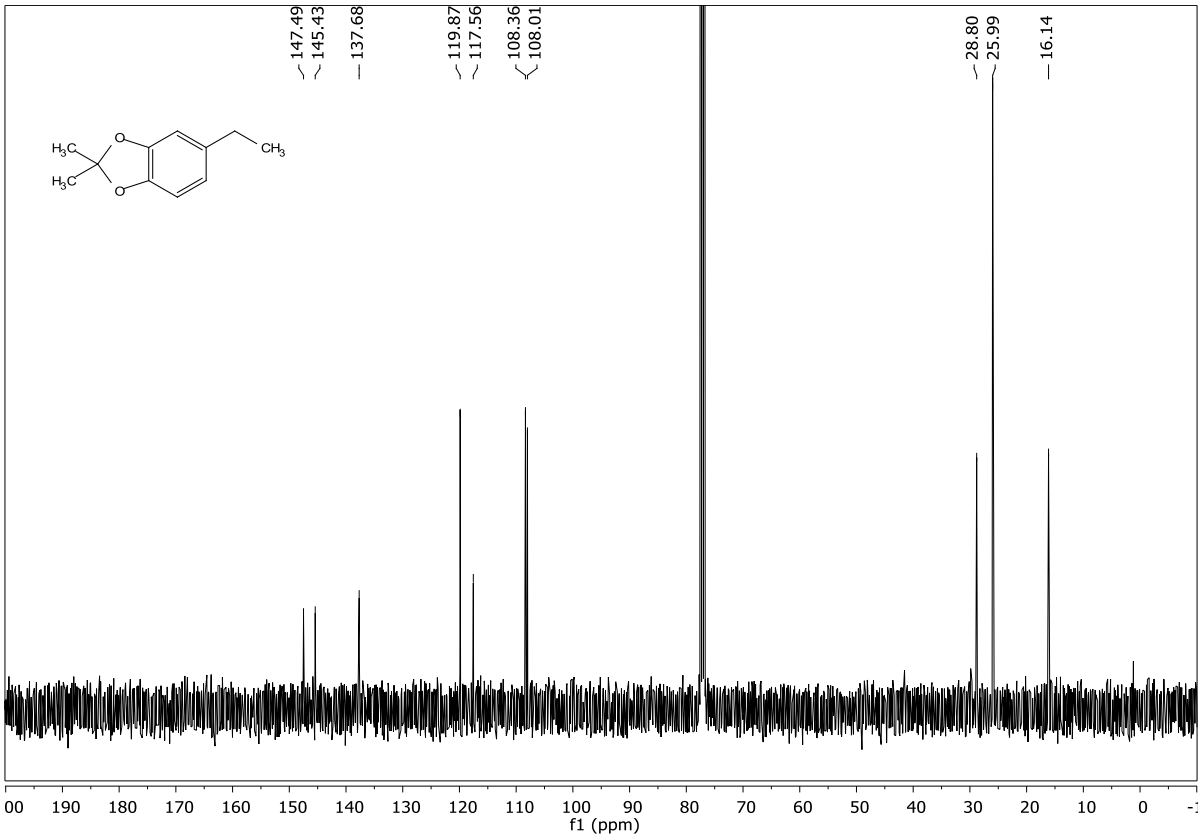

5-Ethyl-2,2-dimethyl-6-nitrobenzo[*d*][1,3]dioxole (**49**)

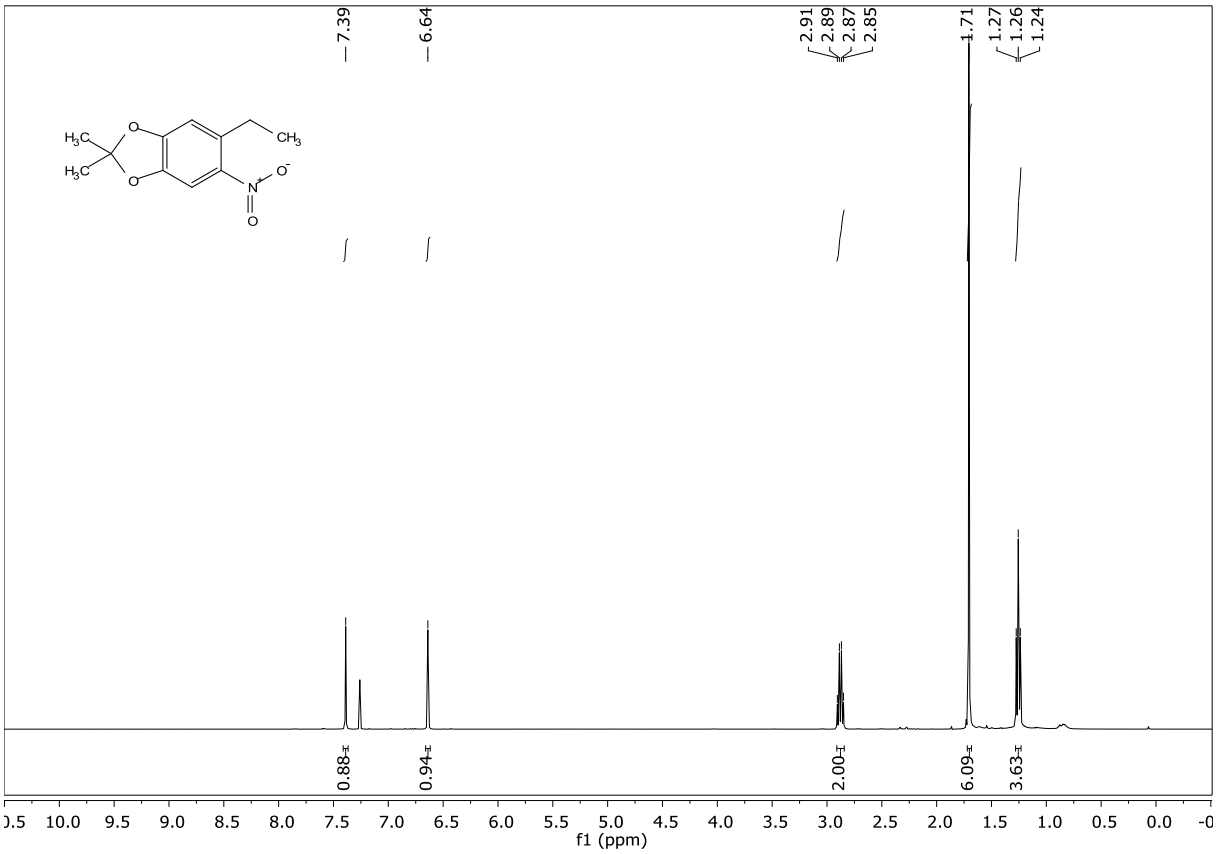

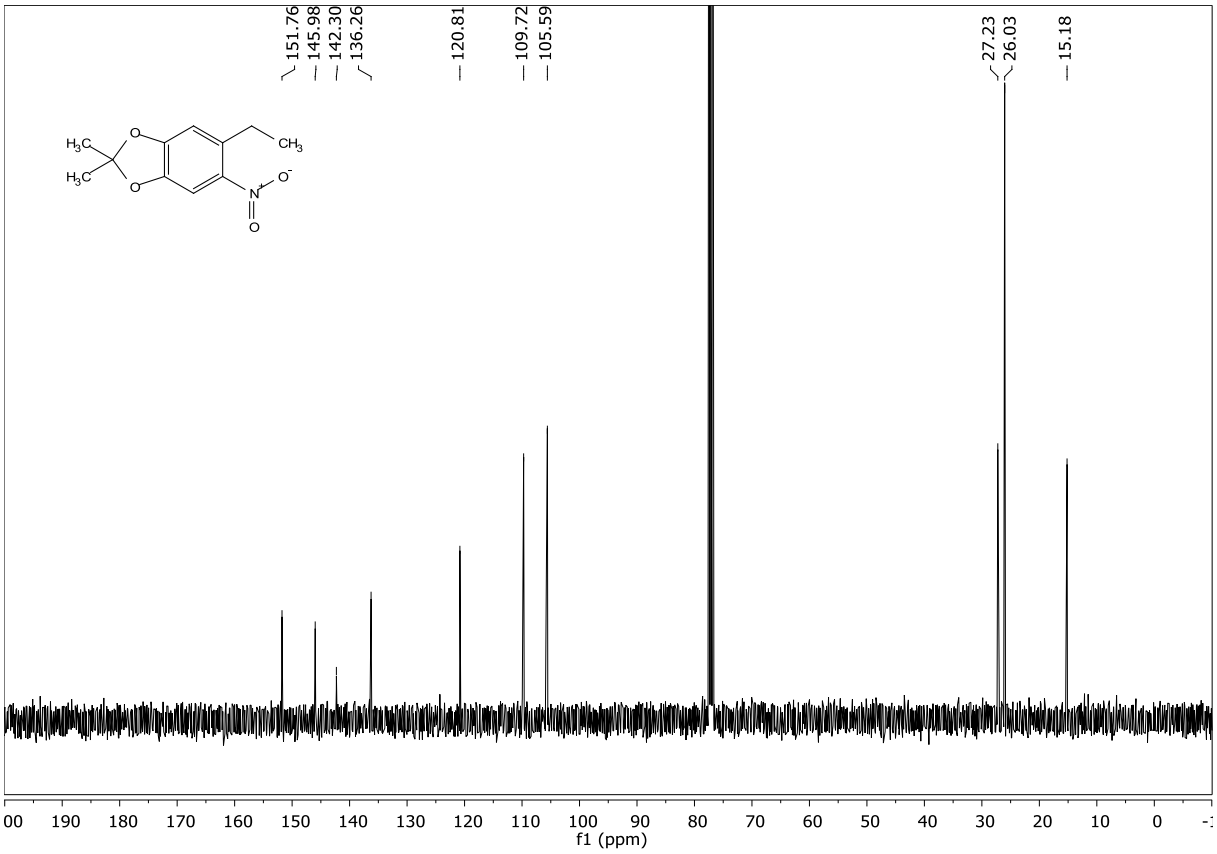

2-(2,2-Dimethyl-6-nitrobenzo[*d*][1,3]dioxol-5-yl)propan-1-ol (**50**)

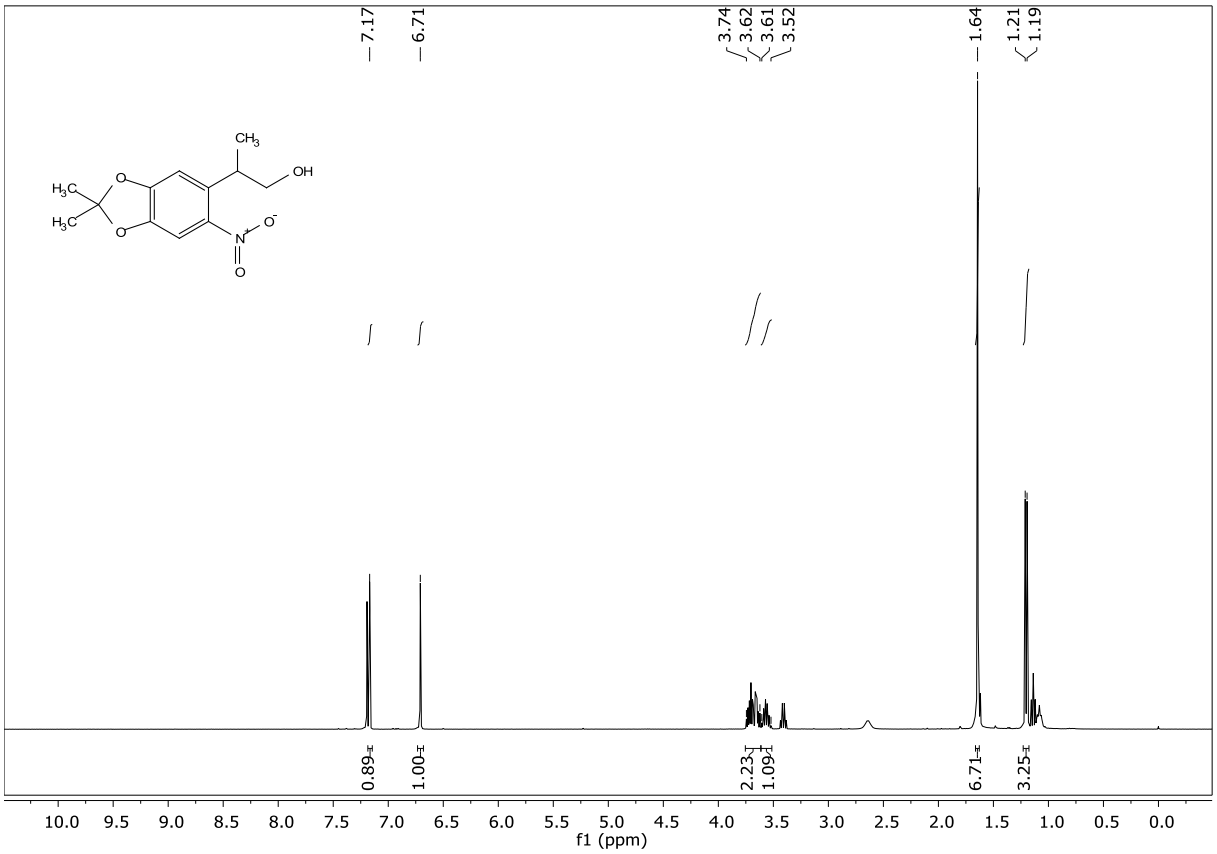

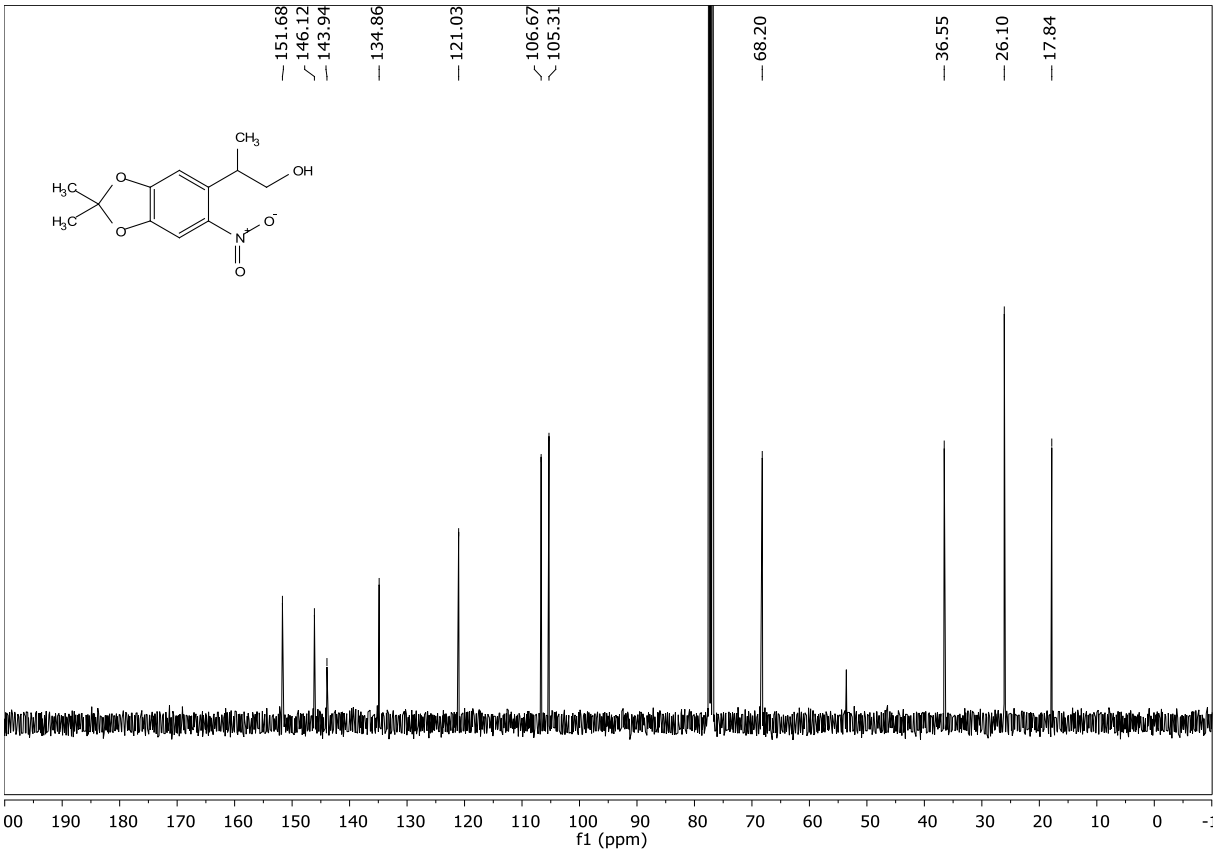

5-(1-(Benzyloxy)propan-2-yl)-2,2-dimethyl-6-nitrobenzo[d][1,3]dioxole (**55**)

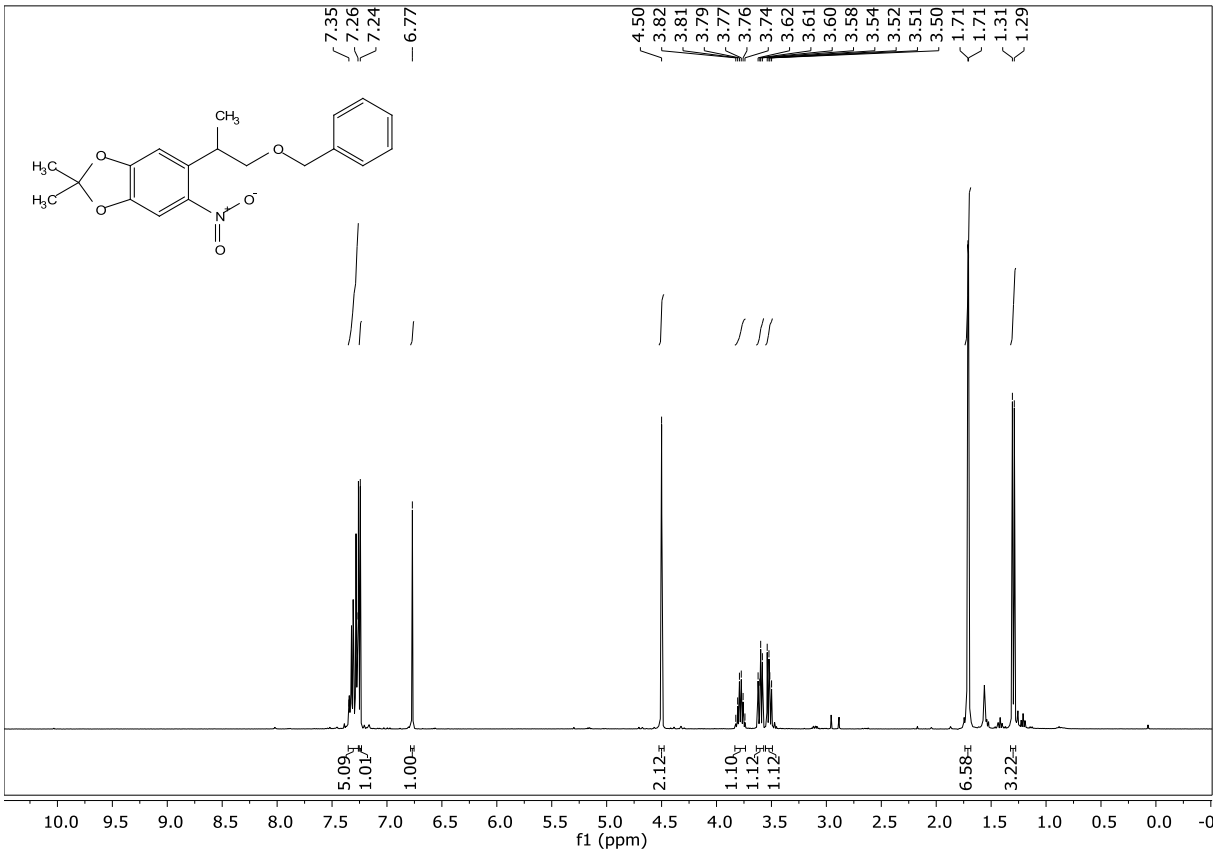

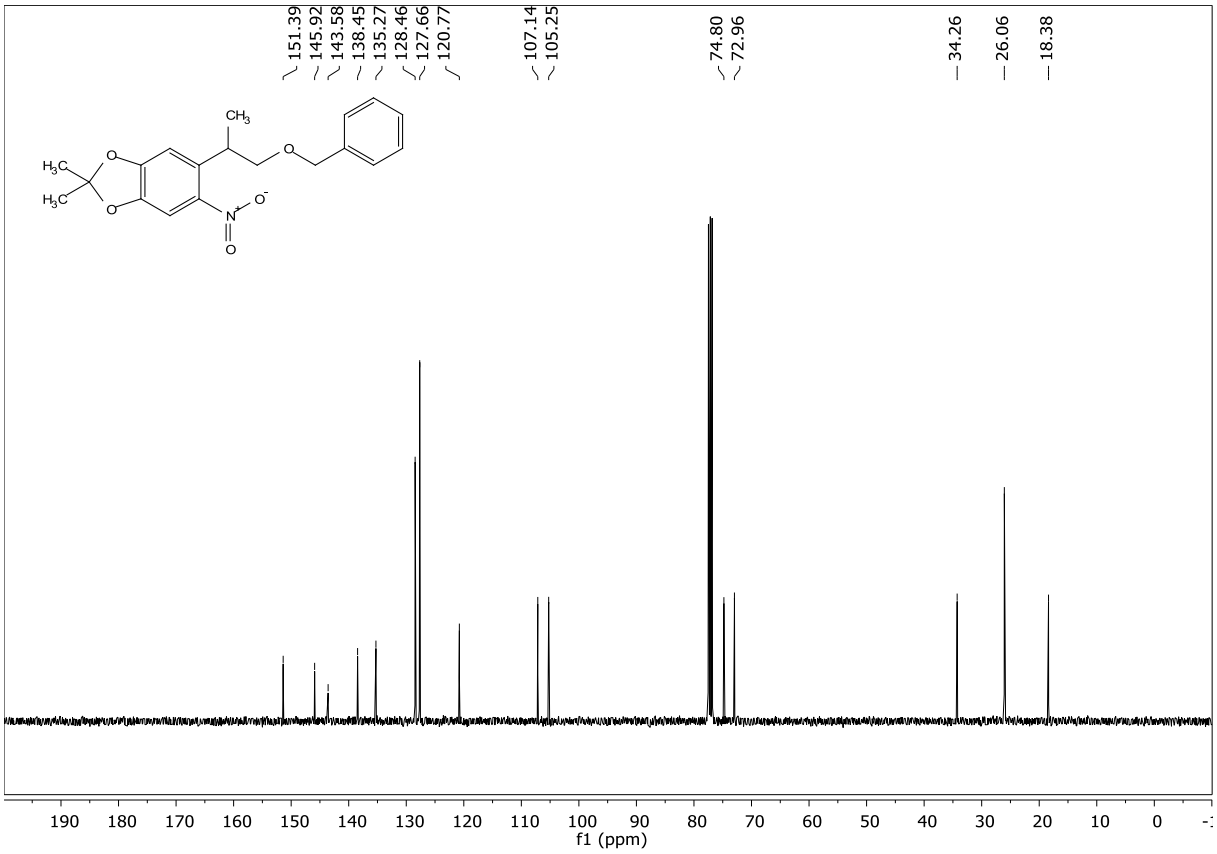

4-(1-(Benzyloxy)propan-2-yl)-5-nitrobenzene-1,2-diol (**56**)

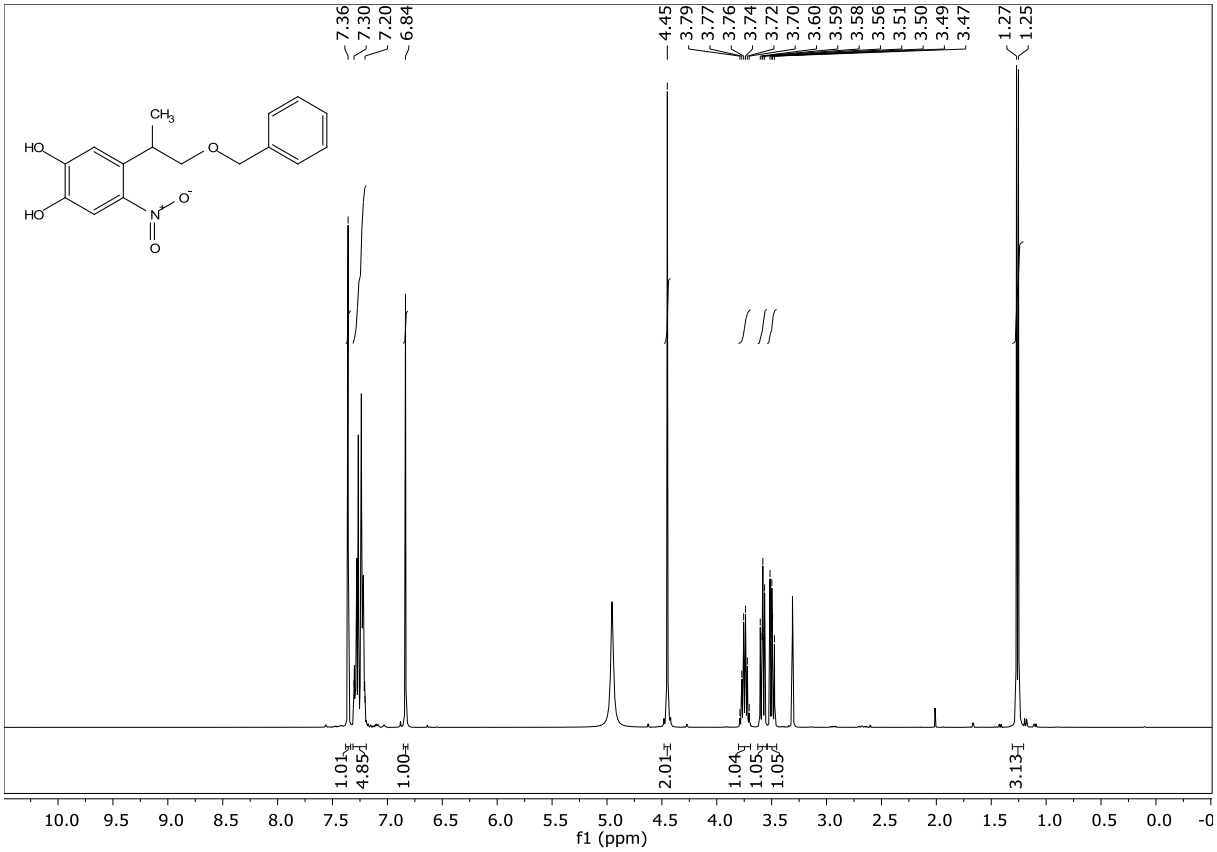

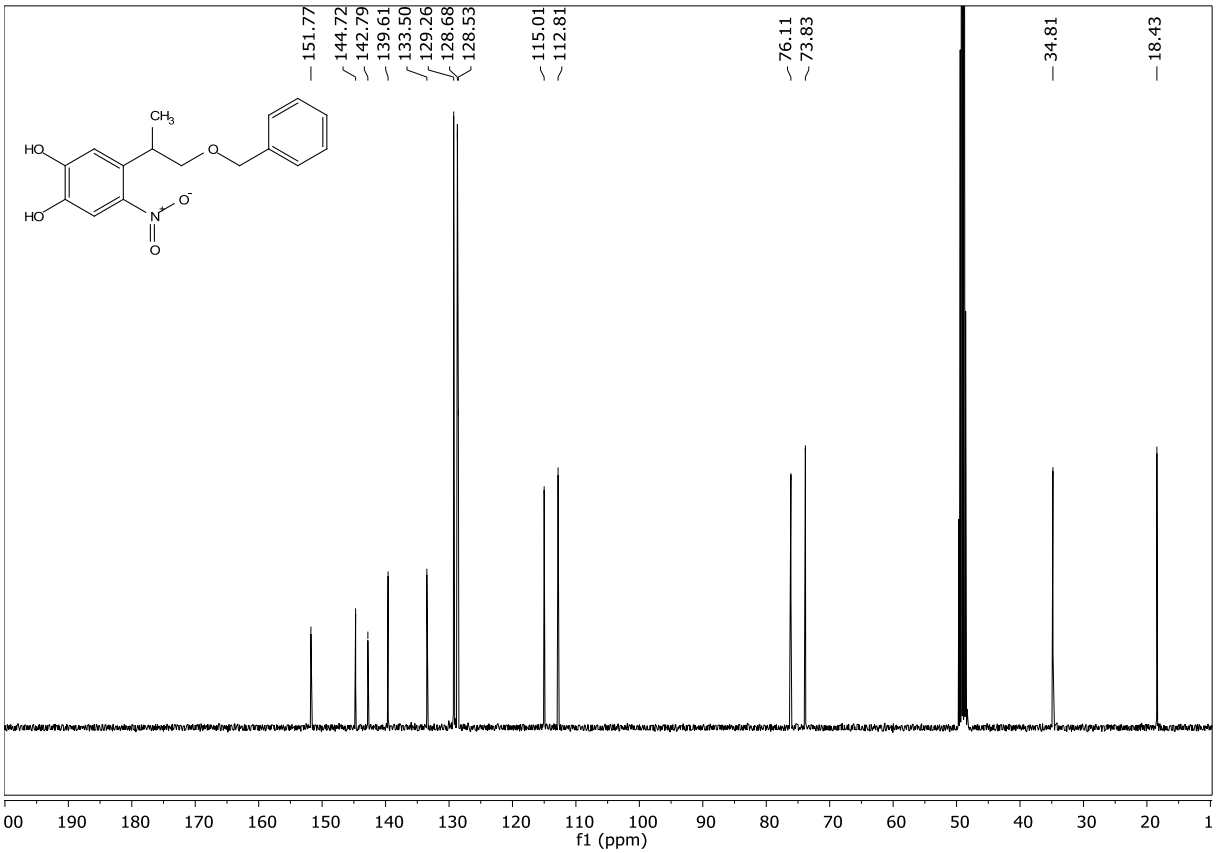

2-(2,2-Dimethyl-6-nitrobenzo[*d*][1,3]dioxol-5-yl)propanal (**57**)

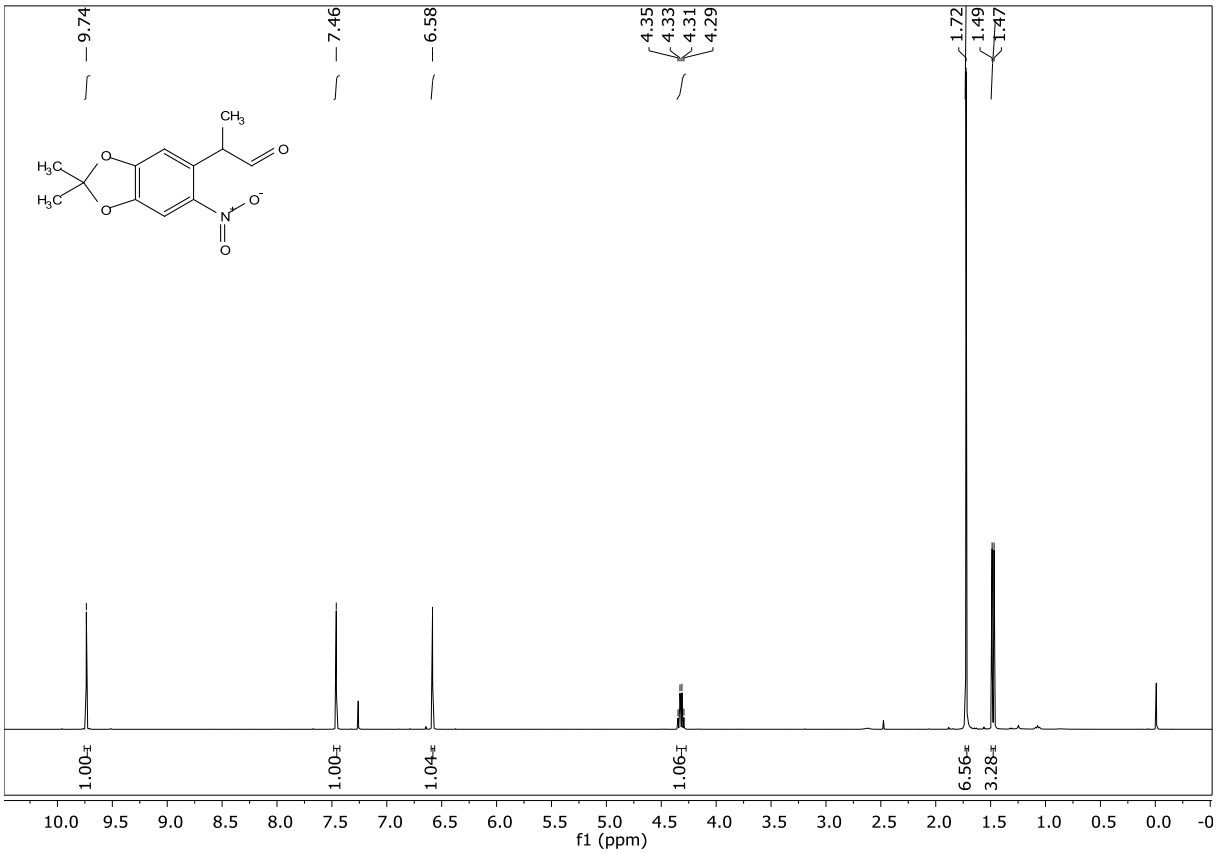

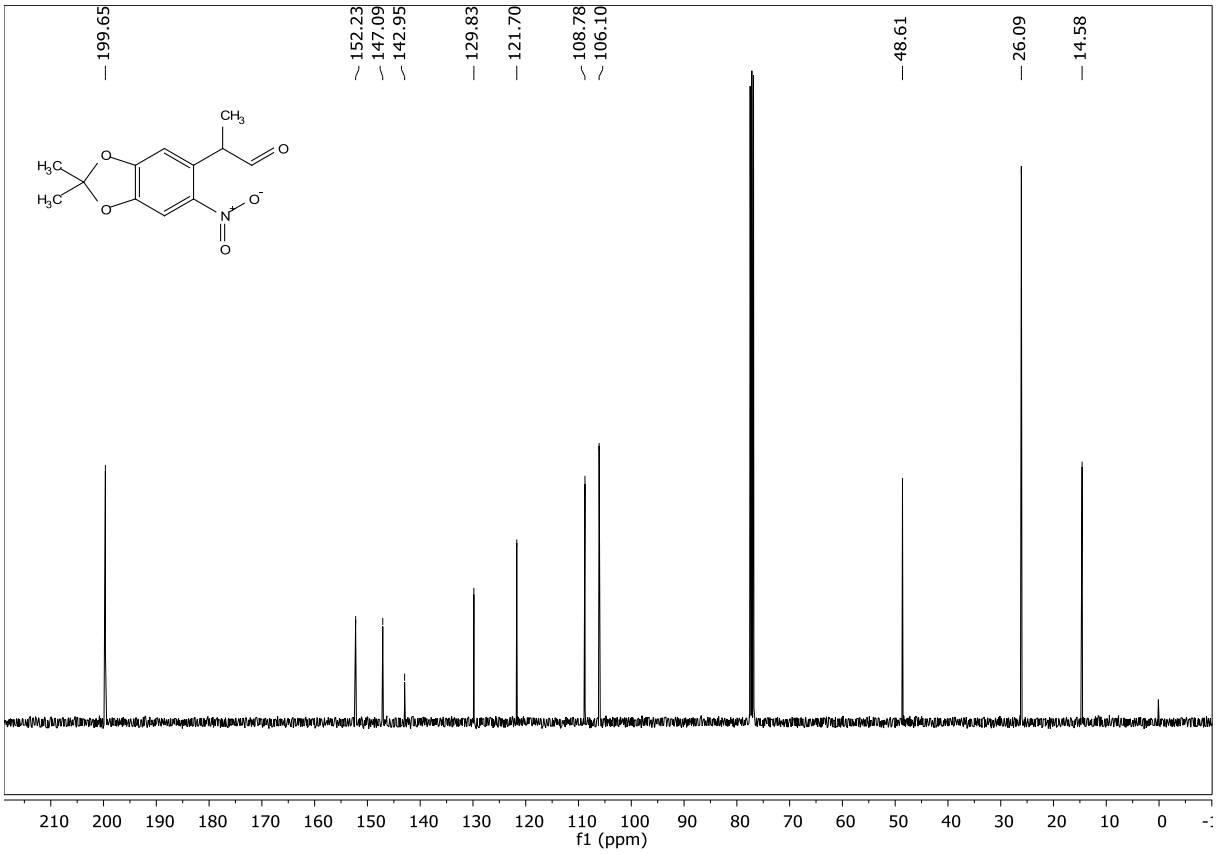

N-Benzyl-2-(2,2-dimethyl-6-nitrobenzo[*d*][1,3]dioxol-5-yl)propan-1-amine (**58**)

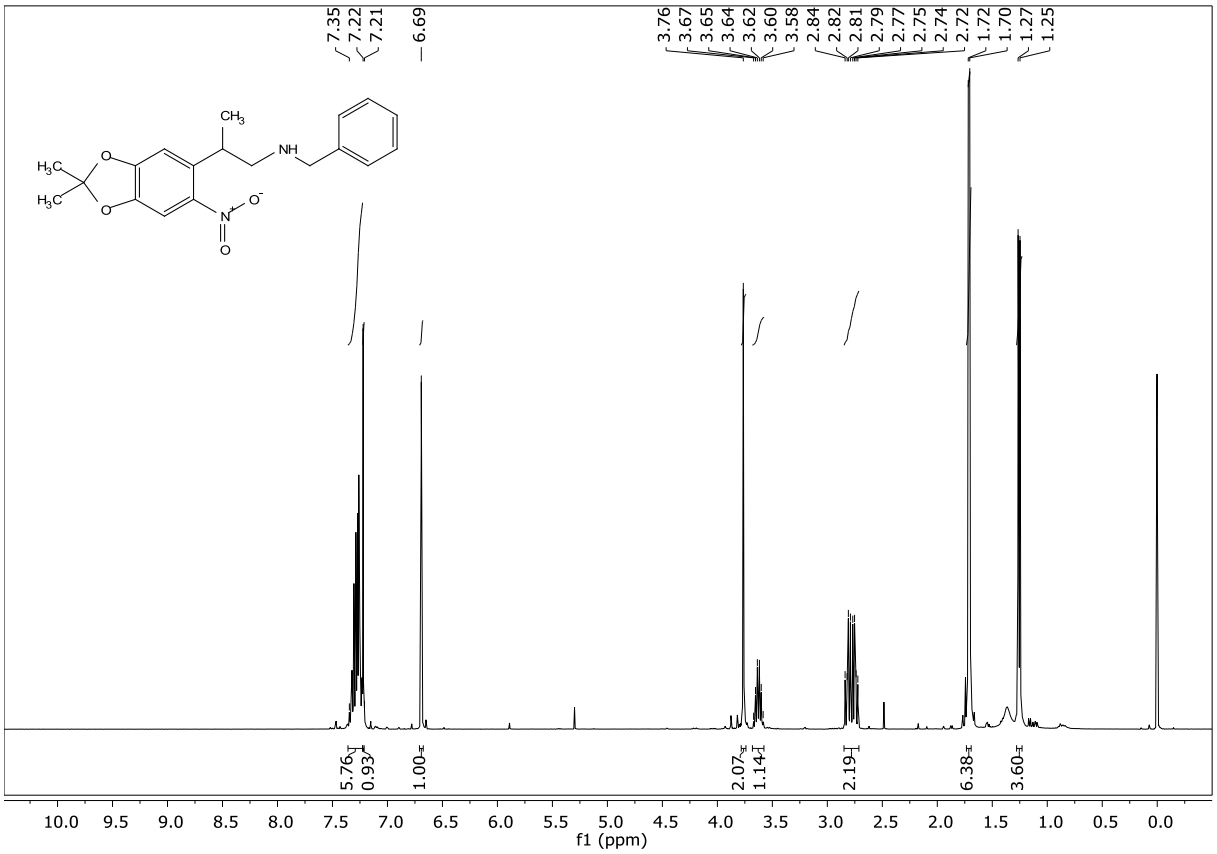

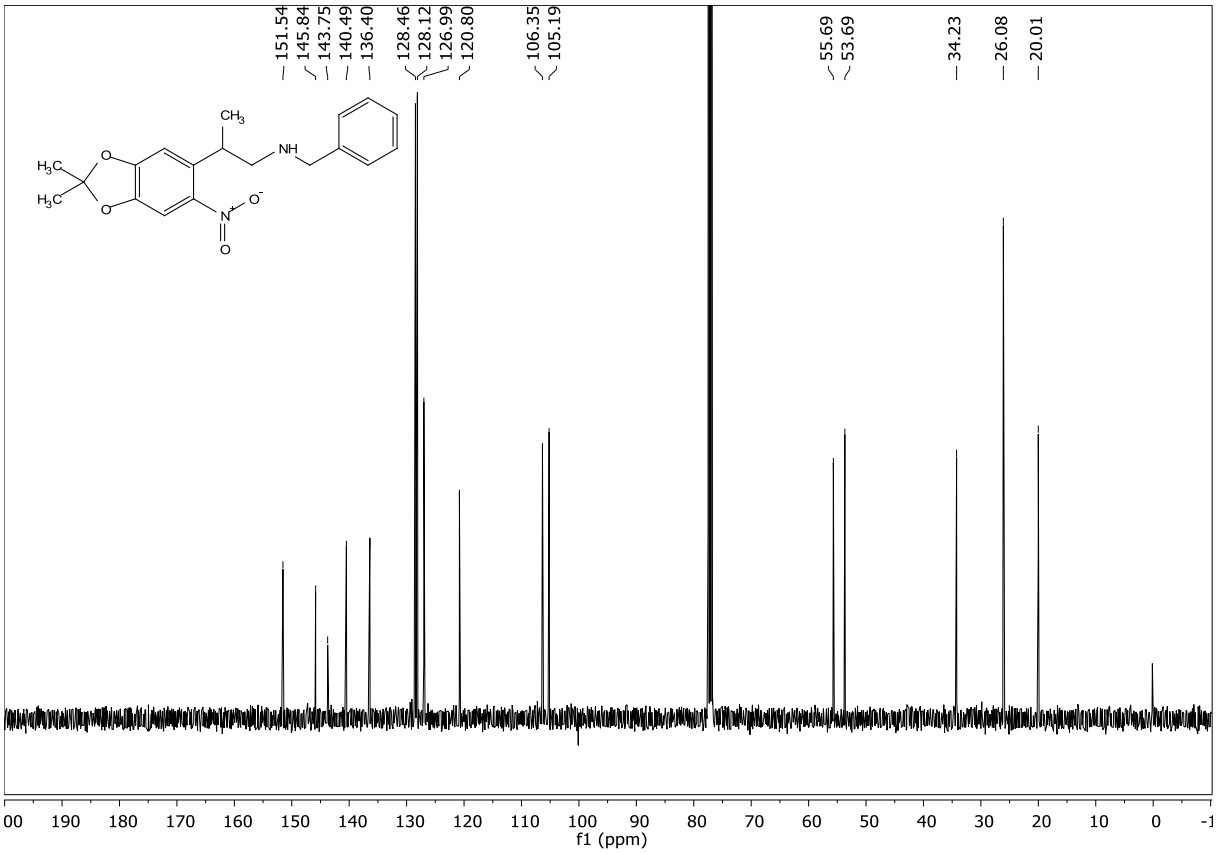

4-(1-(Benzylamino)propan-2-yl)-5-nitrobenzene-1,2-diol (**59**)

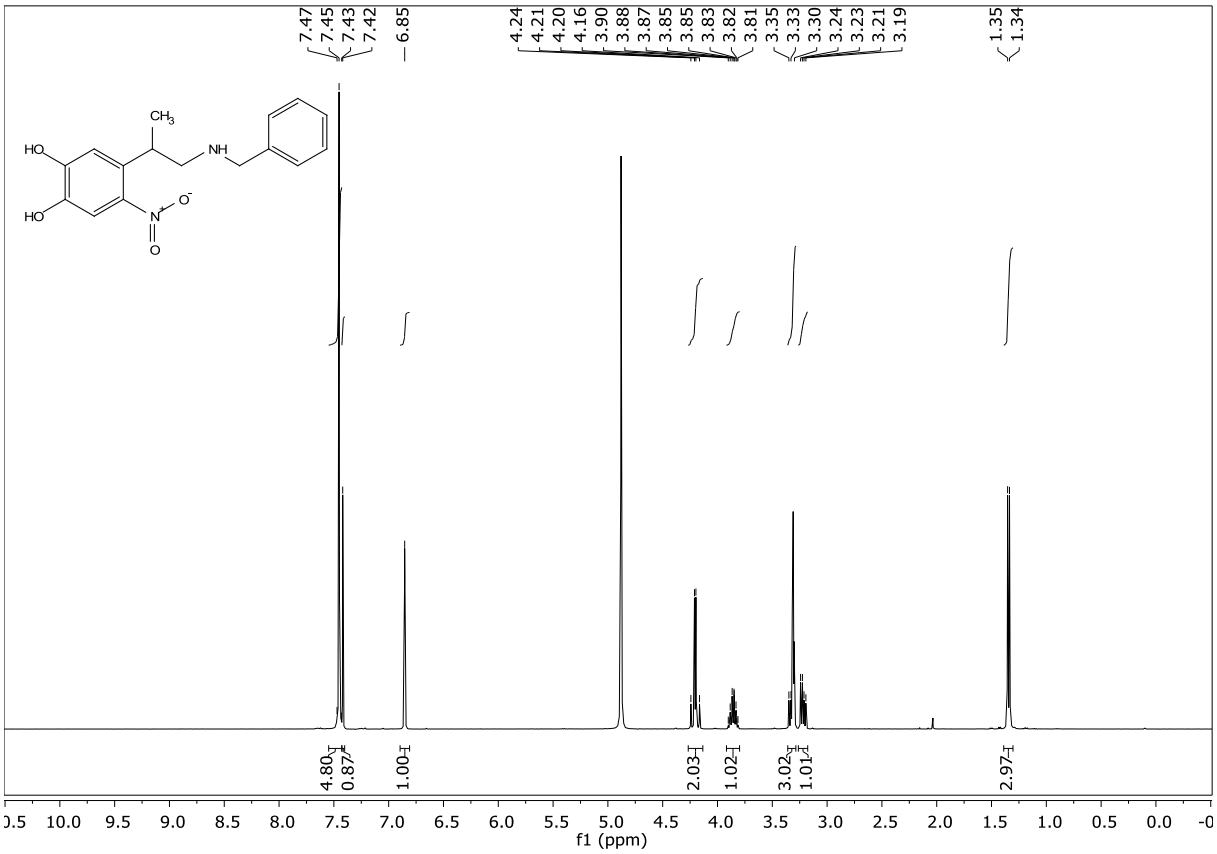

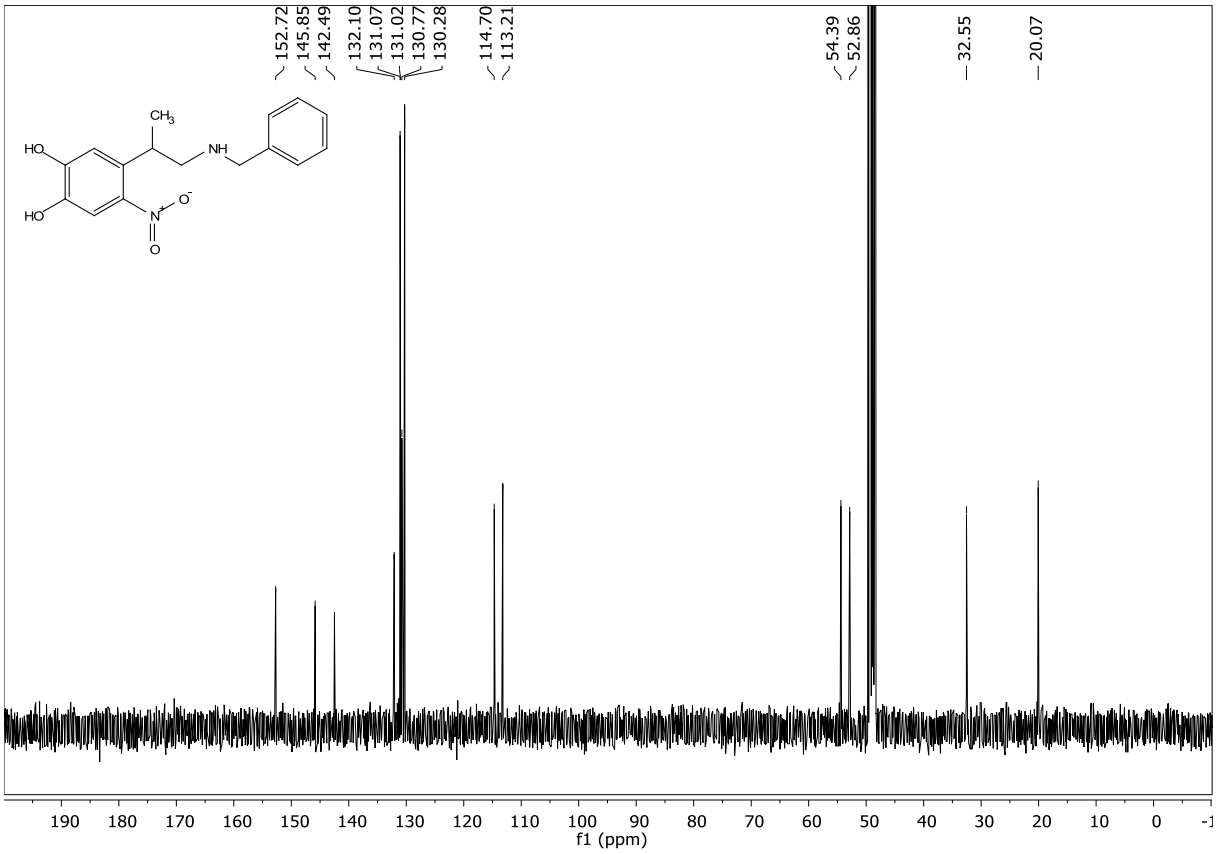

5-(1-Bromopropan-2-yl)-2,2-dimethyl-6-nitrobenzo[*d*][1,3]dioxole (**62**)

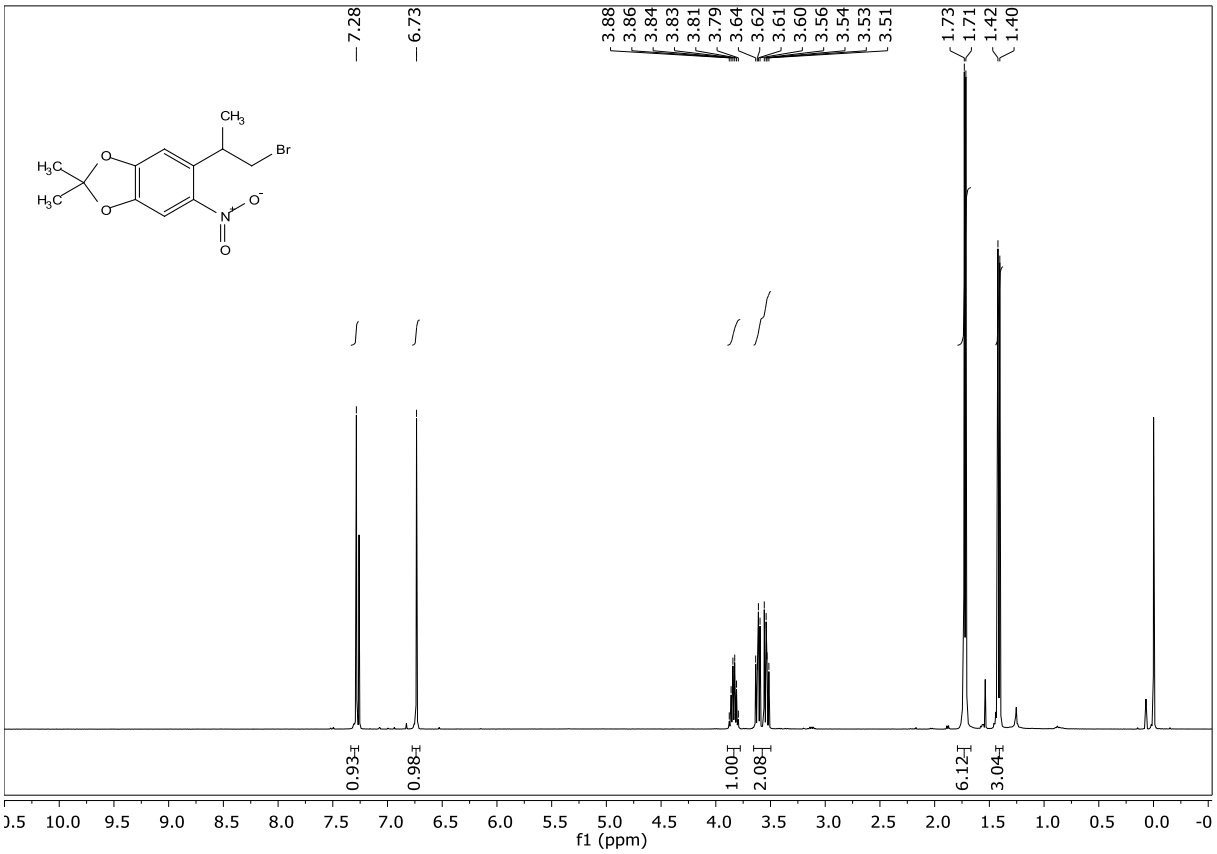

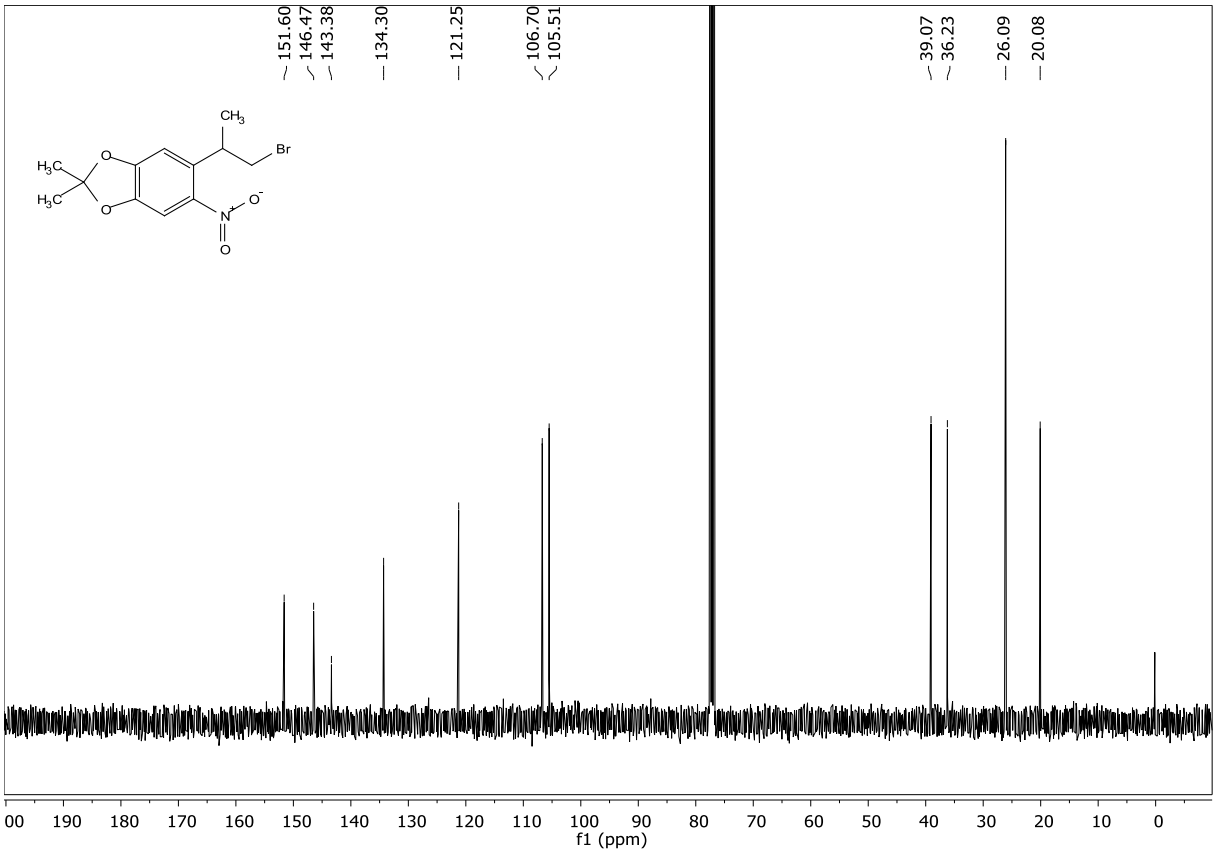

Benzyl (2-(2,2-dimethyl-6-nitrobenzo[*d*][1,3]dioxol-5-yl)propyl)carbonate (**65**)

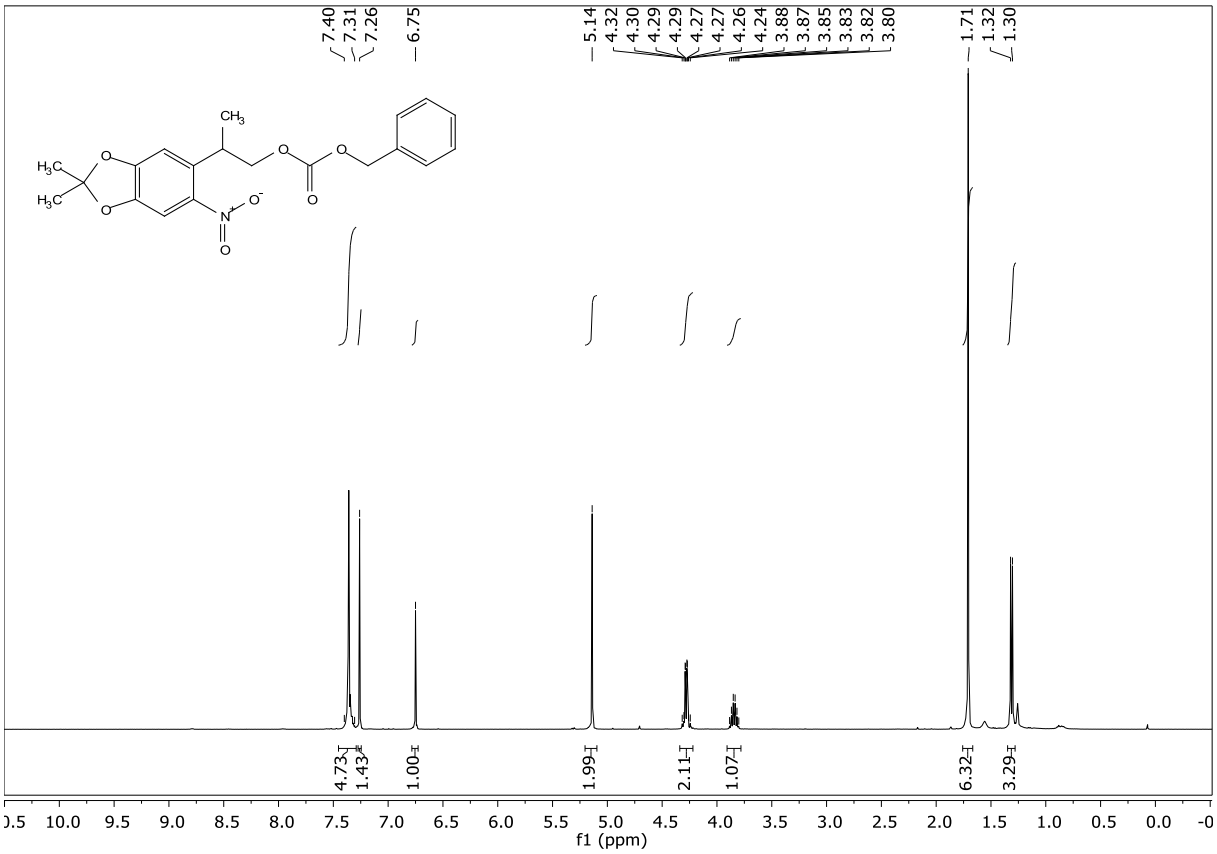

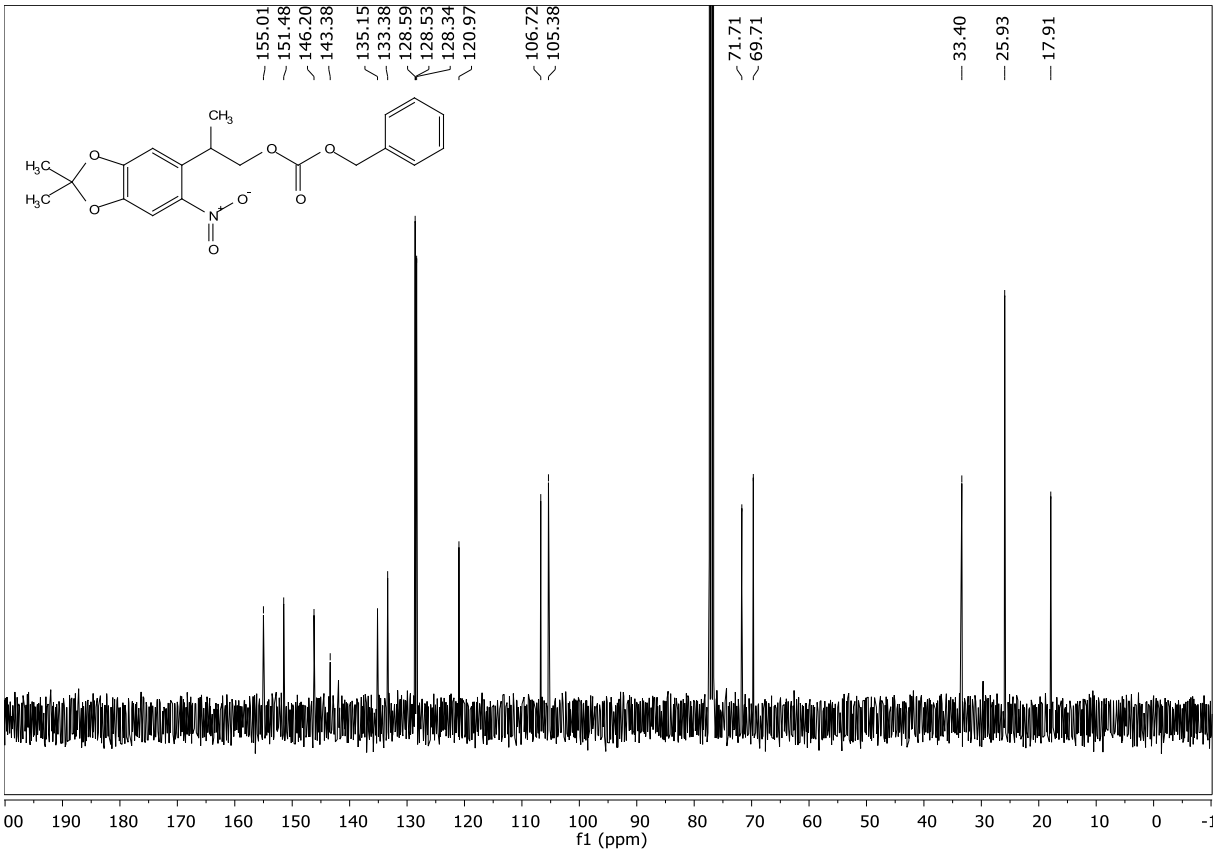

Benzyl (2-(4,5-dihydroxy-2-nitrophenyl)propyl) carbonate (**66**)

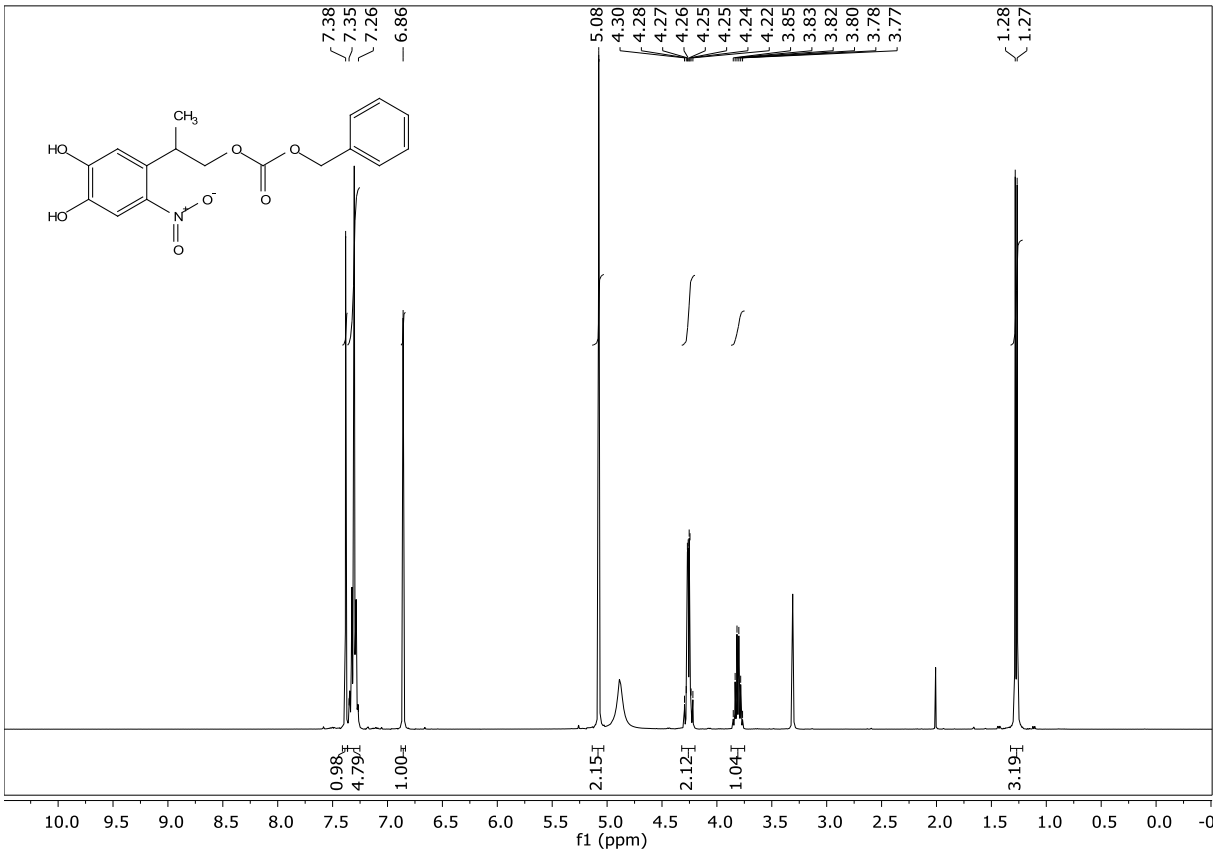

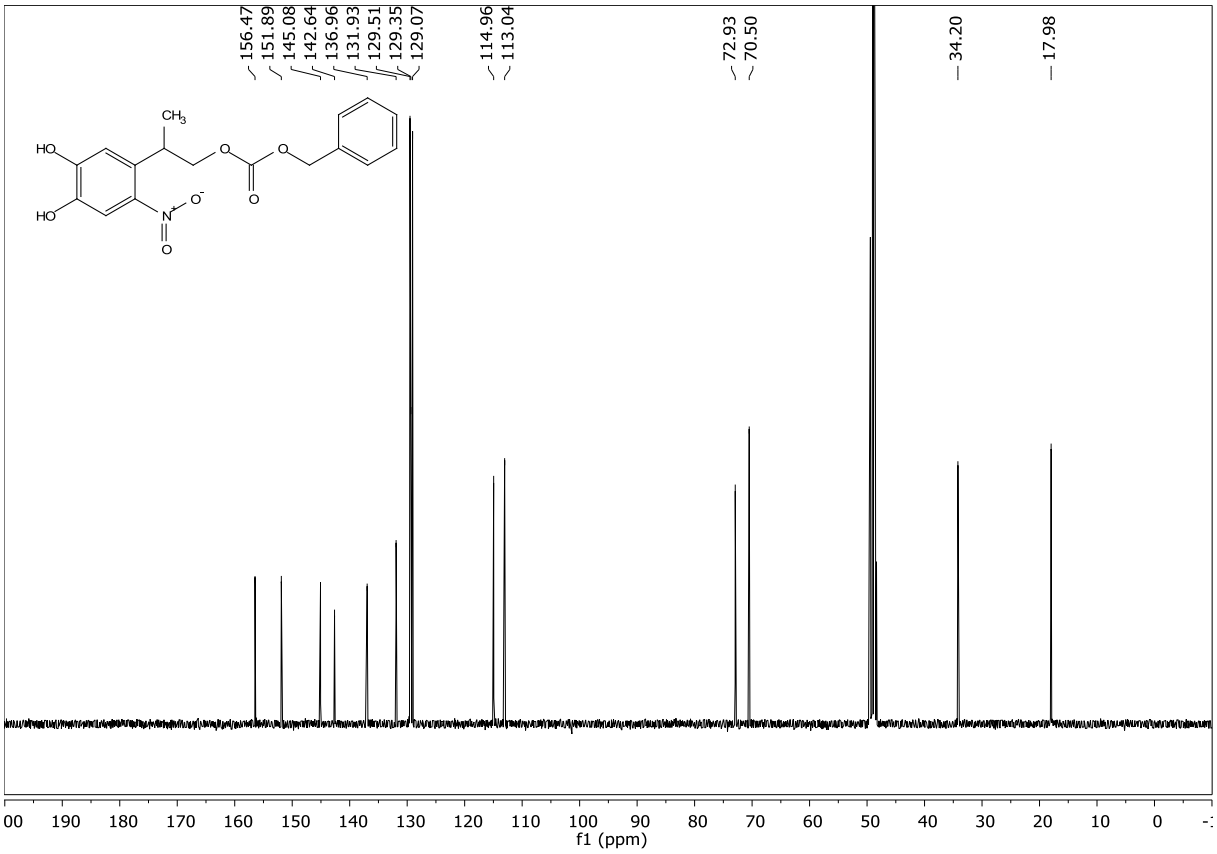

2-(2,2-Dimethyl-6-nitrobenzo[*d*][1,3]dioxol-5-yl)propyl benzylcarbamate (**67**)

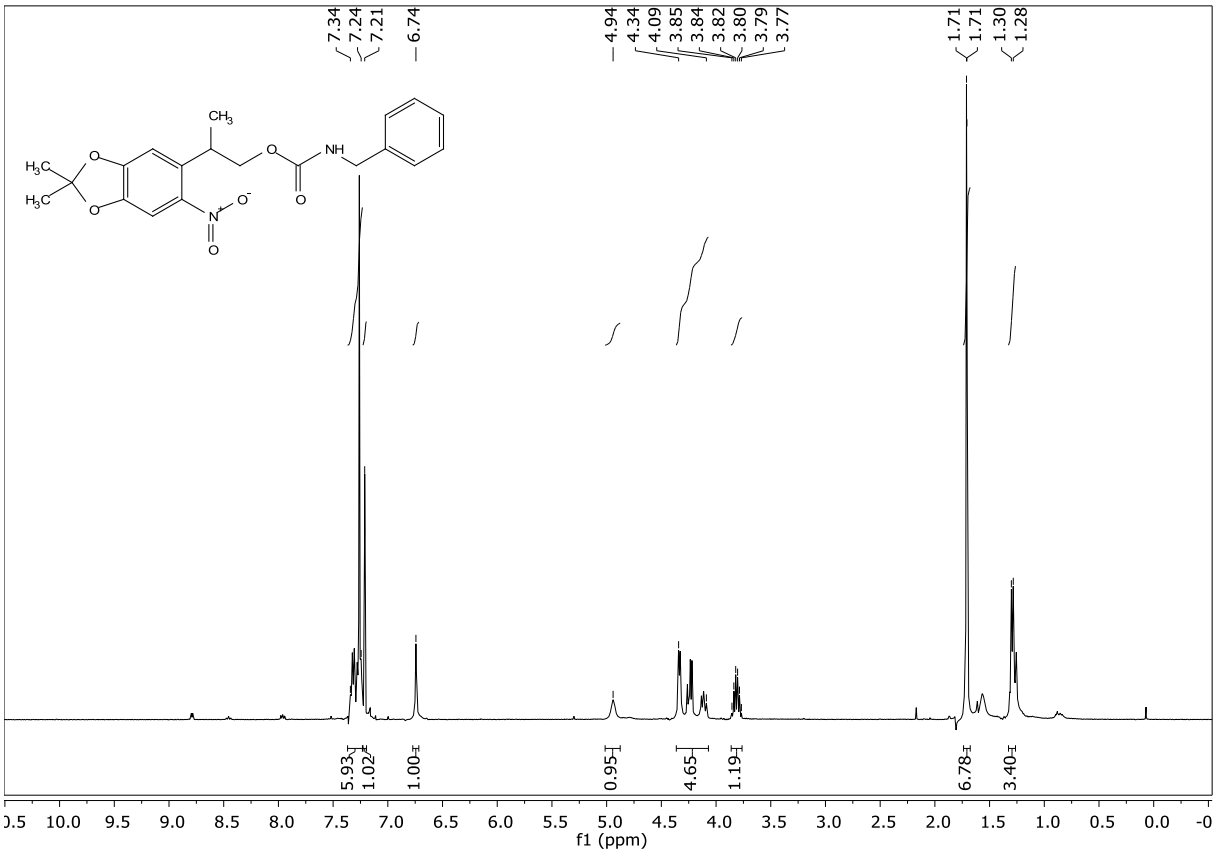

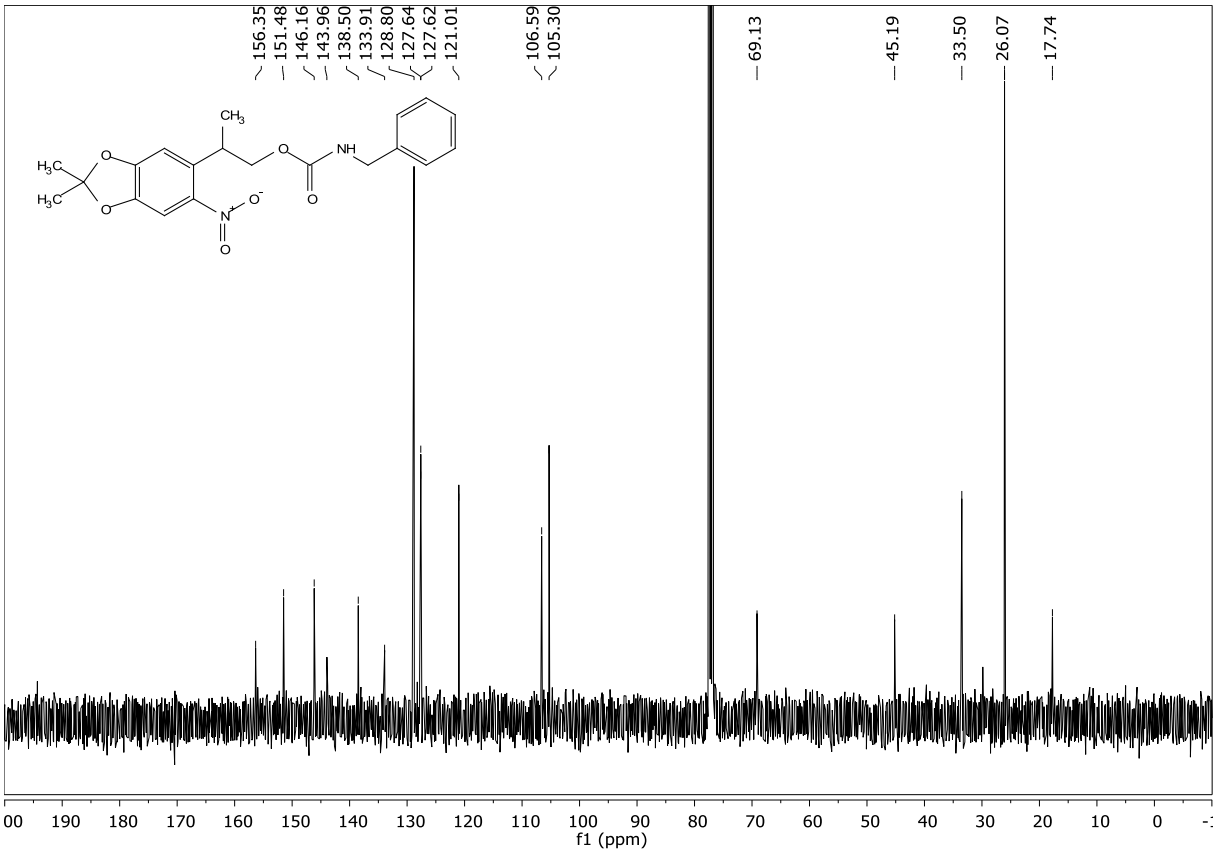

2-(4,5-Dihydroxy-2-nitrophenyl)propyl benzylcarbamate (**68**)

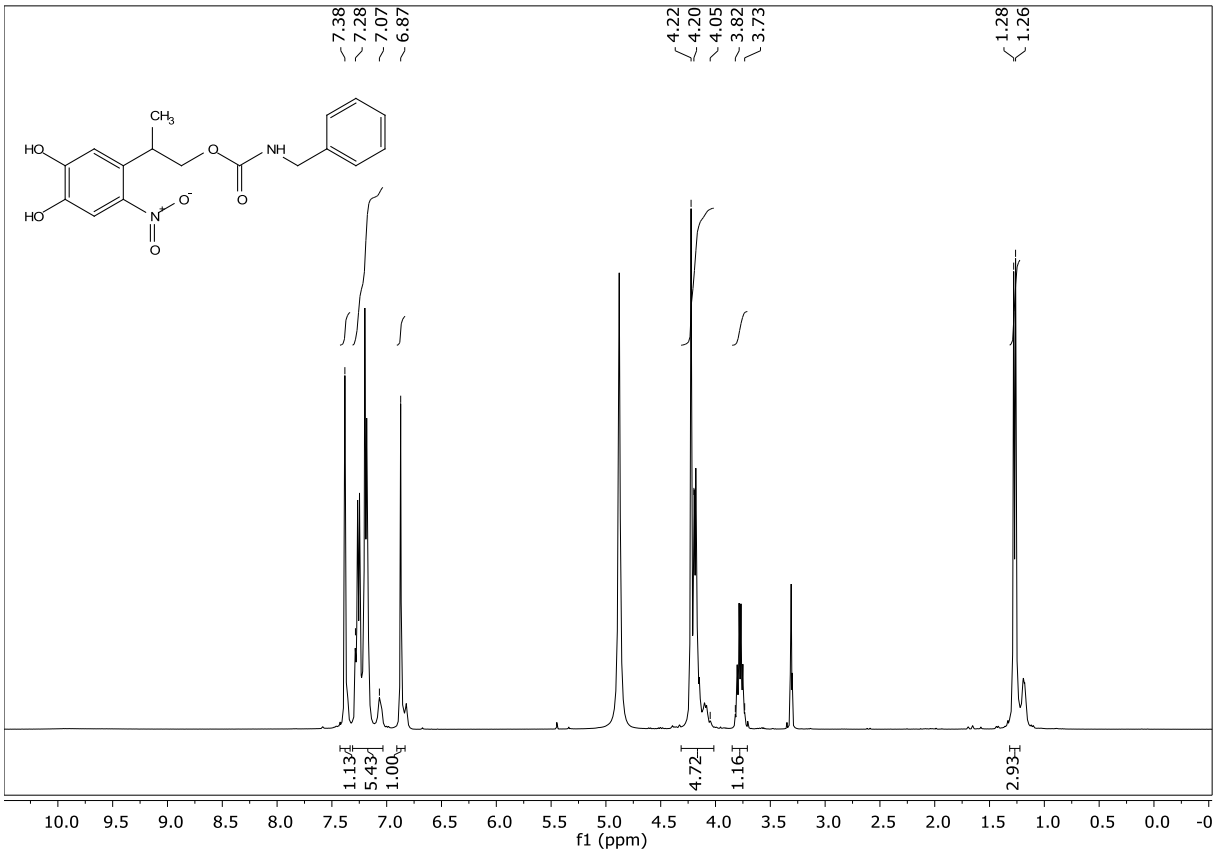

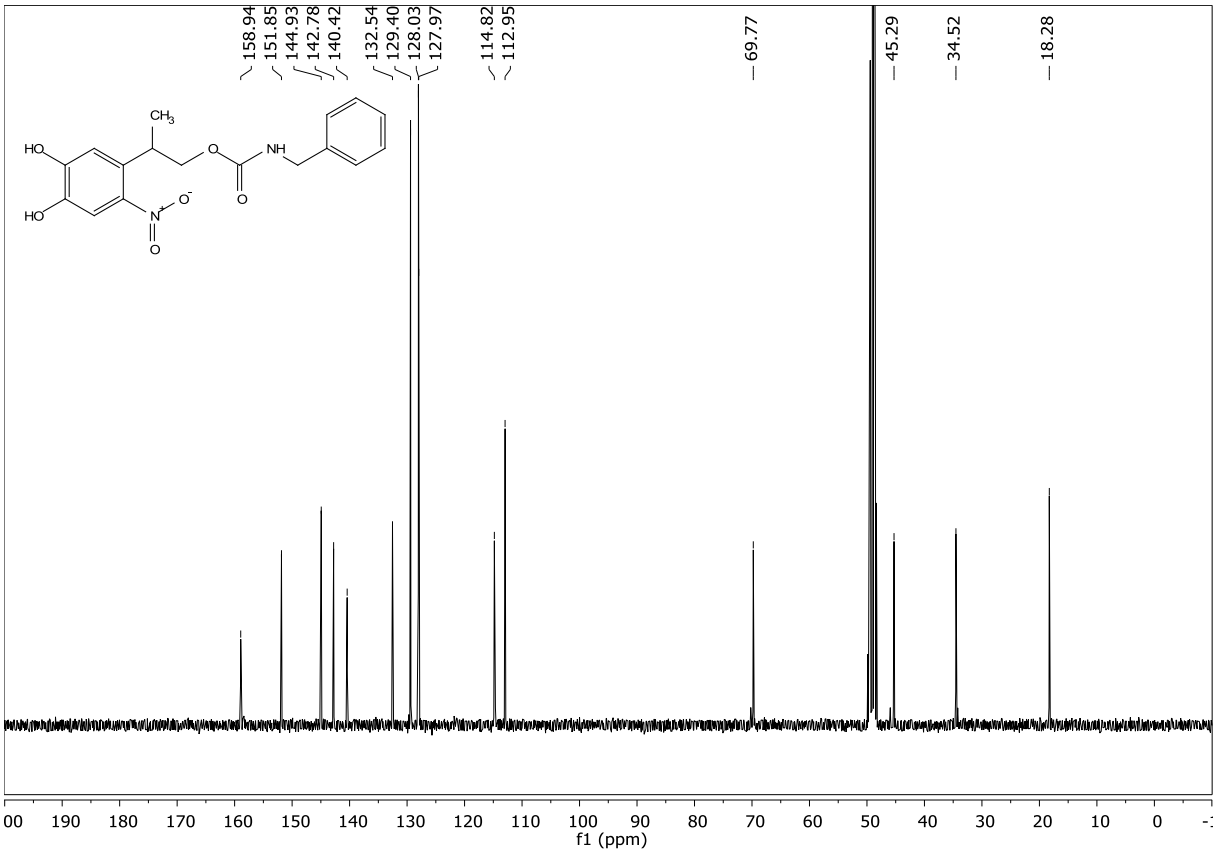

2-(2,2-Dimethyl-6-nitrobenzo[*d*][1,3]dioxol-5-yl)propyl 2-phenylacetate (**69**)

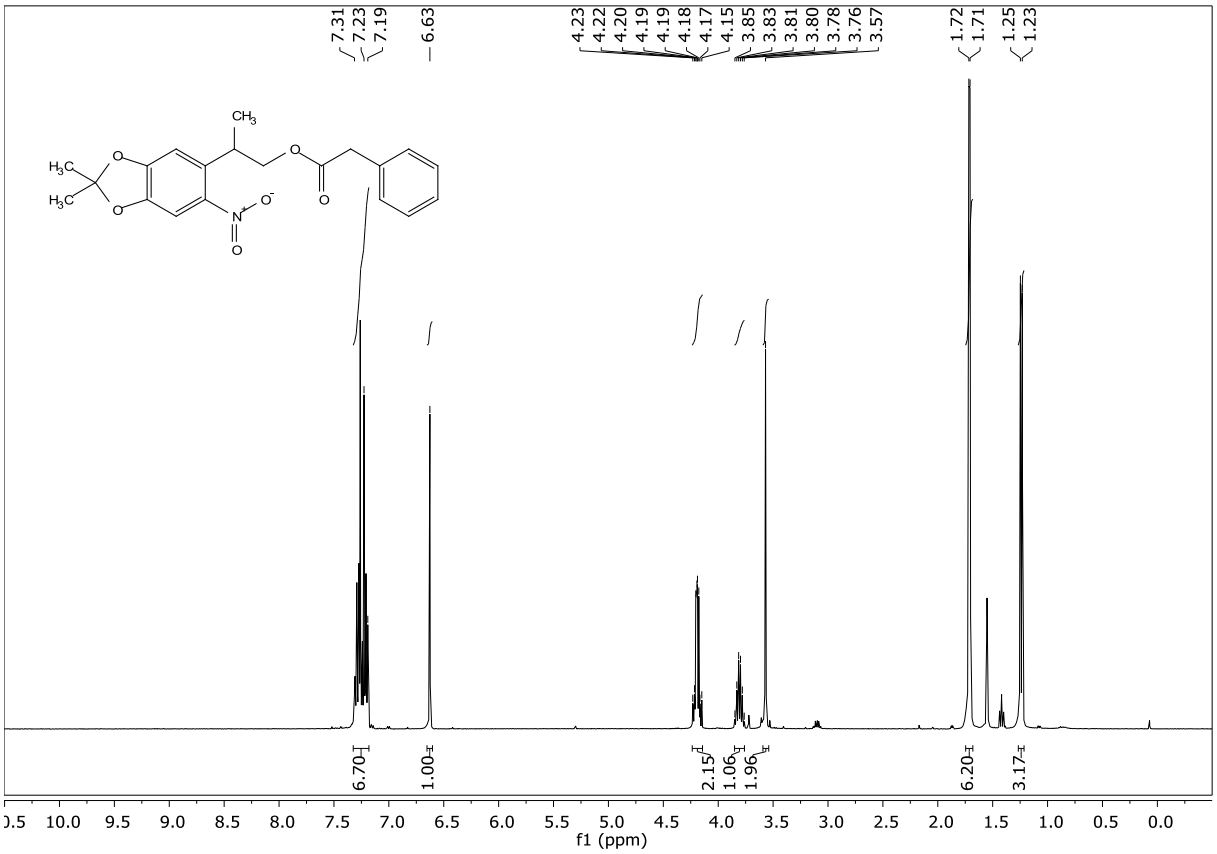

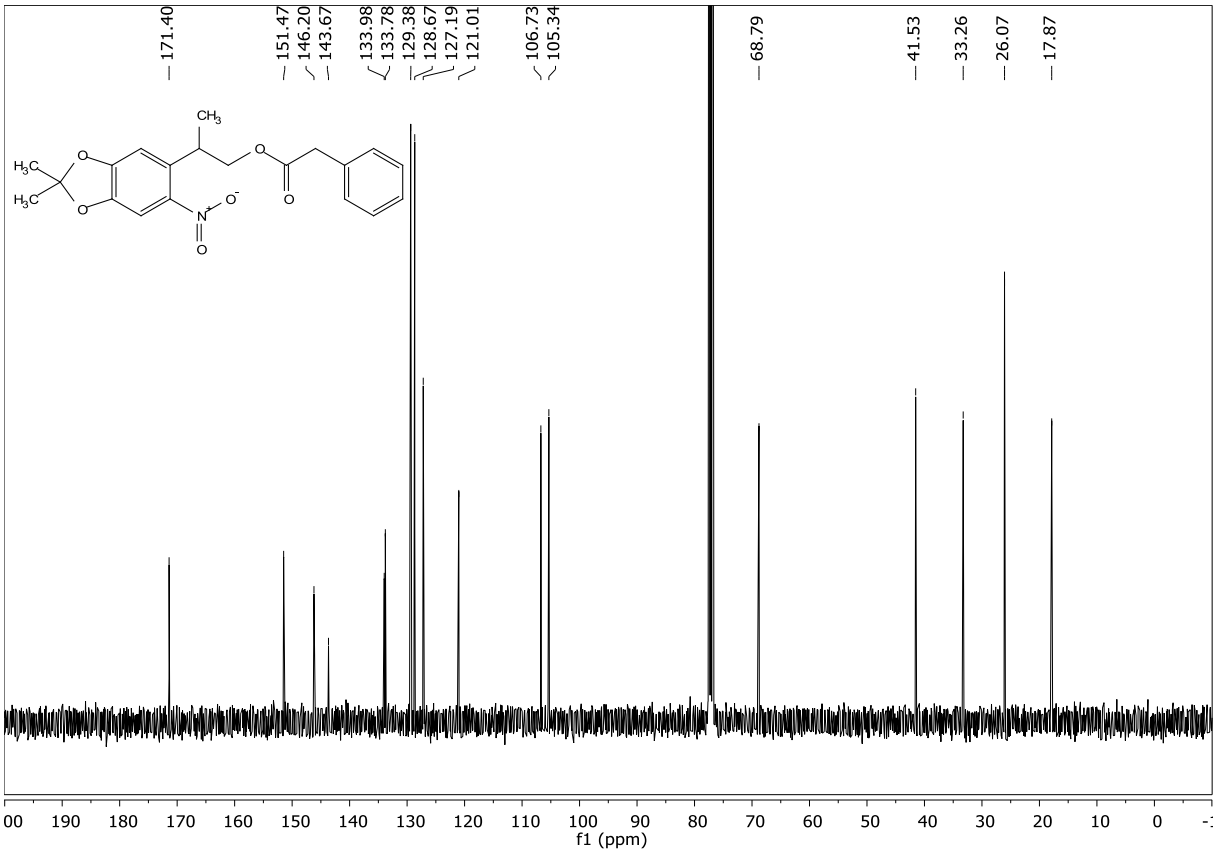

2-(2,2-Dimethyl-6-nitrobenzo[*d*][1,3]dioxol-5-yl)propyl 2,2-diphenylacetate (**71**)

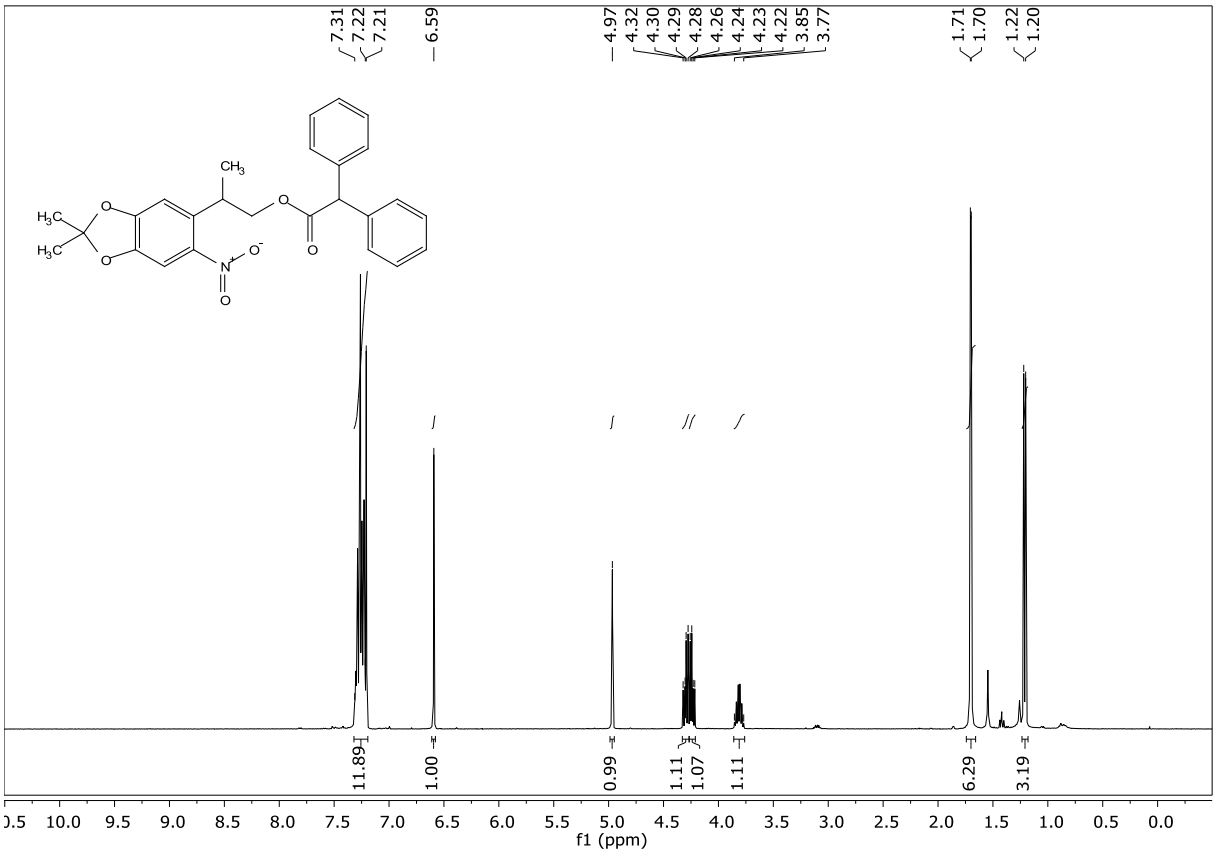

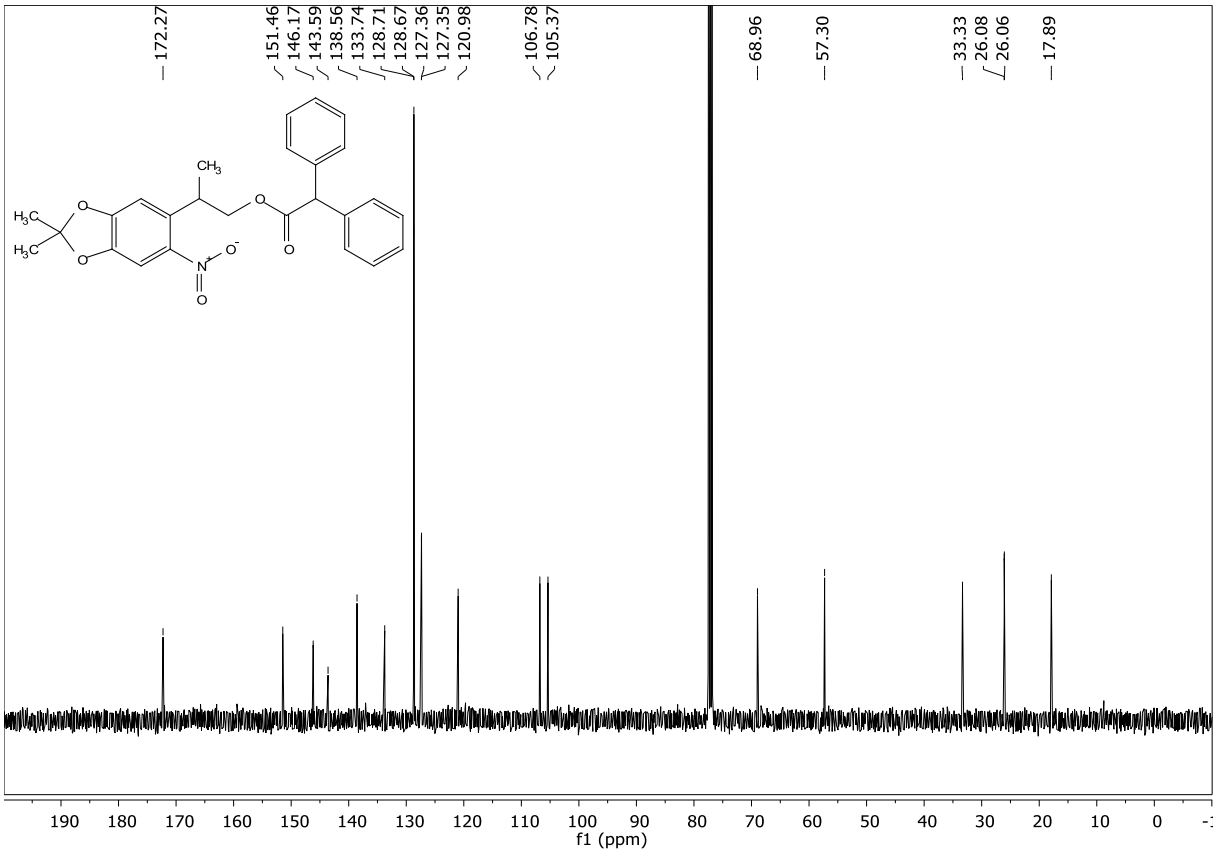

2-(4,5-Dihydroxy-2-nitrophenyl)propyl 2,2-diphenylacetate (**72**)

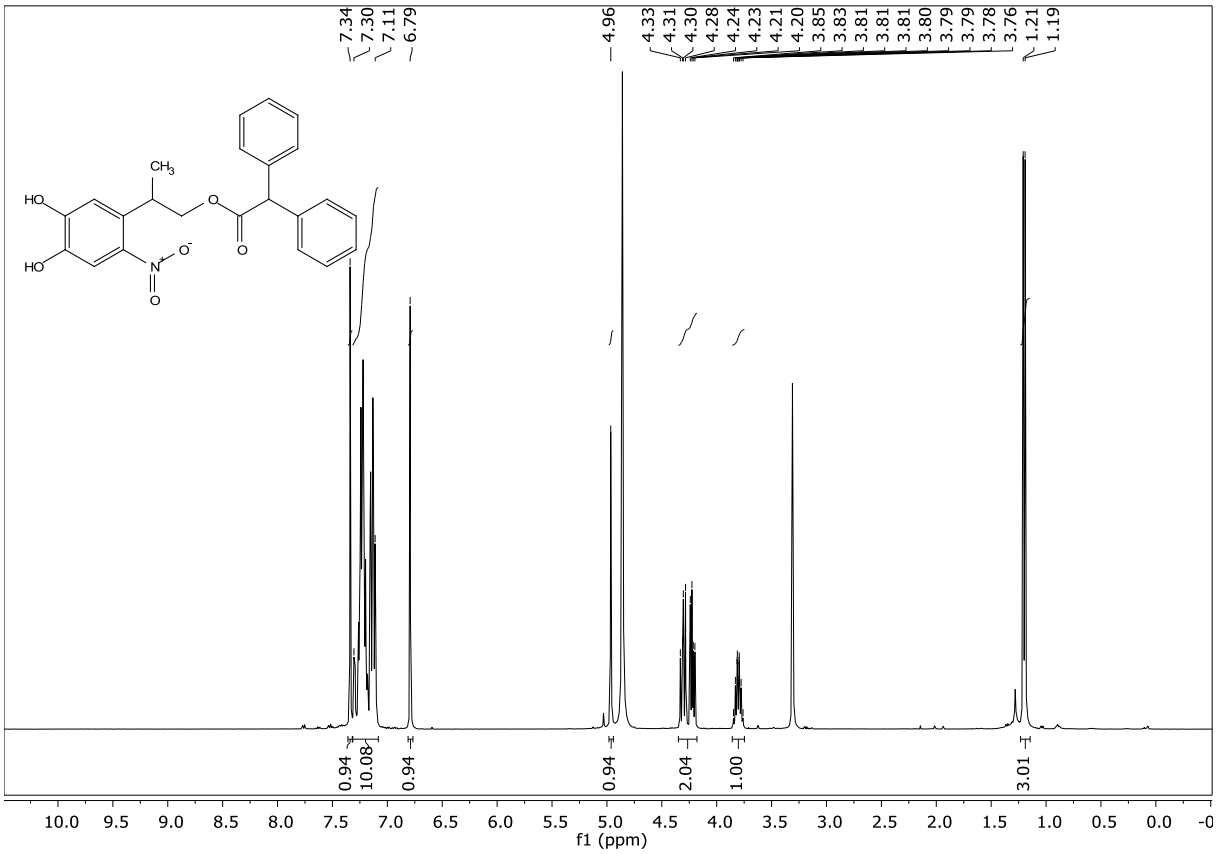

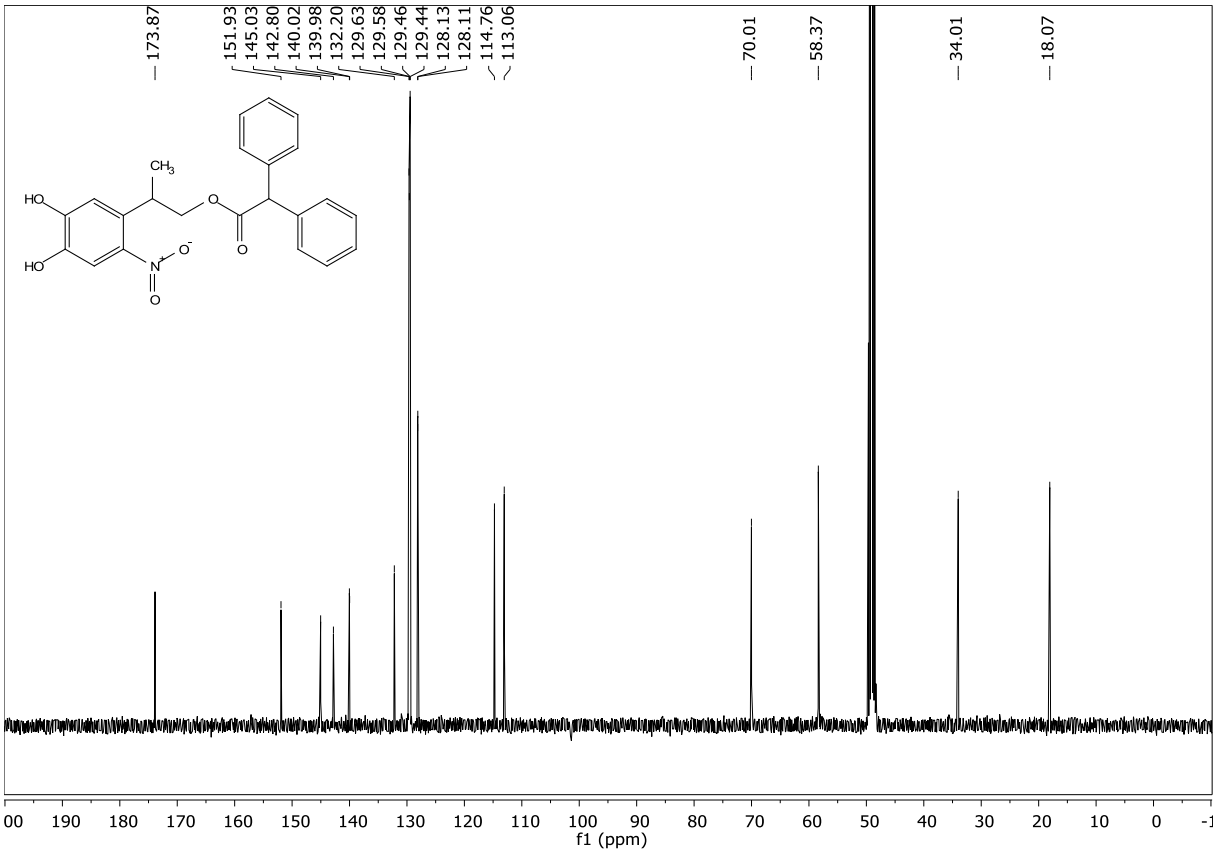

5-Bromo-6-ethyl-2,2-dimethylbenzo[d][1,3]dioxole (**86**)

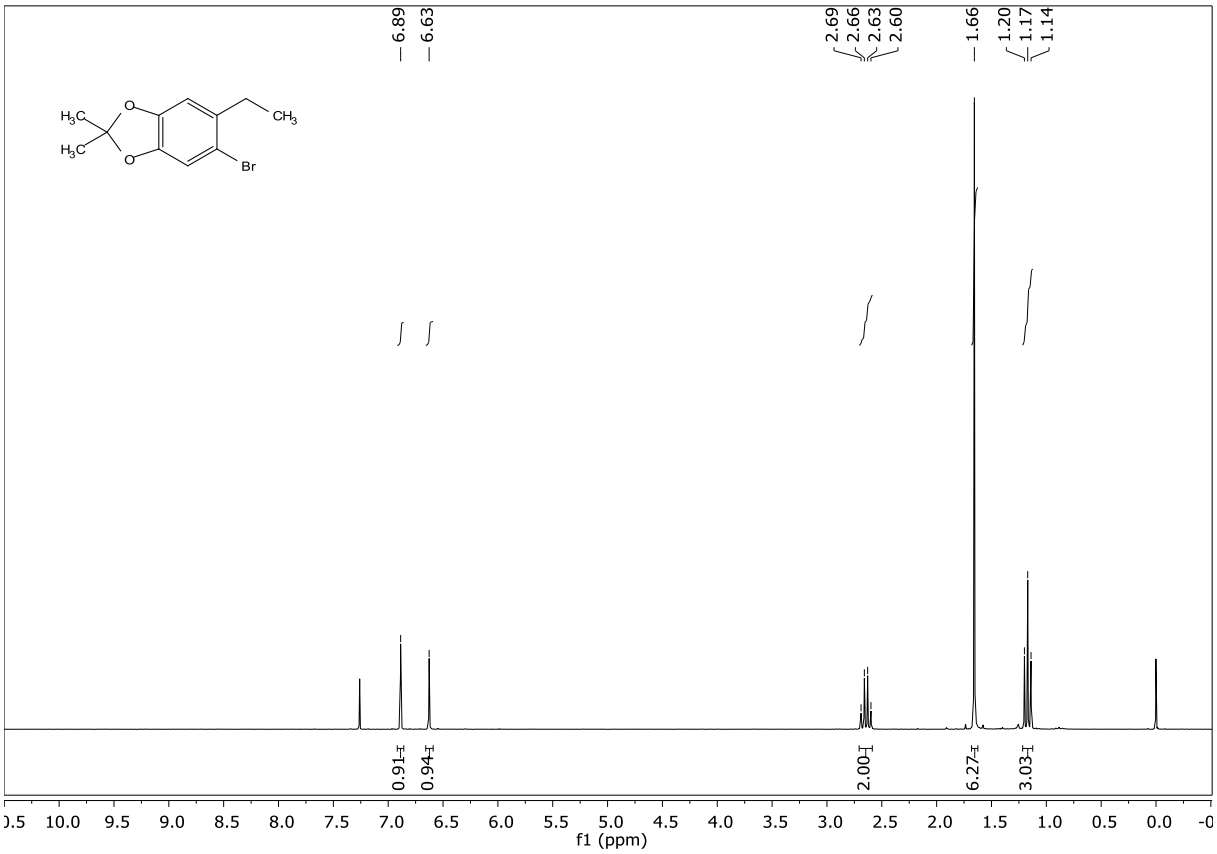

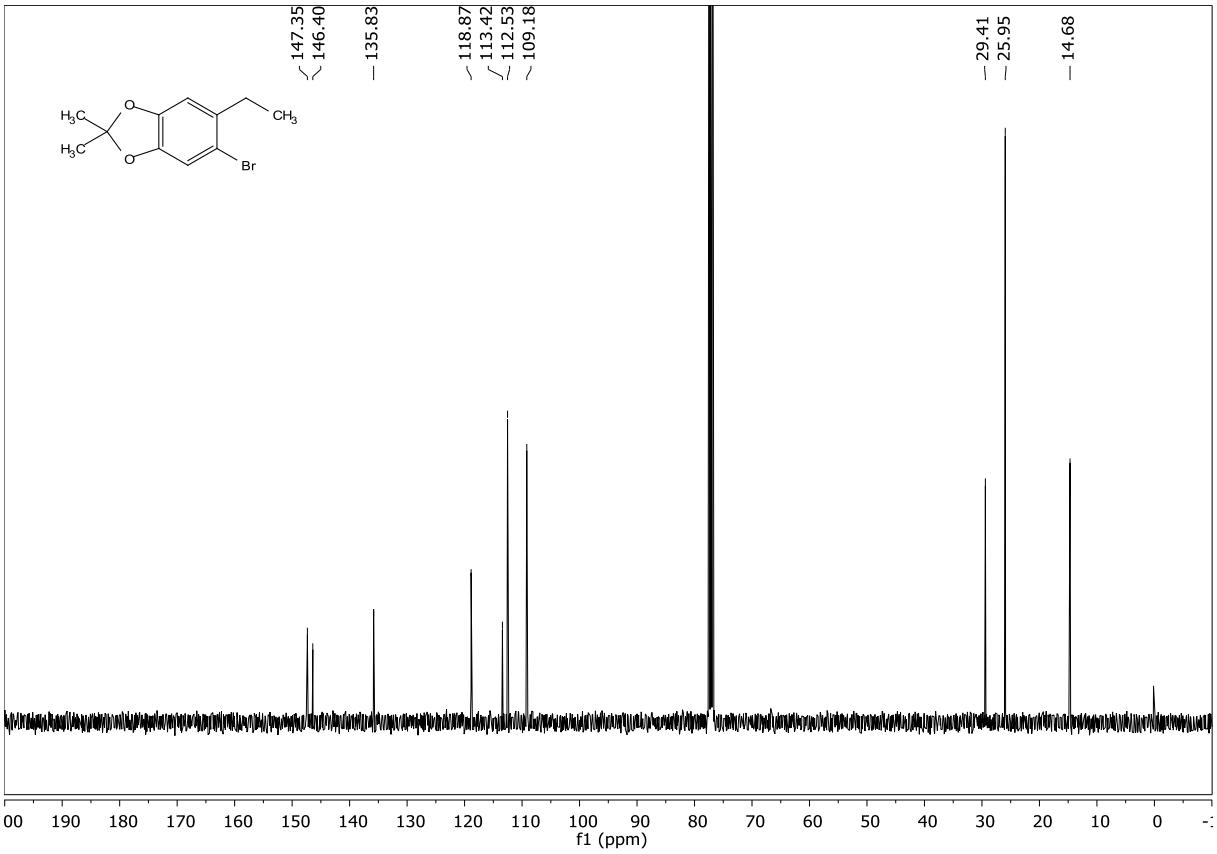

Methyl 2-(6-chloro-2,2-dimethylbenzo[*d*][1,3]dioxol-5-yl)acetate (**97**)

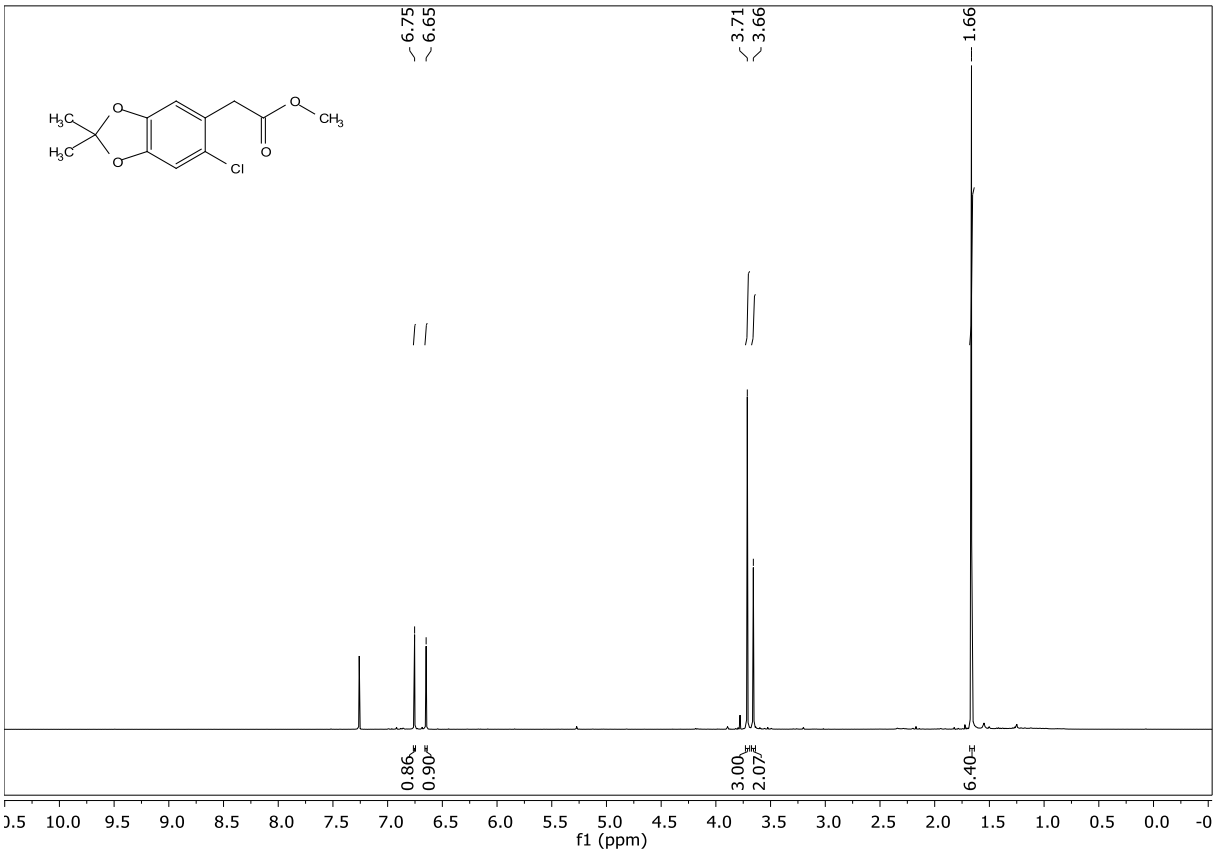

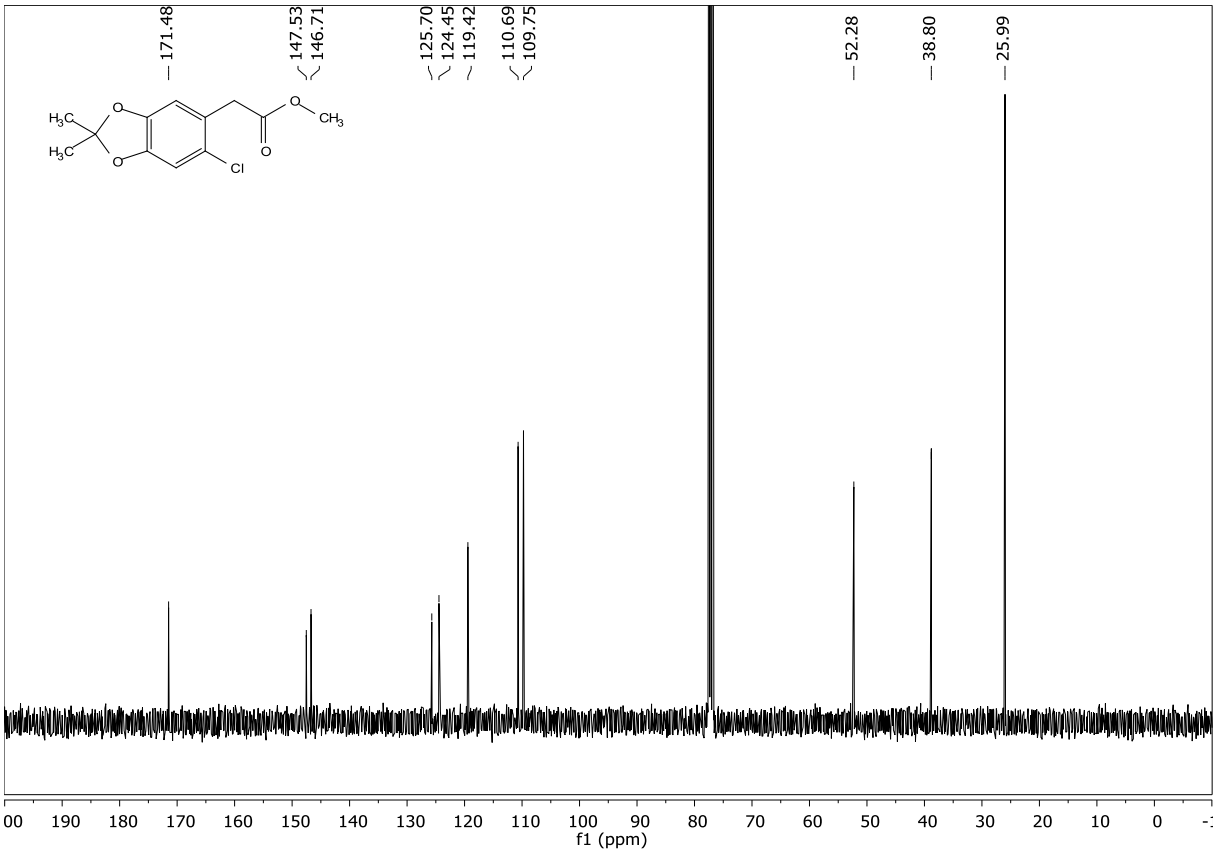

Methyl 2-(6-bromo-2,2-dimethylbenzo[*d*][1,3]dioxol-5-yl)acetate (**98**)

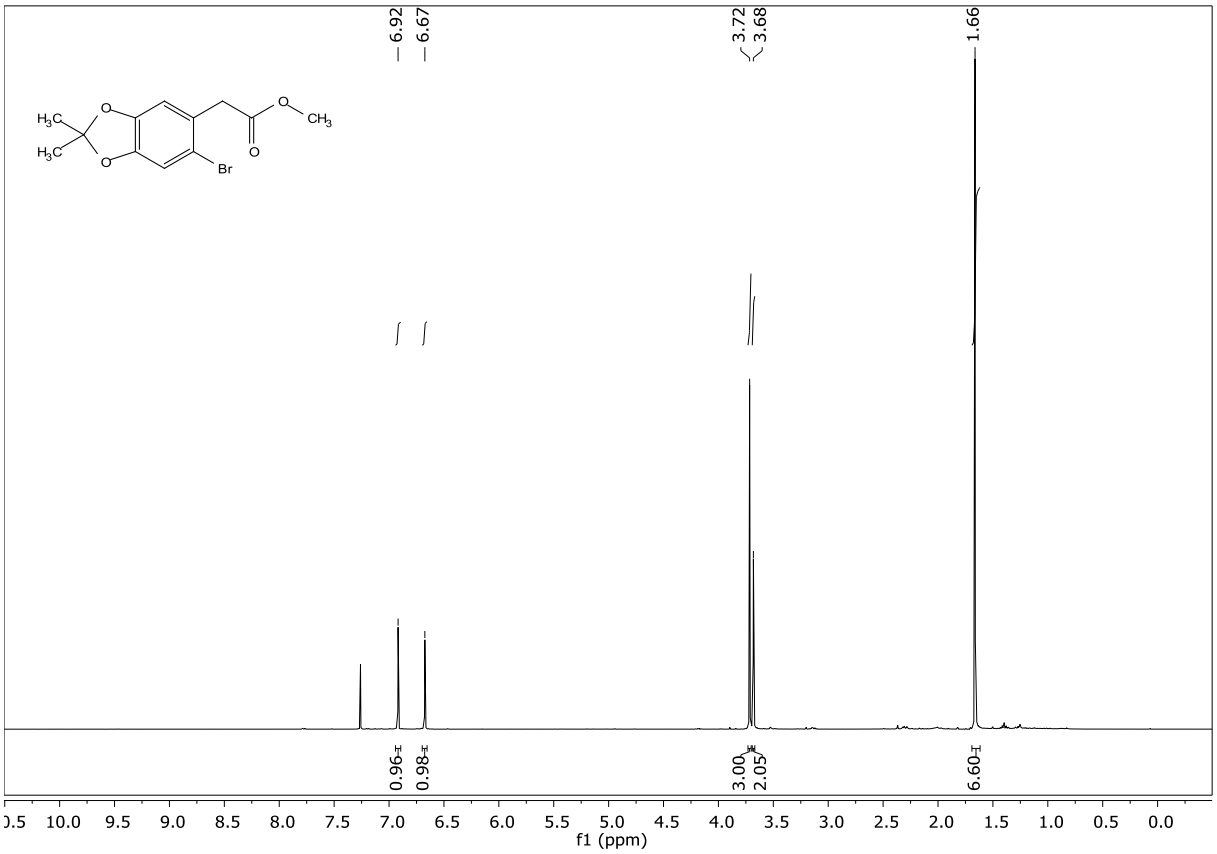

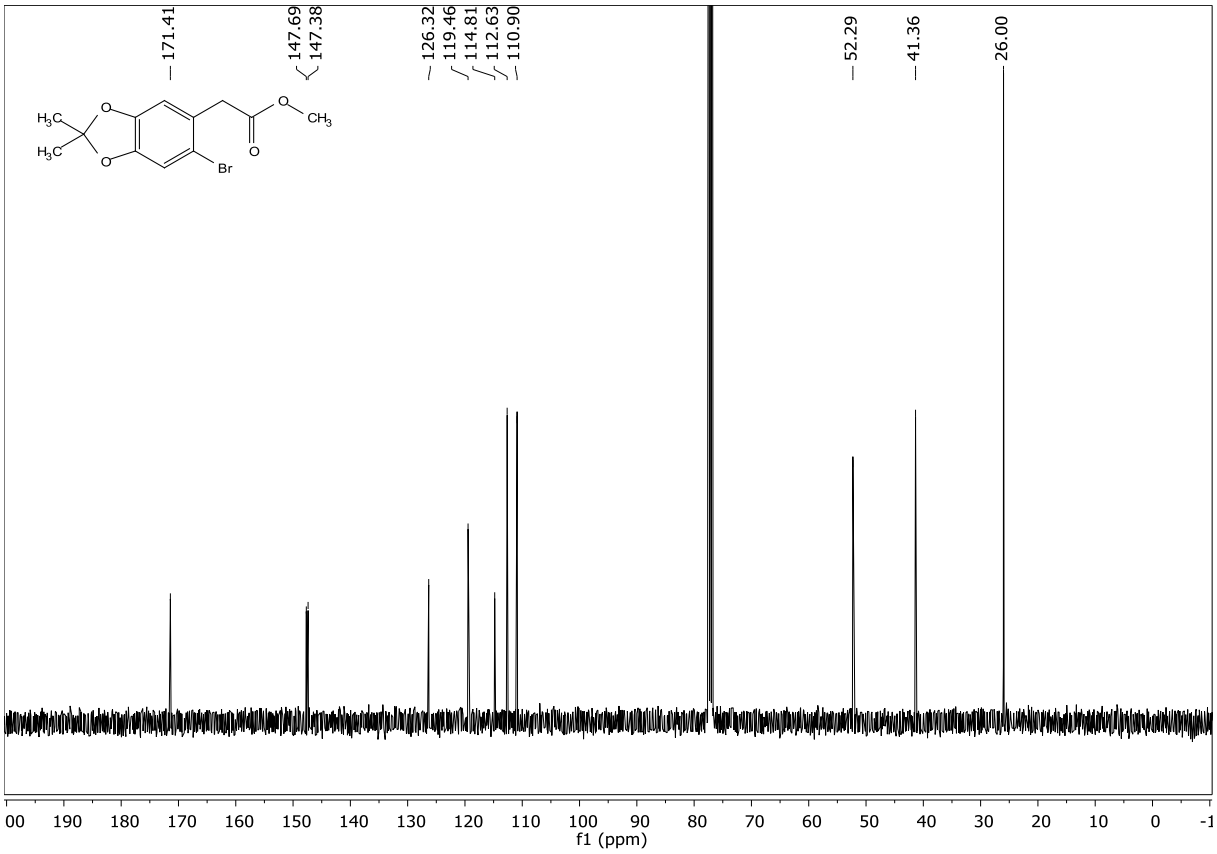

Methyl 2-(6-iodo-2,2-dimethylbenzo[*d*][1,3]dioxol-5-yl)acetate (**99**)

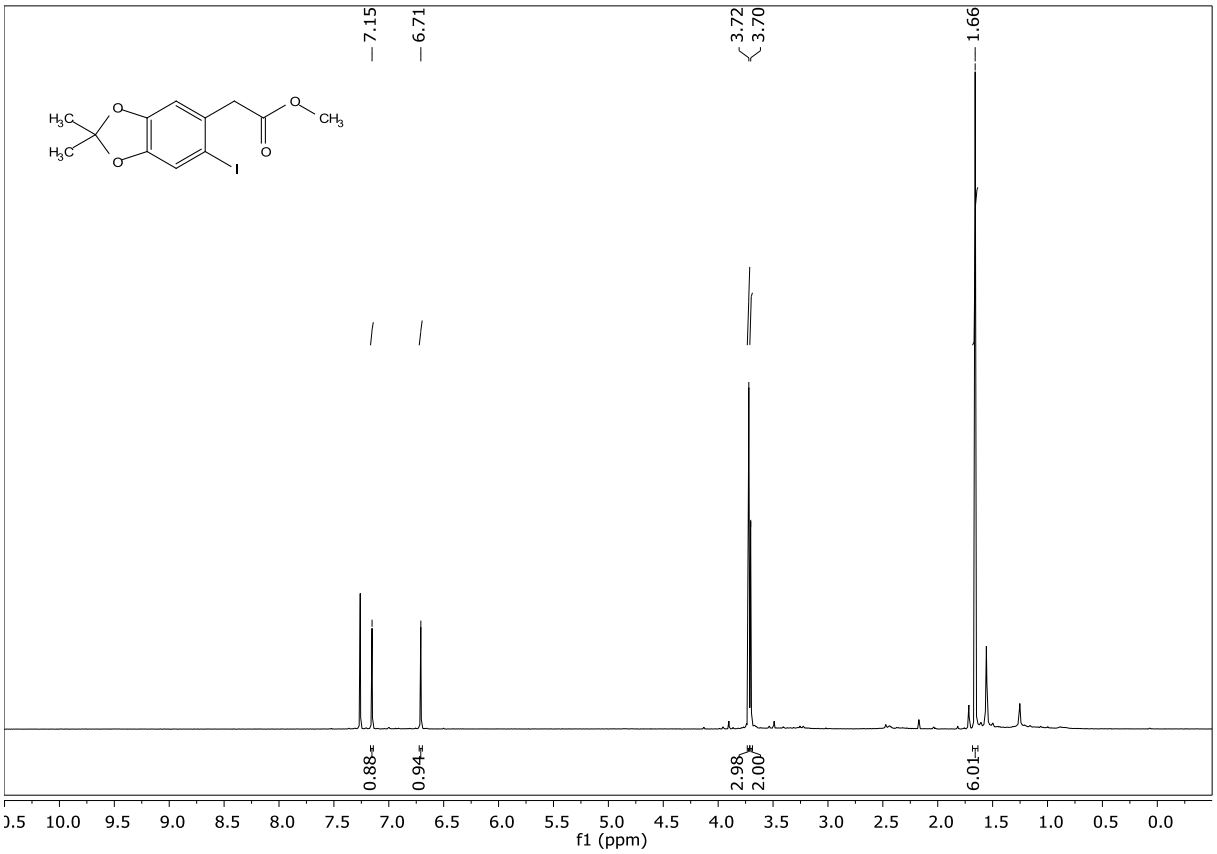

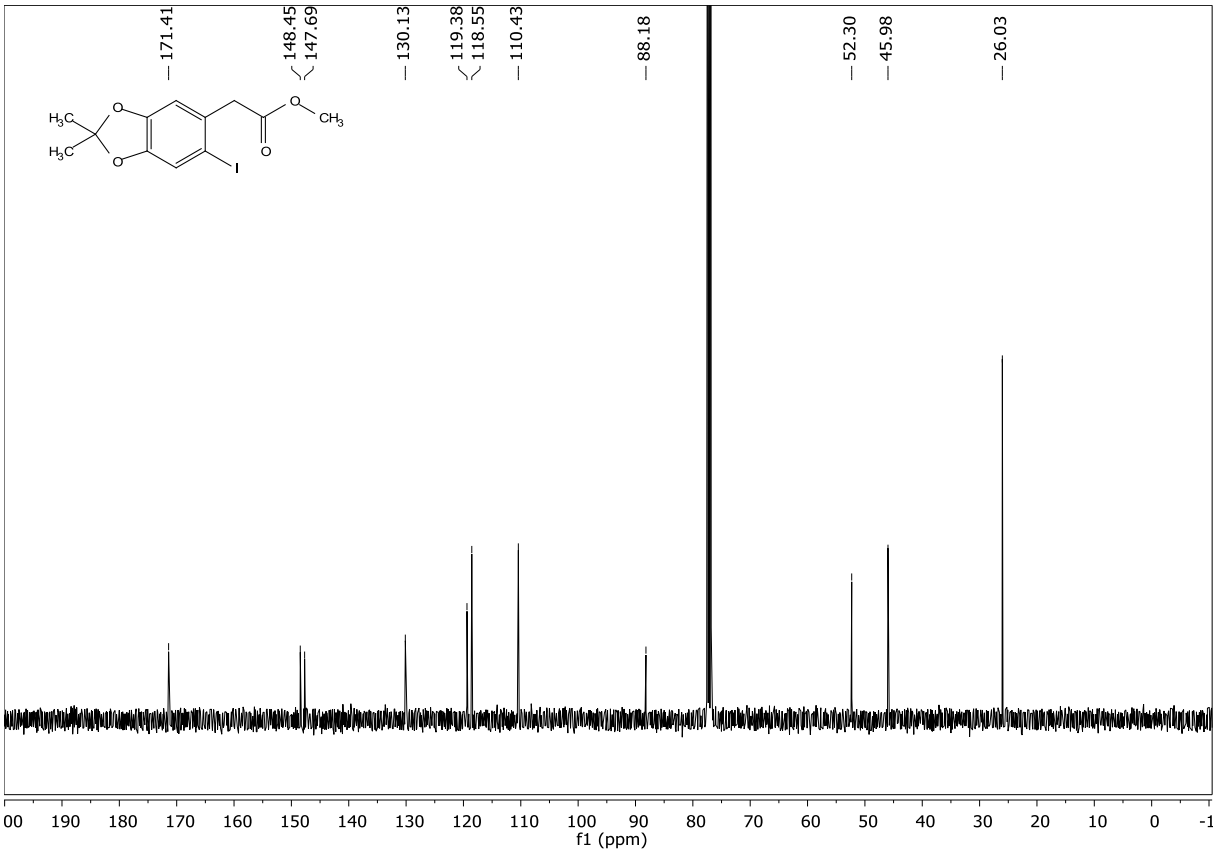

Methyl 2-(2,2-dimethyl-6-(trifluoromethyl)benzo[*d*][1,3]dioxol-5-yl)acetate (**100**)

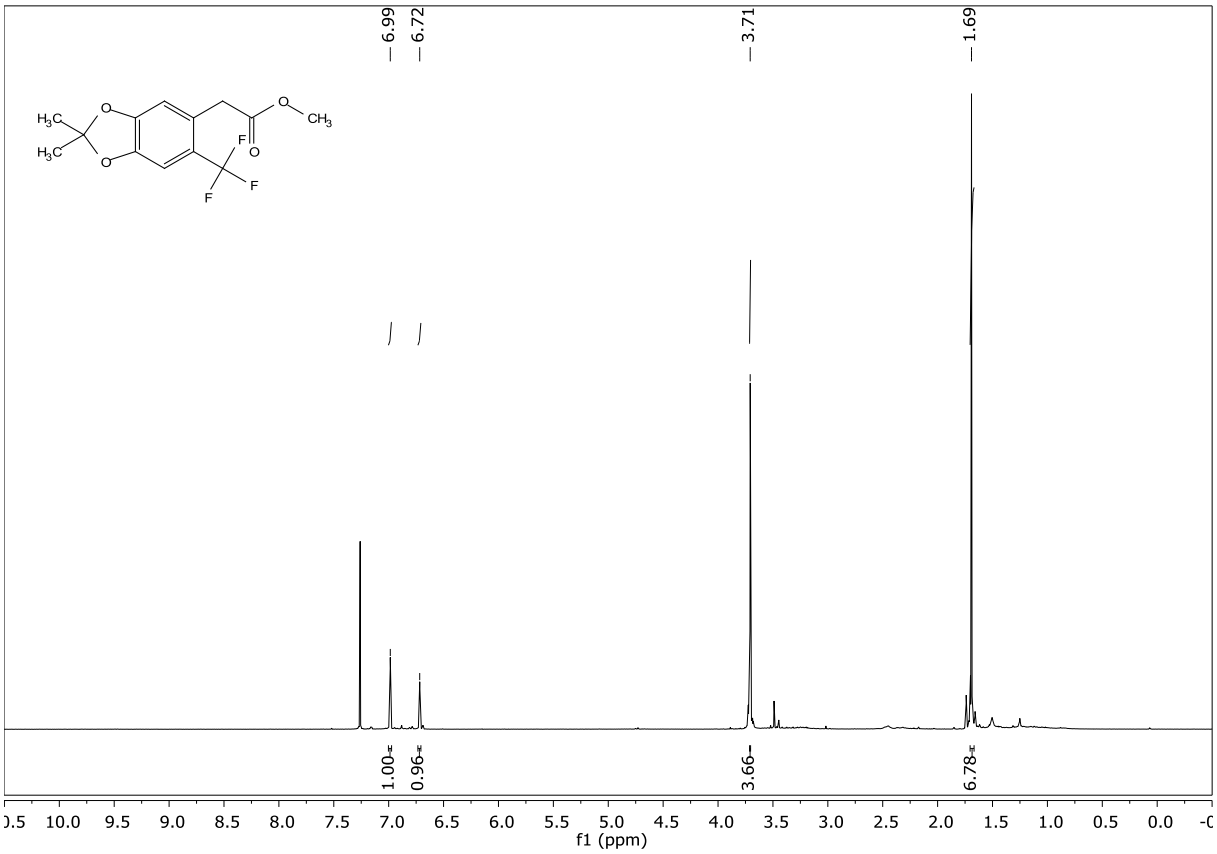

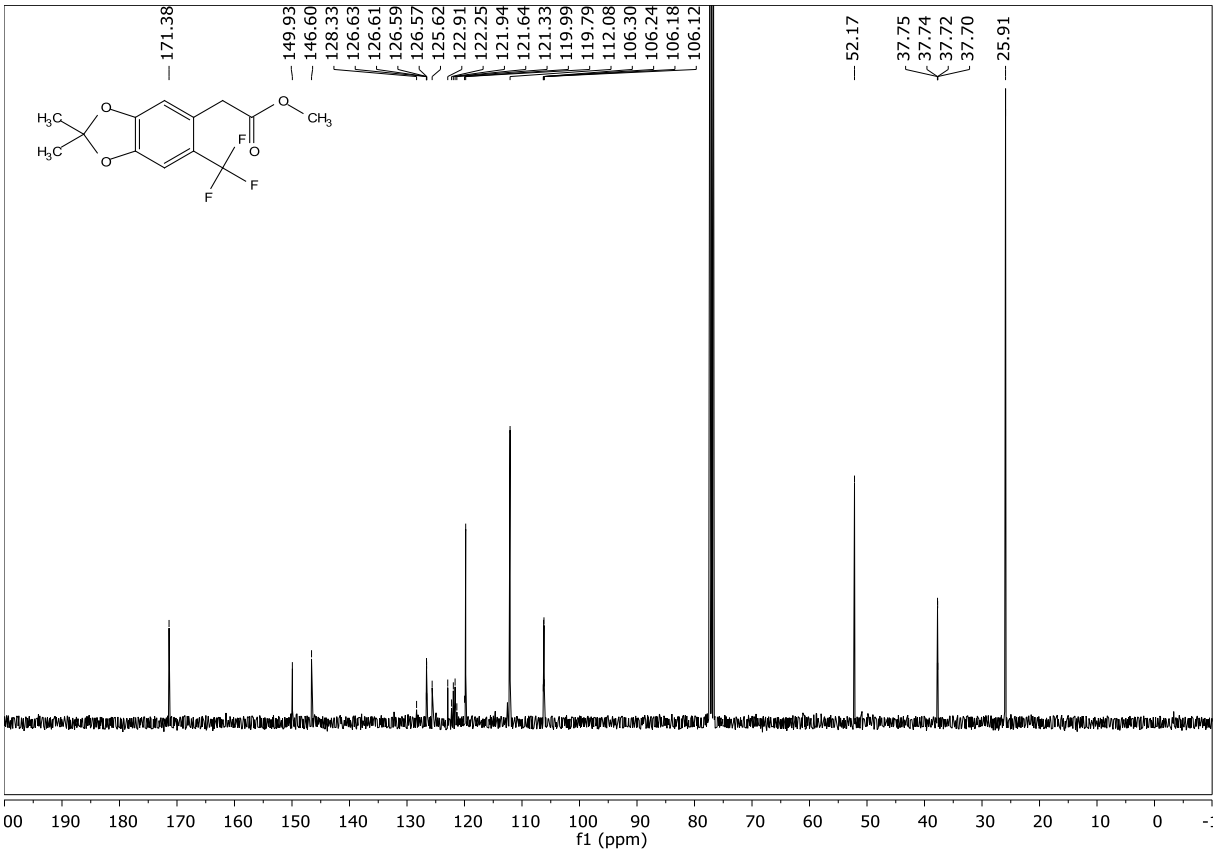

Methyl 2-(2,2-dimethyl-6-(methylsulfonyl)benzo[*d*][1,3]dioxol-5-yl)acetate (**101**)

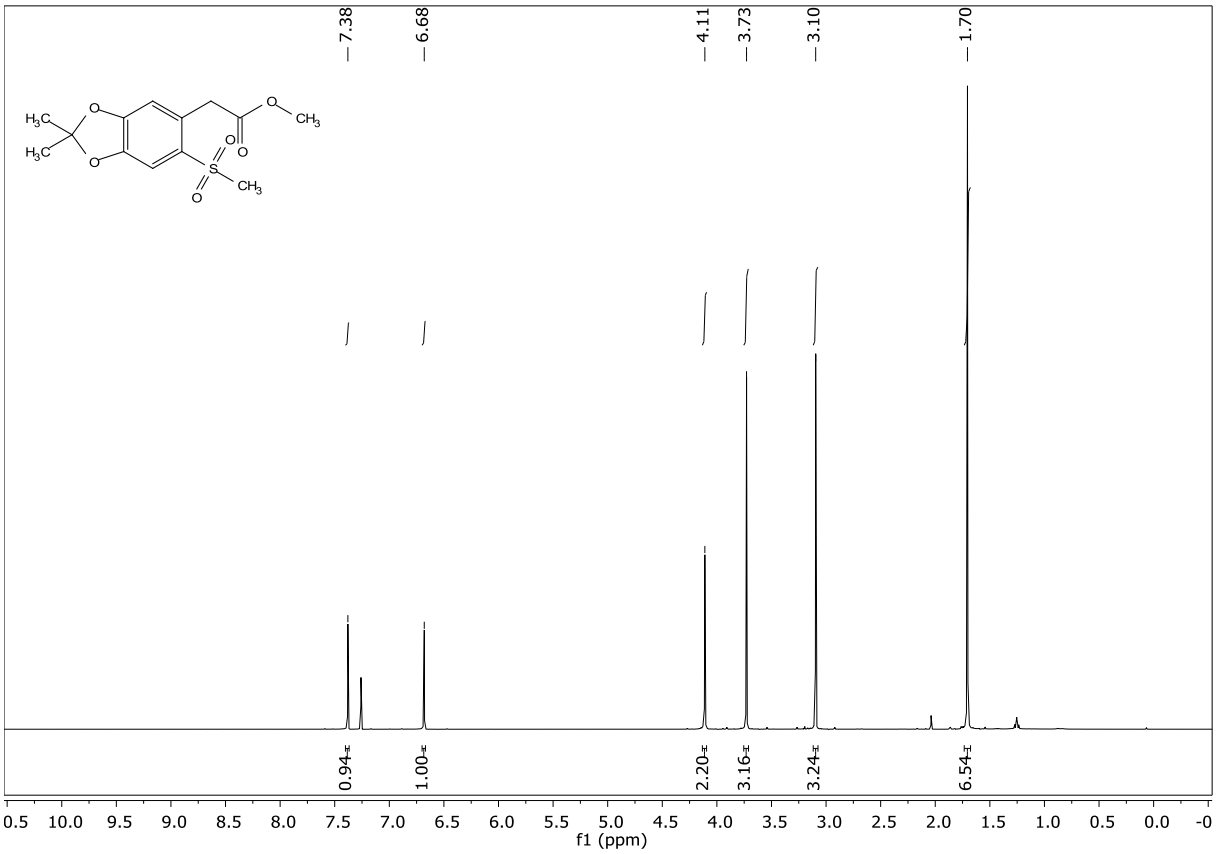

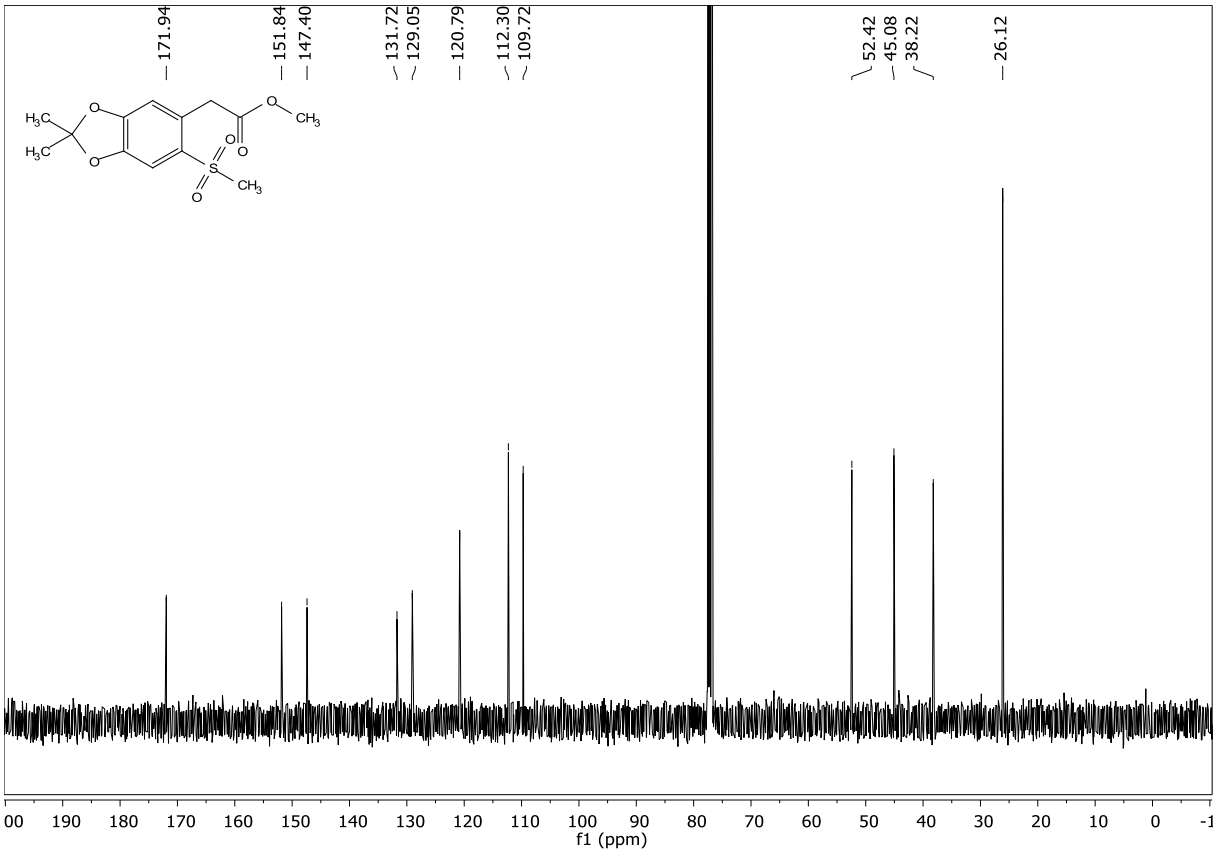

2-(6-Chloro-2,2-dimethylbenzo[*d*][1,3]dioxol-5-yl)acetic acid (**102**)

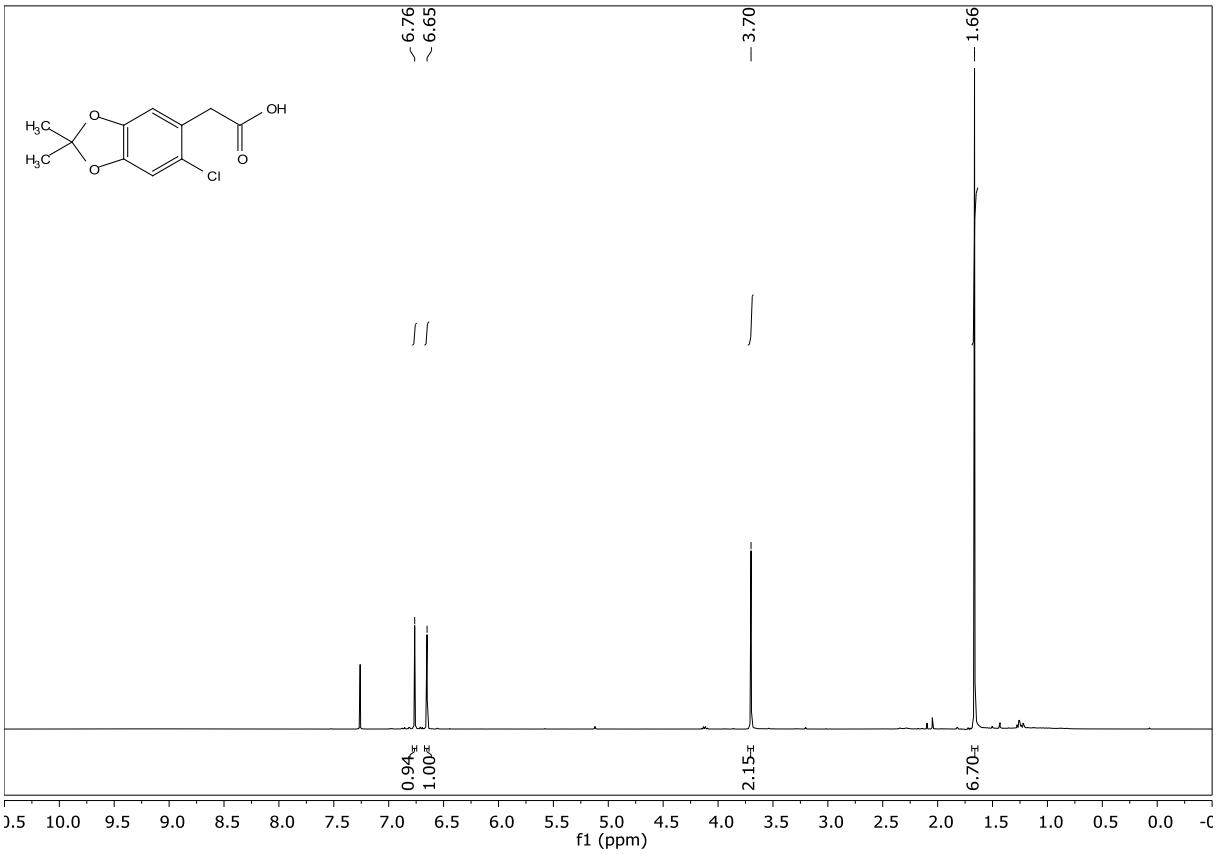

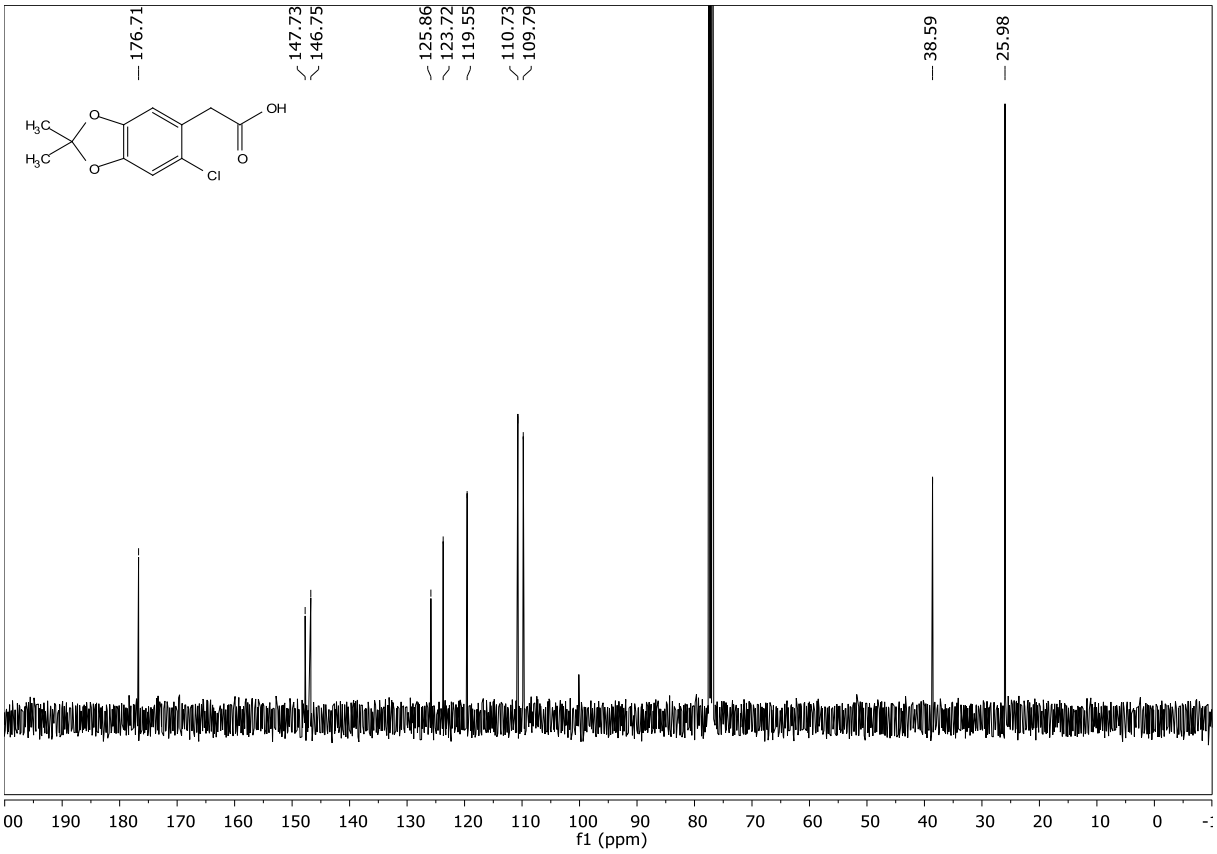

2-(6-Bromo-2,2-dimethylbenzo[*d*][1,3]dioxol-5-yl)acetic acid (**103**)

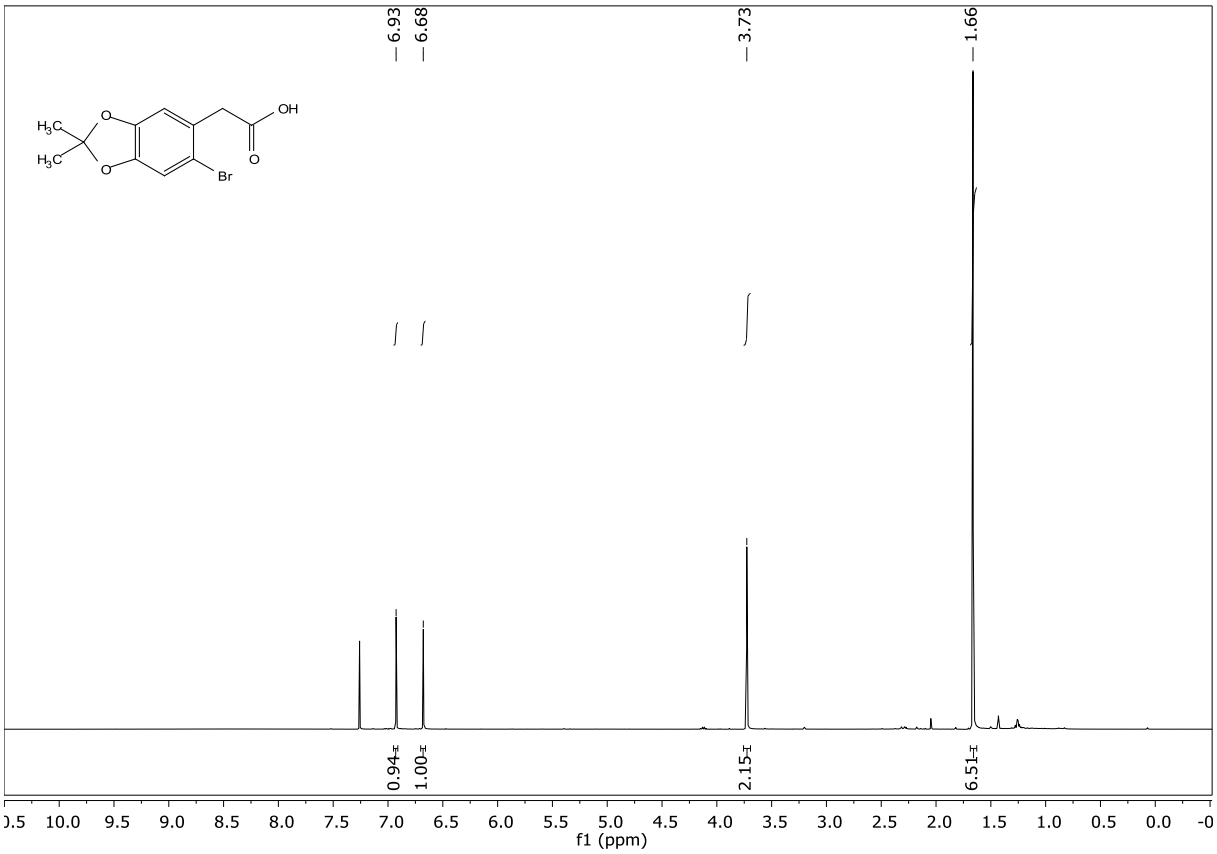

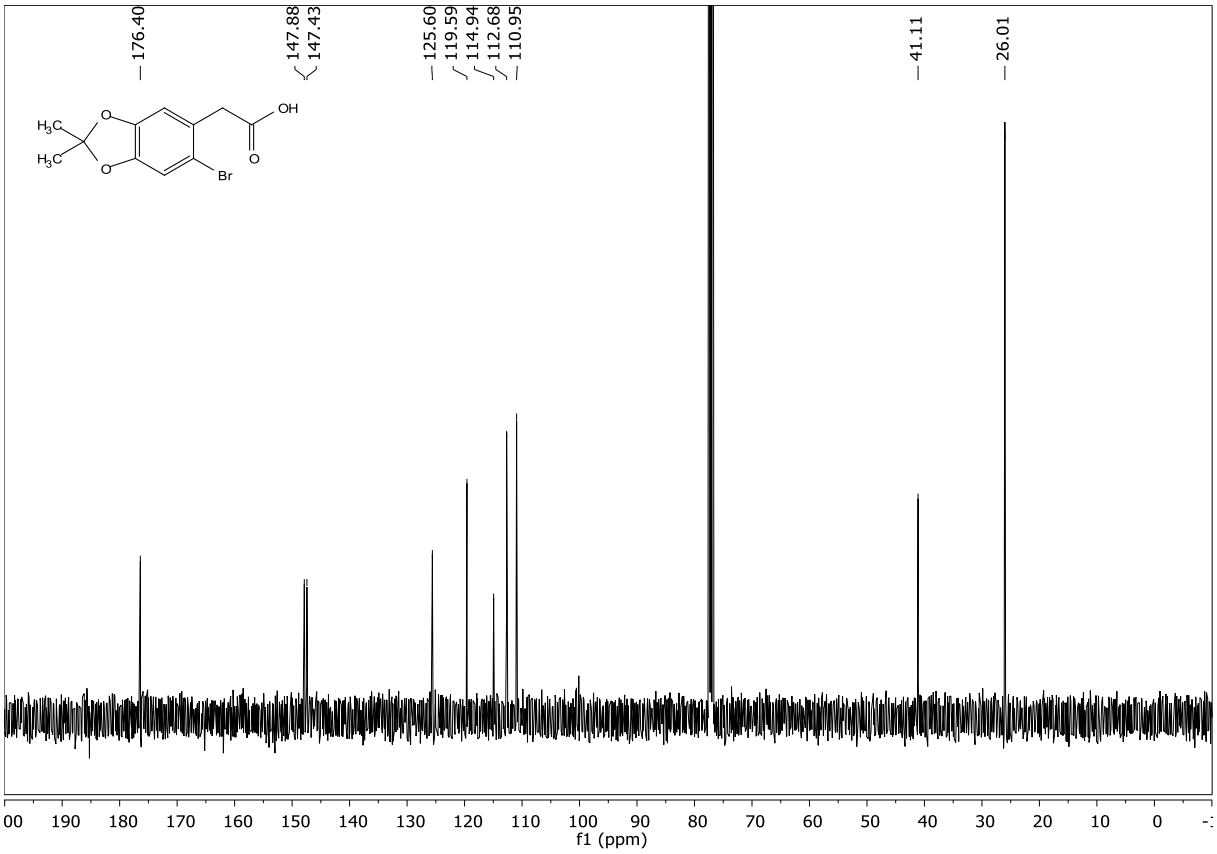

2-(6-Iodo-2,2-dimethylbenzo[*d*][1,3]dioxol-5-yl)acetic acid (**104**)

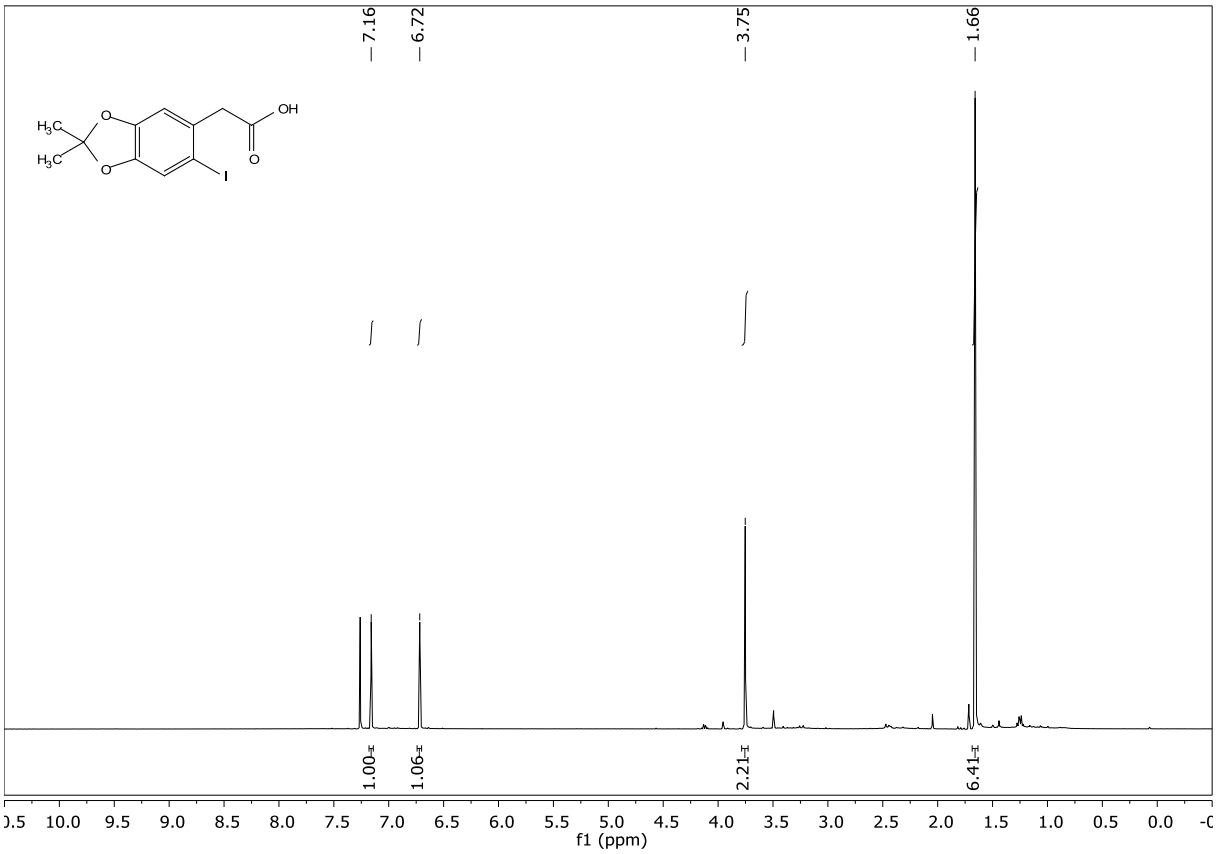

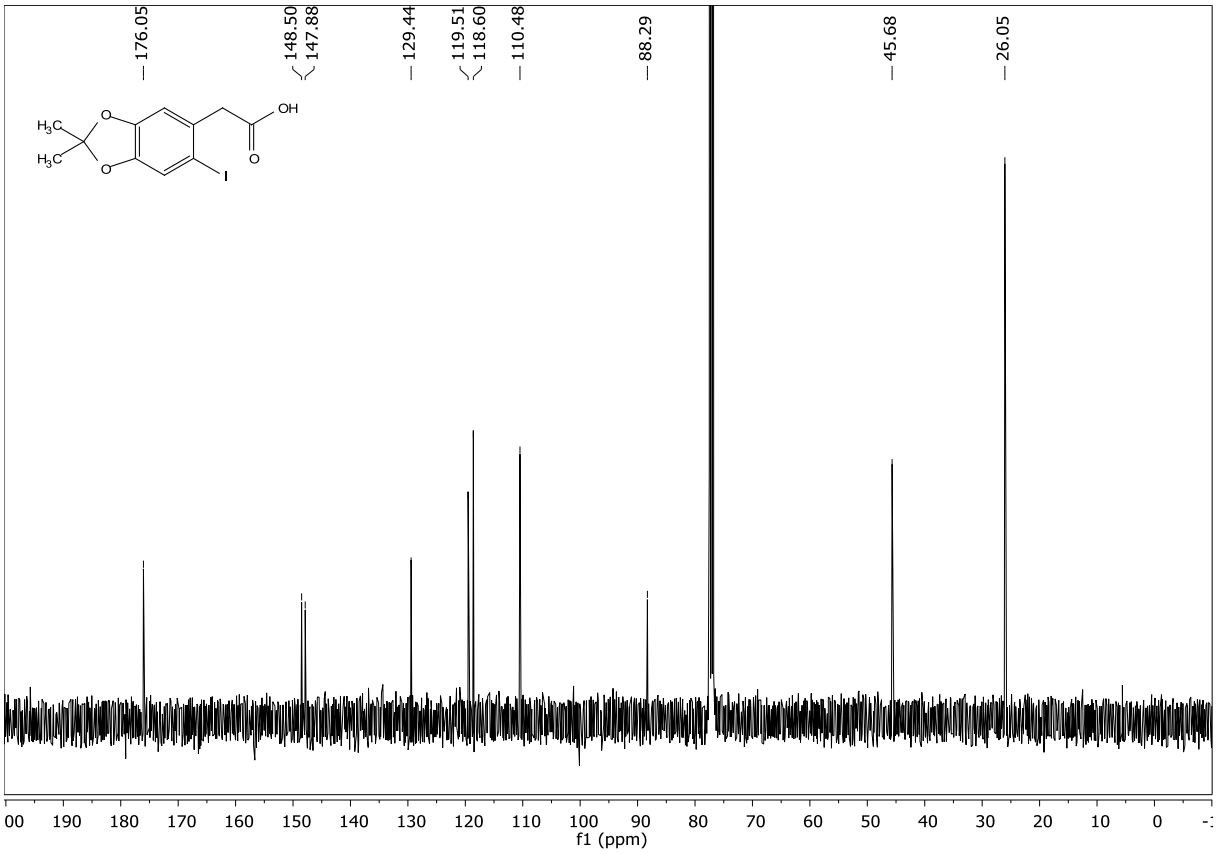

2-(2,2-Dimethyl-6-(trifluoromethyl)benzo[*d*][1,3]dioxol-5-yl)acetic acid (**105**)

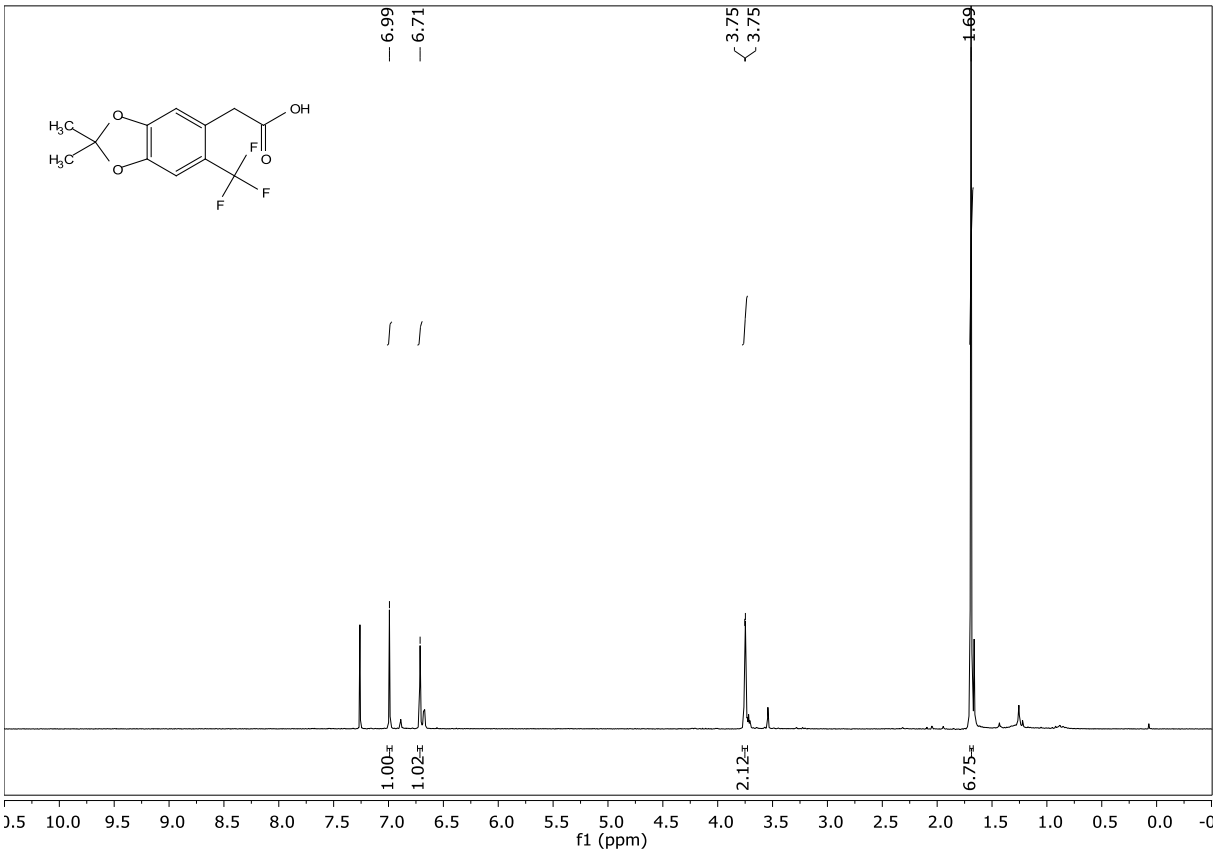

2-(2,2-Dimethyl-6-(methylsulfonyl)benzo[*d*][1,3]dioxol-5-yl)acetic acid (**106**)

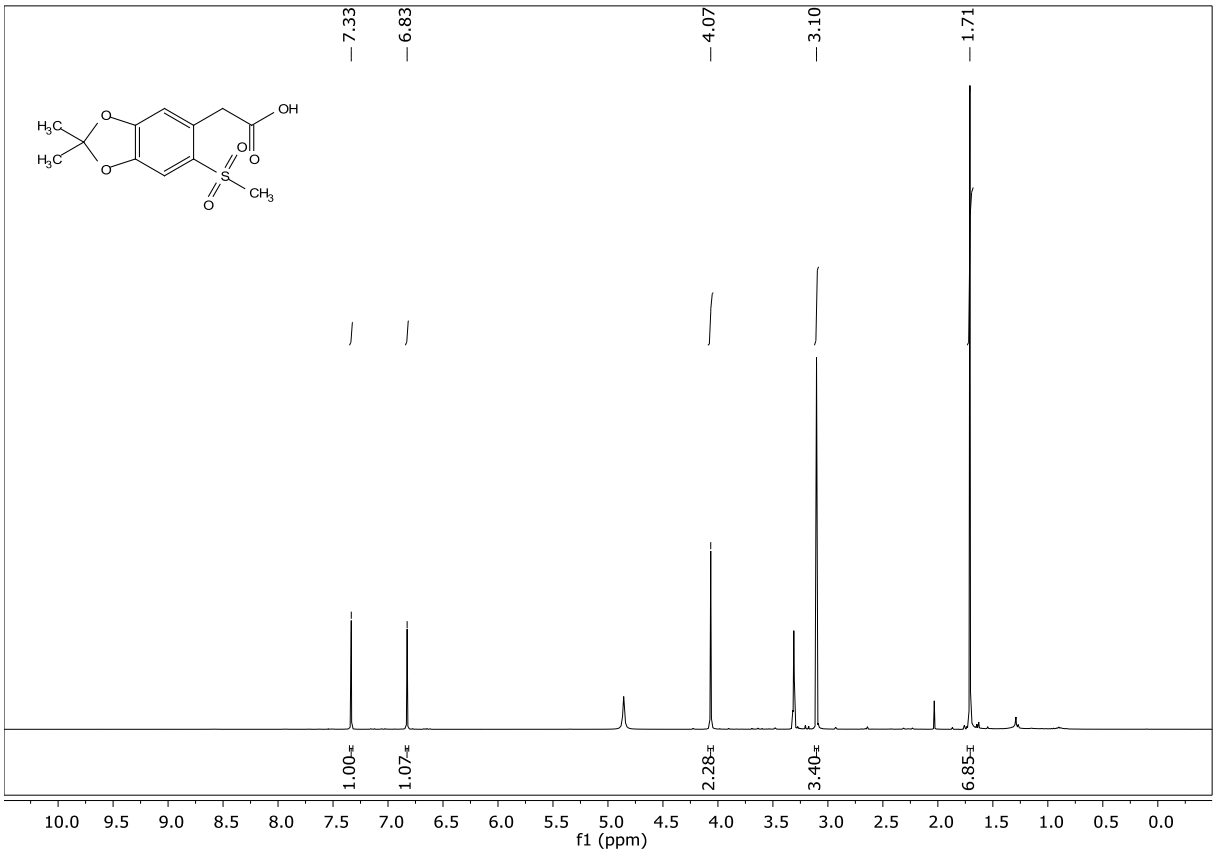

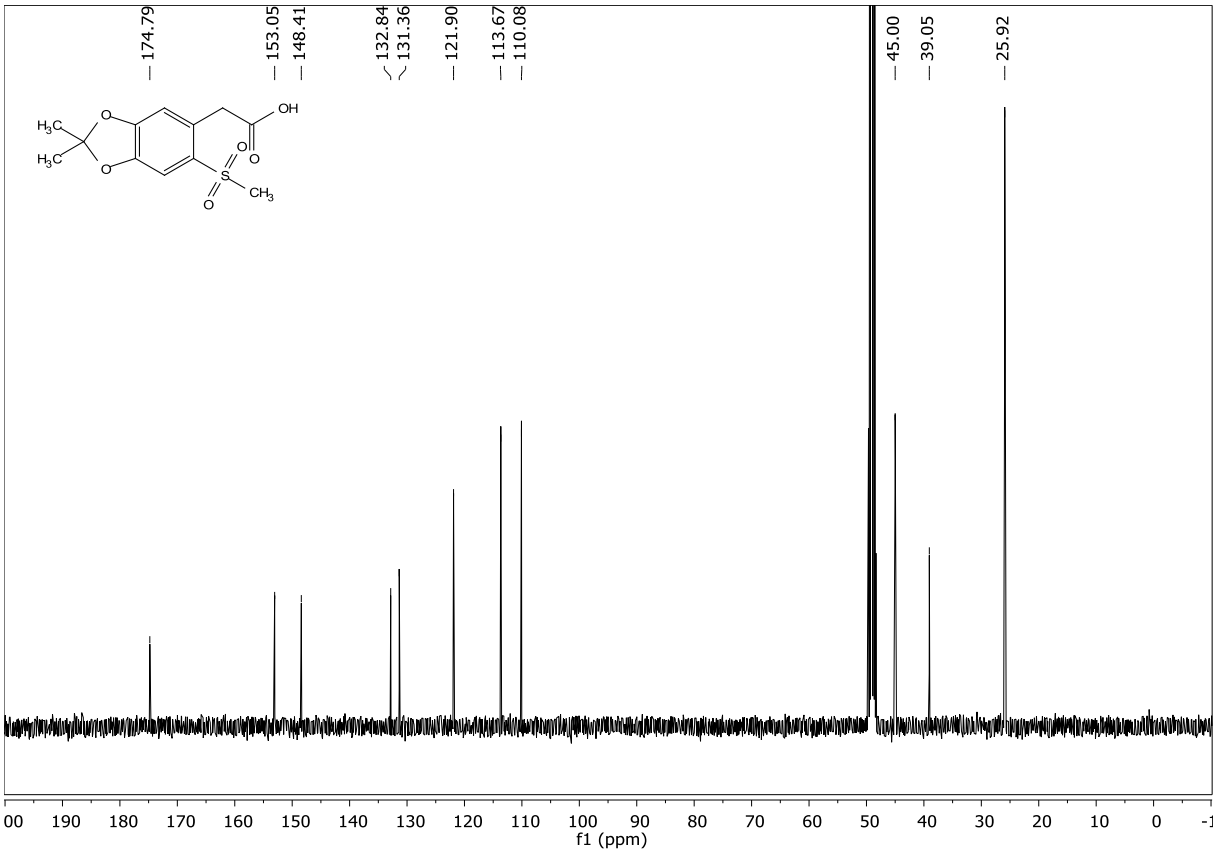

Methyl 2-(2-bromo-4,5-dihydroxyphenyl)acetate (**108**)

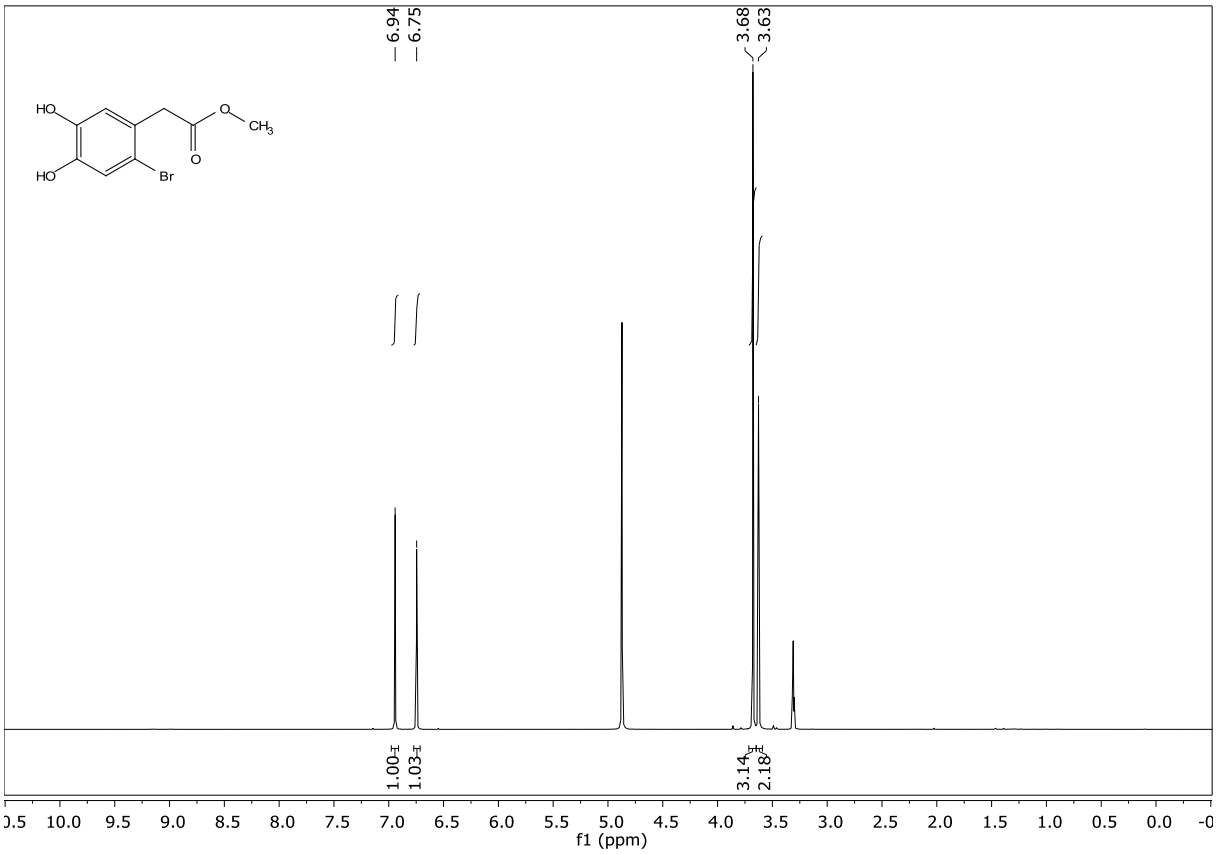

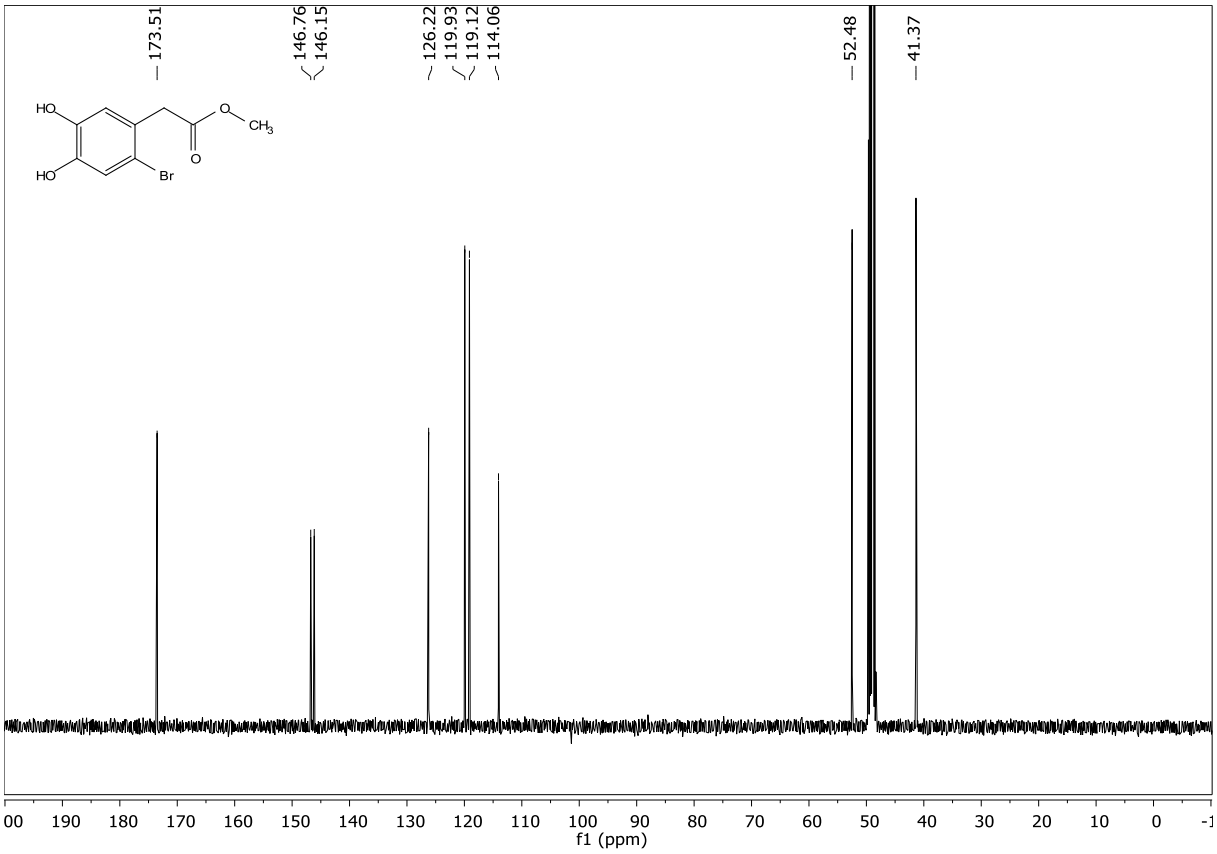

Methyl 2-(4,5-dihydroxy-2-iodophenyl)acetate (**109**)

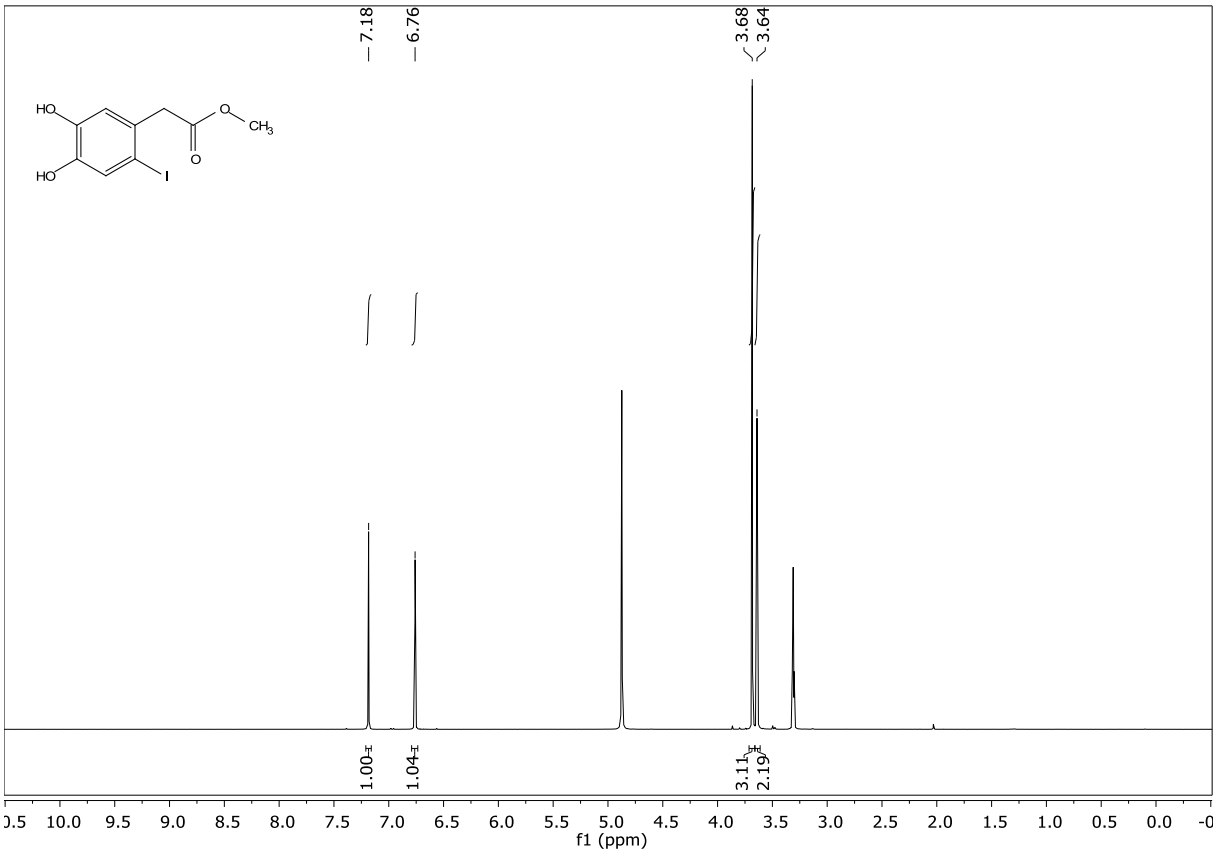

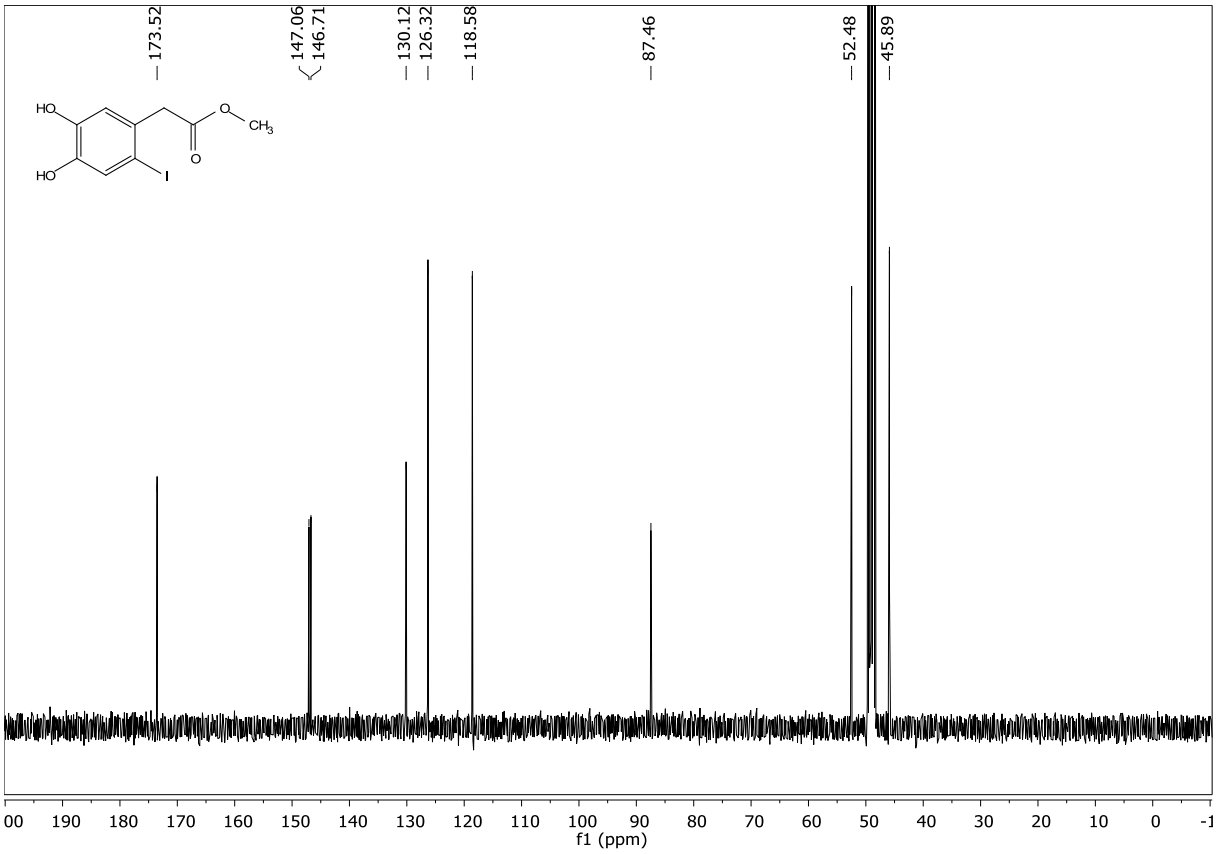

Methyl 2-(4,5-dihydroxy-2-(trifluoromethyl)phenyl)acetate (**110**)

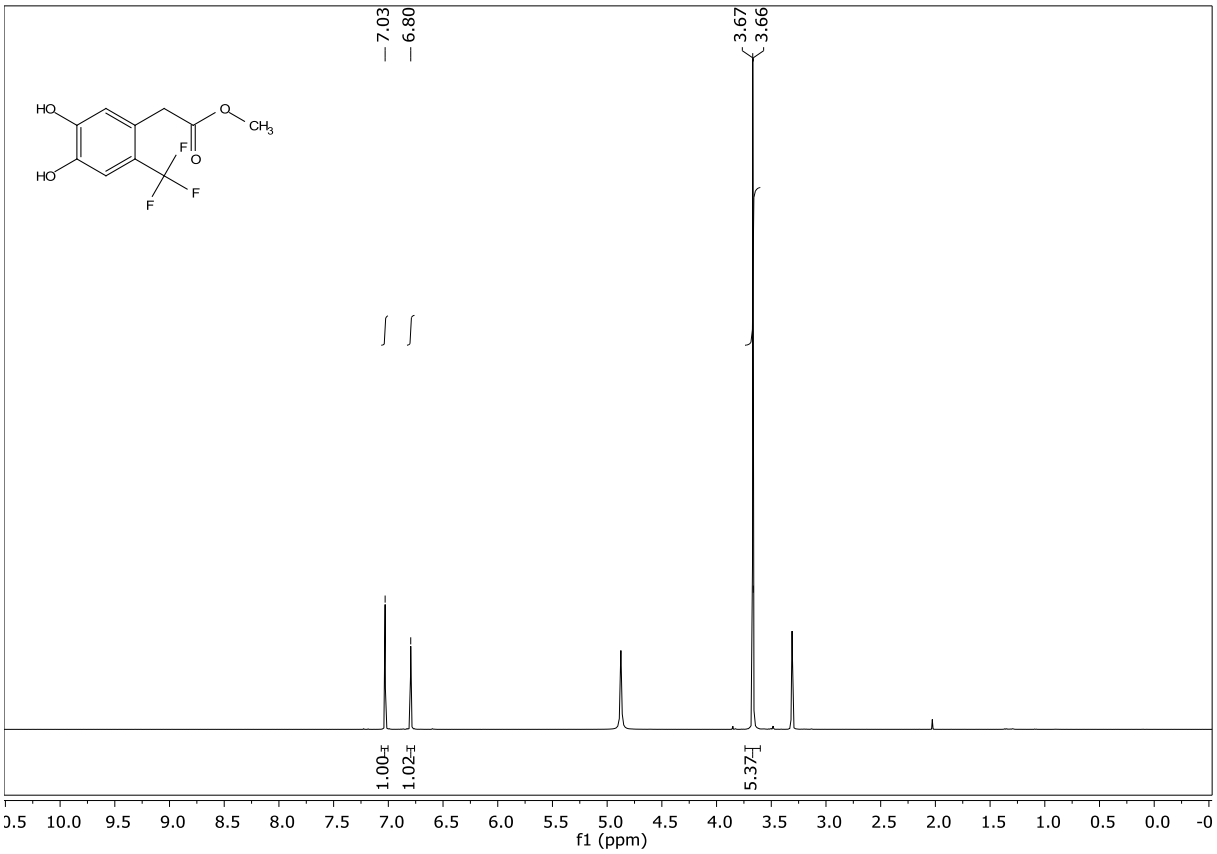

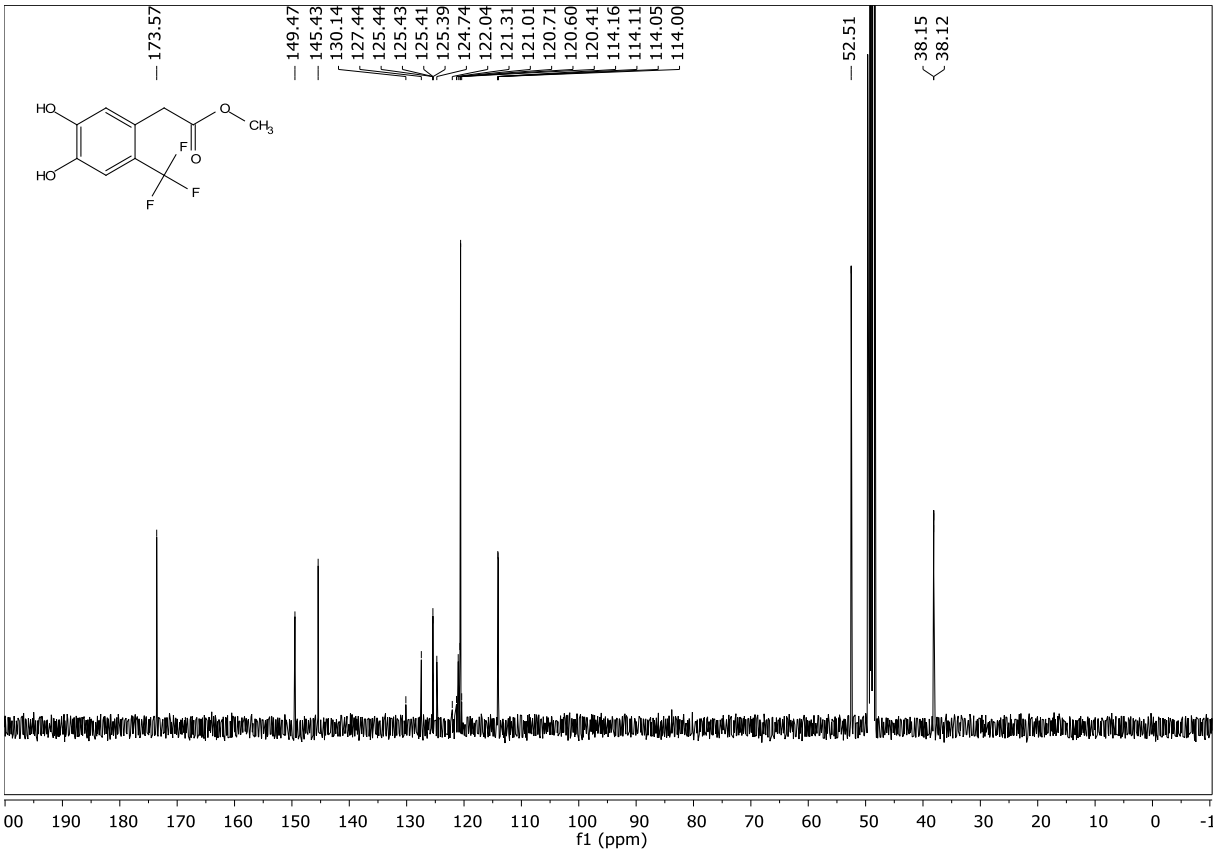

Methyl 2-(4,5-dihydroxy-2-(methylsulfonyl)phenyl)acetate (**111**)

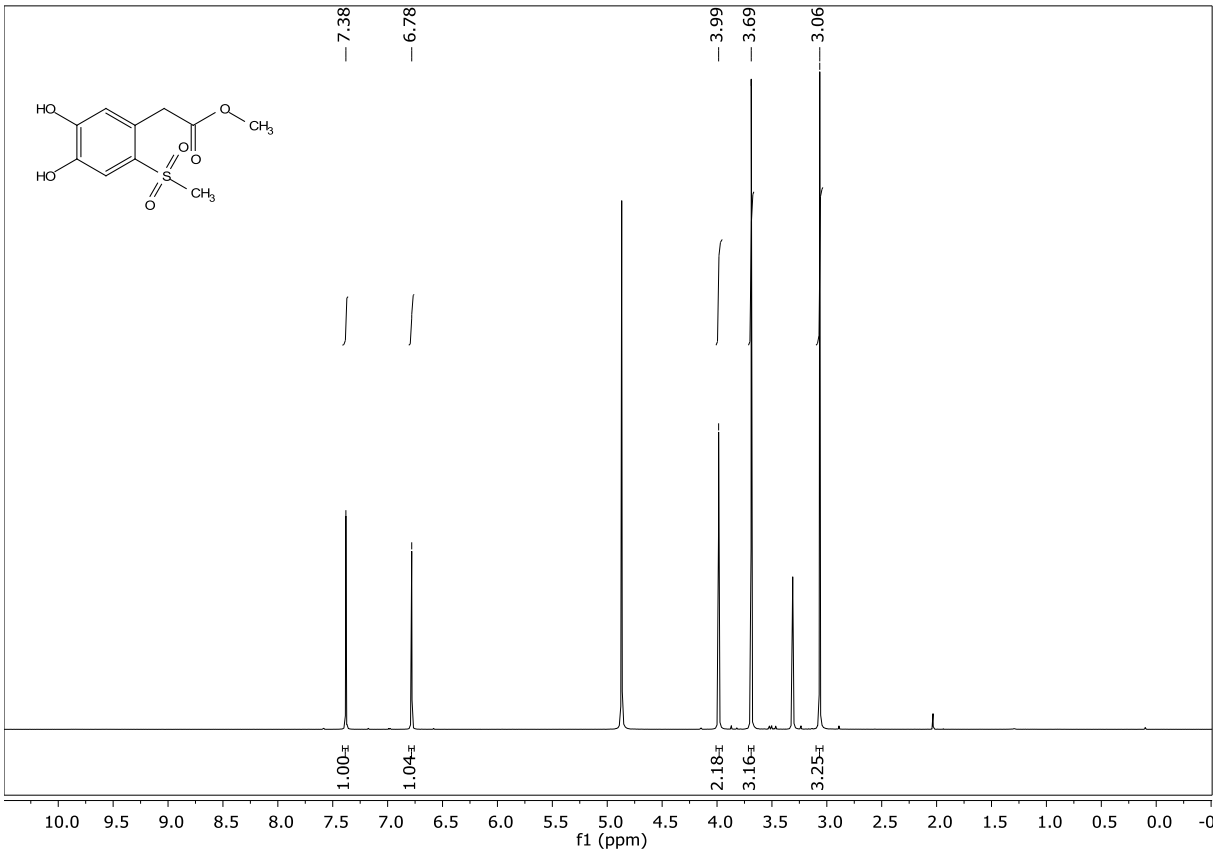

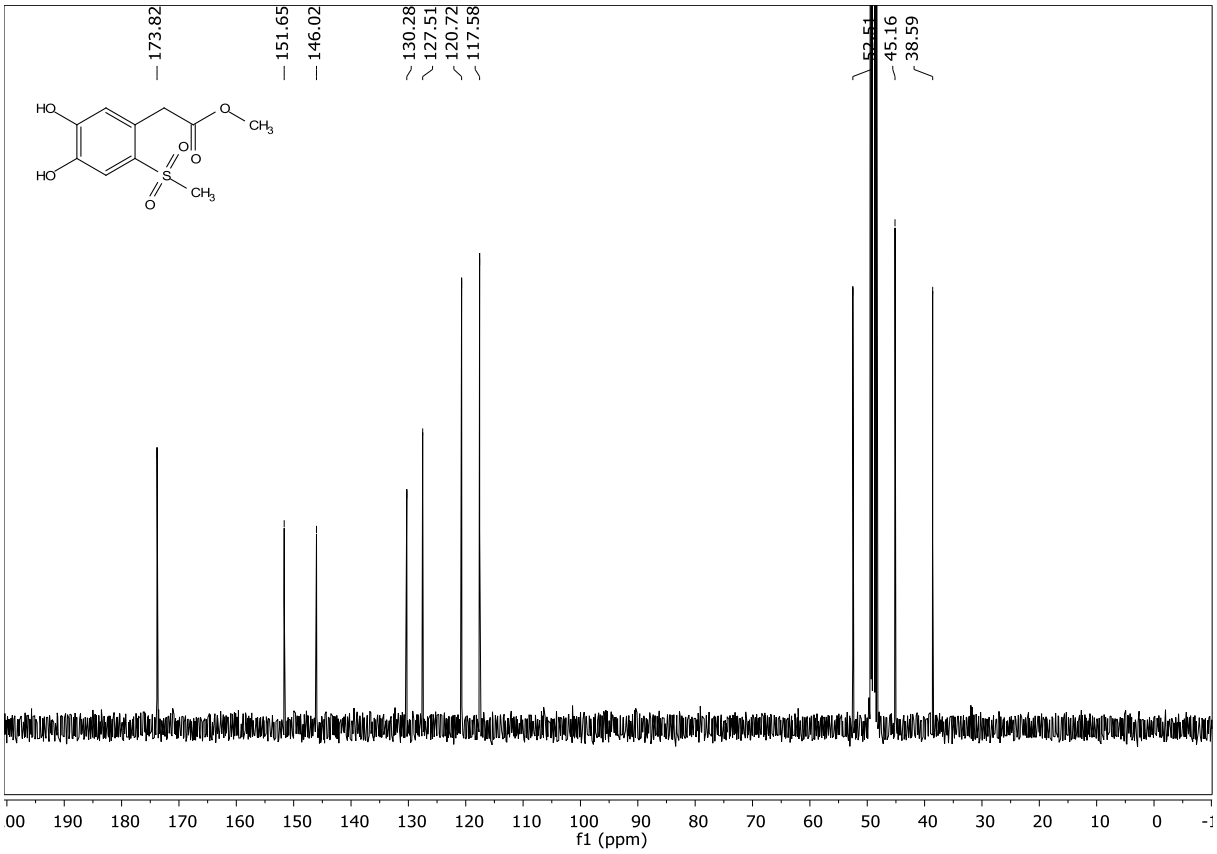

2,2-Dimethylnaphtho[1,8-*de*][1,3]dioxine (**137**)

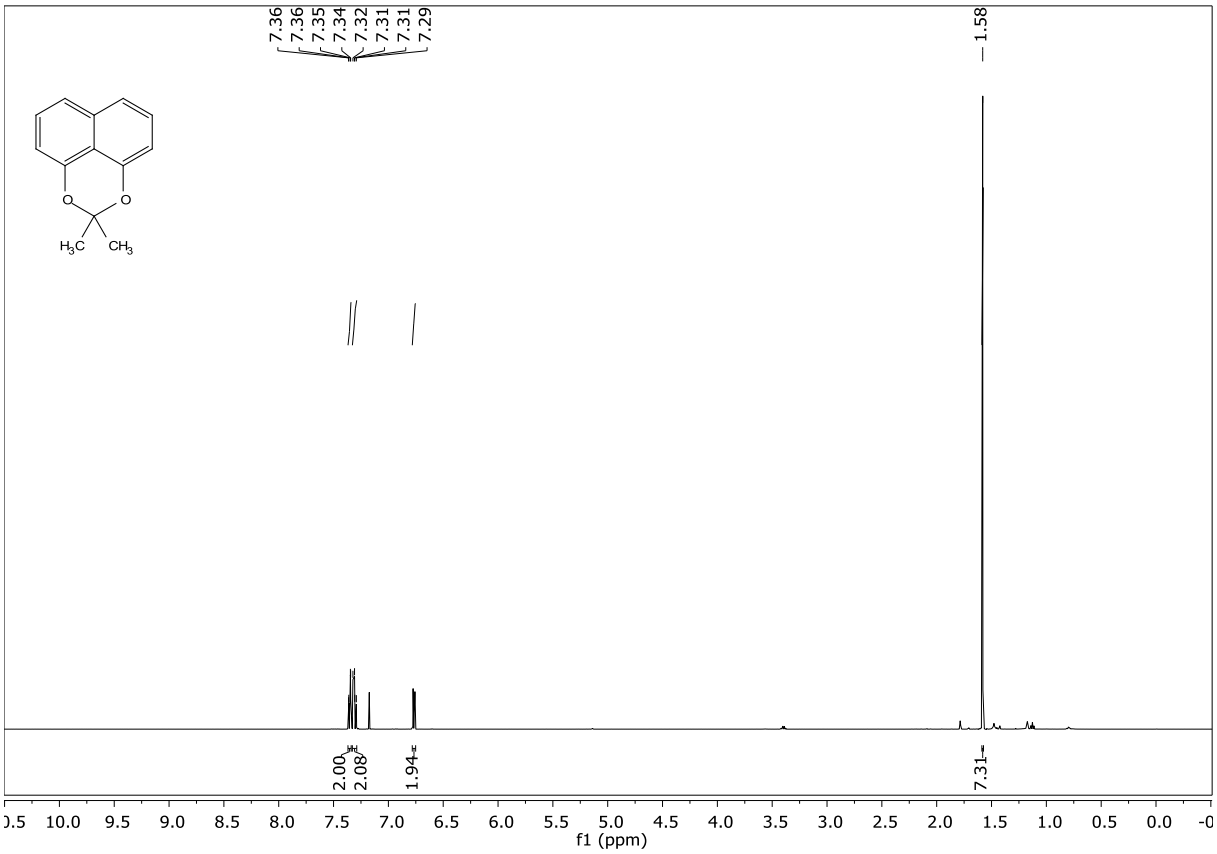

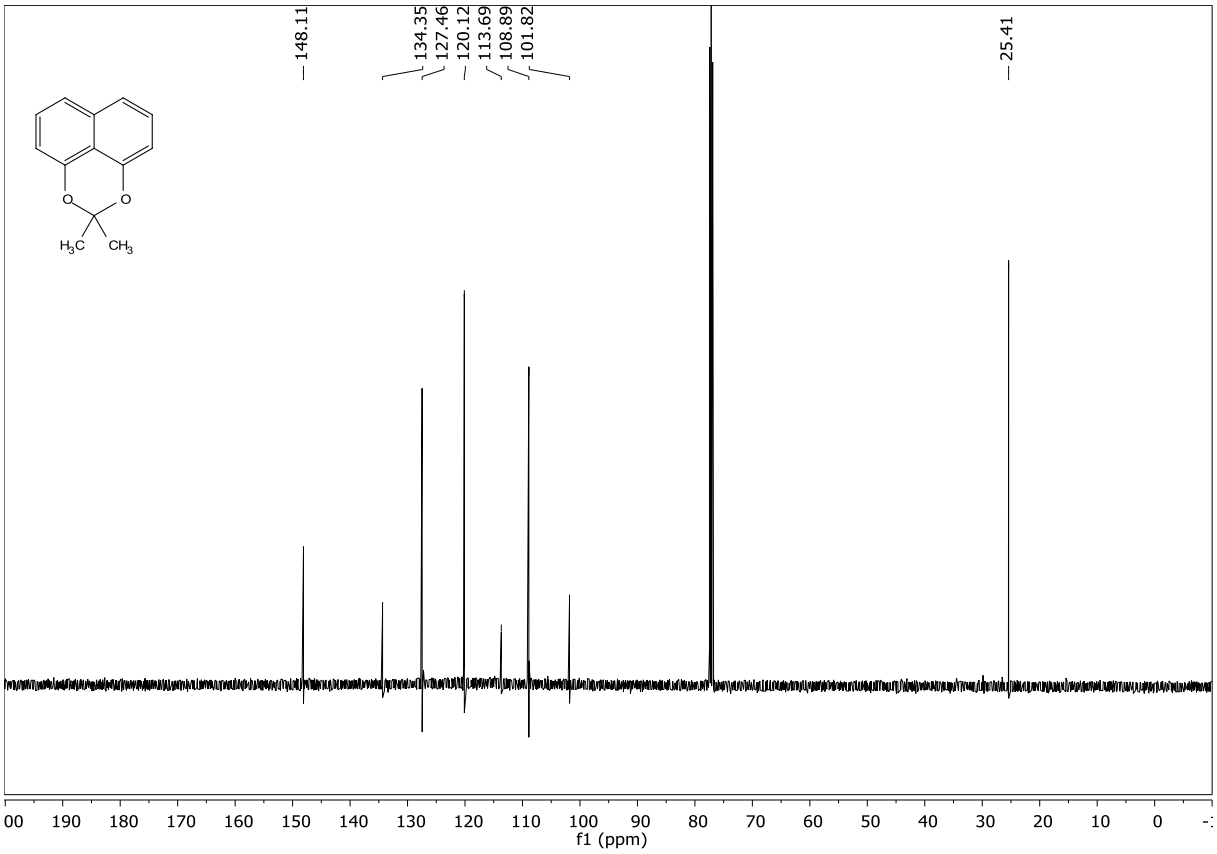

2,2-Dimethyl-6,7-dinitronaphtho[1,8-*de*][1,3]dioxine (**138**)

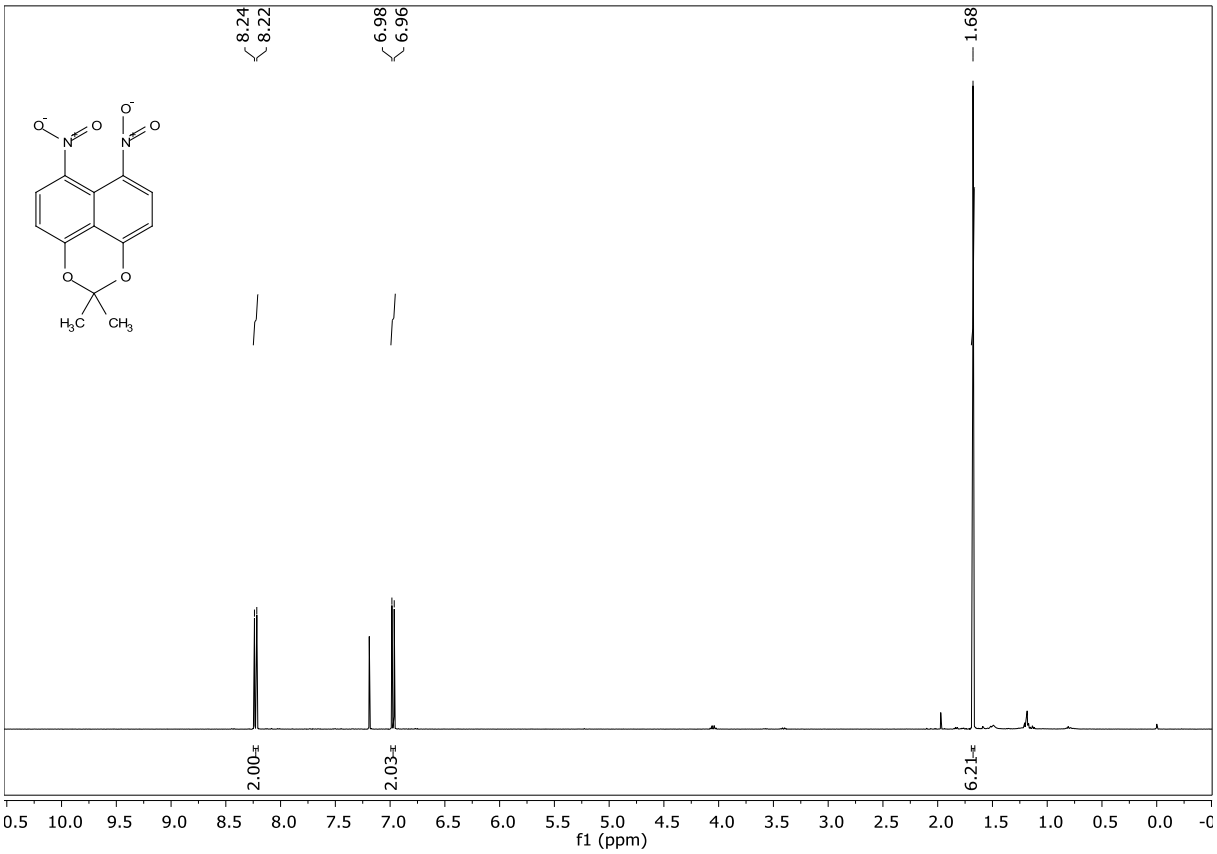

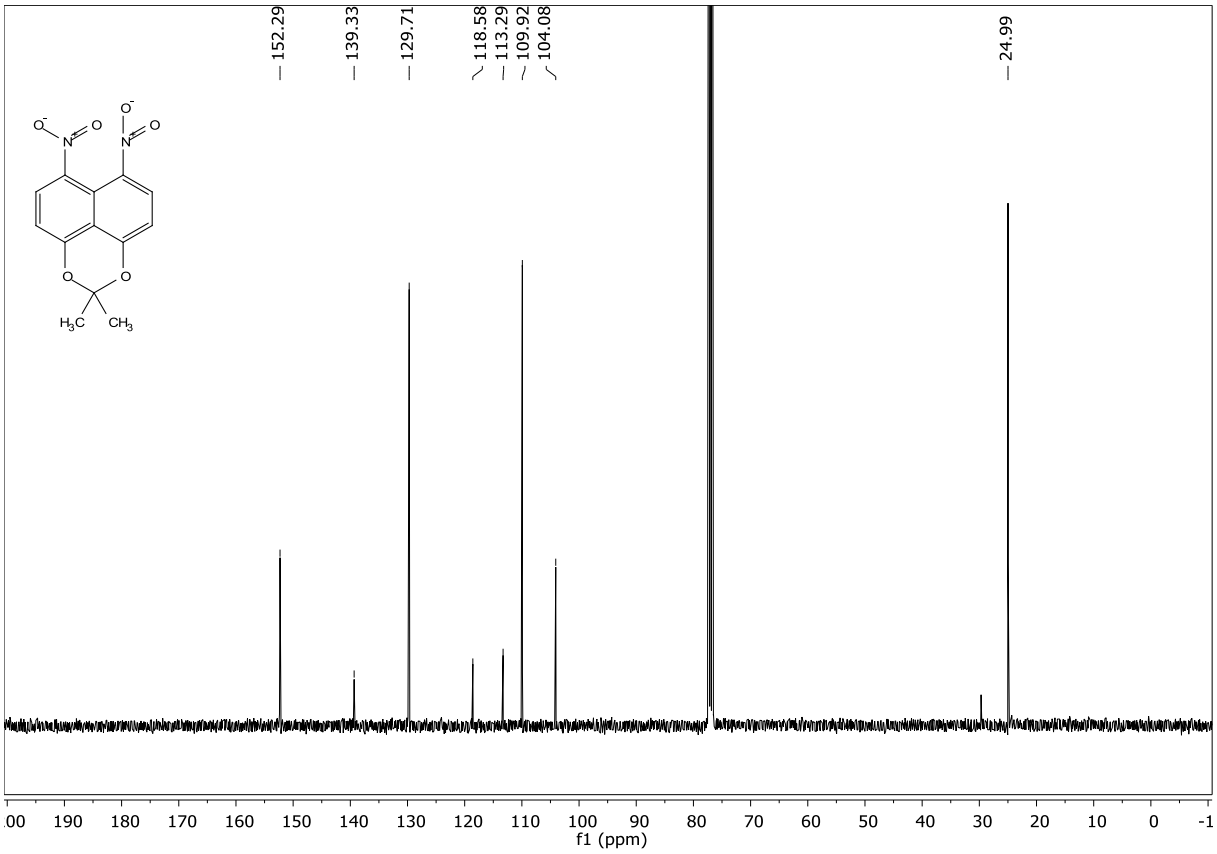

1-(2,2-Dimethylnaphtho[1,8-*de*][1,3]dioxin-6-yl)ethan-1-one (**139**)

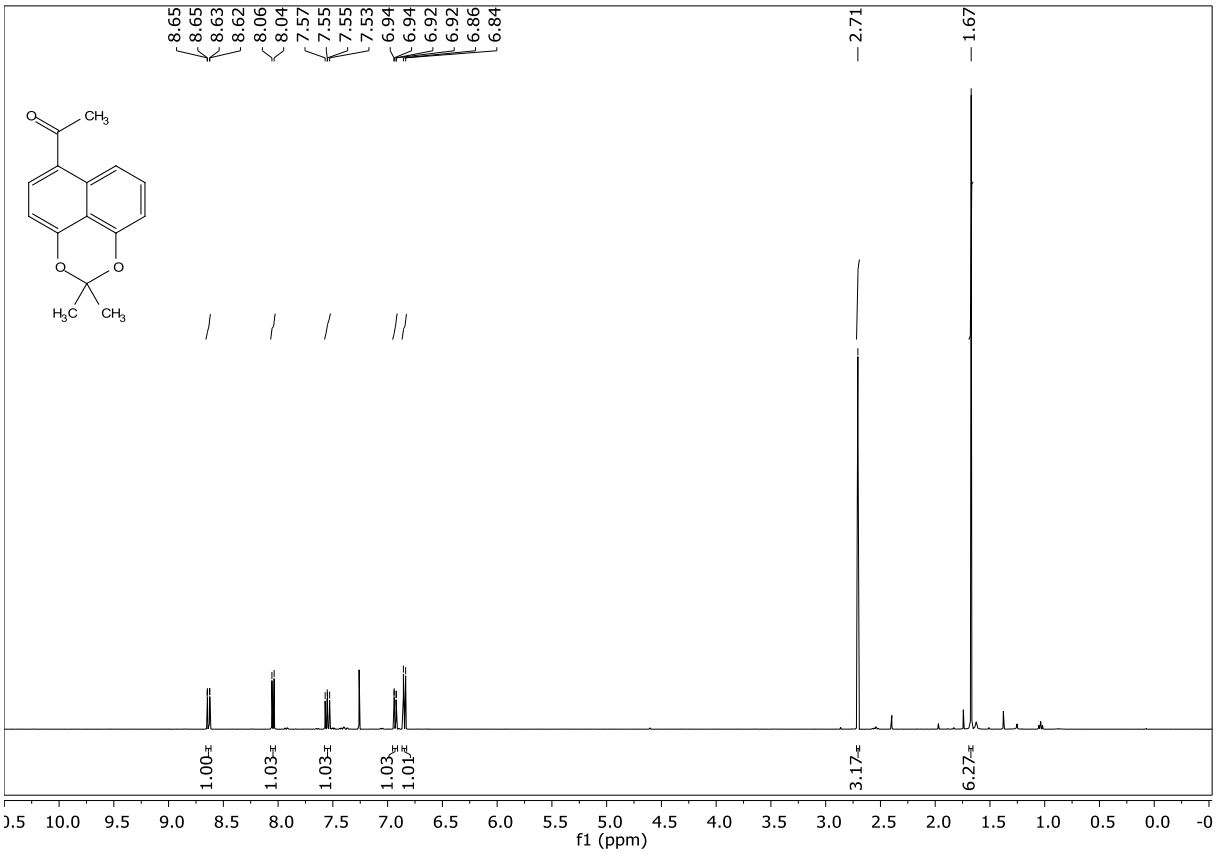

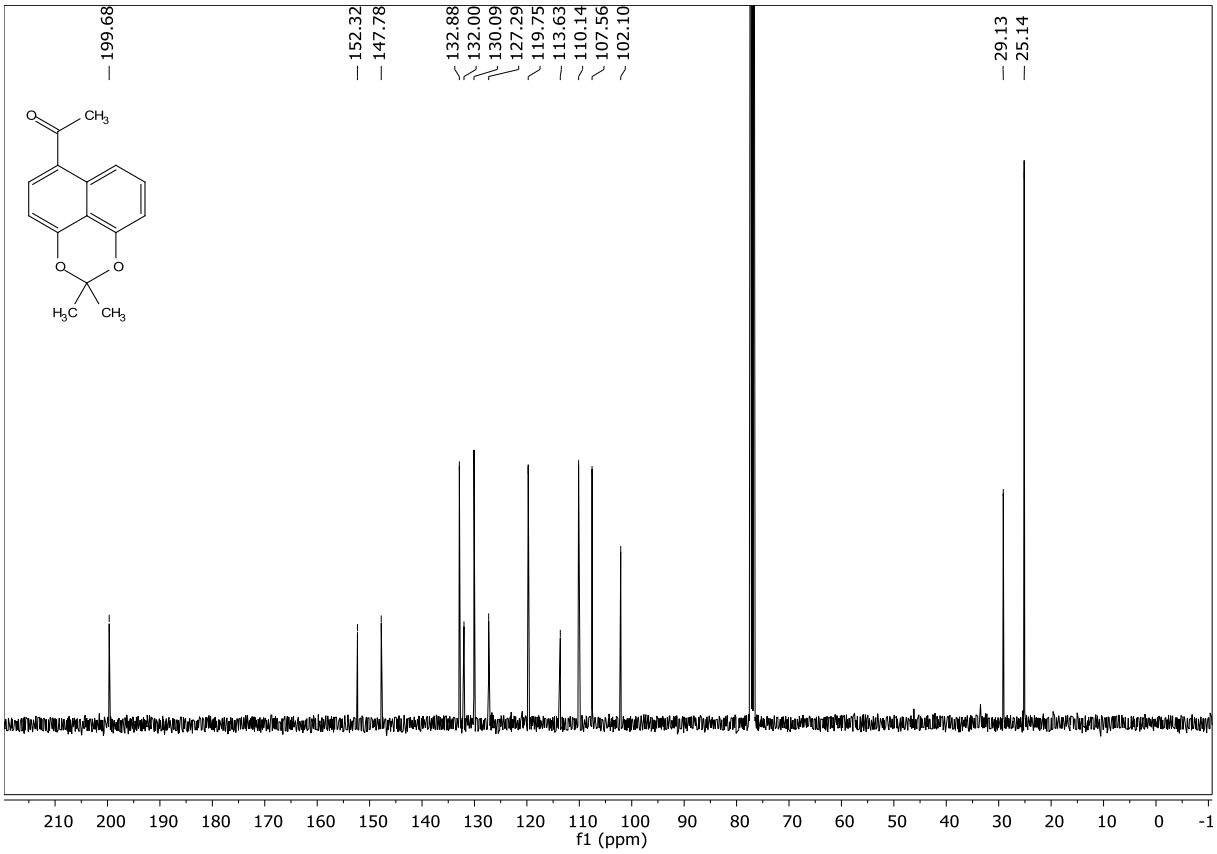

1-(2,2-Dimethyl-7-nitronaphtho[1,8-*de*][1,3]dioxin-6-yl)ethan-1-one (**140**)

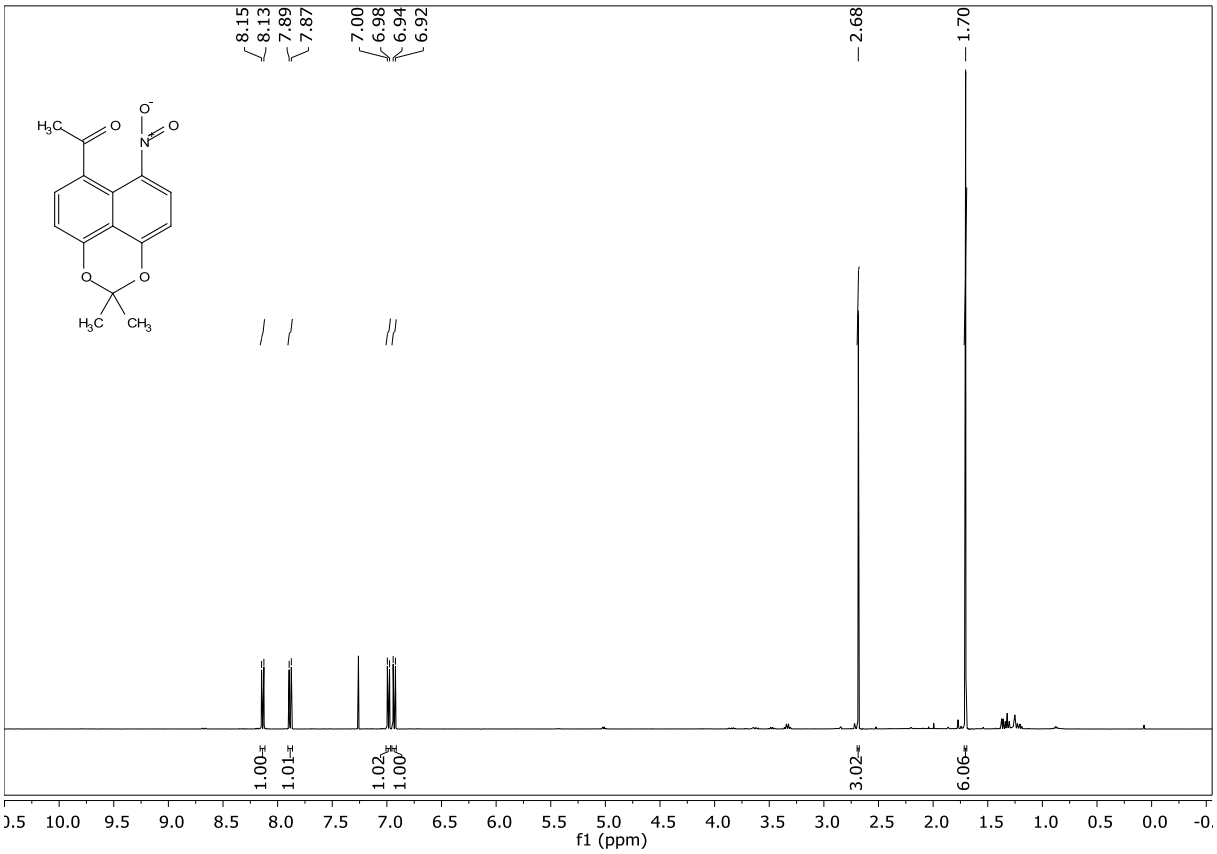

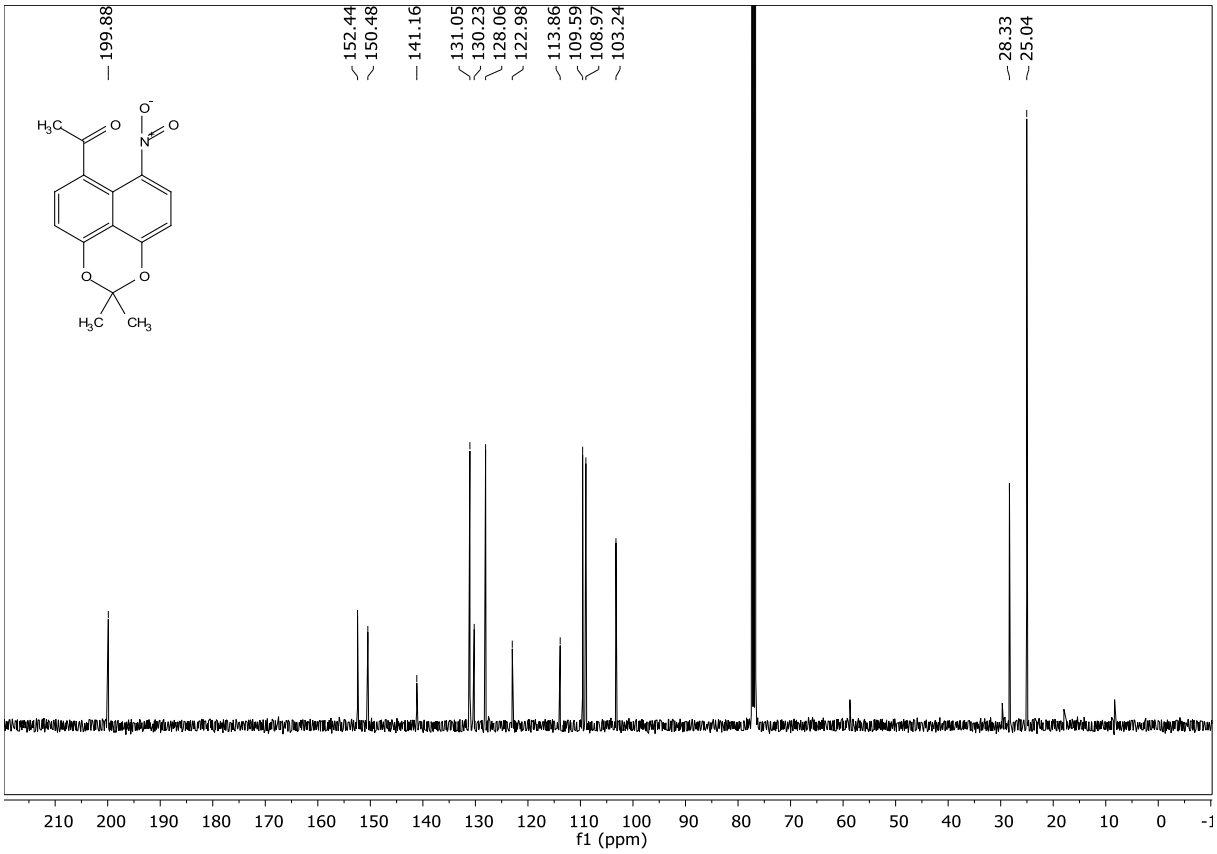

tert-Butyl (6-(5-((3a*S*,4*S*,6a*R*)-2-oxohexahydro-1H-thieno[3,4-*d*]imidazol-4-yl)¬pentan-amido)¬hexyl) carbamate (**154**)

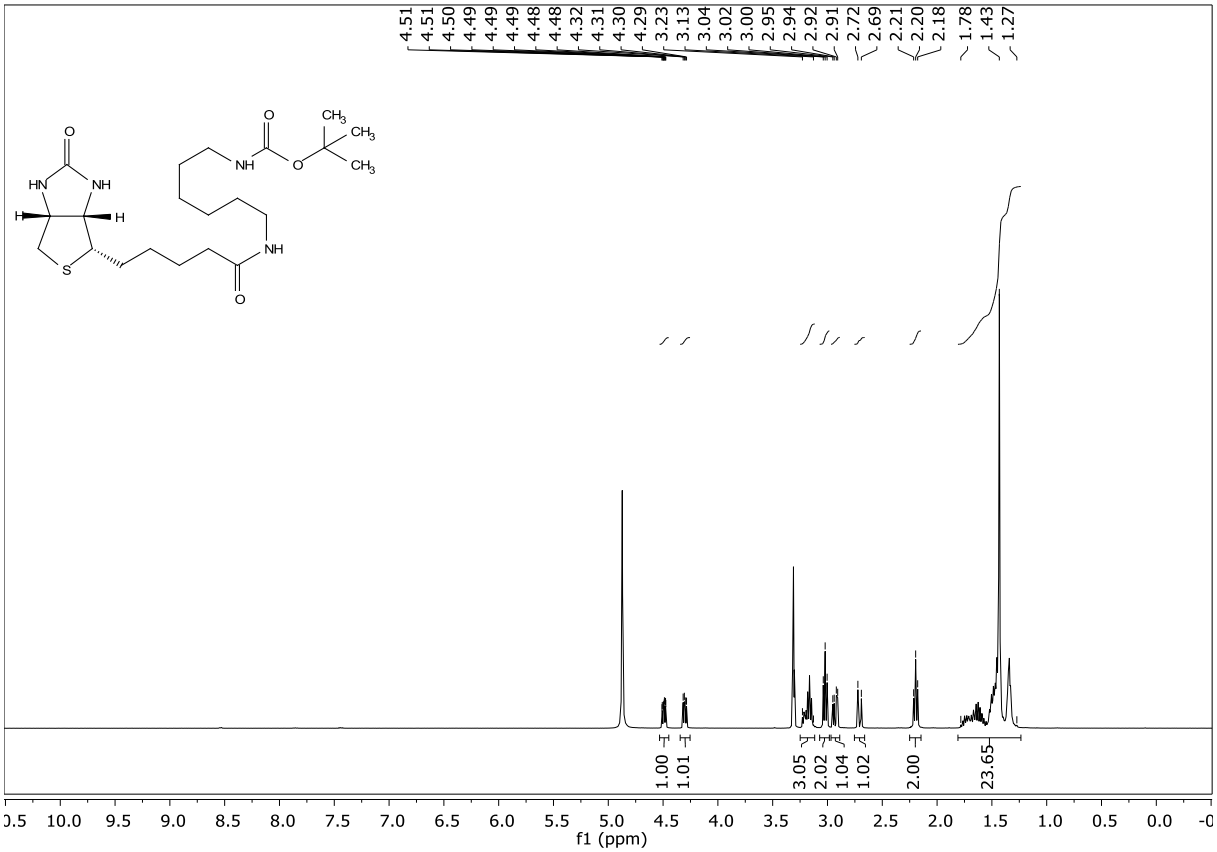

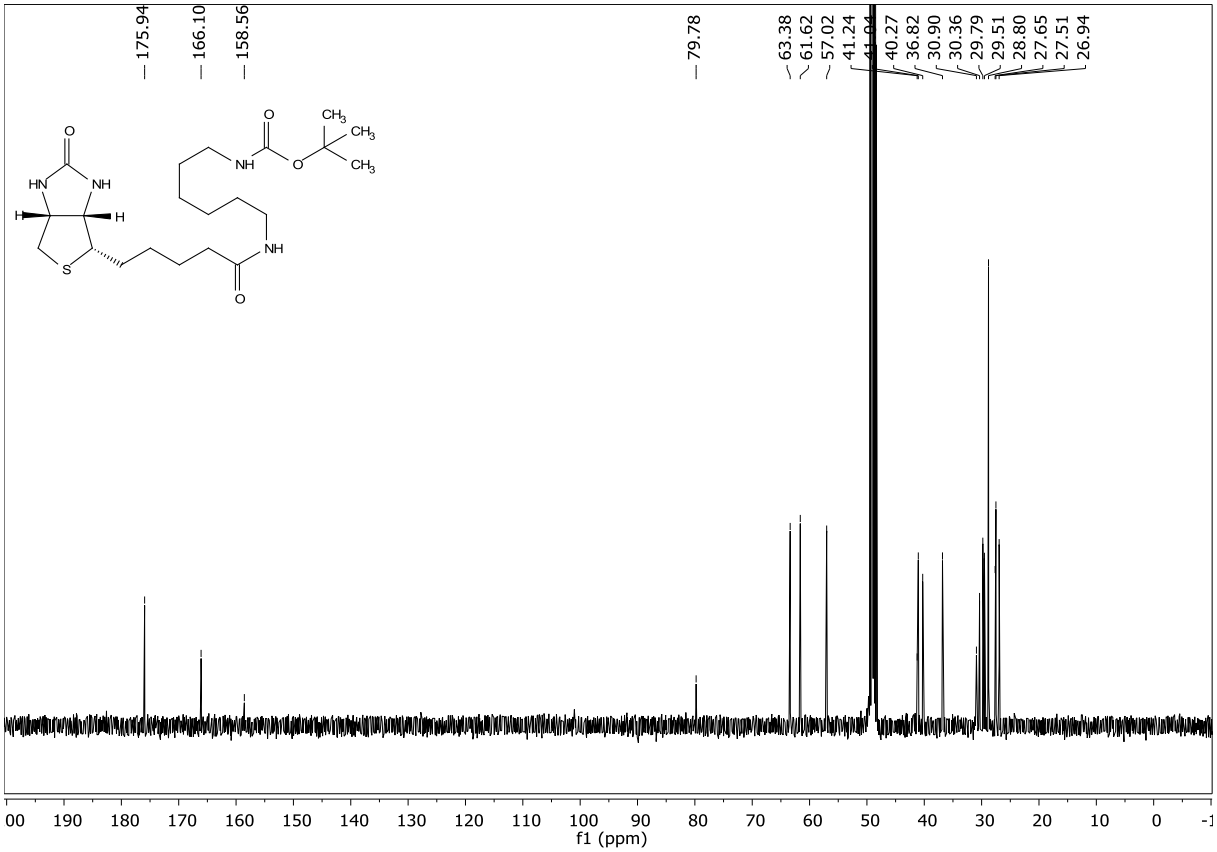

N-Biotinyl-1,6-hexanediamine (**155**)

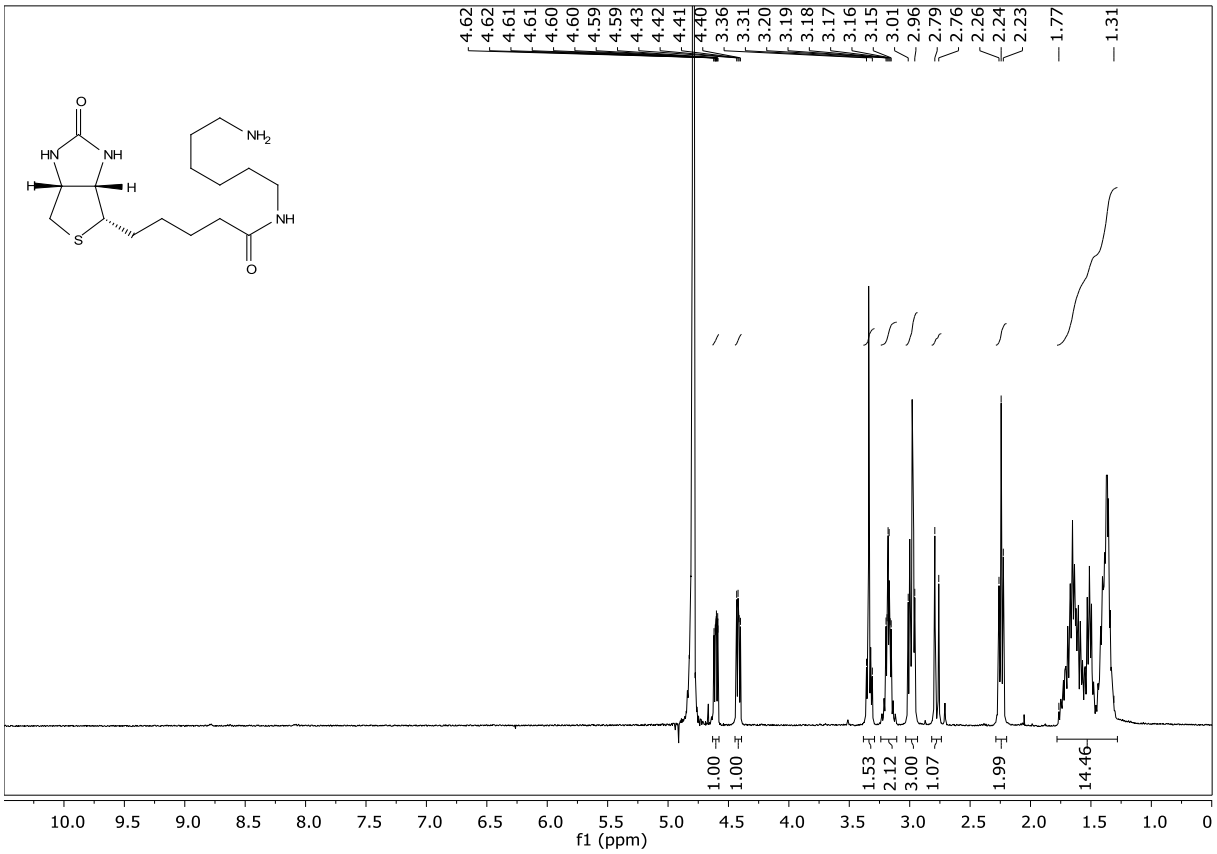

N-Biotinyl-*N'*-Boc-cystamine (**159**)

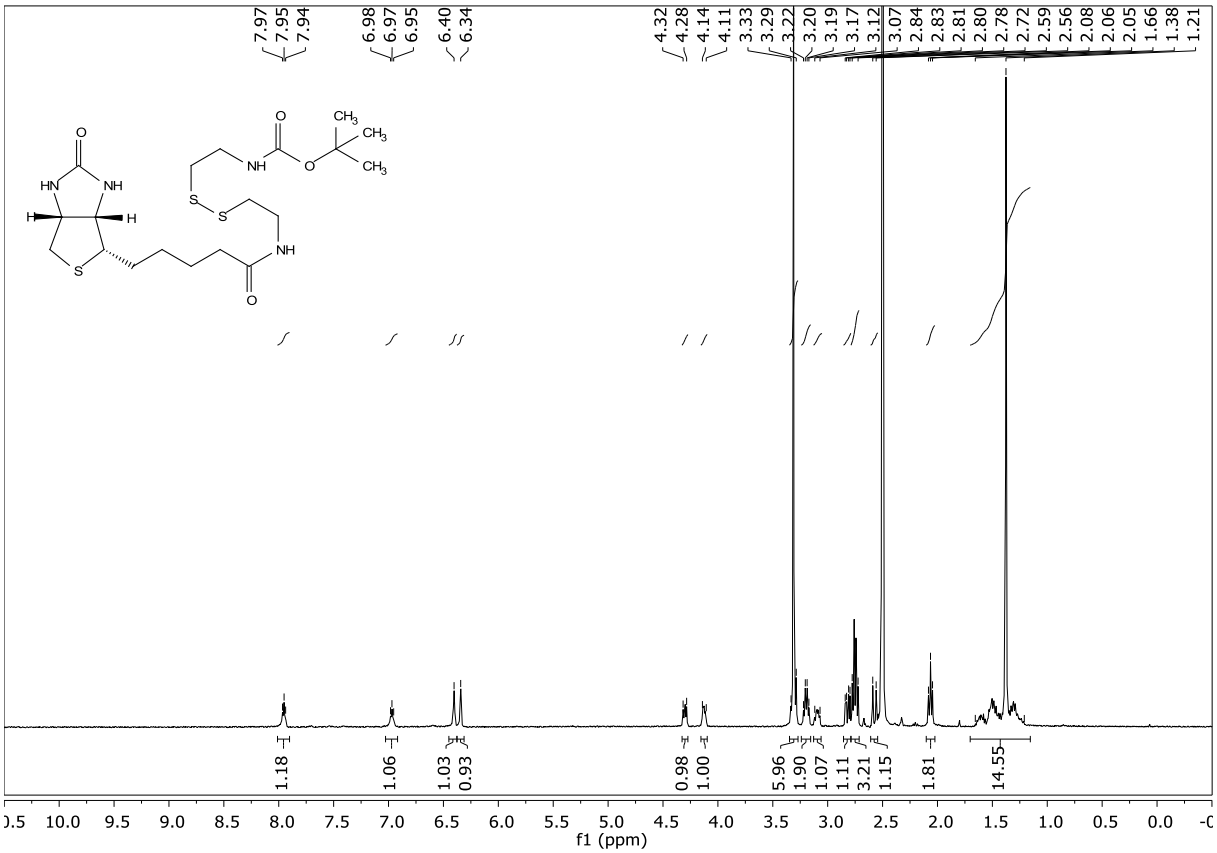

Cystaminyl biotinate hydrochloride (**160**)

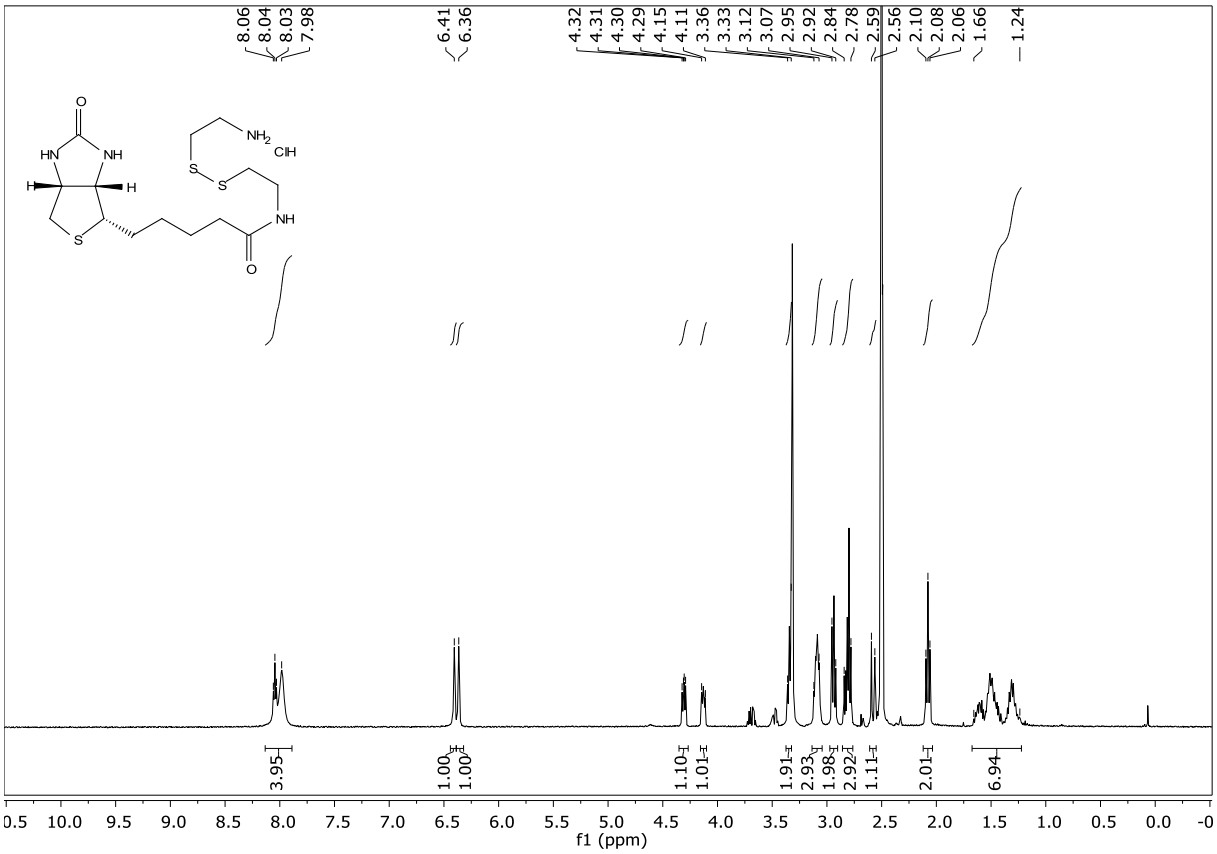

tert-Butyl (15,18,27-trioxo-31-((3a*S*,4*S*,6a*R*)-2-oxohexahydro-1H-thieno[3,4-*d*]imidazol-4-yl)-4,7,10-trioxa-22,23-dithia-14,19,26-triazahentriacontyl)carbamate (**163**)

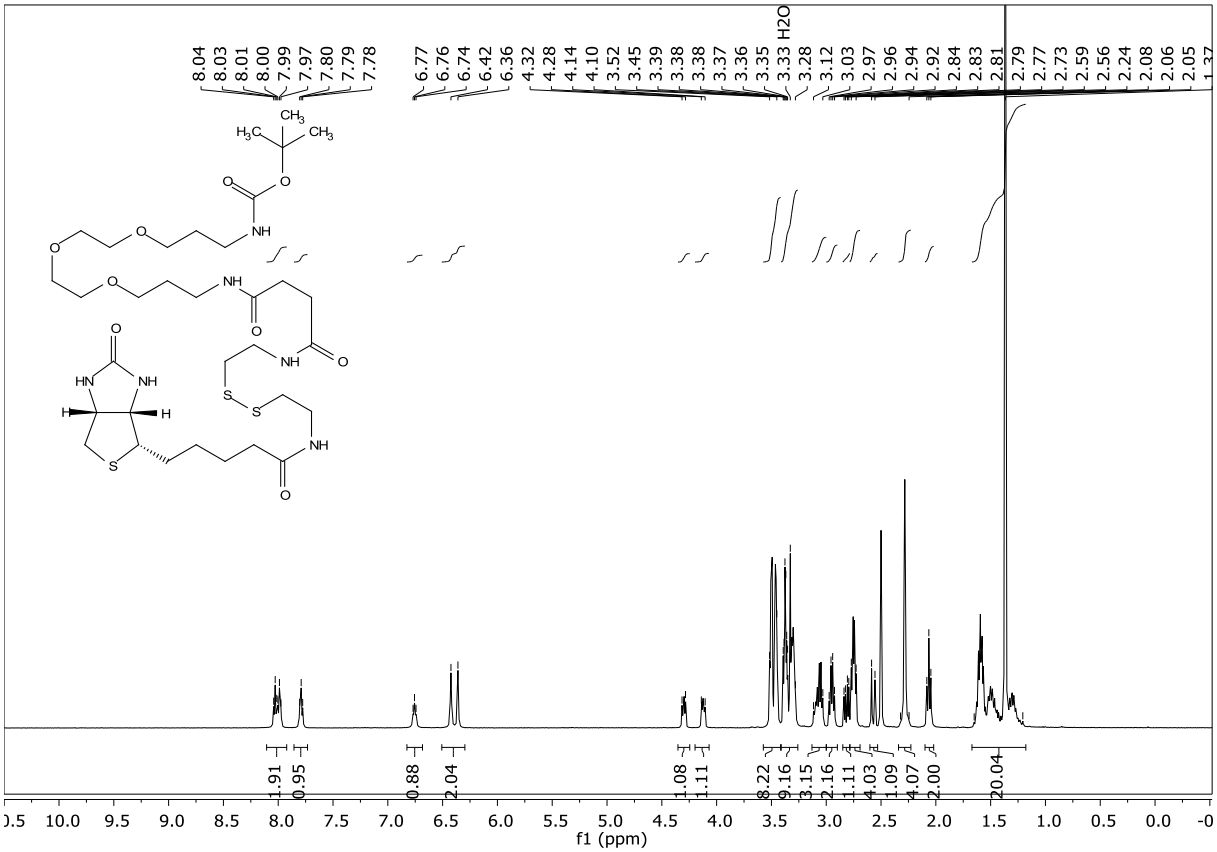

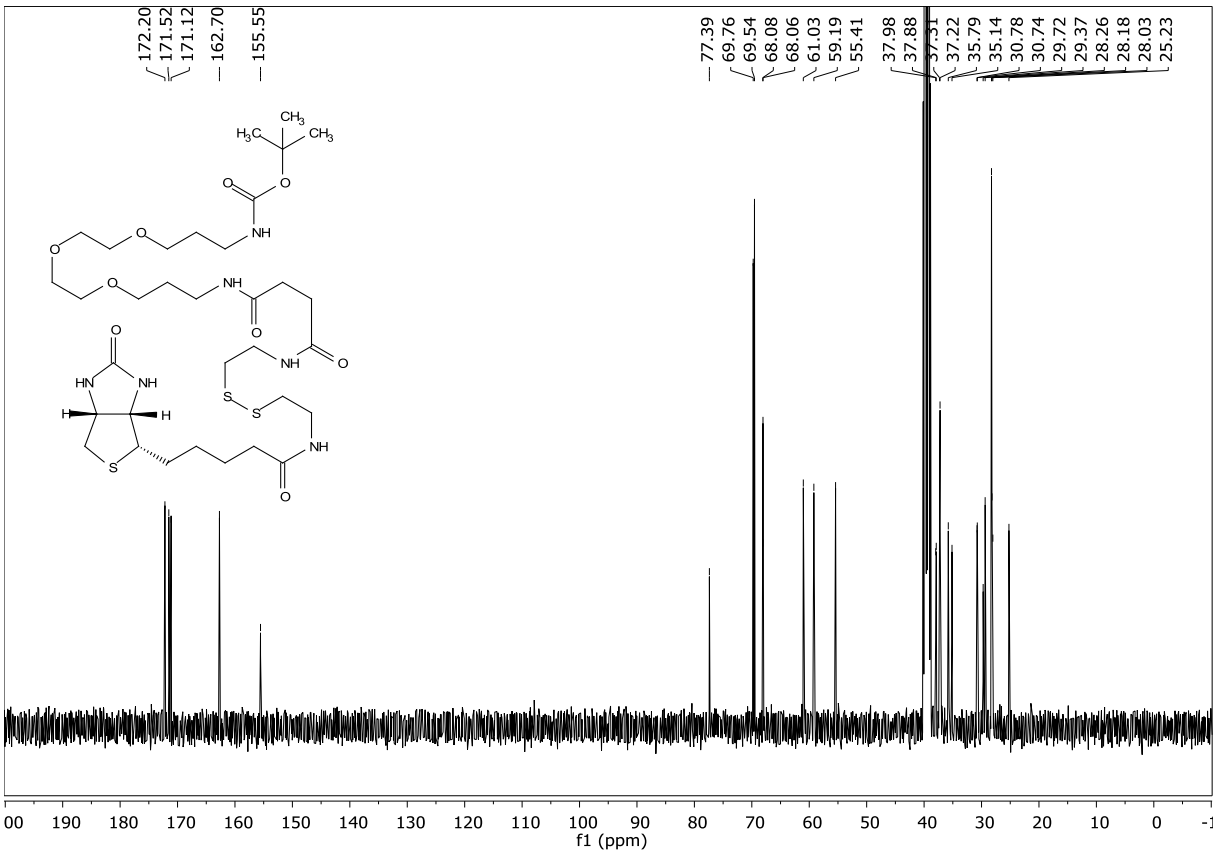

(*R*)-4-((*tert*-Butyldiphenylsilyl)oxy)cyclohex-2-en-1-one (**312**)

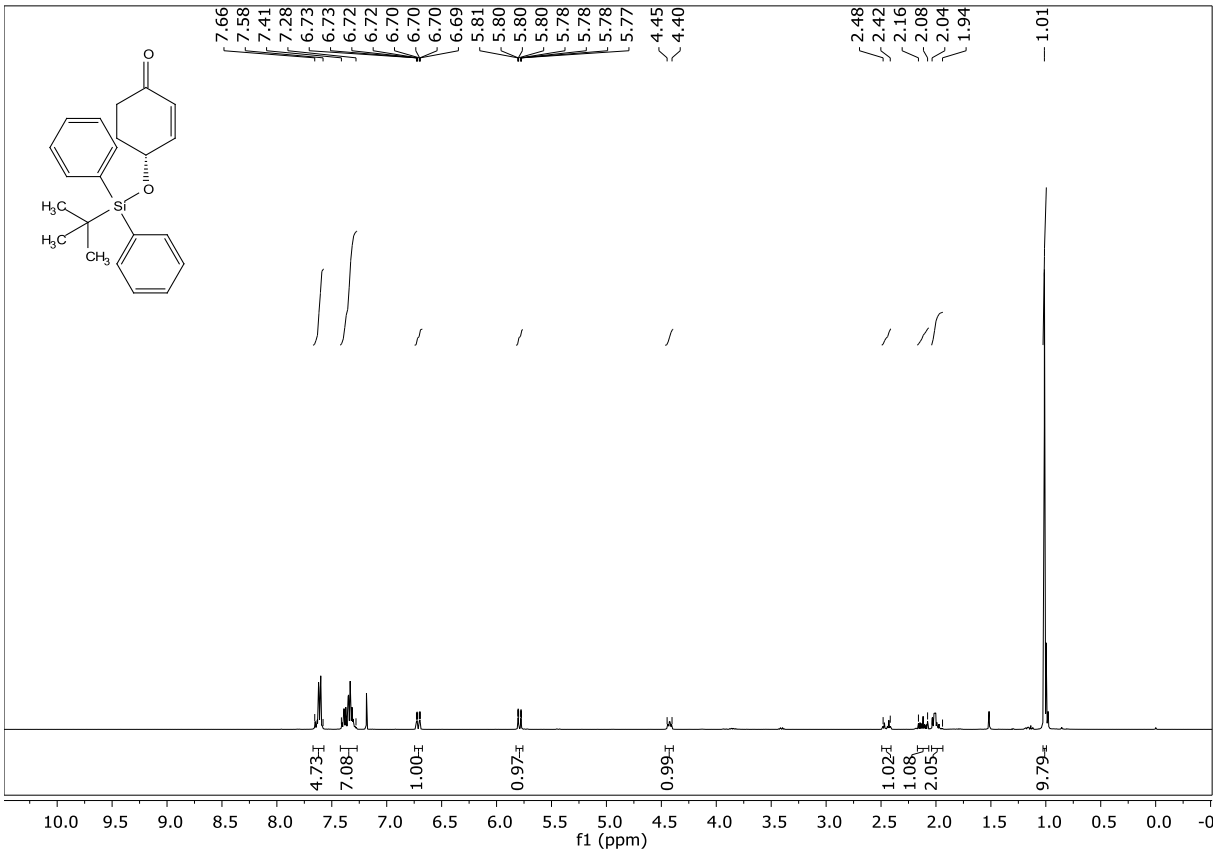

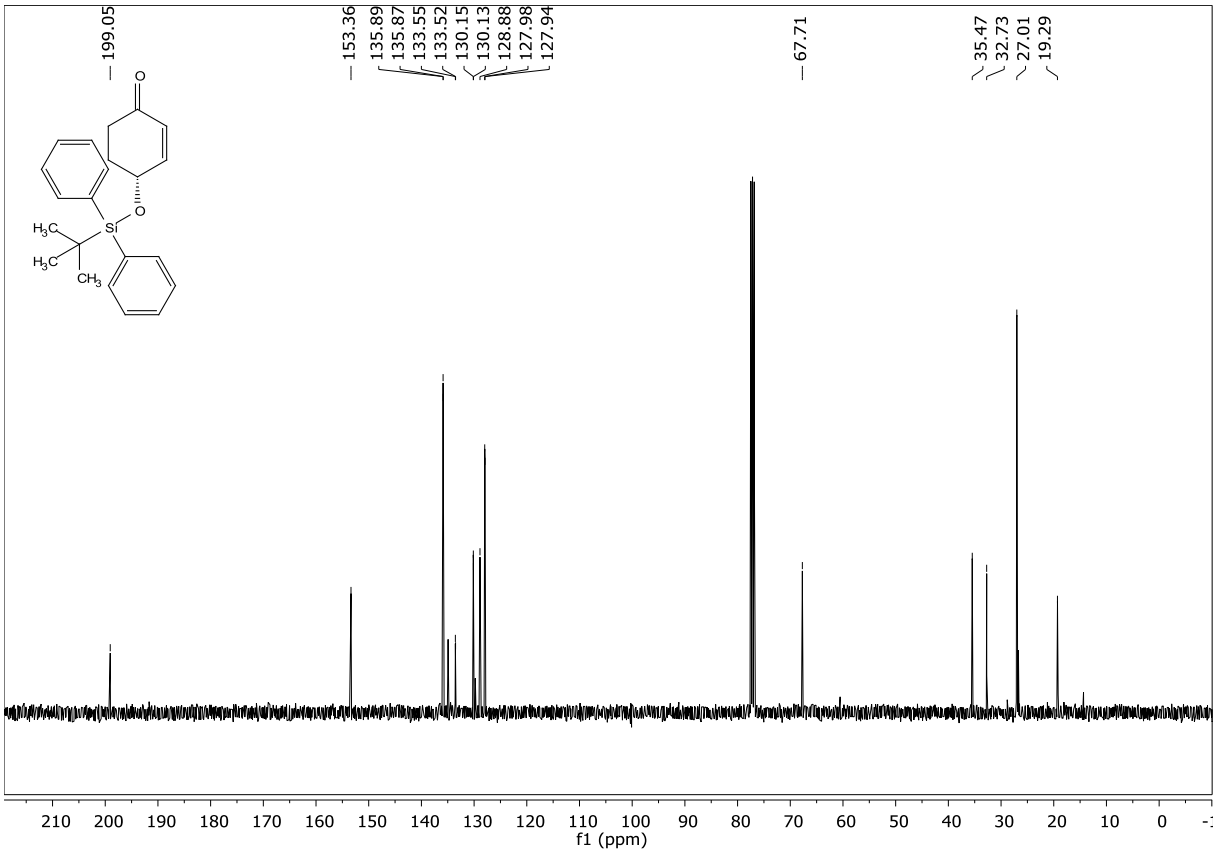

(6*R*,7a*R*)-6-((*tert*-Butyldiphenylsilyl)oxy)-7,7a-dihydrobenzofuran-2(6*H*)-one (**288**)

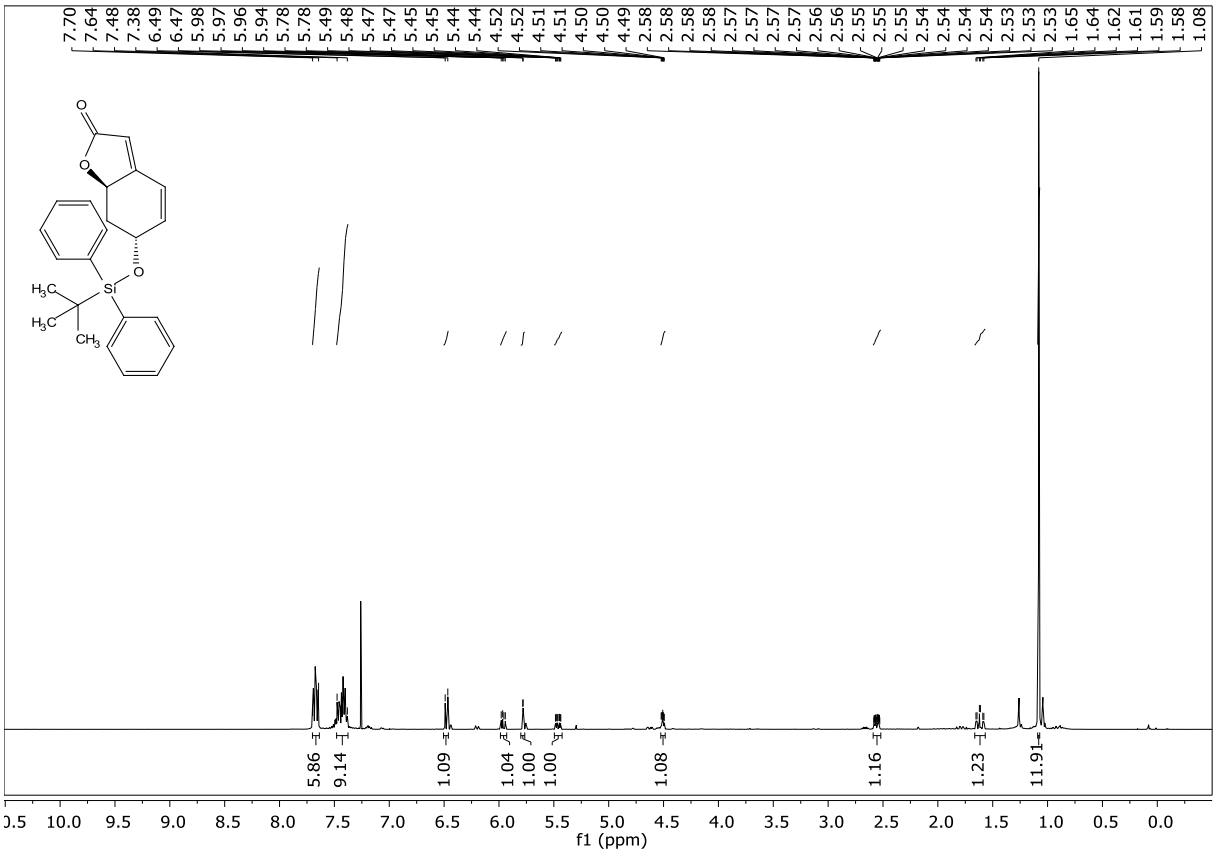

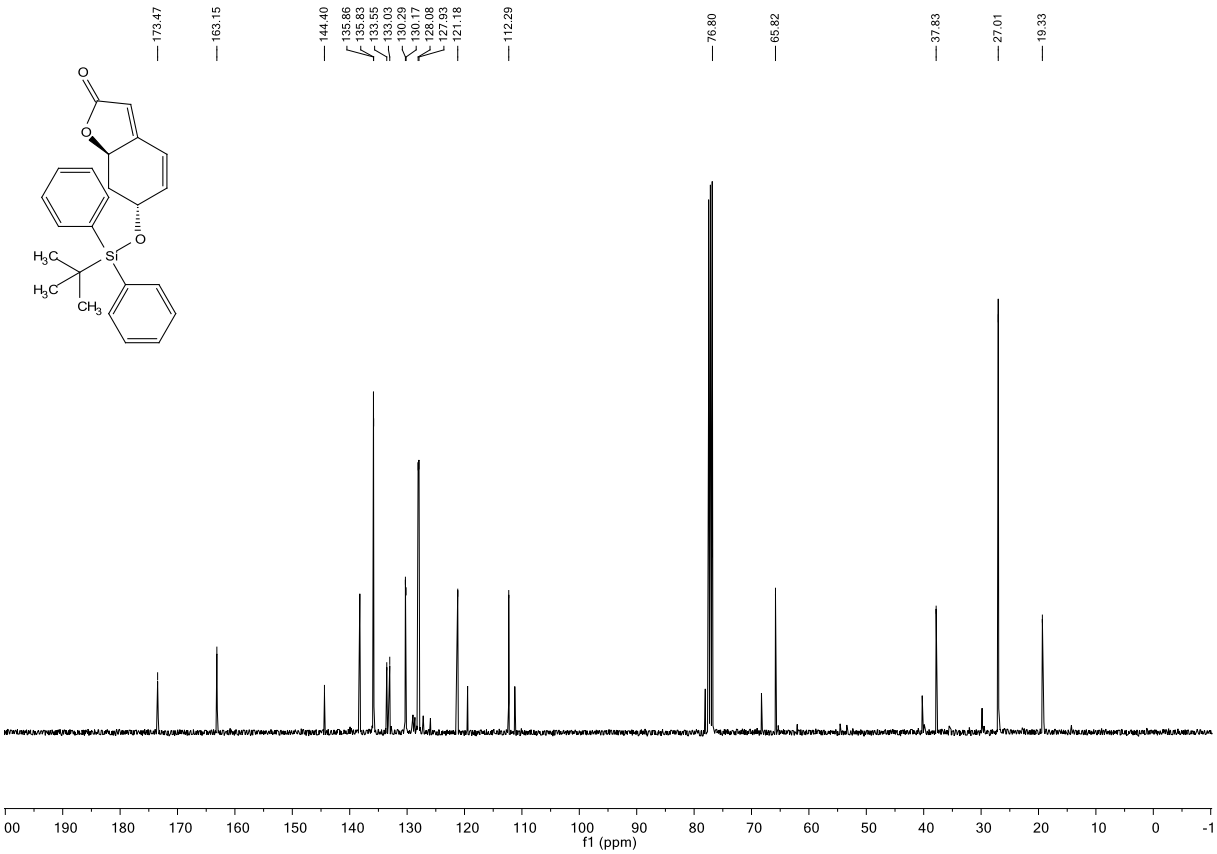

tert-Butyl (*S*)-2-((6*R*,7a*S*)-6-((*tert*-butyldiphenylsilyl)oxy)-2-oxo-6,7-dihydro-benzofuran-7a(2*H*)- yl)piperidine-1-carboxylate (**275**)

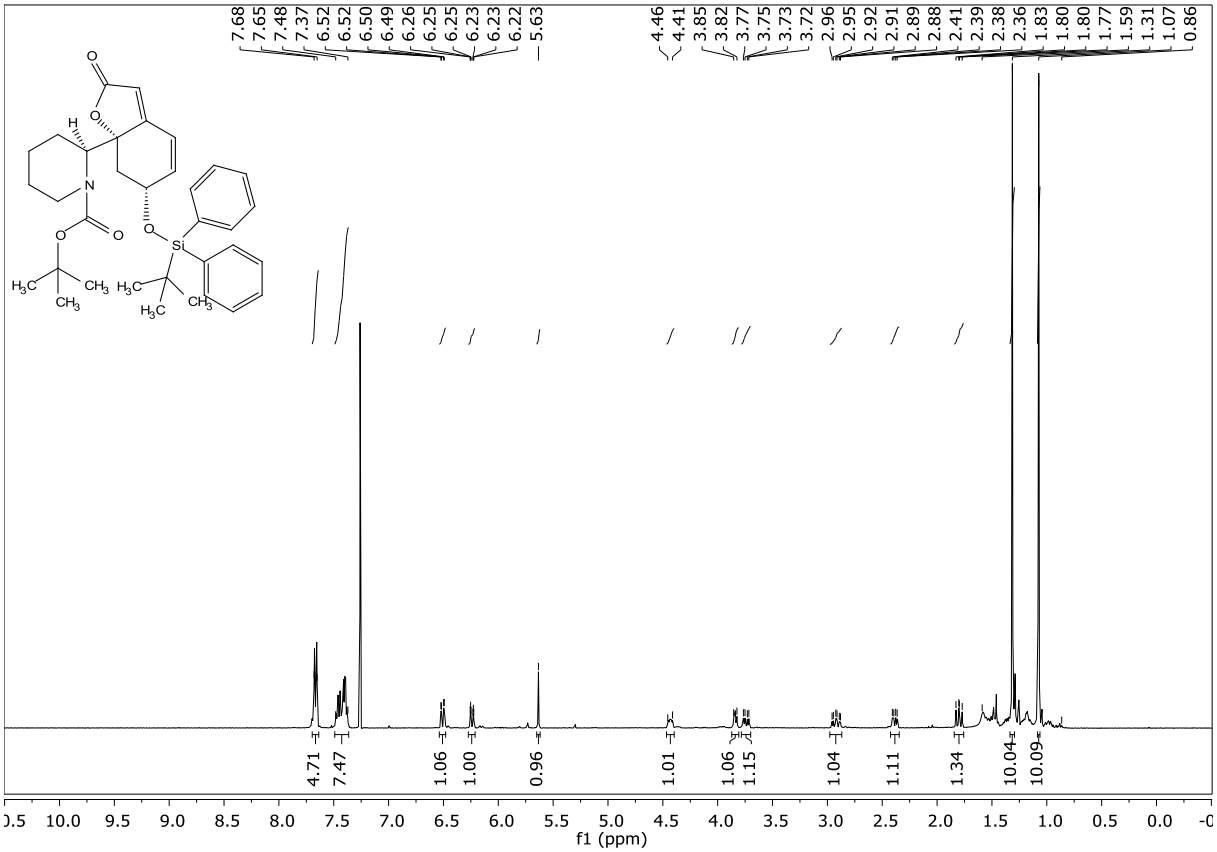

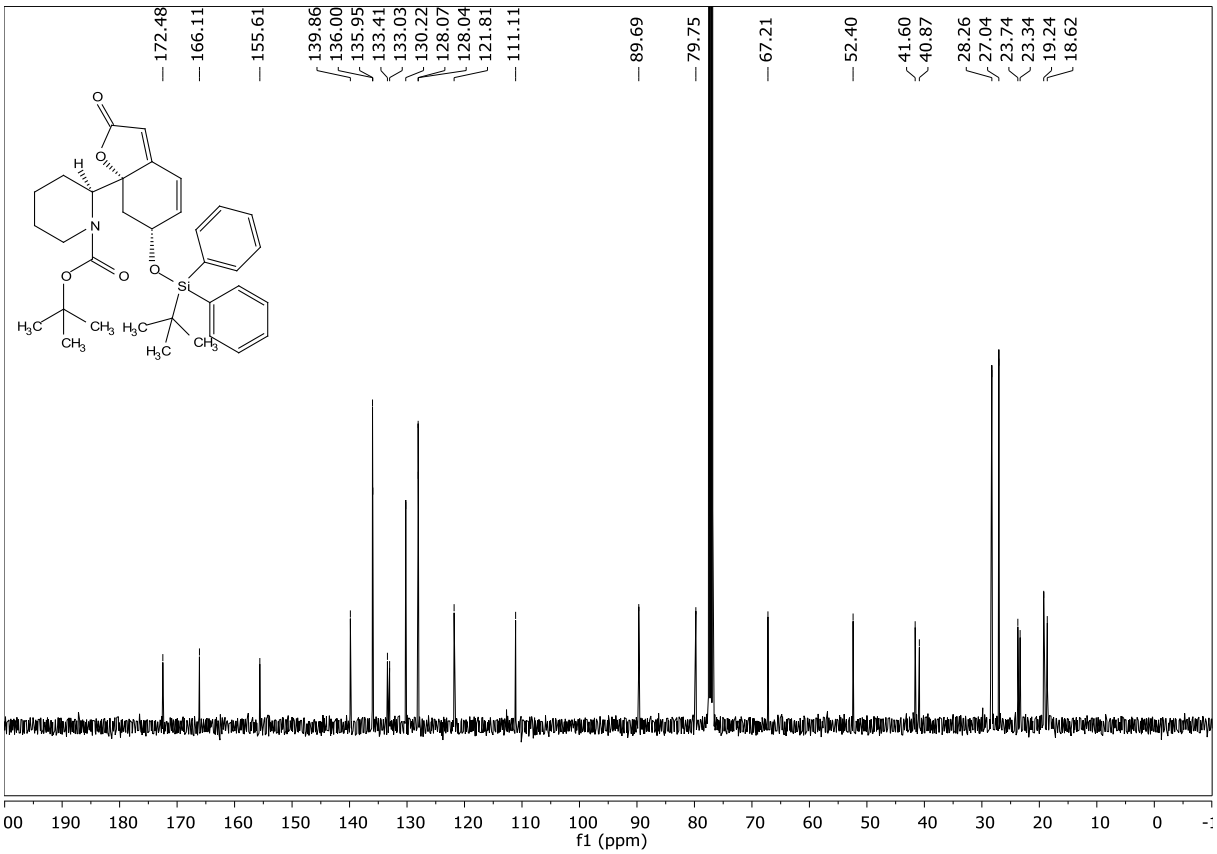

(*S*)-2-((6*R*,7a*S*)-6-((*tert*-Butyldiphenylsilyl)oxy)-2-oxo-6,7-dihydrobenzofuran-7a(2*H*)-yl)piperidin-1- ium chloride (**325**)

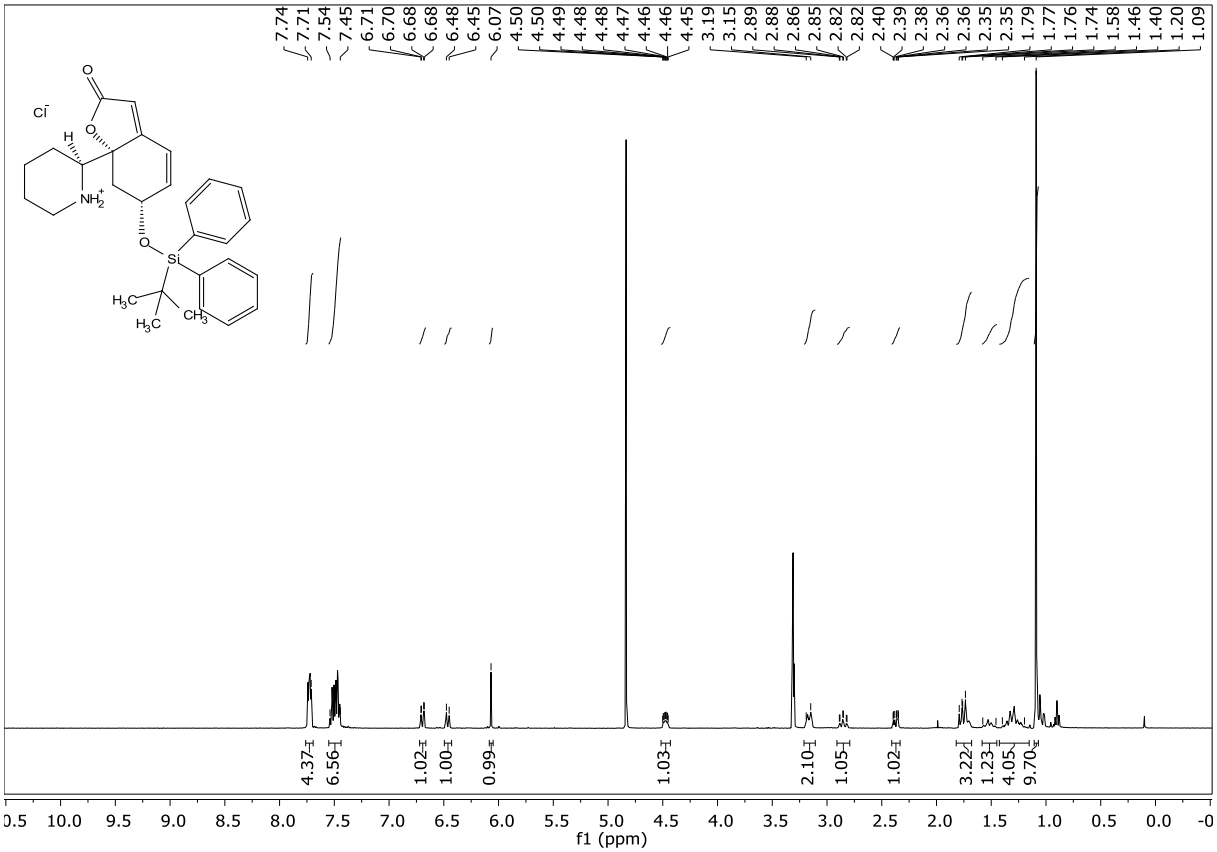

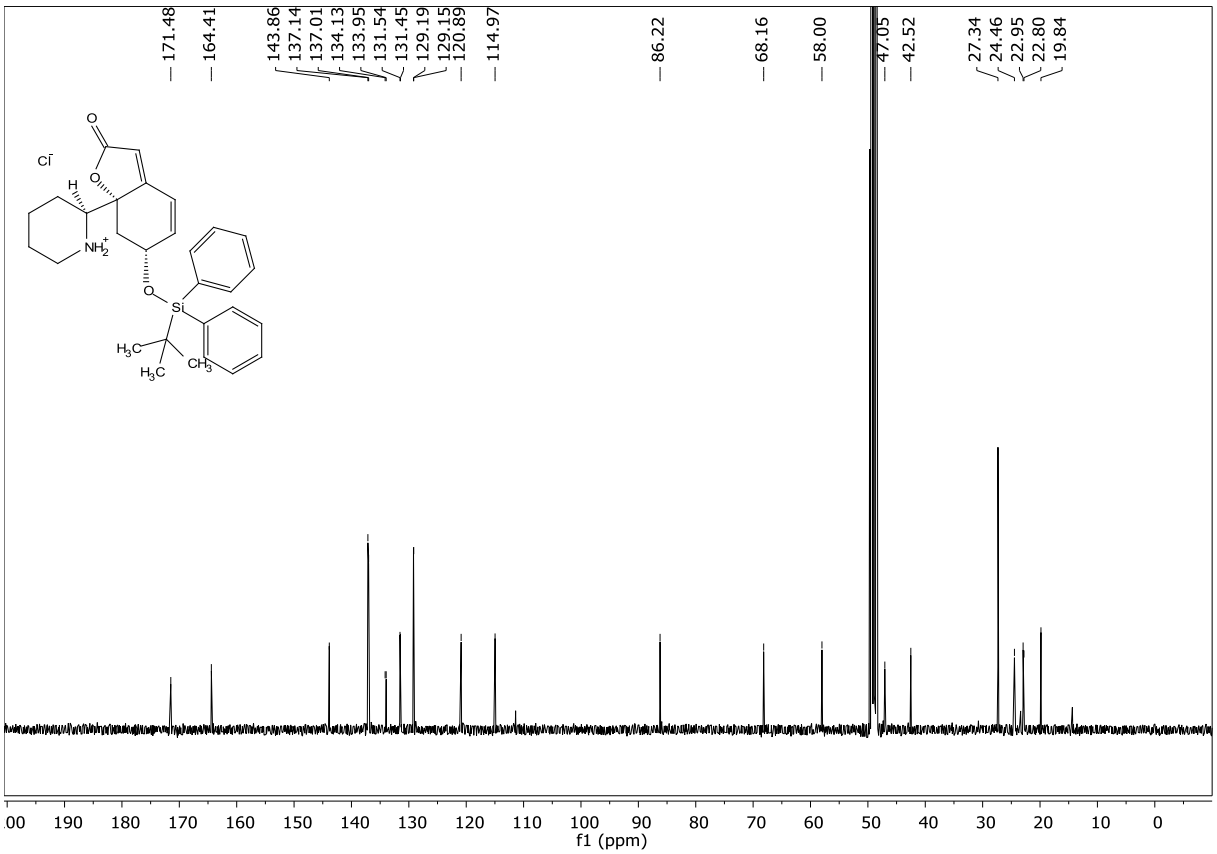

(5*R*,10a*S*,12*R*)-12-((*tert*-Butyldiphenylsilyl)oxy)-4,5,8,9,10,10a-hexahydro-2*H*,7*H*-5,10b-ethanofuro[2,3-a]quinolizin-2-one (**326**)

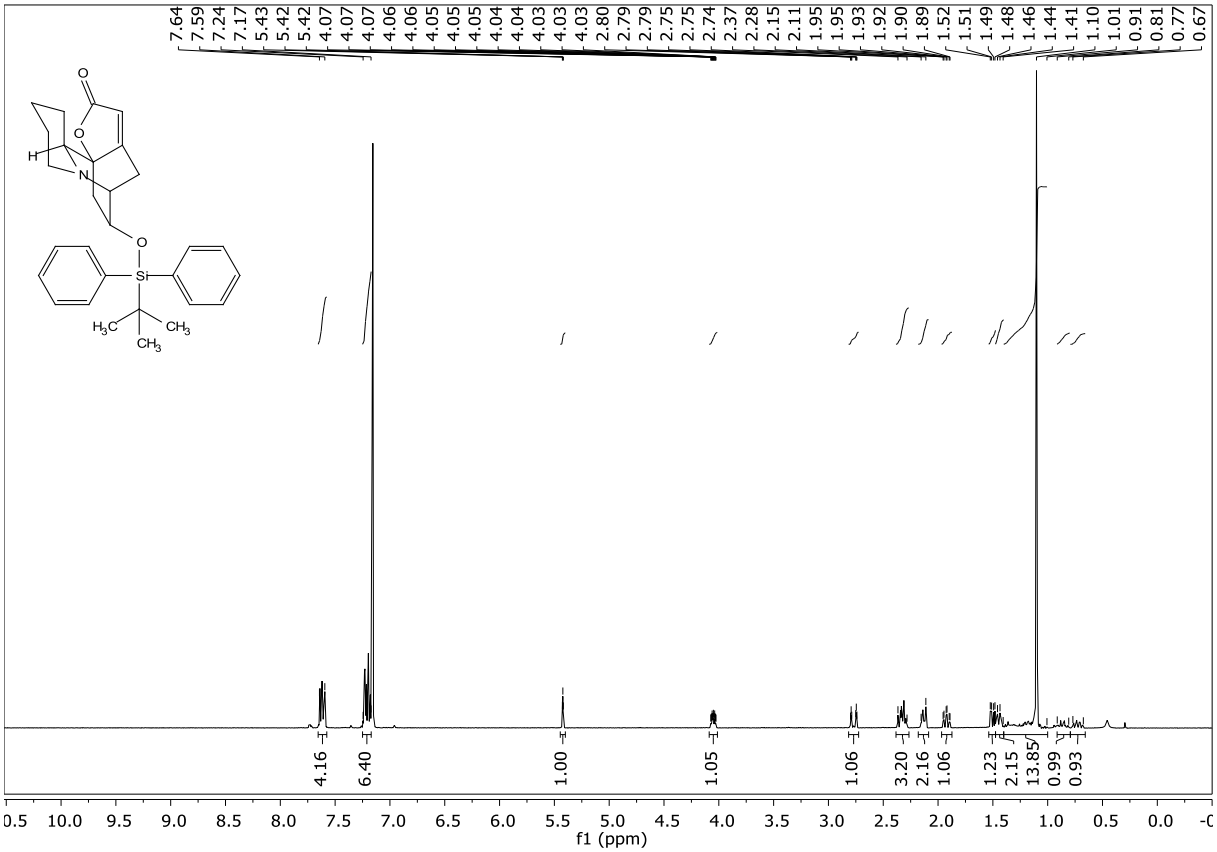

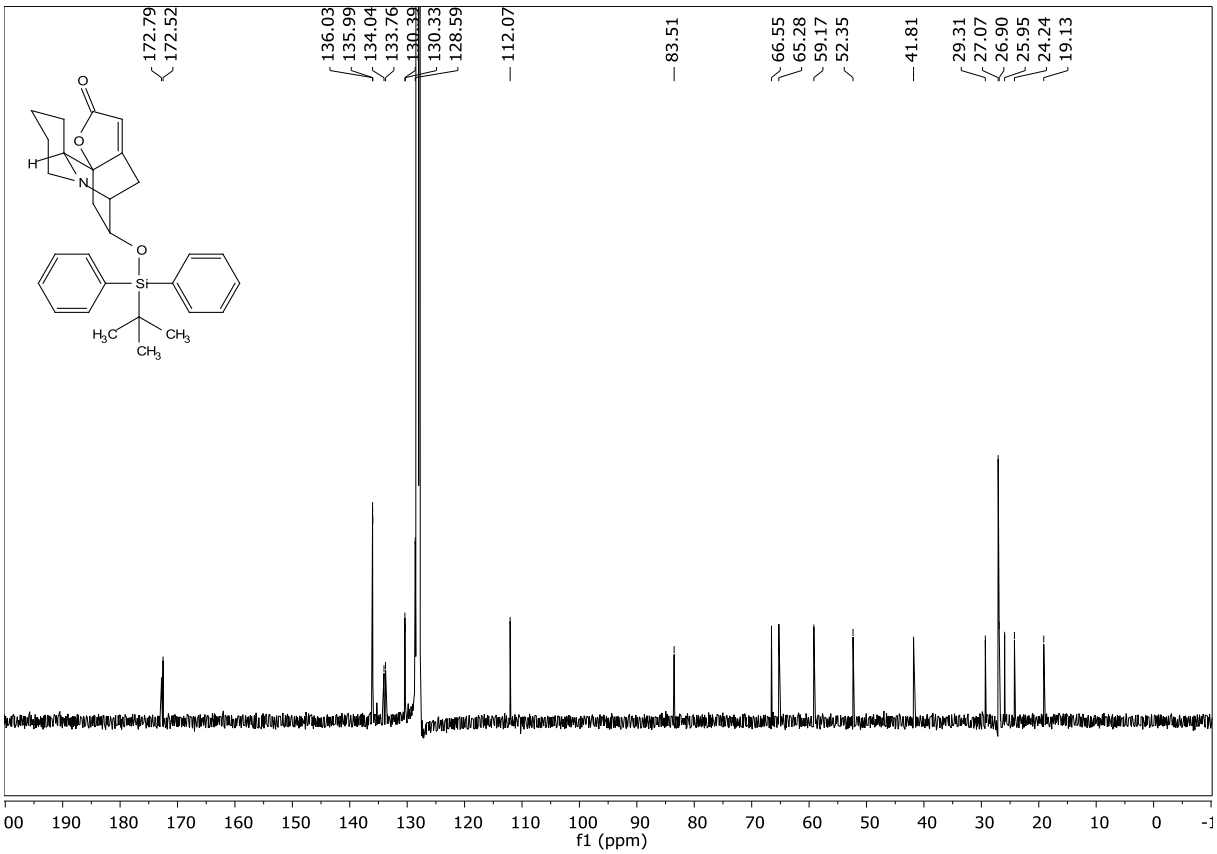

Secu’amamine E (**296**)

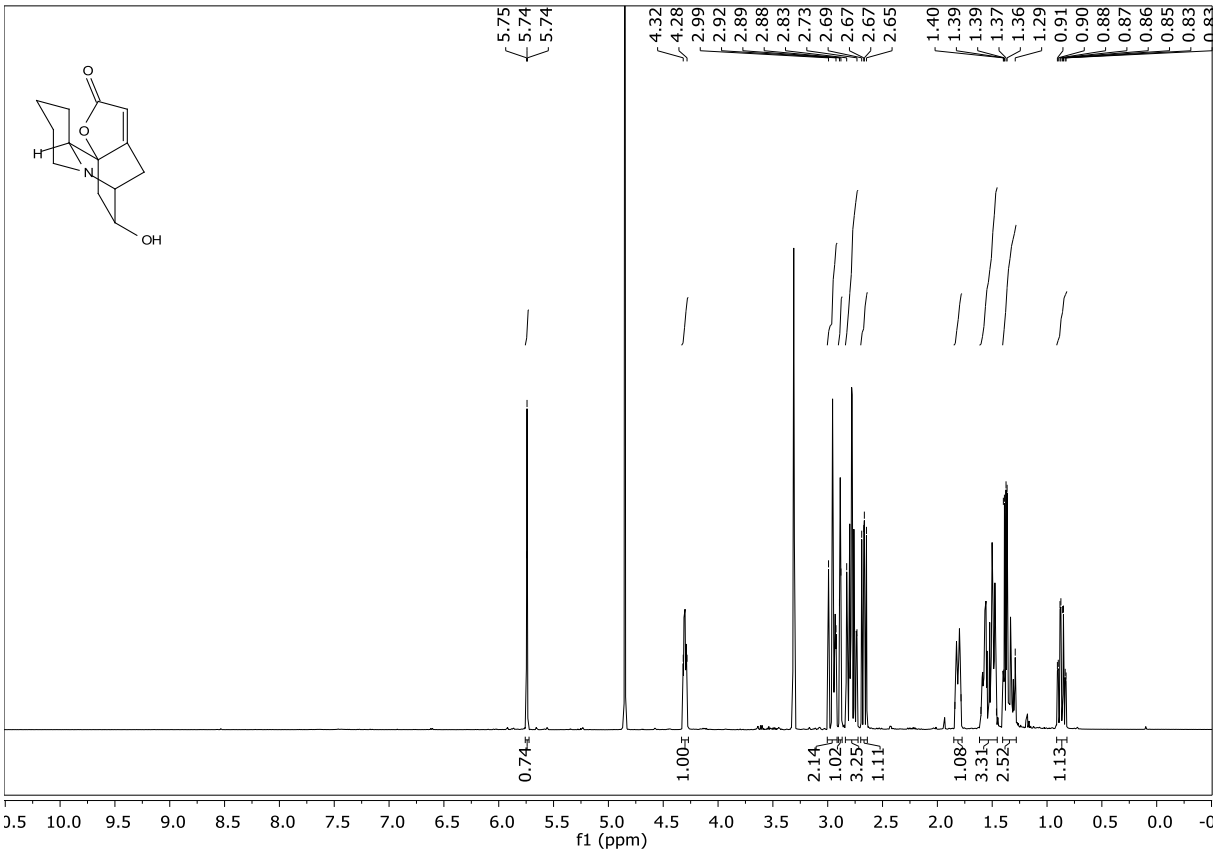

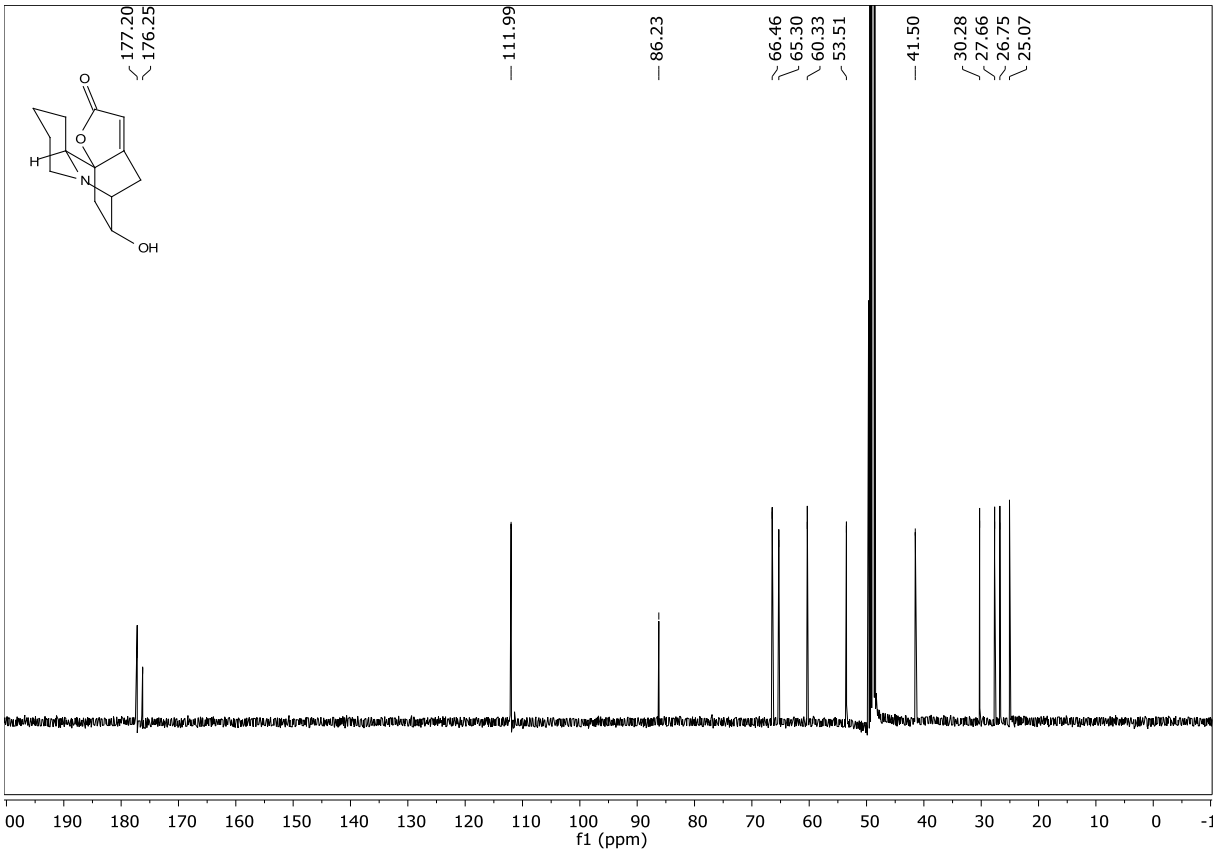

Allosecurinine (**172**)

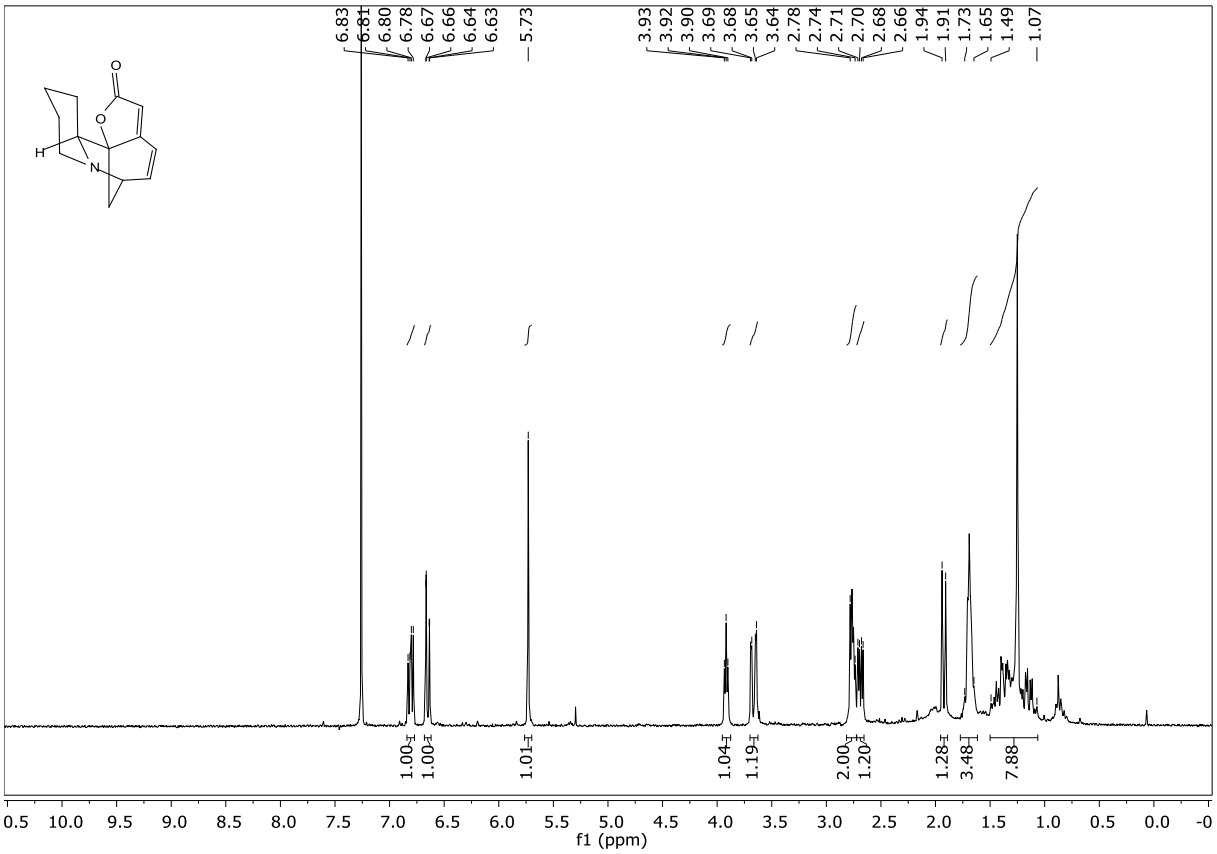

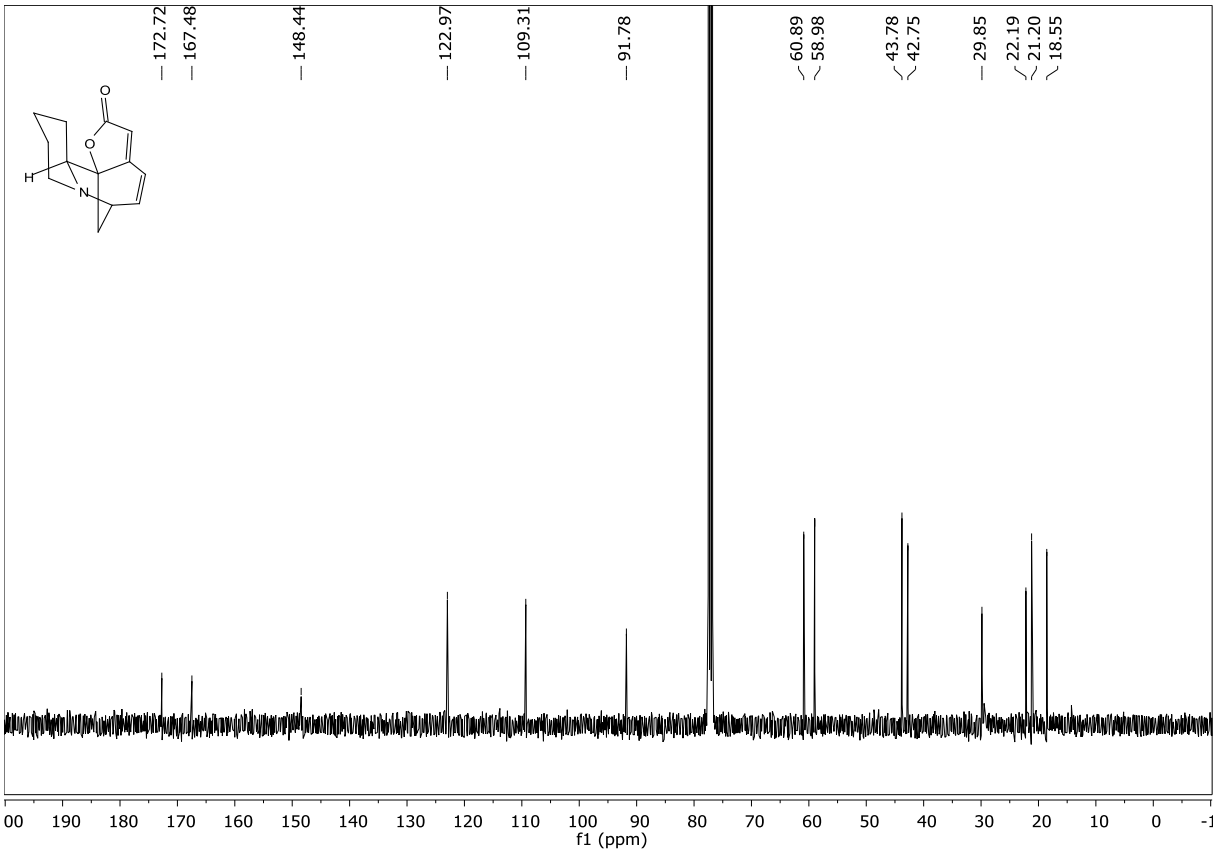

(−)-Allonorsecurinine (**329**)

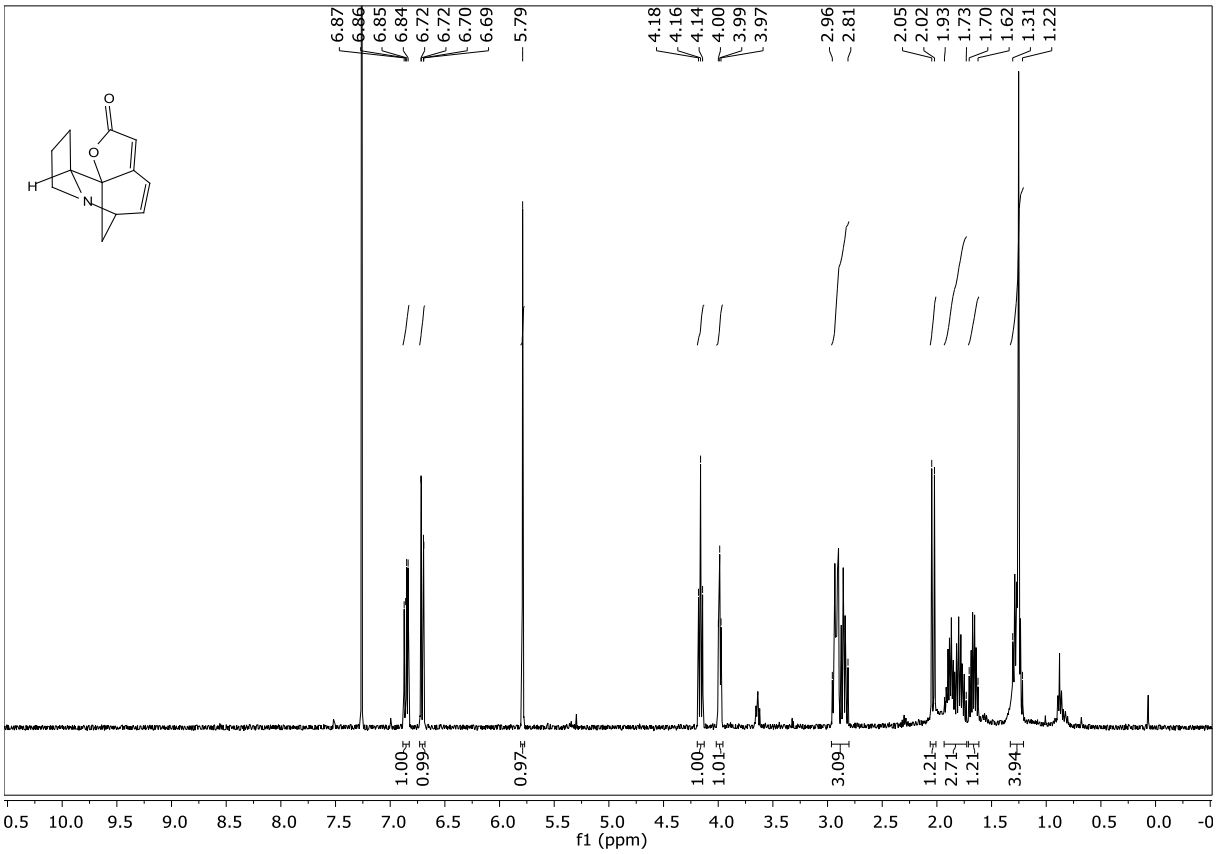

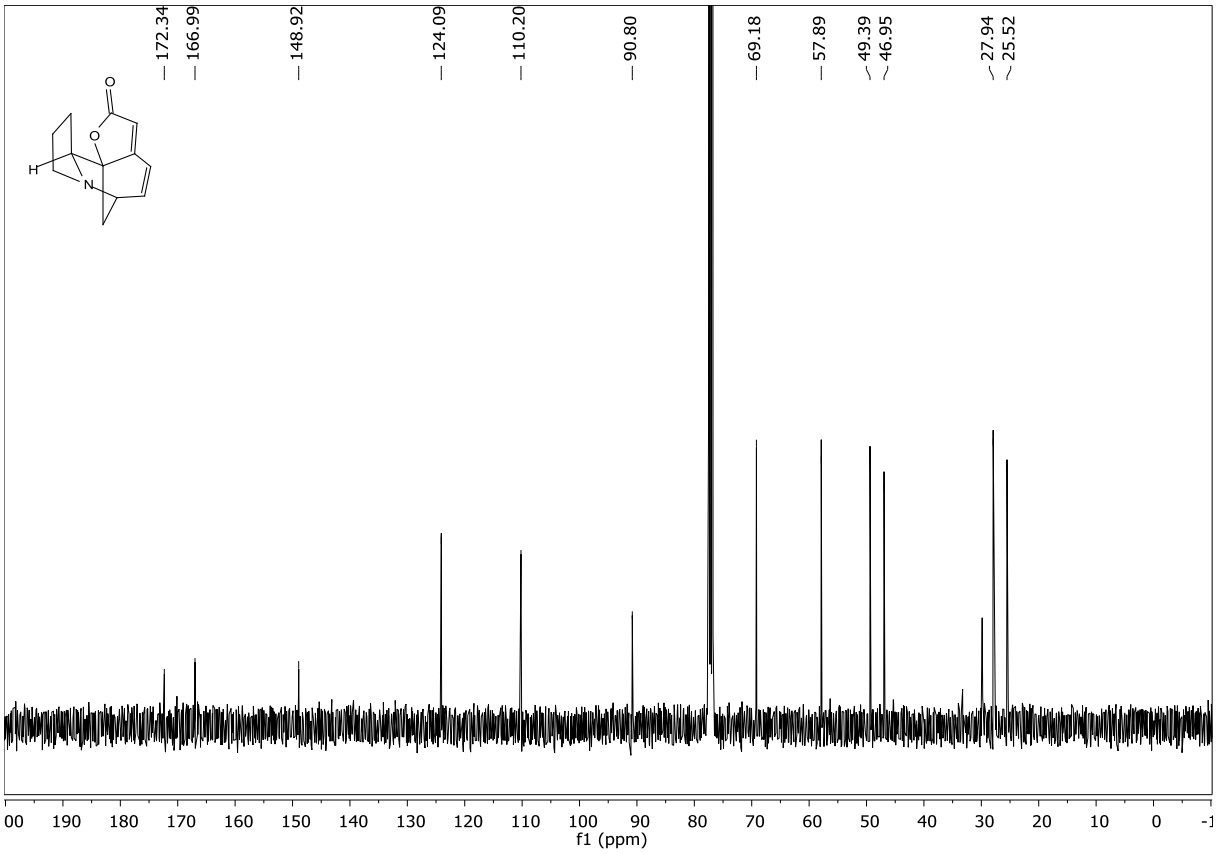

Bubbialine mesylate (**330**)

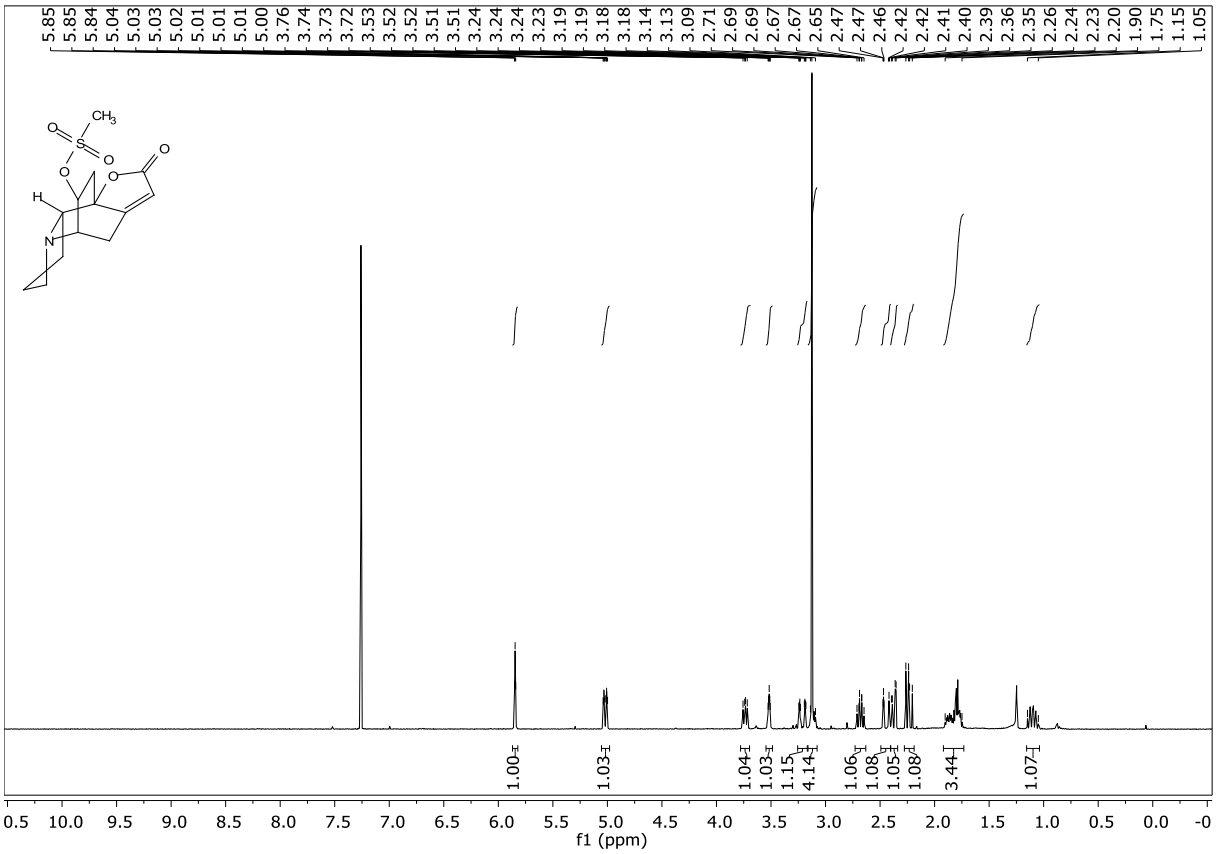

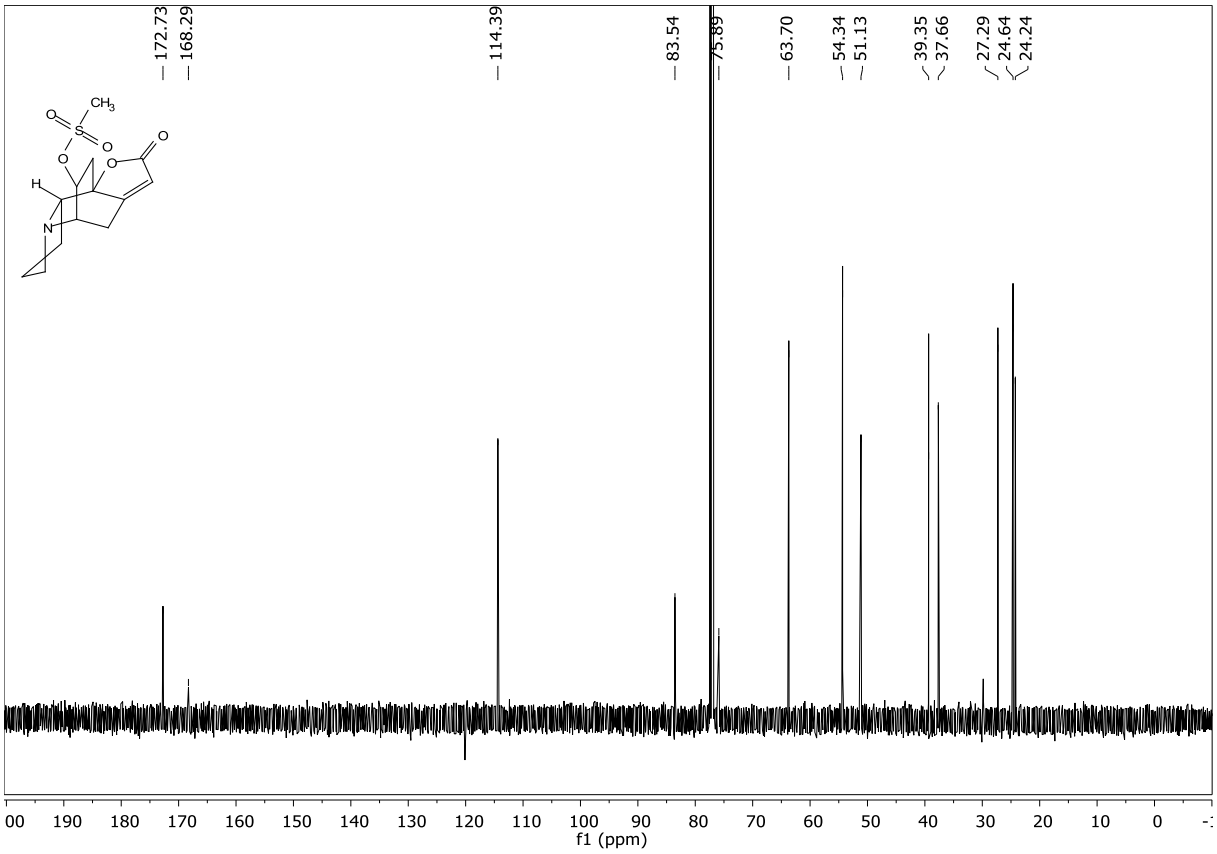

(+)-Allonorsecurinine (**331**)

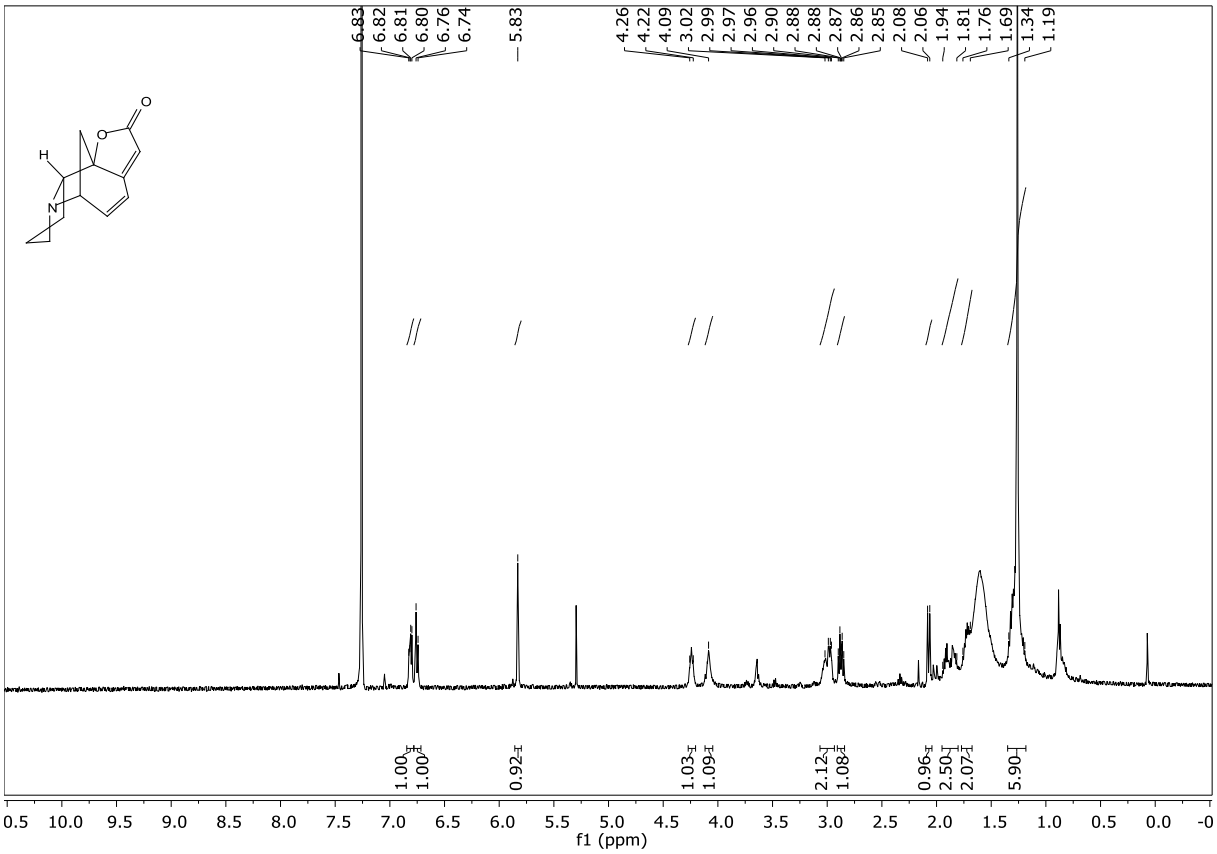

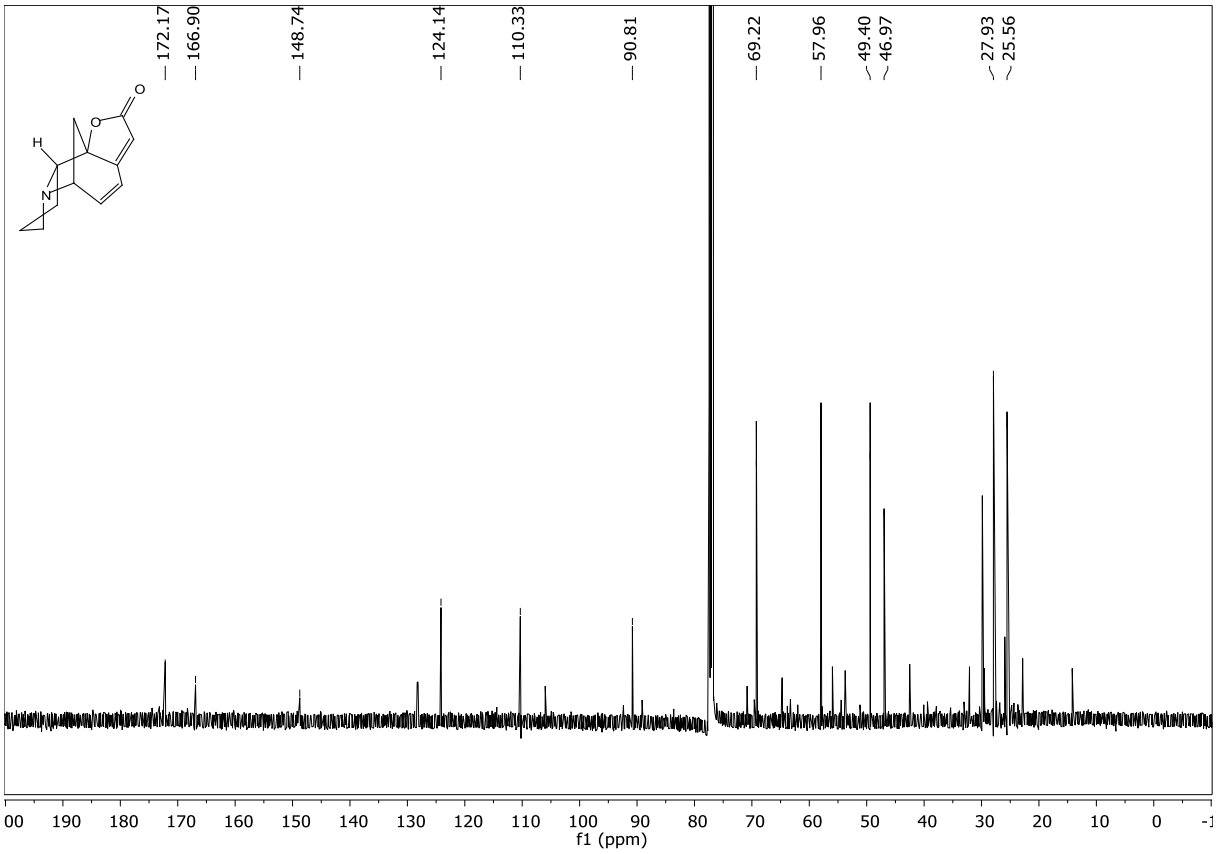

Acknowledgements

My sincerest gratitude goes to my Doktorvater Prof. Dr. *Karl Gademann* for giving me the chance to conduct the research presented in this work and for taking me into the Gademann group family. I am more than thankful for all the inspiration, motivation, education, support, and trust he provided me with during the past years.

I thank Prof. Dr. *Konrad Tiefenbacher* for accepting the co-examination of my thesis.

Dr. *Regina Berg*, Dr. *Nadine Bohni*, Dr. *Florian Huber*, and *Mathieu Szponarski* are thanked for proofreading this manuscript.

I am thankful to *Simone Grendelmeier* and *Andrea Meier* for contributing to this work in a Master's thesis and a Wahlpraktikum, respectively.

I am grateful to all the past and present members of the Gademann research group for their guidance and advice but especially for the countless great times we have spent together. Thank you all for the nice working atmosphere, for all the fun we had in and outside of the lab, for being my second family, and for always supporting me: Dr. *Johannes Hoecker*, Dr. *Suman De Sarkar*, Dr. *José Gomes*, Dr. *Samuel Bader*, Dr. *Hideki Miyatake-Ondozabal*, Dr. *Patrick Burch*, Dr. *Malika Makhlouf*, Dr. *Elamparuthi Elangovan*, Dr. *Verena Grundler*, Dr. *Christophe Thommen*, Dr. *Erika Crane*, Dr. *Christophe Daeppen*, Dr. *Elias Kaufmann*, Dr. *Fabian Schmid*, Dr. *Simon Sieber*, Dr. *Manuel Scherer*, Dr. *Isabel Kerschgens*, Dr. *Regina Berg*, Dr. *Nadine Bohni*, *Raphael Liffert*, *Mathieu Szponarski*, *Hiromu Hattori*, *Ellen Piel*, *Simone Grendelmeier*, *Jan Hanusch*, *Joël Rösslein*, *Andrea Meier*, *Agron Ilazi*, *Chien-Chi Hsiao*, *Bin Huang*, and *Inga Shchelik*.

Special thanks go to all my mates in labs 102 and 32E78, particularly my direct neighbors, who could not run away when I was in a bad mood, but were always there for me: my former Master student, colleague, and friend *Simone Grendelmeier*; my soulmate Dr. *Fabian Schmid*; and my NCCR buddy and frequent travel companion Dr. *Simon Sieber*.

I am thankful to Prof. Dr. *Christof Sparr* and *Achim Link*, *Dominik Lotter*, *Reto Witzig*, *Christian Fischer* and *Vincent Fäseke* from the Sparr research group for all the great discussions and good moments we shared.

I am grateful to all my friends at the Department Chemie of the University of Basel for the many great evenings we spent together.

I thank all the analytical, technical, and administrative staffs at the Universities of Basel and Zurich.

I acknowledge the financial support provided by the Universities of Basel and Zurich.

Besonders danken möchte ich der Karlsruher Gang *Marcel, Patrick, Kathi, Moe, Christian, Flo, Marbo, Chrissi, den Matzes* und allen anderen für den seelischen Beistand. Danke, dass ihr auch nach so vielen Jahren immer einen Platz für mich freihaltet und stets für die richtige Balance in meinem Alltag sorgt.

Mein herzlichster Dank gilt meiner gesamten Familie für die unermessliche Unterstützung auf dem bisherigen Weg. Ohne euch wäre all dies nicht möglich gewesen. Ich danke euch für die unablässige Hilfe mit den grossen und kleinen Dingen im Leben, für euer Vertrauen, eure Geduld, euer stetes Interesse an meiner Arbeit und die Motivation immer weiter zu machen auch in den schwersten Zeiten.